Epidemiological models for the transmission of HIV/AIDS and relevant coinfections

Ana Rita Moreira Carvalho
Doctoral Program in Applied Mathematics
Mathematics Department
2018

Orientador
Carla Manuela Alves Pinto, Adjunct Professor, School of Engineering, Polytechnic of Porto
Coorientador
João Nuno Domingues Tavares, Associate Professor, Faculty of Sciences, University of Porto

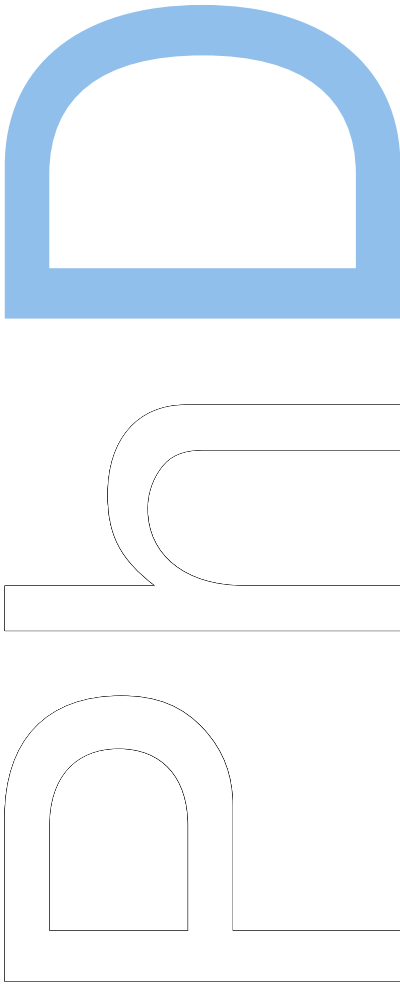

Acknowledgements

First of all, I would like to express my thanks to Professor Carla Pinto for the opportunity she gave me to start this joint work in my master's thesis, which encouraged this doctoral thesis. Secondly, for her always wise, generous and patient orientation regarding the doubts that the research put me. But also because of the challenging requirements with which she guided me, always pushing me to go further in the direction of clarity and scientific rigor. Thirdly, I would like to express my gratitude for all the opportunities for learning and work she has given me, which have greatly enriched this work. I also want to thank Professor João Nuno for his great initiative and for the work team he created around this theme, which allowed me to establish contacts with professionals from other areas and helped me to enrich my work.

Secondly, I want to thank my family, my parents, my brother and my grandmother, a huge thank you for always believing in me and always encouraging me to fight for my dreams. In particular, I want to thank my grandfather, who regardless of not being physically with me, I know he is my guardian angel. I'm dedicating this thesis to you! I know you will be thrilled that your girl has succeeded. I remember perfectly how happy you were when I decided to take my PhD. For you, knowledge was the most important and you always encouraged us to learn more and more. Over the years, I always saw you learn what the world brought as new, never being intimidated by technology. And this thirst of yours, of wanting to understand everything and not letting yourself be overlooked, was always a pride to me! I'm really sorry you're not here to see the culmination of this phase! I hope that this stage, which I now conclude, can somehow reciprocate everything you have taught me and I hope to continue to follow your teachings!

To you, Miguel, I want to thank you for all the love, tolerance, understanding for the lack of time and by appeasing my stress and anxiety by the end of this stage.

Finally, I thank my friends, especially João, for being always available to help me. Thank you all for the patience and the motivation you have always given me to conclude this

work.

The research of was supported by a FCT grant with reference SFRH/BD/96816/2013.

Abstract

Every year millions of people die worldwide due to infectious diseases, the like human immunodeficiency virus infection and acquired immune deficiency syndrome (HIV/AIDS), tuberculosis (TB) and hepatitis C virus (HCV). Although there are many distinguishing factors associated with each disease, mathematical models can provide reliable predictions for disease progression, and help decision makers devising public health policies. This thesis begins by reviewing the existing models in the literature, concerning the dynamics of HIV/AIDS transmission and relevant coinfections. Five models for the transmission dynamics of HIV/AIDS, HIV and HCV, HIV and TB, are detailed and analyzed mathematically and epidemiologically.

Two deterministic models for HIV virus are proposed. First in model I, it is considered a model for the dynamics of HIV epidemics under distinct highly active antiretroviral therapy (HAART) regimes. Model I predicts HIV patterns of untreated HIV patients for all stages of HIV infection. The local and the global stability of the disease-free equilibrium of the model are calculated. Simulations of the model are done for two distinct HIV patients, the rapid progressors (RP) and the long-term non-progressors (LTNP). The effects of equal reverse transcriptase inhibitors (RTIs) and protease inhibitors (PIs) efficacies, as well as distinct drug efficacies, namely RTI-based and PI-based therapeutics, are studied. Treatment is initiated when the CD4^+ T cells count is less than 350 cells mm^{-3}. PI-based drugs seem to produce better outcomes, with respect to disease progression, than RTI-based regimes. Model II is a simple delay mathematical model for the dynamics of AIDS-related cancers, where treatment for HIV and chemotherapy is included. The main goal of this model are the study of the effects of the delay and of treatment (HAART and chemotherapy) in cancer cells growth. The model is simulated for several biologically reasonable values of the delay, of HAART efficacies and of chemotherapeutic drugs decay rates. Results show that HAART may benefit HIV-infected patients not only by reducing HIV viral load but also by controlling cancer cell growth. Important inferences are drawn for designing treatment protocols.

Next, two deterministic coinfection models for HIV and HCV are presented. Model III describes HIV and HCV coinfection. The model predicts four distinct equilibria, the disease free, the HIV endemic, the HCV endemic, and the full endemic equilibria. The local and global stability of the disease free equilibria are calculated for the full model and for the HIV and HCV submodels. Simulations of the qualitative changes of the dynamical behavior of the full model are done for variation of relevant parameters. From the results of the model, are inferred measures which could be implemented to reduce the burden of the coinfection, by the policy makers. In model IV, a new coinfection model for HCV and HIV is developed. The model considers treatment for both diseases, screening, unawareness and awareness of HIV infection, and condom use. The local stability of the disease-free equilibria for the full model and for the two submodels (HCV only and HIV only submodels) are studied. Bifurcation diagrams for different parameters, such as the probabilities that a contact will result in a HIV or an HCV infection, are sketched. Numerical simulations of the full model show HIV, HCV and double endemic equilibria. Moreover, plots of dynamics of the model for variation of relevant parameters are also depicted. The model results are extrapolated to actual measures that could be implemented in order to reduce the number of HIV/HCV infected individuals, such as distributing more condoms to individuals; develop campaign in order to warn individuals about the consequences of having many sexual partners; continuing treatment for AIDS and pursuing the investigation of new and better drugs to combat the virus and regular screening.

Finally, it is presented a non-integer order model for coinfection of HIV and TB, in the presence of multi-drug resistant TB strains (MDR-TB) and treatment for both diseases. The reproduction number of the HIV and TB submodels and of the full model, and the local and global stabilities of the disease-free equilibria are calculated. Numerical simulations show the different dynamics of the model for variation of epidemiologically relevant parameters, and for the order of the fractional derivative $\alpha \in]0, 1]$. The results obtained highlight the importance of treatment for HIV and TB and the role of the MDR-TB strains in the severity of the coinfection. Moreover, the order of the fractional derivative is a significant player in the epidemics theatre.

In conclusion, the models presented in this thesis are mathematically and epidemiologically well posed.

Resumo

Todos os anos milhões de pessoas morrem em todo o mundo devido a doenças infecciosas, como a infeção do vírus da imunodeficiência humana e o síndrome da imunodeficiência adquirida (VIH/SIDA), a tuberculose (TB) e o vírus da hepatite C (VHC). Embora existam muitos fatores distintivos associados a cada doença, os modelos matemáticos podem fornecer previsões confiáveis da progressão da doença e ajudar a tomar decisões sobre a política de saúde pública. Nesta tese começa-se por analisar os modelos existentes na literatura, sobre a dinâmica da transmissão do VIH/SIDA e coinfeções relevantes. São detalhados e analisados matematicamente e epidemiologicamente, cinco modelos para a dinâmica da transmissão do VIH/SIDA, do VIH e do VHC, do VIH e da TB.

São propostos dois modelos determinísticos para a dinâmica da propagação do vírus VIH. Primeiro no modelo I, é considerado um modelo para a dinâmica da epidemia do VIH sob diferentes regimes de terapia antirretroviral altamente ativa (TARV). O modelo I prevê padrões do VIH de pacientes infetados não tratados para todas as etapas da infeção. As estabilidades local e global do equilíbrio livre de doença do modelo são calculadas. O modelo é simulado para dois pacientes distintos infetados com o VIH, os progressores rápidos (RP) e os não-progressores de longo prazo (LTNP). Os efeitos dos inibidores da transcriptase reversa (RTIs) iguais aos inibidores de protease (PIs) são estudados, assim como distintas eficiências das drogas, ou seja, terapias baseadas em RTI e em PI. O tratamento é iniciado quando as células CD4^+ T são inferiores a 350 células mm^{-3}. Os fármacos baseados em PI parecem produzir melhores resultados, em relação à progressão da doença, do que os regimes baseados em RTI. O modelo II é um modelo matemático com atraso para a dinâmica dos cancros relacionados com a SIDA, onde o tratamento para o VIH e a quimioterapia estão incluídos. O objetivo principal deste modelo é o estudo dos efeitos do atraso e do tratamento (TARV e quimioterapia) no crescimento das células cancerígenas. O modelo é simulado para vários valores biologicamente razoáveis do atraso, das eficiências da TARV e das taxas

de decomposição dos fármacos quimioterapêuticos. Os resultados mostram que a TARV pode beneficiar os pacientes infetados pelo VIH, não só por reduzir a carga viral do VIH, mas também por controlar o crescimento de células cancerígenas. As principais conclusões são elaboradas para a conceção de protocolos de tratamento.

Em seguida, são apresentados dois modelos determinísticos para a coinfeção do VIH e do VHC. O modelo III descreve a coinfeção por VIH e VHC. O modelo prevê quatro equilíbrios distintos, o livre de doença, o endémico do VIH, o endémico do VHC e o equilíbrio endémico completo. As estabilidades local e global dos equilíbrios livres de doença são calculadas para o modelo completo e para os submodelos do VIH e do VHC. As mudanças qualitativas do comportamento dinâmico do modelo completo são simuladas para a variação de parâmetros relevantes. A partir dos resultados do modelo, são inferidas medidas que podem ser implementadas para reduzir a coinfeção pelos decisores políticos. No modelo IV é desenvolvido um novo modelo para a coinfeção por VIH e VHC. O modelo considera o tratamento das doenças, o rastreio, a inconsciência e a consciencialização sobre a infeção pelo VIH e o uso de preservativo. São estudadas as estabilidades locais dos equilíbrios livres de doença para o modelo completo e para os dois submodelos (somente para VHC e para o VIH). Os diagramas de bifurcação para diferentes parâmetros, como as probabilidades de que um contacto resulte numa infeção por VIH ou VHC, são esboçados. As simulações numéricas do modelo completo mostram o equilíbrio endémico do VIH, o equilíbrio endémico do VHC e o equilíbrio endémico duplo. Também se mostram os gráficos da dinâmica do modelo para variação dos parâmetros relevantes. Os resultados do modelo são extrapolados para medidas reais que poderiam ser implementadas para reduzir o número de indivíduos infetados pelo VIH/VHC como distribuir mais preservativos pelos indivíduos; desenvolver campanhas para alertar os indivíduos sobre as consequências de ter muitos parceiros sexuais; tratamento contínuo da SIDA e a investigação de novos e melhores medicamentos para combater o vírus e a triagem regular.

Finalmente, é apresentado um modelo de ordem fracionária (FO) para a coinfeção por VIH e TB, na presença de estirpes resistentes da TB a vários medicamentos (MDR-TB) e o tratamento para ambas as doenças. São calculados, os números de reprodução dos submodelos de VIH e da TB e do modelo completo, as estabilidades local e global dos equilíbrios livres de doença. As simulações numéricas mostram as diferentes dinâmicas do modelo para a variação de parâmetros epidemiologicamente relevantes e para a ordem da derivada fracionária $\alpha \in]0, 1]$. Os resultados obtidos destacam a importância do tratamento do VIH e da TB e o papel das estirpes MDR-TB na gravidade da coinfeção. A ordem da derivada fracionária é uma componente importante no

cenário das epidemias.

Em conclusão, os modelos apresentados nesta tese são matematicamente e epidemiologicamente bem definidos.

Keywords

HIV, AIDS, mathematical model, HAART regimes, treatment, drug resistance, rapid progressors, long-term non-progressors, AIDS-related cancer, chemotherapy, delay, HCV, MSM, screening, coinfection, TB, multi-drug resistance, fractional order.

x

Contents

List of Tables

List of Figures

Chapter 1

Introduction

HIV is classified as a member of the *Retroviridae* family, subfamily *Orthoretrovirinae*, genus *Lentivirus* (ICTV, 2009). This virus has a cone-shaped capsid that holds its genome consisting of two single-stranded ribonucleic acid (RNA) molecules. Retroviruses are characterized by the ability of transcribing their RNA genome into a double-stranded deoxyribonucleic acid (DNA) prior to the integration of the virus genome into the host cell chromosome. This process is mediated by an RNA-dependent DNA polymerase called reverse transcriptase [147].

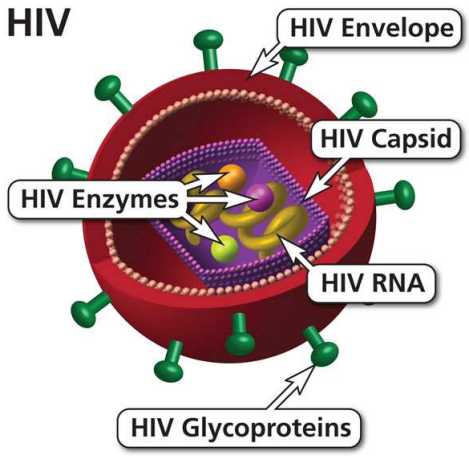

Figure 1.1: HIV [88]

HIV has three structural genes: *gag*, responsible for viral capsid synthesis; *pol* (polymerase), which encodes the PR (protease), RT (reverse transcriptase), IN (integrase) proteins and *env* (envelope), responsible for the production of the viral surface glycoproteins. In addition, HIV has two regulatory genes (*tat* and *rev*) and four accessory

genes (*vpr*, *vpu*, *nef* and *vif*) (see Figure 1.2).

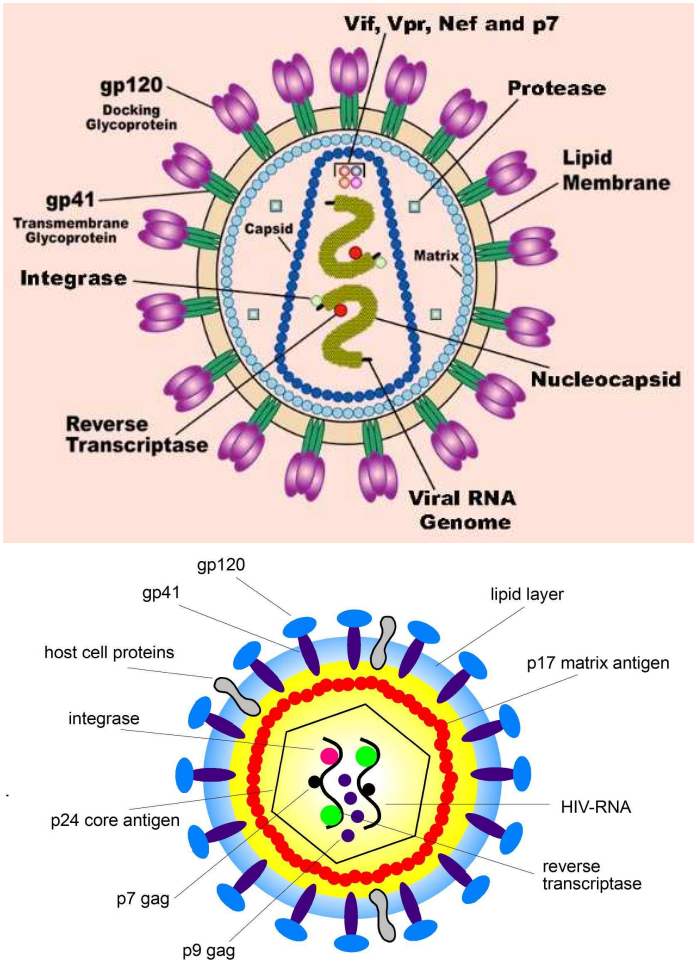

Figure 1.2: Structure of an HIV virion particle [89, 121]

As shown in the Figure 1.2, HIV has a lipoprotein envelope derived from the membrane of the target cell, which exposes to its surface glycoproteins (gp120), that are anchored in the virus through interactions with transmembrane glycoproteins (gp41) [147]. In addition to these proteins, there are others that are also derived from the host cell membrane during the virus entry process in the cell, which are Principal Histocompatibility Complex antigens, actin and ubiquitin [9]. HIV has a structural matrix consisting of matrix proteins (p17), viral capsid (p24), nucleocapsid (p7), which involves both copies of the viral genome and p6 [44]. PR, RT and IN are present inside the capsid. The HIV genome is also responsible for encoding the regulatory proteins Tat (transcriptional transcriptivator) and Rev (transcriptional regulator of the viral gene), as well as the accessory proteins Vpr, Vpu, Nef and Vif. These proteins are important for the viral

transcription process and, consequently, for host pathogenesis [44].

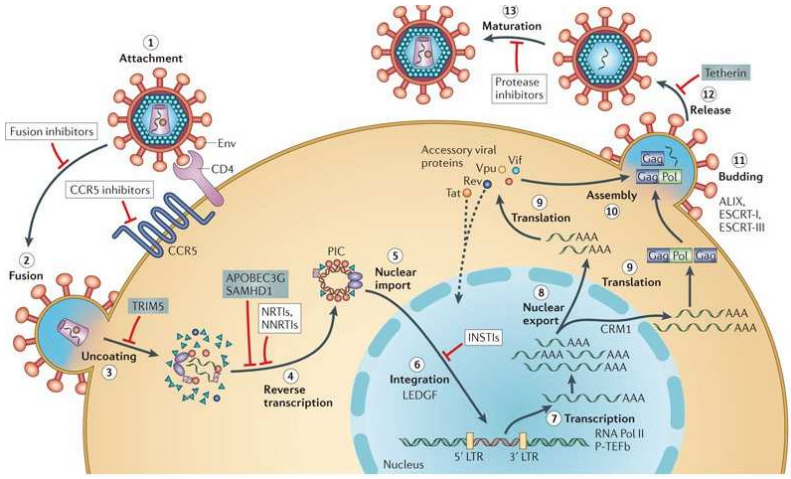

Figure 1.3: Schematic overview of the HIV-1 replication cycle [39]

As shown in Figure 1.3, viral replication begins with the specific binding of HIV virus particles to cells which have, on their surface, CD4 type receptors, a protein that has immune function. This binding occurs through specific interactions between the viral envelope glycoproteins (gp120) and the amino-terminal immunoglobulin domain of CD4, which is essential for the binding, but not sufficient for the infection. The HIV virus requires an additional surface protein present in the host cell for fusion between the viral envelope and the host cell membrane. These proteins are the co-receptors CCR5 (β-chemokine receptor) and CXCR4 (α-chemokine receptor), which direct fusion between membranes [82]. Initially, the gp120 molecule binds to the CD4 molecule, present in the membrane of the target cell. This molecular interaction generates conformational changes in the gp120 molecule, exposing new binding sites, thus allowing the molecular interaction between gp120 and co-receptors CCR5 or CXCR4. Such interactions lead to modifications in the conformation now in the gp41 molecule, exposing a hydrophobic region called fusion peptide. The later is inserted into the cell membrane allowing its fusion with the viral envelope [44]. After this fusion, the viral capsid is introduced into the cell cytoplasm, being digested and thus releasing the viral genome associated with the viral enzymes PR, RT and IN. These enzymes become active, thus initiating the viral replication cycle [44]. Viral RNA is transcribed by the RT enzyme, firstly by forming a hybrid RNA/DNA molecule, which will then give rise to a double-stranded linear DNA molecule [143]. RT is a multifunctional enzyme that exhibits both DNA and RNA-dependent DNA polymerase as well as ribonuclease H (RNase H) activities. RNase H acts on the formation of the hybrid RNA/DNA molecule, through the specific cleavage

of viral RNA tape. This proviral DNA will be associated with the IN, MA, RT and Vpr viral proteins, forming a preintegration complex (PIC). This complex will be transported to the cell nucleus where it can be integrated into the genome of the infected cell [126]. Integration is an essential step in replication and hence persistence of infection [111].

HIV is associated with impairment and destruction of the immune system's response, mostly by depletion of $CD4^+$ T cells. HIV infects several types of these cells, but its primary targets are the $CD4^+$ T helper cells. The depletion of $CD4^+$ T cells may have destructive effects in immune regulation [96]. These include reduced antibody development capacity for new attackers, abnormal function of macrophages and decrease in production of chemical messengers [90]. Macrophages play a major role in adaptive and innate immune response [65]. However, their relevance for HIV transmission, propagation and pathogenesis is not yet completely understood [62]. This is mainly due to the variation of macrophages susceptibility to infection and capacity to actively replicate the virus, with the tissue localization and cytokine activity. Nevertheless, macrophages live longer and become good HIV reservoirs [112], preventing its eradication from the body.

Cytotoxic T cells (CTLs) are important players in the control of viral infections. Some results show that the level of viral load is determined by the efficacy of CTLs and that the degree of the response to viruses may influence the outcome of the disease. Nevertheless, there are viruses able to escape the host immune responses and establish persistent infections. HIV is one of those virus. In the acute (first) phase of HIV infection, the CTL response to HIV is mostly linked with the viral set-point, influencing the rate of HIV disease progression. In the chronic phase of the infection, CTL response is associated with the partial containment of HIV replication [13].

As shown in Figure 1.4, a typical HIV infection is, in the absence of treatment, characterized by three stages [107]. The first is the acute phase, where there is a spike in HIV load and a sharp decrease in the $CD4^+$ T cells count. Patients in this stage suffer commonly from fever, headaches, rash, pharyngitis. The second stage is the chronic phase, characterized by a dramatic drop in the viral load, approaching a quasi-steady state, and an increase in the CD4 cells count. This behavior is explained by the balance between virus production and clearance rates [158]. After the chronic phase, the acquired immunodeficiency syndrome (AIDS) takes place. In the later, the number of $CD4^+$ T cells declines steadily and the viral load increases rapidly. AIDS leaves the human body vulnerable to life-threatening opportunistic infections and cancers, such that is a deadly disease in untreated patients. In these cases, time since initial infection till death is approximately 9-10 years.

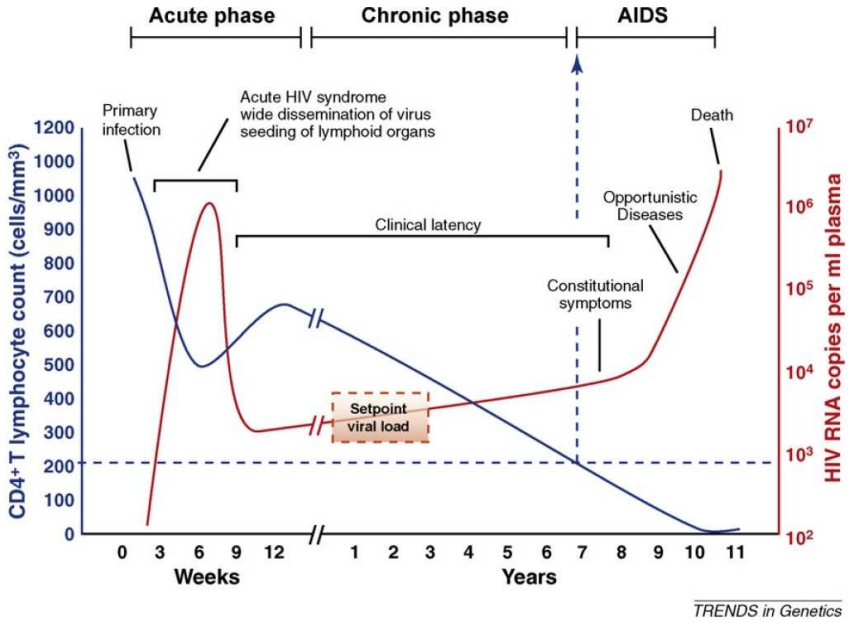

Figure 1.4: Time course of HIV infection [7]

Treatment for HIV/AIDS relies in antiretroviral therapy (ART) that suppress HIV viral load below the limit of detection (50 copies mL^{-1}), particularly if initiated in early stages of the infection. The major five drug classes to fight HIV/AIDS are the reverse transcriptase inhibitors (RTIs), the protease inhibitors (PIs), the fusion/entry inhibitors (FEIs), the integrase inhibitors (IIs), and the multidrug combinations. RTIs prevent the transcription of RNA virus into a complementary DNA sequence, blocking the viral genome to become incorporated into the host DNA. PIs hamper the ability of the viral protease to cleave viral polypeptide into functional enzymes, thus interfering with continued infection. FEI interfere with the ability of the virus to bound to the cell membrane. II block the introduction of virus genetic material in the host DNA. Finally, MI combine distinct drugs of the above classes in order to avoid resistance from virus strains to specific antiretroviral drugs. The later is known as highly active antiretroviral therapy (HAART). Drug-resistance is associated with high virus replication and mutation rates, poor adherence to therapy, or poor absorption and pharmacokinetics [154].

HAART may not be effective for certain patients. There are evidence of virus persistence during treatment, or of viral load rebounds shortly after ART interruption [50, 79]. The existent virus reservoirs, in the form of latently infected $CD4^+$ T cells, and infected macrophages and dendritic cells, are responsible for this phenomenon and make the eradication of HIV extremely complex. These cells are infected during the primary phase of infection and remain at a resting state. In the second phase of infection, several cells

contribute to plasma virus, namely the long-lived HIV infected cells (e.g., macrophages), the latent cells, and the release of virus from tissue sources (e.g. lymphoid tissue). Latently infected cells take 6 to 48 months to be activated [110, 129]. Never thought, the significant advances in the development of ART that effectively fight HIV, currently HIV infection is considered a chronic disease. This means that it has no cure, but is treatable. In addition, ART prevents onward HIV transmission. Other forms of HIV transmission prevention are the treatment as prevention (TasP), the pre-exposure prophylaxis (PrEP), the post-exposure prophylaxis (PEP) and HIV counselling and testing (HCT).

TasP uses antiretroviral treatment in HIV prevention programs to reduce the risk of HIV transmission. The treatment reduces the HIV viral load in the body to such low levels that it remains undetectable. This viral suppression leads to these individuals not transmitting HIV. Thus the effectiveness of ART as a prevention tool can be used as a strategy for intervention in public health

PrEP consists on the intake of HIV medicines daily, by people that are at very high risk of being infected with HIV. PrEP acts by halting HIV spread in the body. The risk of getting HIV in sexual intercourse is reduced by 90%. In injecting drug users, it decreases to 70%. PrEP is effective only when following treatment guidelines thoroughly [87]. In 2015, the World Health Organization (WHO) recommended that at-risk populations should be given PrEP as an additional prevention choice [93].

PEP is an ART drug treatment, started immediately after exposure to HIV. One study showed that PEP has little or no effect on the prevention of HIV infection if it is initiated later than 72 hours after exposure to it. PEP is effective in HIV prevention when administered correctly, but not at 100%. Therefore, it does not replace the regular use of other HIV prevention methods, such as PrEP. This treatment is intended to prevent the survival and multiplication of HIV in a person's body, protecting against being exposed to HIV again and reducing the chances of HIV transmission [87]. WHO recommends the use of PEPs for occupational and non-occupational exposures for adults and children [93]

HCT is an important part of an integrated framework for HIV prevention. Knowing one's HIV status is critical to prevent the spread of HIV and access counselling and medical care [87]. Nevertheless, nowadays HCT is limited since 40% of the people living with HIV worldwide are unaware of their status [93].

People infected with HIV are at a higher risk of developing cancer. It is expected that 30% to 40% of HIV-infected people will develop some type of malignancy. Moreover, clinical courses of cancers in HIV-positive individuals are much more aggressive than in HIV-negative ones. The malignancies are of two types: AIDS-related ones and non-

AIDS related ones. In the first type are included the Hodgkin's lymphoma, Kaposi's sarcoma and invasive cervical cancer. These are the majority of cancers affecting HIV/AIDS infected individuals. The second type, aka opportunistic cancers, also affect the HIV-infected people but are not directly associated with AIDS. Examples of the later are: Hodgkin's disease, anal cancer, lung cancer, testicular tumours.

Though some controversy still exists on attributing an oncogenic role to HIV, it is consensual that it fuels tumour growth. Distinct factors may contribute to the development of these AIDS-related and non-related cancers, namely impaired immune surveillance, inability to fight genomic instability, dysregulation of cytokine pathways, cellular proliferation and differentiation imbalance [83].

1.1 Mathematical models in epidemiology

Epidemiology studies, among others, the incidence of transmissible diseases in large populations. Over the years, the epidemiologists applied statistics to describe their data and formulate their hypothesis. The classic epidemiology is highly associated with the description of the number of disease cases per thousands of inhabitants, per geographical area, and/or per unit of time. This description can consist of simple bar charts, mapping techniques or even in sophisticated multivariate analysis methods. In the last decades, there were also significant developments in the understanding of the transmission of epidemic diseases in large populations, based in the application of mathematical models. The conclusions drawn from these models are extremely important in the conception of control programs and strategic interventions in developed and developing countries.

The infection, pathology and symptomatology of most human infectious diseases is reasonably understood. This knowledge, however, is not enough to predict how the diseases will propagate in a large population. For that, it is necessary to consider factors that considerably complicate the investigation. These factors are related to the biology of the infectious agent (lifecycle, vulnerability to climate factors), the demographic features of the population to be infected (infected mortality of infected and non-infected, age, spatial distribution), behavioural aspects (contact rates among individuals, hygiene) and, of course, possible control measures (vaccination, isolation of infected, distribution of condoms and syringes, amongst others). The complexity of the problem makes it impossible to make predictions for the course of an epidemic, based only on intuition. On the contrary, it is necessary to integrate all the relevant information effectively and

this can be done using mathematical models.

Mathematics offers appropriate tools to express complex relations, in a way that makes it relatively easy to evaluate their consequences. Thus, mathematics offers a concise and powerful way to expose exactly the factors that determine the epidemiology of the diseases.

The mathematical models often used to describe the dynamics of a disease are of compartmental type. Namely, the population is divided into categories or compartments. These compartments translate the way an individual gets infected and show how the infection spreads. In a very large population, the movement of individuals between compartments may be considered a continuous phenomenon. Therefore, it is possible to represent mathematically the variation of the number of individuals within each compartment, 'as time goes by', by systems of differential equations. These systems of equations may have useful analytical solutions, but, when the model has a minimum of realism, this rarely happens and it becomes necessary to implement computationally tools.

The first compartmental model was introduced in 1864 by Guldberg and Waage [127]. It is the SIR (Susceptible - Infected - Recovered) model. In 1911, Ross [119] analysed the dynamics of malaria through the mosquito-borne pathogen transmission. Ross, Kermach and McKendrick continued to work and founded the field of deterministic compartmental epidemic modeling in 1927 [58].

Chapter 2

Literature review

This chapter, contains the state-of-the-art in modeling of HIV/AIDS dynamics and relevant coinfections (HIV and HCV, HIV and TB). There are many more modeling papers than could be reviewed here. Nevertheless, are highlighted only a few which were considered to be more relevant for the theme/development of the thesis.

2.1 HIV

Throughout the years, mathematical models have contributed to a better understanding of the mechanisms behind the immune response against HIV [98].

2.1.1 Within-host models

In 1996, Perelson *et al.* [97] studied a model for viral load data, collected from infected patients, after administration of a PI. They calculated the lifespan of productively infected cells and of plasma virions, the virions production rate, and the HIV-1 generation time (namely, the intracellular delay from the time virions are released until they infect another cell, and cause the release of new viruses). Spouge *et al.* [134] described two models for HIV dynamics, considering virus-to-cell transmission in one model and cell-to-cell transmission in the other. The authors concluded that both models show similar asymptotic behaviors, using realistic parameter regimes. In 1998, Wein *et al.* [159] presented a mathematical model to predict the role of drug regimens, based on combinations of PIs and RTIs, in the eradication of HIV-1 or in the maintenance of low viral loads. The

model included the CD4^+ T cells, macrophages (as long-lived cells) and sensitive and resistant virus. From the model the authors infer that the behaviour of the cells and virus, and the eradication of the virus, are dependent on the strength of the combined therapy against the mutant strain and the maximum achievable increase in the uninfected CD4^+ T cell concentration. Under certain conditions, the model suggests that a successful formula to control HIV infection would be to start with a strong inductive therapy to reduce viral load, and proceed with a weaker maintenance regime. In 2000, Arnout *et al.* [8] concluded that during the administration of antiretroviral drugs, priming the CTL response can lead to better immune responses from the patients. Viral load decreases rapidly when CTLs are abundant and less quickly otherwise. In 2005, Jones *et al.* [56] used mathematical models to show that the amplitude and duration of the viral blips, in well-suppressed chronically infected HIV patients, under HAART, can be generated by opportunistic infections. In 2006, Asquith *et al.* [10] analysed multiple sets of HIV data and estimated that only 2% of infected CD4$^+$ T cells is due to CTLs, recognising only one epitope. The authors suggested that CTLs are responsible for the killing of a considerable number of infected T helper cells, but nonetheless the majority of infected cells are killed by other cells of the immune system. Kim and Perelson [59] studied the persistence of the latently infected cells and low levels of plasma virus in HIV-infected patients. Simulations of the model revealed that the intrinsic stability of latently infected resting memory CD4^+ T cells is the key factor to their long-term persistence. The role of ongoing viral replication to the stability of the latent reservoir is meaningless. The presented model is also used to assess the contribution of long-lived infected cells to plasma virus. It is found that these cells have a significant contribution to plasma virus only in the first few months of therapy, when the viral load is above 50 copies/ml. In 2007, Wodarz *et al.* [162] showed that HIV virus ability to infect CD4$^+$ T cells induces the dynamics of HIV infection. Moreover, infected CD4$^+$ T cells spread fueled the virus spread at higher virus loads, and it supplied a protection of infected cells during drug therapy. In what concerns vaccination, a larger number of CD4$^+$ T cells might be beneficial to the virus, if CD8^+ T cells were not boosted at the same time. As a consequence, vaccination might precipitate disease progression rather than prevent it [135]. In 2009, Weng *et al.* [161] studied a model that includes virus-to-cell and cell-to-cell transmissions. They demonstrated that cell-to-cell transmission is crucial for the dynamics of HIV infection and it is much more important than virus-to-cell transmission. Hadjandreou *et al.* [48], proposed a model for long term HIV dynamics, subjected to continuous and structured treatment interruptions (STI). Their results showed that an optimized scheduling, where the interplay between the two virus strains (drug-resistant and drug-susceptible) is facilitated, favors better responses from the patients. Opti-

mized STI is thus promising in patients that have developed strong drug-resistance, and for whom continuous therapy fails. In 2011, Sigal *et al.* [128] verified that cell-to-cell transmission can adversely affect the immune system, leading to treatment failure in individuals with risk factors and potentially contribute to viral persistence. In 2012, Roy *et al.* [120] proposed a model for the patterns of HIV and $CD4^+$ T cells, assuming the existence of two helper cell clones, directed against epitopes of the virus. The model predicted that a stronger helper cell clone could exclude a weaker one, since the two clones were infected by the same pathogen. On the other hand, if one of the helper cell clones was too weak to become established in isolation, the presence of a stronger one provided enhanced antigenic stimulation, allowing the weaker clone to persist. Chan *et al.* [25] studied a model for primary and secondary CTL response cells. The model exhibits rich dynamics and the authors observed oscillatory patterns for a wide parameter range. In 2013, Titanji *et al.* [145] determined that protease inhibitors are more efficient in blocking cell-to-cell spread of virus than transcriptase inhibitors. They also found that the efficacy of ART is dependent on the multiplicity of infection. Komarova *et al.* [61] showed that virus-to-cell and cell-to-cell transmission contribute approximately equally to the growth of the virus population. Hernandez-Vargas and Middleton [52] developed a model for the three stages of HIV infection. They concluded that macrophage population plays a key role in the progression to AIDS. In 2014, Li *et al.* [66] studied a mathematical model which describes the dynamics of HIV under treatment. The model exhibits a backward bifurcation and the bistability accompanying it may explain the sudden recovery of the viral load, when treatment is interrupted, and the occurrence of viral blips. In 2015, Agosto *et al.* [3] suggested, based on experimental data, that most ART regimens are effective in blocking cell-to-cell virus transmission and preventing $CD4^+$ T cells depletion. They argued that efforts are to be applied in better understanding HIV pathogenesis *in vivo*, in order to develop smarter ART regimens. The later would alleviate the treatment burden of people living with HIV. In 2016, Carvalho *et al.* [22] proposed a model for the dynamics of HIV under distinct HAART regimes, and study the emergence of drug-resistance. The model is simulated for two distinct HIV patients, the RP and the LTNP. The effects of equal RTIs and PIs efficacies, as well as distinct drug efficacies, namely RTI-based and PI-based therapeutics are studied. The PI-based drugs seem to produce better outcomes, with respect to disease progression, than RTI-based regimes. Wang *et al.* [155] compared the effect of different categories of drugs on the dynamics of the viral load. The authors concluded that when treatment is 100% effective, drugs acting later in the viral replication cycle lead to a rapid decline in the viral load. On the other hand, for a non-100% effective treatment, the drugs acting at intermediate stages of the viral load cycle, induce multiple viral load declines, lowering

also its slope. Lorenzo-Redondo *et al.* [68], proposed a spatial and dynamic model to explain the mechanism behind viral rebound in suppressive HIV patients. The model simulates the dynamics of viral replication subjected to drug-concentration and HIV spread among two spatially distinct compartments of the body. The larger compartment has a high effective drug concentration, the smaller has a lower drug concentration and may be seen as a sanctuary inside the lymphoid tissue. The authors concluded that spatial and dynamic processes contribute to the persistence of HIV-1 within infected cells and prevent drug-resistance even under ART. Thus, the viral reservoir is maintained by the sanctuaries inside lymphoid tissues, where drug concentration is low. These sanctuaries also promote HIV traffic to blood or lymphoid tissue. In 2017, Carvalho *et al.* [23] studied the contributions of within-host (virus-to-cell) and synaptic (cell-to-cell) transmissions in a mathematical model for human immunodeficiency virus dynamics. The cell-to-cell transmission rate has a considerable impact in the value of the reproduction number. This is consistent with biological findings of HIV dynamics in vivo, where at the level of the lymph nodes, cell-to-cell transmission is crucial for the development of the disease.

Time-dependent drug regimens have also been considered in the literature. In 2010, Yang *et al.* [163] analysed a HIV time-dependent model, where drug efficacy changes periodically. They proved that the disease-free equilibrium is stable for a threshold parameter less than unity and unstable for values greater than one. In this case, the model depicts a globally asymptotically stable periodic solution. In 2012, Browne *et al.* [18] considered the effects of the periodic forcing of threshold drug efficacies on the disease-free equilibrium of an HIV infection model. The authors considered two time scales, a larger one for the STIs, and the small one for the daily drug dosages. It was shown that in the first, varying the phase difference between the RTI on-days relative to PI on-days, significantly impacts the treatment results. For small time scales, optimization of the timing between daily dosages of RTI and PI may induce greater treatment effectiveness.

Some of these models include time delays, namely the time needed for infected cells to produce new virus, and the delay in the stimulation of the immune response. In 2006, Ciupe *et al.* [28] modeled the dynamics of the primary HIV infection and the beginning of the latency phase, considering a delay in the CTL response. This delay leads to the appearance of periodic solutions, through a Hopf bifurcation. These oscillations describe the rapid rotation between viral strains and the CTL response, needed to control the infection. In 2009, Ouifki *et al.* [95] proposed a model for HIV-1 infection that included reverse transcriptase inhibitors and three intracellular delays. Authors

observed that introducing delays promoted the appearance of Hopf bifurcations, translated in the model as periodic orbits around the endemic equilibrium. These solutions were consistent with the viral blips seen in HIV patients data. In 2013, Pitchaimani *et al.* [107] studied a model for HIV-1 infection that includes protease inhibitor therapy and three intracellular delays. They showed that the delays reduce the number of infected cells and viruses at the HIV endemic equilibrium, thus lowering the critical efficacy of the PI regimen needed to eliminate the virus. In 2014, Wang *et al.* [156], proposed a model for drug-resistance, that includes intracellular delay and a general form of target cell density, during ART. Authors obtained sustained oscillations, promoted by variation of the T cells growth rate, in a biologically reasonable parameter space. This finding suggested the viral strains rapidly turn over and any successful ART regimen should take this into consideration. Pinto *et al.* [99] studied a model for HIV dynamics in HIV-specific $CD4^+$ T cells, including intracellular delays. The authors argued that a good strategy to control HIV should focus on drugs to prolong the latent period and/or slow down the virus production. In 2016, Huanga *et al.* [55] presented a model for HIV infection with treatment and delayed immune response. They concluded that the higher the delay, the higher the amount of virus and infected T cells in the body and the frequency of oscillations. Prakast *et al.* [109] studied a model for macrophages infection by HIV that includes CTL. The authors concluded that the inclusion of the delay may destabilize the solutions of the model. This could help devise new treatment options.

In the last few years, several mathematical models have been developed to study tumour growth in the presence of HIV [73, 71, 69, 70, 136]. In 2006, Pillis *et al.* [35] proposed a mathematical model to describe cancer growth, on a cell population level, with combination immune, vaccine and chemotherapy treatments. Simulations of the model suggest that neither chemotherapy nor immunotherapy alone are sufficient to control tumour growth, and a combination of the two therapies is able to eliminate the entire tumour. In 2013, Rihan *et al.* [113] developed a delay mathematical model to describe the interactions between a tumour and the immune system in the presence of HIV. The time delay plays an important role in the dynamics of the model, affecting the stability of the disease-free steady state. The delay model is consistent with biological findings. In 2014, Louzoun *et al.* [72] studied a mathematical model of pancreatic cancer. The model shows that tumour growth depends on complex feedback loops between the tumour cells, endothelial cells and the immune response. These loops set the cancer growth rate and its response to immunotherapy. If the immune system is weakened, as in the case of HIV-infected patients, then cancer treatment is not effective.

2.1.2 Epidemic models

In the last decades, researchers have tried to understand the long-term dynamics of HIV epidemics, in order to help devise better HIV prevention programmes nationwide and worldwide. In 2011, Nyabadza *et al.* [85] developed a deterministic model, that incorporated the use of condoms, screening (HCT) and treatment, to infer the impact of HCT in the long-term dynamics of HIV infection. HCT reduced the prevalence of HIV only when the screening campaign efficacy exceeded a given threshold. In 2013, Abbas *et al.* [1] studied ART and PrEP impacts, with overlapping and non-overlapping antiretroviral drugs, on HIV transmission and drug resistance. They concluded that the combination of ART and PrEP prevents more HIV infections than any strategy alone. On the other hand, it may increase drug resistance. In 2017, Simpson *et al.* [132] proposed a deterministic model to assess the impact in an MSM-population of the use of PrEP on the dynamics of HIV disease transmission. Simulations of the model revealed that, at the current rate of administration of ART to HIV patients, the HIV viral load decreases with increasing use of PrEP. Pinto *et al.* [104] assess the impact of HIV prevention strategies, namely PrEP and HCT, in a model for the dynamics of HIV. It is observed that the reproduction number is extremely impacted by the efficacy of the screening and not by the screening rate. This means that future measures to prevent HIV/AIDS transmission should also focus on explicit campaigns highlighting the importance of the screening efficacy. The model without PrEP was fitted to data on the cumulative HIV and AIDS cases in Portugal. This could help policy makers to devise strategies to reduce heavy economical and social burden of HIV infection in Portugal.

2.2 HIV and HCV

HIV and HCV share the same transmission routes, namely by injection drug use, sexual contact, mother to child transmission during pregnancy or birth, blood and blood products transfusion, organs transplantation from infected donors, exposure to blood by health care professionals [6, 138].

Typically, the coinfection of HIV and other diseases is associated with more serious risks and severe consequences for patients. In the coinfection with HCV, HIV accelerates the progression of HCV, moreover, the risk of severe liver disease is higher if the CD4 count falls below 200 cells/mm3 [47]. In addition, there is a higher risk of cirrhosis, end-stage liver disease, hepatocellular carcinoma and liver-related death [144]. In Portugal,

end-stage liver disease is, after tuberculosis, the second leading cause of death among HIV-positive people [47].

The current international consensus, to control the HIV epidemic, focuses on the need for clear leadership on policies and programs for prevention, early diagnosis, treatment that respects human rights, and quality of health care, effective and accessible to everyone. In what concerns coinfection, some successful treatments for HCV using drug combination in individuals coinfected with HIV have been reported. Furthermore, most people with HCV can be treated successfully for HIV [43]. However, more studies are needed to show the efficacy of new antiviral drugs for HCV in people coinfected with HIV.

HIV and HCV infections are major global public health issues. There are 37 million people infected with HIV worldwide, and about 115 million people HCV antibody positive [93]. One-third of HIV-infected patients are infected with HCV [51]. People coinfected with HIV and HCV are more prone to a faster development of HCV infection [51], presenting higher HCV viral loads, and are more efficient in transmitting HCV [108]. Moreover, the spontaneous elimination of HCV is also decreased in untreated HIV coinfected patients [108]. One of the leading causes of death in HIV treated coinfected patients is chronic HCV infection [142], due to drug related hepatoxicity. Chronic infection results in a large number of deaths annualy due to cirrhosis and hepatocellular carcinoma. Moreover, liver transplants, for HCV induced liver disease patients, are a major part of health care costs [137]. On the other hand, there is evidence that treatment for HIV can slow the natural progression of HCV infection and reduce HCV mortality related to liver diseases [51].

In Portugal, it is estimated that about 25% to 40% of the 41.086 people infected with HIV are coinfected with HCV [47]. Portugal is the third country, of Western Europe, with higher prevalence and more new diagnosed cases of HIV/AIDS, per year.

In the last few decades, mathematical models have been applied in the literature to the modeling of infectious diseases. HIV and known coinfections epidemiologies are the research topic of some of those models. In 2008, Vickerman *et al.* [153] proposed a transmission model for HCV/HIV coinfection, aimed at evaluating the cost-effectiveness of needle and syringe programs for injecting drug users (IDUs). They concluded that although the needle/syringe sharing events were defined as low risk in Rawalpindi, the prevalence of HIV/HCV in IDUs would increase. They emphasized the importance of intervention measures in that low prevalence setting, in order to prevent the HIV/HCV prevalence. Recently, in 2011 [152], the authors used a mathematical

model to understand the trends in the prevalence of HIV and HCV. They determined the different epidemiological profiles and how these profiles affect intervention impact. They concluded that there were threshold levels of HCV prevalence below which HIV risk was negligible. Nevertheless, these thresholds varied by setting. The authors infered that HIV and HCV prevalence settings could provide new insights into IDU risk behaviour and intervention impact. In 2012 [36], the authors proved that HCV prevalence could be used as an indicator of risk for successful HIV infection, in an IDU population. In [157], the authors formulated a mathematical model for HIV/AIDS treatment, where vertical transmission from mother to child was included. It is shown that HAART and control of vertical transmission rate were associated with a reduction of the HIV transmission. Alexander *et al.* [5] proposed a model for drug resistance in patients with a chronic viral disease, such as HIV or HCV. They derived dependencies between the parameters of the system that are important factors in driving drug resistance. Rong *et al.* [117] presented a mathematical model of two virus strains, one sensitive and one resistant, to HCV drugs. They provided a theoretical framework to explore the prevalence of pre-existing mutant variants and the evolution of drug resistance during HCV treatment. In 2013, Bhunu *et al.* [16] studied a mathematical model for HIV and HCV coinfection, that includes treatment for both diseases. The model predicted that HCV had an ongoing prolonged negative effect on the population health, irrespective of their HIV status. The authors infered that specific measures to control HCV should be taken/reinforced in resource limited settings. Corson *et al.* [32], proposed a mathematical model to explore the risk of HCV infection through the sharing of injecting paraphernalia (including filters, cookers and water). Namely, the sharing of injecting paraphernalia among IDUs is common, thus, HCV transmission through this route could contribute to the growing burden in healthcare systems associated with it. The authors infered that more work was needed to detail the contribution of the paraphernalia sharing to the spread of HCV, and that health care providers should distribute sterile paraphernalia to prevent HCV infection. In 2014, Carvalho *et al.* [21] studyed a mathematical model for HIV and HCV coinfection, that includes treatment for both diseases, and vertical transmission in the case of HIV. The outcomes suggest that specific measures should be considered, by the policy makers, in order to reduce HIV infection, such as: distributing more condoms to individuals; develop campaigns in order to warn individuals about the consequences of having many sexual partners; continuing treatment for AIDS and pursuing the investigation of new and better drugs to combat HIV, treat new borns infected with HIV and advise pregnant women for the benefits of HIV treatment. Considering HCV infection, treatment is highly recommended as well as other measures (e.g., more informational campaigns about the disease, its transmission routes, amongst others) in order to

decrease the number of infectious and of chronic carriers. Pinto *et al.* [101] developed a new a coinfection model for HCV and HIV, in which it was considered treatment for both diseases, screening, unawareness and awareness of HIV infection, and the use of condoms. The results obtained suggest that specific measures should be considered in order to reduce HIV infection, such as: distributing more condoms to individuals and try to forward the message that condoms should be used during anal intercourse (though this might not be well accepted in MSM population due to unprotected sex negotiation); develop campaign in order to warn individuals about the consequences of having many sexual partners; continuing treatment for AIDS and pursuing the investigation of new and better drugs to combat the virus and regular screening. MSM population is at risk of HCV reinfection following successful treatment and documented clearance of HCV, they should be warned about this important risk. In 2015, Birger *et al.* [17] improved an existing model for HCV infection to include the dynamics of the HIV and HCV coinfection, where an immune system component for infection clearance is incorporated. They found that the progression of HCV infection is more rapid when the immune response is compromised by HIV. A better understanding of the mechanisms behind this immune impairment in coinfection may help to devise better therapeutic regimens and to identify patients more compliant to certain drugs.

2.3 HIV and TB

TB is an infectious disease caused by the bacteria *Mycobacterium tuberculosis* (MTB). It is transmitted through droplets, when people suffering from pulmonary TB expel bacteria, for example, by coughing. In general, a relatively small proportion of people infected with MTB develops active TB, but this proportion is much higher in people with impaired immunity.

The incidence (number of new cases in the population per year) of TB found in various regions of the globe ranges from almost zero to more than 600 cases per 100 000 persons per year. A significant contributing factor to these rates is the phenomenon of exogeneous reinfection. Exogeneous reinfection has, thus, a determinant role in the dynamics and the epidemiology of TB [26, 80, 41, 60]. The transmission of TB differs from other infectious diseases. Approximately only 10% of the infected individuals develop active TB. Most people's immune response to the initial infection limits proliferation of the bacilli and leads to partial immunity. Apparently, the longer the bacilli is in the organism, the less likely people are to develop active TB (unless the immune system

becomes seriously compromised by other diseases, such as HIV/AIDS). Nevertheless, re-exposure to the bacilli through repeated contacts with infectious TB individuals may accelerate the progression to active TB. The phenomenon of exogeneous reinfection is driven by the condition that the risk of a second disease causing infection for a person, who has recovered from a TB episode, is about $7(\pm 4)$ times greater than the risk of a first-time infection that leads to disease [148]. This estimate is in close agreement with actual minimum estimates based on data from a high TB incidence community [151], where the risk of developing a second episode of TB after infection was estimated to be $4 - 7$ times higher than a first episode.

In 2010, there were an estimated 8.8 million new cases of tuberculosis, approximately 13% of which occurred in people living with HIV. In 2010, an estimated 1.1 million HIV-negative people died from tuberculosis, while an additional 0.35 million died from HIV-associated tuberculosis. Since 1990, mortality due to tuberculosis has fallen by just over one third. Treatment of TB is achieved through antibiotics. Treatment takes at least six months and is increasingly hampered by multidrug-resistance. There are 6 types of multidrug-resistant TB [94]. The treatment for TB has had a success rate of 87% worldwide. In EU/EEA this sucess rate drops to 74.3% [42]. Treatment success had been achieved in 76.8% of new pulmonary TB cases, 53.7% of previously treated cases, and 31.6% of multidrug-resistant TB cases. Some first-line drugs used to treat TB are rifampcin, isoniazid, pyrazinamide, ethambtol. The second line drugs includes amikacin, capreomycin, cycloserine, azithromycin, clarithromycin, moxifloxacin, levofloxacin. The exposed individuals are treated with isoniazid.

Resurgence of TB in the 1980's is attributed jointly to the emergence of multi-drug resistant strains (MDR-TB) and the AIDS pandemic, which led the WHO to declare TB as a global emergency in 1983. MDR-TB and, more recently, extensively resistant TB (XDR-TB), jeopardize TB control, and rise concerns of a future of non-effective drugs [46]. In 1993, the WHO declared TB a global emergency by its overall size and consequences, namelly its association with HIV/AIDS, and the emergence of multidrug-resistance. The Global Plan to Stop TB [94] indicates the goals to be achieved in the 'war' against TB. Some of these goals are to determine strategies and costs associated with multidrug-resistant TB, reduce consequences of coinfection with HIV, to aid laboratories to develop research on TB in a consistent and coordinated way, amongst others.

TB and HIV exhibit a kind of synergistic relationship, where each accelerates the progression of the other. In coinfected individuals, TB causes cell activation and excessive cytokine and chemokine productions. The later stimulates HIV replication and accelerates the progression to AIDS. On the other hand, HIV increases twenty times the

odds of TB reactivation and increases the risk of infection by MDR-TB of MTB, since it expands the number of individuals with active TB [75, 93]. Moreover, it may contribute to selection for spontaneous mutations. Factors worsening this scenario are the lack of treatment adherence due to excessive pill burden, the treatment toxic effects, and/or the communication gaps in HIV and TB treatment programs [46].

TB is nowadays one of the 10 top causes of death worldwide. Moreover, in 2015, 35% of HIV infected individuals deaths were due to coinfection with TB, making TB a leading killer of HIV-positive people [93]. Dual infection with HIV and TB contributes heavily to the morbidity and mortality associated with TB. In comparison, there is a 20-fold higher risk of individuals infected with HIV to develop tuberculosis, when compared to those without the HIV virus, in countries where HIV prevalence is at least 1% [94]. The HIV/AIDS pandemic plays an important role in the resurgence of TB, increasing morbidity and mortality worldwide. It decreases the TB latency period, accelerating active disease in people infected with MTB. Namely, an HIV-positive person infected with MTB has a 50% chance of developing active TB, whereas an HIV-negative person has only a 10% chance of developing it [81]. These high figures may be justified by the late diagnosis of TB in HIV infected individuals, or of HIV in individuals infected with TB. Even when diagnosed, this occurs in a very late stage of the disease [49].

Several mathematical models have been derived with the purpose of understanding the dynamics of HIV, and TB, and of the coinfection [130]. In 1997, Castillo-Chavez *et al.* [24], formulated a model for TB where it is possible to determine the survival and spread of naturally resistant strains of TB and resistant strains of TB generated by antibiotics. They concluded that the coexistence of the two strains only occurs in treated individuals and results from the lack of adherence to treatment. In 2006, Cohen *et al.* [29] proposed a mathematical model for TB and HIV co-infection and examine the impact of community-wide implementation of IPT for dually infected individuals. They found that diagnostic and specific treatment policies together with community-wide IPT should be implemented to identify and properly treat the increasing number of individuals drug-resistant to TB. In 2007, Rodrigues *et al.* [115], proposed a model for TB infection, where the dynamics of the drug-resistant and sensitive strains are studied. The long-term behavior of the model reflects how reinfection modifies the conditions for the coexistence of the strains. In 2009, Roeger *et al.* [116], introduced a highly simplified deterministic model that incorporates the joint dynamics of TB and HIV. They observed that increasing the progression rate from latent to active TB in co-infected individuals might play a significant role in the rising prevalence of TB, and the increased HIV to AIDS progression rates translated in an increase of the prevalence level of HIV, while

decreasing TB prevalence, and generated damped oscillations in the system. In 2011, Bhunu [14] studied a mathematical model to evaluate the impact of active treatment of TB (multi-drug sensitive and resistant) in controlling the spread of TB. The results of the analytical and numerical simulations suggest that the quarantine of extensively drug resistant cases will help reduce the spread of tuberculosis. In 2012, Sergeev *et al.* [124] explored the effect of HIV on the dynamics of MDR-TB. An increase in the HIV viral load in coinfected individuals increases the prevalence of MDR-TB within populations. This occurs even as it lowers the average fitness of circulating MDR-TB strains, when compared to similar HIV uninfected populations. Gakkhar and Chavda [45], developed a mathematical model for HIV and TB co-infection. They computed the reproduction numbers of the two diseases. They computed the stability of the disease free equilibrium and of the endemic equilibrium. Authors suggested, as the endemic equilibrium is unstable, that co-infection is not long lasting. In 2014, Trauer *et al.* [146] developed a mathematical model for TB that includes the partial and temporary efficacy of the vaccine, reduction of the risk of active disease after infection, the possibility of reinfection, during the latency period of the infection or after treatment, multidrug-resistant tuberculosis and resistance during treatment. They concluded that improving the treatment of susceptible individuals increases multidrug-resistant tuberculosis. In 2016, Mallela *et al.* [76], studied the effect of early and late HIV treatment in coinfected individuals receiving treatment for TB. The model suggests that the coinfection burden depends highly on the timing of the initiation of ART. Ronoh *et al.* [118] included resistance to tuberculosis in a standard SEIRS model. They found that in the case of patients with active tuberculosis and multi-resistant tuberculosis with both strains, the disease will persist due to lack of permanent immunity. In 2017, McBryde *et al.* [77] studied a mathematical model for tuberculosis and considered multi-drug resistance. In their analysis, they determined that without a renewed focus on prevention, early diagnosis and treatment of multi-resistance cases, TB transmission will be dominated by MDR-TB, which could divert progress towards global control of TB and final elimination.

2.4 Fractional calculus

Fractional calculus (FC) is a generalization of the integer order calculus. Lagrange and Leibniz were the first mathematicians exchanging letters about the possible meaning of a $1/2$-order derivative. They were the predecessors of non-integer-order differentiation and integration, also known as fractional calculus. Since then, the meaning and methods to compute $1/2$-order derivatives or, in general, α-order derivatives, with α non-integer,

has been a major research in mathematics. Some well-known mathematicians that have devoted their work to fractional differentiation and integration are Euler, Abel, Liouville, Riemann, Grünwald, Letnikov, Caputo, amongst others [91, 122].

There are several definitions for a fractional order (FO) derivative. For simplification, consider the interval $[0, t]$ as an index in the differential operator. Suppose that the function $f(t)$ satisfies some smoothness conditions in every finite interval $(0, t)$ with $t \leq T$. The Riemann–Liouville definition is given by:

$$D_{\star}^{\alpha} f(t) = \begin{cases} \frac{1}{\Gamma(m-\alpha)} \frac{d^m}{dt^m} \int_a^t \frac{f(\tau)}{(t-\tau)^{\alpha+1-m}} d\tau, & m-1 < \alpha < m \\ \\ \frac{d^m f(t)}{dt^m}, & \alpha = m \end{cases}$$

The Caputo's fractional derivative is defined as follows.

Definition 2.4.1 *[20] Let $\alpha > 0$, $t > a$, $\alpha,\ a,\ t \in \mathbf{R}$. The fractional operator*

$$D_{\star}^{\alpha} f(t) = \begin{cases} \frac{1}{\Gamma(n-\alpha)} \int_a^t \frac{f^{(n)}(\tau)}{(t-\tau)^{\alpha+1-n}} d\tau, & n-1 < \alpha < n \in \mathbf{N} \\ \\ \frac{d^n}{dt^n} f(t), & \alpha = n \in \mathbf{N} \end{cases}$$

The main advantage using Caputo's fractional derivative is that classical initial conditions can be used without encountering any problem during solvability. Now the main properties of the Caputo operator are revealed. It begins with interpolation.

Lema 2.4.2 *Let $n-1 < \alpha < n$, $n \in \mathbf{N}$, $\alpha \in \mathbf{R}$ and $f(t)$ be such that $D_{\star}^{\alpha} f(t)$ exists. Then:*

$$D_{\star}^{\alpha} f(t) = I^{n-\alpha} D^n f(t)$$

Lema 2.4.3 *Let $n-1 < \alpha < n$, $n \in \mathbf{N}$, $\alpha \in \mathbf{R}$ and $f(t)$ be such that $D_{\star}^{\alpha} f(t)$ exists. Then the following properties hold:*

$$\begin{aligned} \lim_{\alpha \to n} D_{\star}^{\alpha} f(t) &= f^{(n)}(t) \\ \lim_{\alpha \to n-1} D_{\star}^{\alpha} f(t) &= f^{(n-1)}(t) - f^{(n-1)}(0) \end{aligned}$$

The Caputo operator is a linear operator.

Lema 2.4.4 *Let $n-1 < \alpha < n$, $n \in \mathbf{N}$, $\alpha, \lambda \in \mathbf{C}$ and the functions $f(t)$ and $g(t)$ be such that both $D^{\alpha}_{\star} f(t)$ and $D^{\alpha}_{\star} g(t)$ exist. The Caputo fractional derivative is a linear operator, i.e.:*

$$D^{\alpha}_{\star}\left(\lambda f(t) + g(t)\right) = \lambda D^{\alpha}_{\star} f(t) + D^{\alpha}_{\star} g(t)$$

Generally, the Caputo operator is non-commutative.

Lema 2.4.5 *Let $n-1 < \alpha < n$, $n, m \in \mathbf{N}$, $\alpha \in \mathbf{R}$ and the function $f(t)$ is such that $D^{\alpha}_{\star} f(t)$ exists. Then in general*

$$D^{\alpha}_{\star} D^{m} f(t) = D^{\alpha+m}_{\star} f(t) \neq D^{m} D^{\alpha}_{\star} f(t)$$

Lema 2.4.6 *Let $n-1 < \alpha < n$, $\beta = \alpha - (n-1)$, $n \in \mathbf{N}$, $\alpha, \beta \in \mathbf{R}$ and the function $f(t)$ is such that $D^{\alpha}_{\star} f(t)$ exists. Then*

$$D^{\alpha}_{\star} f(t) = D^{\beta}_{\star} D^{n-1} f(t)$$

The algorithm used for the numerical solution of non-linear differential equations of fractional order is presented in [38]. This algorithm allows an efficient analysis of a mathematical model. The algorithm for the numerical solution of these equations is based on a PECE (Predict, Evaluate, Correct, Evaluate) method. This method combines a fractional-order algorithm with a classical method. Thus, the authors choose an Adams-Bashforth-Moulton approach for both integrators. Given that this approach is well known for first-order equations, in the case of the fractional variant, the key to deriving the method is simply to use the trapezoidal quadrature formula of the product. The main properties of the algorithm are: the behavior of the method is independent of the parameter α and behaves very much like the classical method of an Adams-Bashforth-Moulton stage (ie $\alpha = 1$). As for the stability of the method, these properties remain unchanged in the fractional version against the classical algorithm, and therefore it is also clear that the behavior does not depend on the order of the differential operators involved [38].

Fractional models have been used in the literature to understand the behavior of epidemiological models, where the integer-order models fail to give a complete explanation. In 2013, Diethelm [37] proposed a fractional order model for the dynamics of dengue fever. It was shown that the numerical simulations of the model provide better agreement with real data, from the 2009 outbreak of dengue in Cape Verde, than the integer order

model. In 2014, Pinto *et al.* [100] studied a model for HIV and TB co-infection and concluded that the dynamics of the integer and the fractional order versions of the model are very rich and that together these versions may provide a better understanding of the dynamics of the co-infection. In 2015, Pinto *et al.* [102] proposed a fractional complex-order model for HIV dynamics in the three-stages of infection. The fractional model unravels interesting dynamics that may help to understand the differences in individuals' disease progression. In 2016, Pinto *et al.* [103] studied a fractional complex-order model for drug resistance during HIV therapy, that includes three distinct growth rates for the $CD4^+$ T cells. The numerical results suggest that the variation of the complex-order fractional derivative may be compared to the variation of the delay in integer-order systems, in biologically meaning intervals. This happens for all growth rates. It is also observed the appearance of sustained oscillations (blips) as the proliferation rate increases. Sweilan *et al.* [139] proposed a fractional order model for multi-strain TB, which incorporates drug-sensitive, emerging MDR-TB and XDR-TB. They approximated the solutions of the FO model by distinct numerical methods and discussed the results obtained. In [140], the authors formulated an optimal control problem for a FO TB model and studied it using the Pontryagin maximum principle. They considered four controls variables to minimize the cost interventions and two numerical methods to approximate the solutions of the FO optimal control problem. They found that the iterative optimal control method provides better results. In 2017, it was analysed a FO model for HIV infection where latent T helper cells are included [105]. The order of the fractional derivative is associated to a decrease in the severity of the disease. Moreover, the results of the simulations of relevant parameters, such as the fraction of uninfected $CD4^+$ T cells that become latently infected, and the CTLs proliferation rate due to infected $CD4^+$ T cells, are biologically acceptable, for all values of the order of the fractional derivative. Pinto *et al.* [106] proposed a mathematical model with memory for the dynamics of HIV, where two transmission modes, cell-to-cell and virus-to-cell, and drug resistance are considered. The results showed that the cell-to-cell transmission is crucial for the development of the disease. The later highlights the extremely important role of the cell-cell pathway in the progression to AIDS in HIV infected patients. The order of the fractional derivative may be used, in this sense, to explain differences in the progression routes of HIV infected patients, associated with patients' immune system status, specific features in donor and target cell types, genetic profile, age.

Chapter 3

Mathematical models for HIV

3.1 Model I

A.R.M. Carvalho and C.M.A. Pinto, Emergence of drug-resistance in HIV dynamics under distinct HAART regimes, Communications in Nonlinear Science and Numerical Simulation 30, 207–226, 2016.

It is proposed a mathematical model for HIV infection, which includes helper cells, macrophages, CTLs and two viral strains. The main goals are to study the dynamics of the rapid progressors (RP) and of the long-term non-progressors (LTNP), and the effects of RTI and PI efficacies. Initially, the model is described, then the reproduction number and the local and global stability of the disease-free equilibrium are calculated. Finally, several model simulations are analyzed for different treatment regimens and the implications of the results are discussed.

3.1.1 Description of the model

The proposed compartmental model includes nine compartments. It yields the dynamics of uninfected (T, M), and of drug-sensitive (T_s, M_s) and drug-resistant (T_r, M_r) sub-populations of CD4^+ T cells and macrophages, respectively. Moreover it includes the dynamics of CTLs (Z) and of two viral strains (V_s, V_r).

The source of new T and M cells is represented by the first two terms of the corresponding equations. The logistic term of the T cells prevents its number to exceed the maximum concentration T_{max}. T cells are infected by HIV and infected macrophages at

rates k_1 and k_2, respectively. Macrophages are infected by HIV at rate k_4. The death rates of uninfected T cells and infected $T_s,\ T_r$ cells are given by δ_1 and δ_2, respectively. Macrophages populations are eliminated at rate δ_3.

CTLs, Z, are generated by the first three terms of the corresponding equation. Rates k_3 and k_5 refer to the elimination of infected $T_s,\ T_r$ cells and infected $M_s,\ M_r$ macrophages by CTLs, respectively. The natural death rate of CTLs is δ_4.

The sensitive (V_s) and resistant (V_r) virions are produced by the corresponding infected CD4$^+$ T cells and macrophages populations, with bursting sizes of drug-sensitive strain, N_s, and of drug-resistant strain, N_r. Virions are cleared at a rate c.

Parameters $t_1,\ t_2 \in [0, 1]$ in the equations represent the efficacy of RTIs and PIs, respectively. A value of 0 is associated with non-treatment and a value of 1 with full efficacy in the treatment. Drug-resistance is a result of genetic mutations. Viral mutations are accounted in the model via the parameter u, which represents the probability of mutation per replication cycle. Genetic mutations confer resistance to drugs. On the contrary, they reduce the infection rate of mutated virus. I.e., the virus's ability to transcribe its genome and integrate it into the host's genome is diminished, as well as its replicating capacity. As a result, infection rates by mutated viruses are considered to be smaller. As such, it is assumed that mutated virus is less fit than the wild-type. In the model, this is accounted by the parameter ψ. Moreover, drug efficacy in macrophages is lower than in CD4^+ T cells. Therefore, efficacy of the drugs on macrophages is $f_i t_i$, where $f_i \in [0, 1]$ and subindex i refers to each drug.

The schematic diagram of the model can be found in Figure 3.1.

The model is described by the following system of equations:

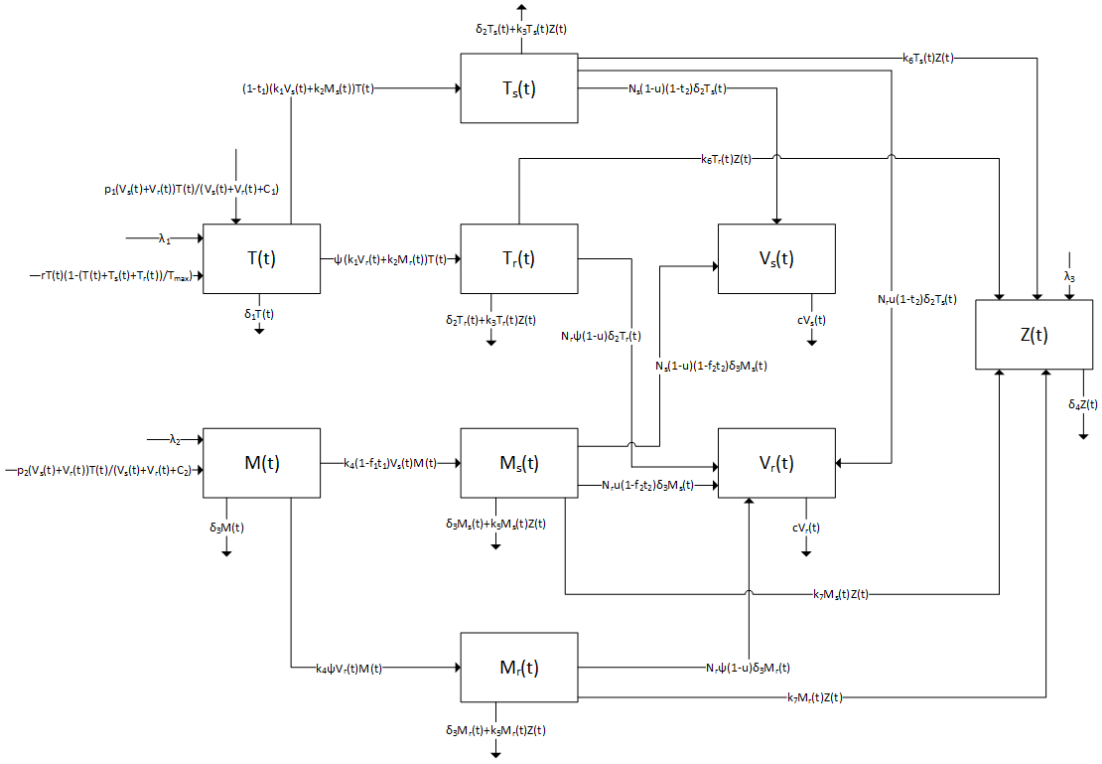

Figure 3.1: Schematic diagram of the model (3.1).

$$
\begin{aligned}
\dot{T}(t) &= \lambda_1 + \tfrac{p_1(V_s(t)+V_r(t))}{V_s(t)+V_r(t)+C_1}T(t) - (1-t_1)(k_1V_s(t)+k_2M_s(t))T(t) - \psi(k_1V_r(t)+k_2M_r(t))T(t) + \\
&\quad + rT(t)(1-(T(t)+T_s(t)+T_r(t))/T_{max}) - \delta_1 T(t);\\
\dot{T}_s(t) &= (1-t_1)(k_1V_s(t)+k_2M_s(t))T(t) - \delta_2 T_s(t) - k_3T_s(t)Z(t)\\
\dot{T}_r(t) &= \psi(k_1V_r(t)+k_2M_r(t))T(t) - \delta_2 T_r(t) - k_3T_r(t)Z(t)\\
\dot{M}(t) &= \lambda_2 + \tfrac{p_2(V_s(t)+V_r(t))}{C_2+V_s(t)+V_r(t)}M(t) - k_4(1-f_1t_1)V_s(t)M(t) - k_4\psi V_r(t)M(t) - \delta_3 M(t)\\
\dot{M}_s(t) &= k_4(1-f_1t_1)V_s(t)M(t) - \delta_3 M_s(t) - k_5M_s(t)Z(t)\\
\dot{M}_r(t) &= k_4\psi V_r(t)M(t) - \delta_3 M_r(t) - k_5M_r(t)Z(t)\\
\dot{V}_s(t) &= N_s(1-u)((1-t_2)\delta_2 T_s(t) + (1-f_2t_2)\delta_3 M_s(t)) - cV_s(t)\\
\dot{V}_r(t) &= N_r(\psi(1-u)(\delta_2 T_r(t)+\delta_3 M_r(t)) + u((1-t_2)\delta_2 T_s(t) + (1-f_2t_2)\delta_3 M_s(t)) - cV_r(t)\\
\dot{Z}(t) &= \lambda_3 + k_6(T_s(t)+T_r(t))Z(t) + k_7(M_s(t)+M_r(t))Z(t) - \delta_4 Z(t)
\end{aligned}
\tag{3.1}
$$

with non-negative initial conditions $T(0) = T^0$, $T_s(0) = T_s^0$, $T_r(0) = T_r^0$, $M(0) = M^0$, $M_s(0) = M_s^0$, $M_r(0) = M_r^0$, $V_s(0) = V_s^0$, $V_r(0) = V_r^0$, and $Z(0) = Z^0$.

3.1.2 Reproduction numbers and stability of the disease-free equilibrium

In this subsection, the reproduction number, R_0, of the model (3.1) is calculated. The basic reproduction number is defined as the number of secondary infections due to a single infection in a completely susceptible population [150].

Two sub-models of model (3.1) are considered. Model (3.2) is obtained from model (3.1) by setting the variables concerning resistance dynamics (T_r, M_r and V_r) to zero. On the other hand, model (3.5) follows from model (3.1) by setting the variables with respect to the sensitive dynamics (T_s, M_s and V_s) to zero.

The reproduction number of system (3.2), R_s, is calculated. The next generation method [150] is used.

$$\begin{aligned}
\dot{T}(t) &= \lambda_1 + \tfrac{p_1 V_s(t)}{V_s(t)+C_1} T(t) - (1-t_1)(k_1 V_s(t) + k_2 M_s(t))T(t) \\
&\quad + rT(t)(1 - (T(t)+T_s(t))/T_{max}) - \delta_1 T(t); \\
\dot{T}_s(t) &= (1-t_1)(k_1 V_s(t) + k_2 M_s(t))T(t) - \delta_2 T_s(t) - k_3 T_s(t) Z(t) \\
\dot{M}(t) &= \lambda_2 + \tfrac{p_2 V_s(t)}{C_2+V_s(t)} M(t) - k_4(1-f_1 t_1) V_s(t) M(t) - \delta_3 M(t) \\
\dot{M}_s(t) &= k_4(1-f_1 t_1) V_s(t) M(t) - \delta_3 M_s(t) - k_5 M_s(t) Z(t) \\
\dot{V}_s(t) &= N_s(1-u)((1-t_2)\delta_2 T_s(t) + (1-f_2 t_2)\delta_3 M_s(t)) - c V_s(t) \\
\dot{Z}(t) &= \lambda_3 + k_6 T_s(t) Z(t) + k_7 M_s(t) Z(t) - \delta_4 Z(t)
\end{aligned} \tag{3.2}$$

The disease-free equilibrium of model (3.2) is given by:

$$\begin{aligned}
P_0^1 &= (T^0, T_s^0, M^0, M_s^0, V_s^0, Z^0) = \\
&= \left(\frac{T_{max}\left[(r-\delta_1) + \sqrt{(r-\delta_1)^2 + \frac{4r\lambda_1}{T_{max}}}\right]}{2r}, 0, \tfrac{\lambda_2}{\delta_3}, 0, 0, \tfrac{\lambda_3}{\delta_4} \right)
\end{aligned} \tag{3.3}$$

Using the notation of [150] in system (3.2), the matrices for the new infection terms, F_1, and the other terms, V_1, are computed as follows:

$$F_1 = \begin{pmatrix} 0 & (1-t_1)k_2T^0 & (1-t_1)k_1T^0 \\ 0 & 0 & k_4(1-f_1t_1)M^0 \\ 0 & 0 & 0 \end{pmatrix}$$

$$V_1 = \begin{pmatrix} \delta_2 + k_3Z^0 & 0 & 0 \\ 0 & \delta_3 + k_5Z^0 & 0 \\ -N_s(1-u)(1-t_2)\delta_2 & -N_s(1-u)(1-f_2t_2)\delta_3 & c \end{pmatrix} = \begin{pmatrix} A & 0 & 0 \\ 0 & B & 0 \\ -N_s(1-u)D & -N_s(1-u)E & c \end{pmatrix}$$

The associative basic reproduction number is calculated to be:

$$R_s = \rho(F_1V_1^{-1}) = \frac{\frac{GD}{A} + \frac{HE}{B} + \sqrt{\left(\frac{GD}{A} + \frac{HE}{B}\right)^2 + 4\frac{HD}{AB}k_2(1-t_1)T^0}}{2} \tag{3.4}$$

where $G = \frac{(1-t_1)k_1T^0N_s(1-u)}{c}$, $H = \frac{(1-f_1t_1)k_4M^0N_s(1-u)}{c}$ and ρ indicates the spectral radius of $F_1V_1^{-1}$. By Theorem 2 [150], one obtains the Lemma 3.1.1.

Lema 3.1.1 *The disease-free equilibrium P_0^1 is locally asymptotically stable if $R_s < 1$ and unstable if $R_s > 1$.*

Proof The matrix of the linearization of model (3.2) around the disease-free equilibrium, P_0^1, is:

$$M_1 = \begin{pmatrix} r\left(1-\frac{2T^0}{T_{max}}\right) - \delta_1 & -\frac{rT^0}{T_{max}} & 0 & -(1-t_1)k_2T^0 & \frac{p_1T^0}{C_1} - (1-t_1)k_1T^0 & 0 \\ 0 & -\delta_2 - k_3Z^0 & 0 & (1-t_1)k_2T^0 & (1-t_1)k_1T^0 & 0 \\ 0 & 0 & -\delta_3 & 0 & \frac{p_2M^0}{C_2} - k_4(1-f_1t_1)M^0 & 0 \\ 0 & 0 & 0 & -\delta_3 - k_5Z^0 & k_4(1-f_1t_1)M^0 & 0 \\ 0 & N_s(1-u)(1-t_2)\delta_2 & 0 & N_s(1-u)(1-f_2t_2)\delta_3 & -c & 0 \\ 0 & k_6Z^0 & 0 & k_7Z^0 & 0 & -\delta_4 \end{pmatrix}$$

The following eigenvalues are easily obtained:

$$\left(1 - \frac{2T^0}{T_{max}}\right) - \delta_1, \qquad -\delta_3, \qquad -\delta_4,$$

The remaining eigenvalues are the roots of the characteristic equation of a 3×3 matrix, M_2, given by:

$$M_2 = \begin{pmatrix} -\delta_2 - k_3 Z^0 & (1-t_1)k_2 T^0 & (1-t_1)k_1 T^0 \\ 0 & -\delta_3 - k_5 Z^0 & k_4(1-f_1 t_1)M^0 \\ N_s(1-u)(1-t_2)\delta_2 & N_s(1-u)(1-f_2 t_2)\delta_3 & -c \end{pmatrix} = \begin{pmatrix} -A & (1-t_1)k_2 T^0 & (1-t_1)k_1 T^0 \\ 0 & -B & k_4(1-f_1 t_1)M^0 \\ N_s(1-u)D & N_s(1-u)E & -c \end{pmatrix}$$

The determinant $|M_2 - \lambda I_3| = 0$ is equivalent to:

$$(-A-\lambda)(-B-\lambda)(-c-\lambda) + (1-t_1)k_2 T^0 k_4(1-f_1 t_1)M^0 N_s(1-u)D -$$
$$-N_s(1-u)D(-B-\lambda)(1-t_1)k_1 T^0 - N_s(1-u)E k_4(1-f_1 t_1)M^0(-A-\lambda) = 0$$

$$(-A-\lambda)(-B-\lambda)(-c-\lambda) + (1-t_1)k_2 T^0 HcD - GcD(-B-\lambda) - HcE(-A-\lambda) = 0$$

$$\lambda^3 + (A+B+c)\lambda^2 + (AB + Ac + Bc - GcD - HcE)\lambda +$$
$$+ABc - (1-t_1)k_2 T^0 HcD - BGcD - HcEA = 0$$

where I_3 is the identity matrix of order 3. By the Routh-Hurwitz criteria, the three roots of the characteristic equation $\lambda^3 + a_1\lambda^2 + a_2\lambda + a_3 = 0$ have negative real parts if and only if $a_1, a_3 > 0$ and $a_1 a_2 - a_3 > 0$. It is proved below for $a_1 = A + B + c$, $a_2 = AB + Ac + Bc - GcD - HcE$, and $a_3 = ABc - (1-t_1)k_2 T^0 HcD - BGcD - HcEA$. It is easy to show that $a_1 = A + B + c = \delta_2 + k_3 Z^0 + \delta_3 + k_5 Z^0 + c > 0$. Next, it is shown the proof of $a_3 > 0$.

$$ABc > c((1-t_1)k_2 T^0 HD + BGD + HEA) \Leftrightarrow AB > (1-t_1)k_2 T^0 HD + BGD + HEA \Leftrightarrow$$
$$\Leftrightarrow (1-t_1)k_2 T^0 \tfrac{HD}{AB} + \tfrac{GD}{A} + \tfrac{HE}{B} < 1$$

This last inequality $(1-t_1)k_2 T^0 \frac{HD}{AB} + \frac{GD}{A} + \frac{HE}{B} < 1$ is equivalent to $R_s < 1$ (see below).

$$R_s < 1 \;\Leftrightarrow\; \frac{\frac{GD}{A} + \frac{HE}{B} + \sqrt{\left(\frac{GD}{A} + \frac{HE}{B}\right)^2 + 4\frac{HD}{AB}k_2(1-t_1)T^0}}{2} < 1$$

$$\Leftrightarrow\; \sqrt{\left(\tfrac{GD}{A} + \tfrac{HE}{B}\right)^2 + 4\tfrac{HD}{AB}k_2(1-t_1)T^0} < 2 - \tfrac{GD}{A} - \tfrac{HE}{B} \Leftrightarrow$$

$$\Leftrightarrow\; \left(\tfrac{GD}{A} + \tfrac{HE}{B}\right)^2 + 4\tfrac{HD}{AB}k_2(1-t_1)T^0 < 4\left(1 - \tfrac{GD}{A} - \tfrac{HE}{B}\right) + \left(\tfrac{GD}{A} + \tfrac{HE}{B}\right)^2 \Leftrightarrow$$

$$\Leftrightarrow\; \tfrac{HD}{AB}k_2(1-t_1)T^0 + \tfrac{GD}{A} + \tfrac{HE}{B} < 1$$

Thus, $a_3 > 0$ if $R_s < 1$. Some algebraic manipulations are now performed to prove that $a_1 a_2 - a_3 > 0$.

$$(A+B+c)(AB+Ac+Bc-GcD-HcE)-ABc+(1-t_1)k_2T^0HcD+BGcD+HcEA>0$$

$$A^2B+A^2c+ABc-AGcD-AHcE+AB^2+ABc+B^2c-BGcD-BHcE+ABc+Ac^2+$$
$$+Bc^2-Gc^2D-Hc^2E-ABc+(1-t_1)k_2T^0HcD+BGcD+HcEA>0$$

$$A^2B+A^2c+ABc-AGcD+AB^2+B^2c-BHcE+ABc+Ac^2+Bc^2-Gc^2D-Hc^2E+$$
$$+(1-t_1)k_2T^0HcD>0$$

$$A^2B+2ABc+AB^2+Ac(A-GD)+Bc(B-HE)+c^2(A-GD)+c^2(B-HE)+$$
$$+(1-t_1)k_2T^0HcD>0$$

It follows that, for $R_s<1$, all eigenvalues of the linearization matrix M_1 have negative real parts, then the disease-free equilibrium P_0^1 is locally asymptotically stable.

■

It follows the computation of the reproduction number of model (3.5), R_r.

$$\begin{aligned}
\dot{T}(t) &= \lambda_1+\tfrac{p_1V_r(t)}{V_r(t)+C_1}T(t)-\psi(k_1V_r(t)+k_2M_r(t))T(t)+\\
&\quad +rT(t)(1-(T(t)+T_r(t))/T_{max})-\delta_1T(t);\\
\dot{T}_r(t) &= \psi(k_1V_r(t)+k_2M_r(t))T(t)-\delta_2T_r(t)-k_3T_r(t)Z(t)\\
\dot{M}(t) &= \lambda_2+\tfrac{p_2V_r(t)}{C_2+V_r(t)}M(t)-k_4\psi V_r(t)M(t)-\delta_3M(t)\\
\dot{M}_r(t) &= k_4\psi V_r(t)M(t)-\delta_3M_r(t)-k_5M_r(t)Z(t)\\
\dot{V}_r(t) &= N_r(\psi(1-u)(\delta_2T_r(t)+\delta_3M_r(t)))-cV_r(r)\\
\dot{Z}(t) &= \lambda_3+k_6T_r(t)Z(t)+k_7M_r(t)Z(t)-\delta_4Z(t)
\end{aligned} \tag{3.5}$$

The disease-free equilibrium state P_0^2 of model (3.5) is given by:

$$\begin{aligned}
P_0^2 &= (T^0,T_r^0,M^0,M_r^0,V_r^0,Z^0)\\
&= \left(\frac{T_{max}\left[(r-\delta_1)+\sqrt{(r-\delta_1)^2+\frac{4r\lambda_1}{T_{max}}}\right]}{2r},0,\tfrac{\lambda_2}{\delta_3},0,0,\tfrac{\lambda_3}{\delta_4}\right)
\end{aligned} \tag{3.6}$$

Using the notation of [150] in system (3.5), the matrices for the new infection terms, F_2, and the other terms, V_2, are calculated as:

$$F_2 = \begin{pmatrix} 0 & \psi k_2 T^0 & \psi k_1 T^0 \\ 0 & 0 & k_4(1-f_1 t_1)M^0 \\ 0 & 0 & 0 \end{pmatrix}$$

$$V_2 = \begin{pmatrix} \delta_2 + k_3 Z^0 & 0 & 0 \\ 0 & \delta_3 + k_5 Z^0 & 0 \\ -N_r\psi(1-u)\delta_2 & -N_r\psi(1-u)\delta_3 & c \end{pmatrix} = \begin{pmatrix} A & 0 & 0 \\ 0 & B & 0 \\ -N_r(1-u)D_1 & -N_r(1-u)E_1 & c \end{pmatrix}$$

The associative basic reproduction number is given by:

$$R_r = \rho(F_2 V_2^{-1}) = \frac{\frac{ID_1}{A} + \frac{JE_1}{B} + \sqrt{\left(\frac{ID_1}{A} + \frac{JE_1}{B}\right)^2 + 4\frac{JD_1}{AB}\psi k_2 T^0}}{2} \tag{3.7}$$

where $I = \frac{\psi k_1 T^0 N_r(1-u)}{c}$, $J = \frac{\psi k_4 M^0 N_r(1-u)}{c}$ and ρ indicates the spectral radius of $F_2 V_2^{-1}$. By Theorem 2 [150], the following lemma is obtained.

Lema 3.1.2 *[150] The disease-free equilibrium P_0^2 is locally asymptotically stable if $R_r < 1$ and unstable if $R_r > 1$.*

Proof The linearization of model (3.5) around the disease-free equilibrium, P_0^2 is given by:

$$M_3 = \begin{pmatrix} r\left(1 - \frac{2T^0}{T_{max}}\right) - \delta_1 & -\frac{rT^0}{T_{max}} & 0 & -\psi k_2 T^0 & \frac{p_1 T^0}{C_1} - \psi k_1 T^0 & 0 \\ 0 & -\delta_2 - k_3 Z^0 & 0 & \psi k_2 T^0 & \psi k_1 T^0 & 0 \\ 0 & 0 & -\delta_3 & 0 & \frac{p_2 M^0}{C_2} - k_4 \psi M^0 & 0 \\ 0 & 0 & 0 & -\delta_3 - k_5 Z^0 & k_4 \psi M^0 & 0 \\ 0 & N_r\psi(1-u)\delta_2 & 0 & N_r\psi(1-u)\delta_3 & -c & 0 \\ 0 & k_6 Z^0 & 0 & k_7 Z^0 & 0 & -\delta_4 \end{pmatrix}$$

The following eigenvalues are easily obtained:

$$\left(1 - \frac{2T^0}{T_{max}}\right) - \delta_1, \qquad -\delta_3, \qquad -\delta_4,$$

The remaining eigenvalues are the roots of the characteristic equation of a 3×3 matrix, M_4, given by:

$$M_4 = \begin{pmatrix} -\delta_2 - k_3 Z^0 & \psi k_2 T^0 & \psi k_1 T^0 \\ 0 & -\delta_3 - k_5 Z^0 & k_4 \psi M^0 \\ N_r \psi (1-u)\delta_2 & N_r \psi (1-u)\delta_3 & -c \end{pmatrix} = \begin{pmatrix} -A & \psi k_2 T^0 & \psi k_1 T^0 \\ 0 & -B & k_4 \psi M^0 \\ N_r(1-u)D_1 & N_r(1-u)E_1 & -c \end{pmatrix}$$

The determinant $|M_4 - \lambda I_3| = 0$ is equivalent to:

$$(-A-\lambda)(-B-\lambda)(-c-\lambda) + \psi k_2 T^0 k_4 \psi M^0 N_r(1-u)D_1 - N_r(1-u)D_1(-B-\lambda)\psi k_1 T^0 - \\ -N_r(1-u)E_1 k_4 \psi M^0(-A-\lambda) = 0$$

$$(-A-\lambda)(-B-\lambda)(-c-\lambda) + \psi k_2 T^0 JcD_1 - IcD_1(-B-\lambda) - JcE_1(-A-\lambda) = 0$$

$$\lambda^3 + (A+B+c)\lambda^2 + (AB + Ac + Bc - IcD_1 - JcE_1)\lambda + ABc - \psi k_2 T^0 JcD_1 - IcD_1 B - JcE_1 A = 0$$

where I_3 is the identity matrix of order 3. By the Routh-Hurwitz criteria, the three roots of the characteristic equation $\lambda^3 + a_1\lambda^2 + a_2\lambda + a_3 = 0$ have negative real parts if and only if $a_1, a_3 > 0$ and $a_1 a_2 - a_3 > 0$. This is shown for $a_1 = A + B + c$, $a_2 = AB + Ac + Bc - IcD_1 - JcE_1$, and $a_3 = ABc - \psi k_2 T^0 JcD_1 - IcD_1 B - JcE_1 A$.

It is trivial to show that $a_1 = A + B + c = \delta_2 + k_3 Z^0 + \delta_3 + k_5 Z^0 + c > 0$. Now it's proven that $a_3 = ABc - \psi k_2 T^0 JcD_1 - IcD_1 B - JcE_1 A > 0$ if $R_r < 1$.

$$ABc > c(\psi k_2 T^0 JD_1 + ID_1 B + JE_1 A) \Leftrightarrow AB > \psi k_2 T^0 JD_1 + ID_1 B + JE_1 A \Leftrightarrow$$

$$\Leftrightarrow \psi k_2 T^0 \tfrac{JD_1}{AB} + \tfrac{ID_1}{A} + \tfrac{JE_1}{B} < 1$$

Last inequality is equivalent to $R_r < 1$.

$$\begin{aligned} R_r < 1 \quad &\Leftrightarrow \quad \frac{\frac{ID_1}{A} + \frac{JE_1}{B} + \sqrt{\left(\frac{ID_1}{A} + \frac{JE_1}{B}\right)^2 + 4\frac{JD_1}{AB}k_2\psi T^0}}{2} < 1 \Leftrightarrow \\ &\Leftrightarrow \quad \sqrt{\left(\frac{ID_1}{A} + \frac{JE_1}{B}\right)^2 + 4\frac{JD_1}{AB}k_2\psi T^0} < 2 - \frac{ID_1}{A} - \frac{JE_1}{B} \Leftrightarrow \\ &\Leftrightarrow \quad \left(\frac{ID_1}{A} + \frac{JE_1}{B}\right)^2 + 4\frac{JD_1}{AB}k_2\psi T^0 < 4\left(1 - \frac{ID_1}{A} - \frac{JE_1}{B}\right) + \left(\frac{ID_1}{A} + \frac{JE_1}{B}\right)^2 \Leftrightarrow \\ &\Leftrightarrow \quad \frac{JD_1}{AB}k_2\psi T^0 + \frac{ID_1}{A} + \frac{JE_1}{B} < 1 \end{aligned}$$

It is shown that $a_1a_2 - a_3 > 0$.

$$(A+B+c)(AB+Ac+Bc-IcD_1-JcE_1)-ABc+\psi k_2T^0JcD_1+IcD_1B+JcE_1A>0$$

$$A^2B+A^2c+ABc-AIcD_1-AJcE_1+AB^2+ABc+B^2c-BIcD_1-BJcE_1+ABc+$$
$$+Ac^2+Bc^2-Ic^2D_1-Jc^2E_1-ABc+\psi k_2T^0JcD_1+IcD_1B+JcE_1A>0$$

$$A^2B+A^2c+ABc-AIcD_1+AB^2+B^2c-BJcE_1+ABc+Ac^2+Bc^2-$$
$$-Ic^2D_1-Jc^2E_1+\psi k_2T^0JcD_1>0$$

$$A^2B+2ABc+AB^2+Ac(A-ID_1)+Bc(B-JE_1)+c^2(A-ID_1)+c^2(B-JE_1)+$$
$$+\psi k_2T^0JcD_1>0$$

Last inequality is true since $A > ID_1$ and $B > JE_1$. It follows that all eigenvalues of the linearization matrix of model (3.5) have negative real parts. Thus, the disease-free equilibrium P_0^2 is locally asymptotically stable if $R_r < 1$.

■

The calculation of the reproduction number of the full model (3.1), R_0 proceeds. The disease-free equilibrium state, P_0, of the full model (3.1) is given by:

$$\begin{aligned} P_0 &= (T^0, T_s^0, T_r^0, M^0, M_s^0, M_r^0, V_s^0, V_r^0, Z^0) \\ &= \left(\frac{T_{max}\left[(r-\delta_1)+\sqrt{(r-\delta_1)^2+\frac{4r\lambda_1}{T_{max}}}\right]}{2r}, 0, 0, \frac{\lambda_2}{\delta_3}, 0, 0, 0, 0, \frac{\lambda_3}{\delta_4} \right) \end{aligned} \tag{3.8}$$

Using the notation in [150] on system (3.1), the matrices for the new infection terms, F, and the other terms, V, are calculated as:

$$F = \begin{pmatrix} 0 & 0 & (1-t_1)k_2T^0 & 0 & (1-t_1)k_1T^0 & 0 \\ 0 & 0 & 0 & \psi k_2T^0 & 0 & \psi k_1T^0 \\ 0 & 0 & 0 & 0 & k_4(1-f_1t_1)M^0 & 0 \\ 0 & 0 & 0 & 0 & 0 & k_4\psi M^0 \\ 0 & 0 & 0 & 0 & 0 & 0 \\ 0 & 0 & 0 & 0 & 0 & 0 \end{pmatrix}$$

$$V = \begin{pmatrix} \delta_2 + k_3 Z^0 & 0 & 0 & 0 & 0 & 0 \\ 0 & \delta_2 + k_3 Z^0 & 0 & 0 & 0 & 0 \\ 0 & 0 & \delta_3 + k_5 Z^0 & 0 & 0 & 0 \\ 0 & 0 & 0 & \delta_3 + k_5 Z^0 & 0 & 0 \\ -N_s(1-u)(1-t_2)\delta_2 & 0 & -N_s(1-u)(1-f_2 t_2)\delta_3 & 0 & c & 0 \\ -N_r u(1-t_2)\delta_2 & -N_r\psi(1-u)\delta_2 & -N_r u(1-f_2 t_2)\delta_3 & -N_r\psi(1-u)\delta_3 & 0 & c \end{pmatrix}$$

$$= \begin{pmatrix} A & 0 & 0 & 0 & 0 & 0 \\ 0 & A & 0 & 0 & 0 & 0 \\ 0 & 0 & B & 0 & 0 & 0 \\ 0 & 0 & 0 & B & 0 & 0 \\ -N_s(1-u)D & 0 & -N_s(1-u)E & 0 & c & 0 \\ -N_r u D & -N_r(1-u)D_1 & -N_r u E & -N_r(1-u)E_1 & 0 & c \end{pmatrix}$$

The associative basic reproduction number, R_0, is computed to be:

$$R_0 = \rho(FV^{-1}) = \max\{R_s, R_r\} \tag{3.9}$$

where ρ indicates the spectral radius of FV^{-1}. By Theorem 2 [150], get the following lemma.

Lema 3.1.3 *The disease-free equilibrium P_0 is locally asymptotically stable if $R_0 < 1$ and unstable if $R_0 > 1$.*

Proof The linearization matrix of model (3.1) around the disease-free equilibrium, P_0, is:

$$M_5 = \begin{pmatrix} r\left(1-\frac{2T^0}{T_{max}}\right)-\delta_1 & -\frac{rT^0}{T_{max}} & -\frac{rT^0}{T_{max}} & 0 & -(1-t_1)k_2T^0 & -\psi k_2T^0 & \frac{p_1}{C_1}T^0-(1-t_1)k_1T^0 & \frac{p_1}{C_1}T^0-\psi k_1T^0 & 0 \\ 0 & -\delta_2-k_3Z^0 & 0 & 0 & (1-t_1)k_2T^0 & 0 & (1-t_1)k_1T^0 & 0 & 0 \\ 0 & 0 & -\delta_2-k_3Z^0 & 0 & 0 & \psi k_2T^0 & 0 & \psi k_1T^0 & 0 \\ 0 & 0 & 0 & -\delta_3 & 0 & 0 & \frac{p_2}{C_2}M^0-k_4(1-f_1t_1)M^0 & \frac{p_2}{C_2}M^0-k_4\psi M^0 & 0 \\ 0 & 0 & 0 & 0 & -\delta_3-k_5Z^0 & 0 & k_4(1-f_1t_1)M^0 & 0 & 0 \\ 0 & 0 & 0 & 0 & 0 & -\delta_3-k_5Z^0 & 0 & k_4\psi M^0 & 0 \\ 0 & N_s(1-u)(1-t_2)\delta_2 & 0 & 0 & N_s(1-u)(1-f_2t_2)\delta_3 & 0 & -c & 0 & 0 \\ 0 & N_ru(1-t_2)\delta_2 & N_r\psi(1-u)\delta_2 & 0 & N_ru(1-f_2t_2)\delta_3 & N_r\psi(1-u)\delta_3 & 0 & -c & 0 \\ 0 & k_6Z^0 & k_6Z^0 & 0 & k_7Z^0 & k_7Z^0 & 0 & 0 & -\delta_4 \end{pmatrix}$$

The following eigenvalues are easily obtained:

$$\left(1-\frac{2T^0}{T_{max}}\right)-\delta_1, \qquad -\delta_3, \qquad -\delta_4,$$

The remaining eigenvalues are the roots of the characteristic equation of a 6×6 matrix, M_6, given by:

$$M_6 = \begin{pmatrix} -\delta_2-k_3Z^0 & 0 & (1-t_1)k_2T^0 & 0 & (1-t_1)k_1T^0 & 0 \\ 0 & -\delta_2-k_3Z^0 & 0 & \psi k_2T^0 & 0 & \psi k_1T^0 \\ 0 & 0 & -\delta_3-k_5Z^0 & 0 & k_4(1-f_1t_1)M^0 & 0 \\ 0 & 0 & 0 & -\delta_3-k_5Z^0 & 0 & k_4\psi M^0 \\ N_s(1-u)(1-t_2)\delta_2 & 0 & N_s(1-u)(1-f_2t_2)\delta_3 & 0 & -c & 0 \\ N_ru(1-t_2)\delta_2 & N_r\psi(1-u)\delta_2 & N_ru(1-f_2t_2)\delta_3 & N_r\psi(1-u)\delta_3 & 0 & -c \end{pmatrix}$$

$$= \begin{pmatrix} -A & 0 & (1-t_1)k_2T^0 & 0 & (1-t_1)k_1T^0 & 0 \\ 0 & -A & 0 & \psi k_2T^0 & 0 & \psi k_1T^0 \\ 0 & 0 & -B & 0 & k_4(1-f_1t_1)M^0 & 0 \\ 0 & 0 & 0 & -B & 0 & k_4\psi M^0 \\ N_s(1-u)D & 0 & N_s(1-u)E & 0 & -c & 0 \\ N_ruD & N_r(1-u)D_1 & N_ruE & N_r(1-u)E_1 & 0 & -c \end{pmatrix}$$

The determinant $|M_6 - \lambda I_6| = 0$ is equivalent to:

$$[(-A-\lambda)(-B-\lambda)(-c-\lambda) - (-A-\lambda)N_r(1-u)E_1k_4\psi M^0 +$$
$$+N_r(1-u)D_1k_4\psi M^0\psi k_2T^0 - N_r(1-u)D_1\psi k_1T^0(-B-\lambda)] \times$$

$$\times [(-A-\lambda)(-B-\lambda)(-c-\lambda) + N_s(1-u)D(1-t_1)k_2T^0k_4(1-f_1t_1)M^0 -$$
$$-N_s(1-u)D(-B-\lambda)(1-t_1)k_1T^0 - (-A-\lambda)N_s(1-u)Ek_4(1-f_1t_1)M^0] = 0$$

The first factor of the characteristic equation of matrix M_6 is the characteristic equation of matrix M_4, and the second factor is the characteristic equation of the matrix M_2. Thus, as it has already been shown that the disease-free equilibria of subsystems (3.2)-(3.5) are stable for $R_s < 1$ and $R_r < 1$, respectively, one concludes that the disease-free equilibrium P_0 is locally asymptotically stable if $R_0 = \max\{R_s, R_r\} < 1$.

■

3.1.3 Global stability of disease-free equilibria

In this subsection, the global stability of the disease-free equilibrium of the full model (3.1) is calculated. Again, one begins by the stability of the disease-free equilibria of the two submodels.

Lema 3.1.4 *The disease-free equilibrium P_0^1 is globally asymptotically stable if $R_s < 1$.*

Proof The rate of change of the variables (T_s, M_s, V_s) of system (3.2) can be rewritten as follows.

$$\begin{pmatrix} \dot{T}_s \\ \dot{M}_s \\ \dot{V}_s \end{pmatrix} = (F_1 - V_1) \begin{pmatrix} T_s \\ M_s \\ V_s \end{pmatrix} - \begin{pmatrix} (1-t_1)(k_1V_s + k_2M_s)(T^0 - T) + k_3T_sZ \\ k_4(1-f_1t_1)V_s(M^0 - M) + k_5M_sZ \\ 0 \end{pmatrix} \tag{3.10}$$

where F_1 and V_1 are as defined above. Now let's prove that system (3.10) satisfies:

$$\begin{pmatrix} \dot{T}_s \\ \dot{M}_s \\ \dot{V}_s \end{pmatrix} \leq (F - V) \begin{pmatrix} T_s \\ M_s \\ V_s \end{pmatrix} \tag{3.11}$$

The proof starts by showing that $T(t) \leq T^0$. Consider the helper T cells' growth function $f_1(T) = \lambda_1 + rT\left(1 - \frac{T}{T_{max}}\right) - \delta_1 T$. This function satisfies assumptions $(A1)$ and $(A2)$ below.

$(A1)$ $\exists T_0$ such that $f_1(T_0) = 0$ and $f_1'(T_0) < 0$.

$$\begin{aligned} f_1(T_0) = 0 &\Leftrightarrow \lambda_1 + rT_0\left(1 - \tfrac{T_0}{T_{max}}\right) - \delta_1 T_0 = 0 \\ &\Leftrightarrow -\tfrac{r}{T_{max}}(T^0)^2 + (r - \delta_1)T_0 + \lambda_1 = 0 \\ &\Leftrightarrow T_0 = T^0 = \frac{T_{max}\left[(r-\delta_1) \pm \sqrt{(r-\delta_1)^2 + \frac{4r\lambda_1}{T_{max}}}\right]}{2r} \end{aligned}$$

Proof continues with the calculation of the first derivative of function $f_1(t)$.

$$f_1'(T_0) = r - \frac{2rT_0}{T_{max}} - \delta_1$$

This derivative has negative sign at $T_0 = T^0$:

$$f_1'(T^0) = -\sqrt{(r - \delta_1)^2 + \frac{4r\lambda_1}{T_{max}}} < 0$$

$(A2)$ $f_1(T) > 0$, $T \in (0, T_0)$ and $f_1(T) < 0$, $T > T_0$.

At $T_0 = T^0$, it is obtained:

$$f_1(T) > 0 \Leftrightarrow \frac{r}{T_{max}}(T^0)^2 + (r - \delta_1)T^0 + \lambda_1 > 0 \tag{3.12}$$

As this function has the shape of a parable with concavity facing down, then it is positive between 0 and T^0 and negative for $T > T^0$.

The equation $\dot{T}(t)$ and assumptions $(A1)$ and $(A2)$ imply that $\limsup T(t) \leq T^0$, $t \to \infty$.

Now, it is proven that $M(t) \leq M^0$. Consider the macrophages growth rate $f_2(M) = \lambda_2 - \delta_3 M$. This function satisfies assumptions $(A3)$ and $(A4)$ below - analogous to assumptions $(A1)$ and $(A2)$.

$(A3)$ $\exists M_0$ such that $f_2(M_0) = 0$ and $f_2'(M_0) < 0$.

$$f_2(M) = 0 \Leftrightarrow \lambda_2 - \delta_3 M_0 = 0 \Leftrightarrow M_0 = \frac{\lambda_2}{\delta_3} = M^0$$

The first derivative of $f_2(t)$, $f_2'(M) = -\delta_3$, is negative $\forall M$, in particular for $M_0 = M^0$.

$(A4)$ $f_2(M) > 0$, $M \in (0, M_0)$ and $f_2(M) < 0$, $M > M_0$.

$$f_2(M) > 0 \Leftrightarrow \lambda_2 - \delta_3 M > 0 \Leftrightarrow M < \frac{\lambda_2}{\delta_3} = M_0 = M^0$$

$$f_2(M) < 0 \Leftrightarrow \lambda_2 - \delta_3 M < 0 \Leftrightarrow M > \frac{\lambda_2}{\delta_3} = M_0 = M^0$$

Assumptions $(A3)$ and $(A4)$ and the form of equation $\dot{M}(t)$ of (3.2) imply that

$$\limsup M(t) \leq M^0, \qquad t \to \infty.$$

Thus, the inequality (3.11) is proven. If $R_s < 1$, then $\rho(F_1 V_1^{-1}) < 1$, which is equivalent to the matrix $F_1 - V_1$ having all its eigenvalues in the left-half plane [150]. It follows that the linear system given by equality (3.11) is stable whenever $R_s < 1$, and hence $(T_s(t), M_s(t), V_s(t)) \to (0, 0, 0)$ as $t \to \infty$. Consequently, after using a standard comparison theorem [63, 133], it is obtained $(T_s(t), M_s(t), V_s(t)) \to (0, 0, 0)$, for the nonlinear system given by the equations of submodel (3.2). Returning now to the equations of this submodel and substituting $T_s = M_s = V_s = 0$, one obtains a linear system, where $T(t) = T^0$, $M(t) = M^0$ and $Z(t) = Z^0$. Thus,

$$(T(t), T_s(t), M(t), M_s(T), V_s(t), Z) \to (T^0, 0, M^0, 0, 0, Z^0)$$

as $t \to \infty$. It is concluded that, if $R_s < 1$ then P_0^1 is globally asymptotically stable.

■

Now, the same procedure for the computation of the global stability of the disease-free equilibrium of submodel (3.5) is repeated.

Lema 3.1.5 *The disease-free equilibrium P_0^2 is globally asymptotically stable if $R_r < 1$.*

Proof The rate of change of the variables (T_r, M_r, V_r) of system (3.5) can be rewritten as:

$$\begin{pmatrix} \dot{T}_r \\ \dot{M}_r \\ \dot{V}_r \end{pmatrix} = (F_2 - V_2) \begin{pmatrix} T_r \\ M_r \\ V_r \end{pmatrix} - \begin{pmatrix} \psi(k_1 V_r + k_2 M_r)(T^0 - T) + k_3 T_r Z \\ k_4 \psi V_r (M^0 - M) + k_5 M_r Z \\ 0 \end{pmatrix} \tag{3.13}$$

where F_2 and V_2 are as defined previously. Since $T(t) \leq T^0$, $M(t) \leq M^0$ and $Z(t) \geq 0$ for all $t \geq 0$, then:

$$\begin{pmatrix} \dot{T}_r \\ \dot{M}_r \\ \dot{V}_r \end{pmatrix} \leq (F - V) \begin{pmatrix} T_r \\ M_r \\ V_r \end{pmatrix} \tag{3.14}$$

In [150] it is proven that if the reproduction number is less than 1, the matrix $F_2 - V_2$ has all its eigenvalues in the left-half plane. Thus, if $R_r < 1$, the linear system given by the equality (3.14) is stable, and hence $(T_r(t), M_r(t), V_r(t)) \to (0, 0, 0)$ as $t \to \infty$. Consequently, after using a standard comparison theorem [63, 133], it is obtained $(T_r(t), M_r(t), V_r(t)) \to (0, 0, 0)$ for the nonlinear system, given by the equations of (3.5). Returning now to the equations of this submodel and substituting $T_r = M_r = V_r = 0$, one obtains a linear system with $T(t) = T^0$, $M(t) = M^0$ and $Z(t) = Z^0$. Thus, if $R_r < 1$, $(T(t), T_r(t), M(t), M_r(t), V_r(t), Z(t)) \to (T^0, 0, M^0, 0, 0, Z^0)$ as $t \to \infty$, which proves that P_0^2 is globally asymptotically stable.

■

A similar procedure for the computation of the global stability of the disease-free equilibrium of the full model (3.1) follows.

Lema 3.1.6 *The disease-free equilibrium P_0 is globally asymptotically stable if*

$$R_0 = \max\{R_s, R_r\} < 1.$$

Proof The rate of change of the variables $(T_s, T_r, M_s, M_r, V_s, V_r)$ of system (3.1) can be rewritten as:

$$\begin{pmatrix} \dot{T}_s \\ \dot{T}_r \\ \dot{M}_s \\ \dot{M}_r \\ \dot{V}_s \\ \dot{V}_r \end{pmatrix} = (F-V) \begin{pmatrix} T_s \\ T_r \\ M_s \\ M_r \\ V_s \\ V_r \end{pmatrix} - \begin{pmatrix} (1-t_1)(k_1V_s + k_2M_s)(T^0 - T) + k_3T_sZ \\ \psi(k_1V_r + k_2M_r)(T^0 - T) + k_3T_rZ \\ k_4(1-f_1t_1)V_s(M^0 - M) + k_5M_sZ \\ k_4\psi V_r(M^0 - M) + k_5M_rZ \\ 0 \\ 0 \end{pmatrix} \tag{3.15}$$

where F and V are as defined above for system (3.1). Since $T(t) \leq T^0$, $M(t) \leq M^0$ and $Z(t) \geq 0$ for all $t \geq 0$, then:

$$\begin{pmatrix} \dot{T}_s \\ \dot{T}_r \\ \dot{M}_s \\ \dot{M}_r \\ \dot{V}_s \\ \dot{V}_r \end{pmatrix} \leq (F-V) \begin{pmatrix} T_s \\ T_r \\ M_s \\ M_r \\ V_s \\ V_r \end{pmatrix} \tag{3.16}$$

If $\max\{R_s, R_r\} < 1$, then $\rho(FV^{-1}) < 1$, which is equivalent to the matrix $F - V$ having all its eigenvalues in the left-half plane [150]. It follows that the linear system given by the equality (3.16) is stable whenever $\max\{R_s, R_r\} < 1$, and hence $(T_s(t), T_r(t), M_s(t), M_r(t), V_s(t), V_r(t)) \to (0, 0, 0, 0, 0, 0)$ as $t \to \infty$ for this linear ODE system. Consequently, applying a standard comparison theorem [63, 133], results in $(T_s(t), T_r(t), M_s(t), M_r(t), V_s(t), V_r(t)) \to (0, 0, 0, 0, 0, 0)$ for the nonlinear system, given by the equations of (3.1). Returning now to the equations of this model and substituting $T_s = T_r = M_s = M_r = V_s = V_r = 0$, one gets a linear system with $T(t) = T^0$, $M(t) = M^0$ and $Z(t) = Z^0$. Thus, if $\max\{R_s, R_r\} < 1$,

$$(T(t), T_s(t), T_r(t), M(t), M_s(t), M_r(t), V_s(t), V_r(t), Z(t)) \to (T^0, 0, 0, M^0, 0, 0, 0, 0, Z^0),$$

as $t \to \infty$, and P_0 is globally asymptotically stable.

■

3.1.4 Numerical results

The model (3.1) is simulated. The parameters used in the simulations are given in Table 3.1 and the initial conditions are set to $T(0) = 1000$, $M(0) = 30$, $Z(0) = 333$, and

all other variables are set to 0.001.

Parameter	DF	RP	LTNP	Units	Reference
λ_1	10	11	35	mm^{-3} day^{-1}	[48]
λ_2	0.15	0.15	0.15	mm^{-3} day^{-1}	[48]
λ_3	5	5	4	mm^{-3} day^{-1}	[48]
δ_1	0.02	0.02	0.01	day^{-1}	[48]
δ_2	0.28	0.33	0.28	day^{-1}	[48]
δ_3	0.005	0.004	0.005	day^{-1}	[48]
δ_4	0.015	0.015	0.028	day^{-1}	[48]
r	0.03	0.072	0.072	day^{-1}	[48]
c	23	23	10	day^{-1}	[156, 48]
T_{max}	1500	1500	1500	mm^{-3}	[156]
C_1	300	188	300	mm^{-3}	[52, 48]
C_2	200	220	200	mm^{-3}	[52]
t_1	0	0	0		[48]
t_2	0	0	0		[48]
u	0.001	0.005	0.001		[48]
ψ	0.9	0.6	0.9		[48]
p_1	0.01	0.01	0.065	day^{-1}	[48]
p_2	0.02	0.0089	0.0068	day^{-1}	[48]
k_1	2.4×10^{-5}	4.0×10^{-5}	2.5×10^{-5}	mm^3 day^{-1}	[74]
k_2	1×10^{-6}	1×10^{-8}	9.8×10^{-9}	mm^3 day^{-1}	[74]
k_3	9.9×10^{-4}	9.9×10^{-4}	9.9×10^{-4}	mm^3 day^{-1}	[74]
k_4	4.22×10^{-8}	4.22×10^{-8}	4.22×10^{-8}	mm^3 day^{-1}	[74]
k_5	6.6×10^{-6}	6.6×10^{-6}	9.6×10^{-6}	mm^3 day^{-1}	[74]
k_6	2.3×10^{-4}	2.3×10^{-4}	3.93×10^{-4}	mm^3 day^{-1}	[74]
k_7	5.28×10^{-9}	5.28×10^{-9}	6.6×10^{-9}	mm^3 day^{-1}	[74]
N_s	200	3000	3000		[156]
N_r	50	2000	2000		[156]
f_1	0.34	0.34	0.34		[48]
f_2	0.34	0.34	0.34		[48]

Table 3.1: Parameters used in the numerical simulations of model (3.1). DF - disease-free equilibrium; RP - rapid progressor; LTNP - long-term non progressor.

In Figure 3.2 it is depicted the disease-free equilibrium of model (3.1).

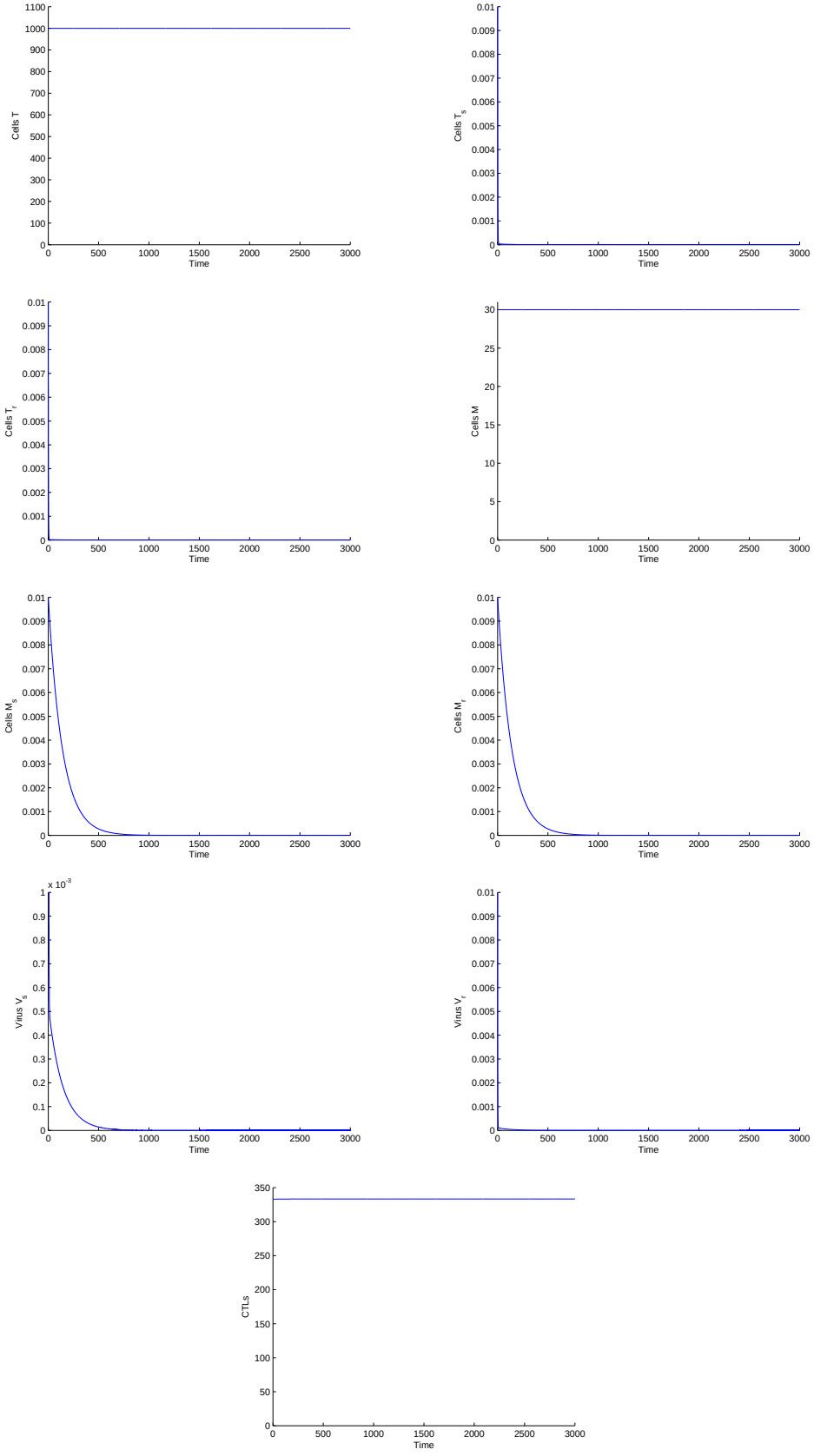

Figure 3.2: Disease-free equilibrium of the model (3.1).

In Figs 3.3-3.4, the patterns of the rapid progressors (RP) and long-term non progressors (LTNP) of model (3.1) are shown. RP are a 10% of untreated HIV patients, whose $CD4^+$ T cells decrease below the AIDS threshold after, approximately, 3-5 years after infection [11]. LTNP are a special class of HIV patients, who without therapy, manage to escape the common route to AIDS for 15-20 years. LTNP account for 10-17%, of HIV infected patients [64]. The generality of untreated HIV infected patients progress to AIDS, after initial infection, within 8-10 years. The distinct routes of progression to AIDS have been associated with patients' immune system status, genetic profile, and age [11].

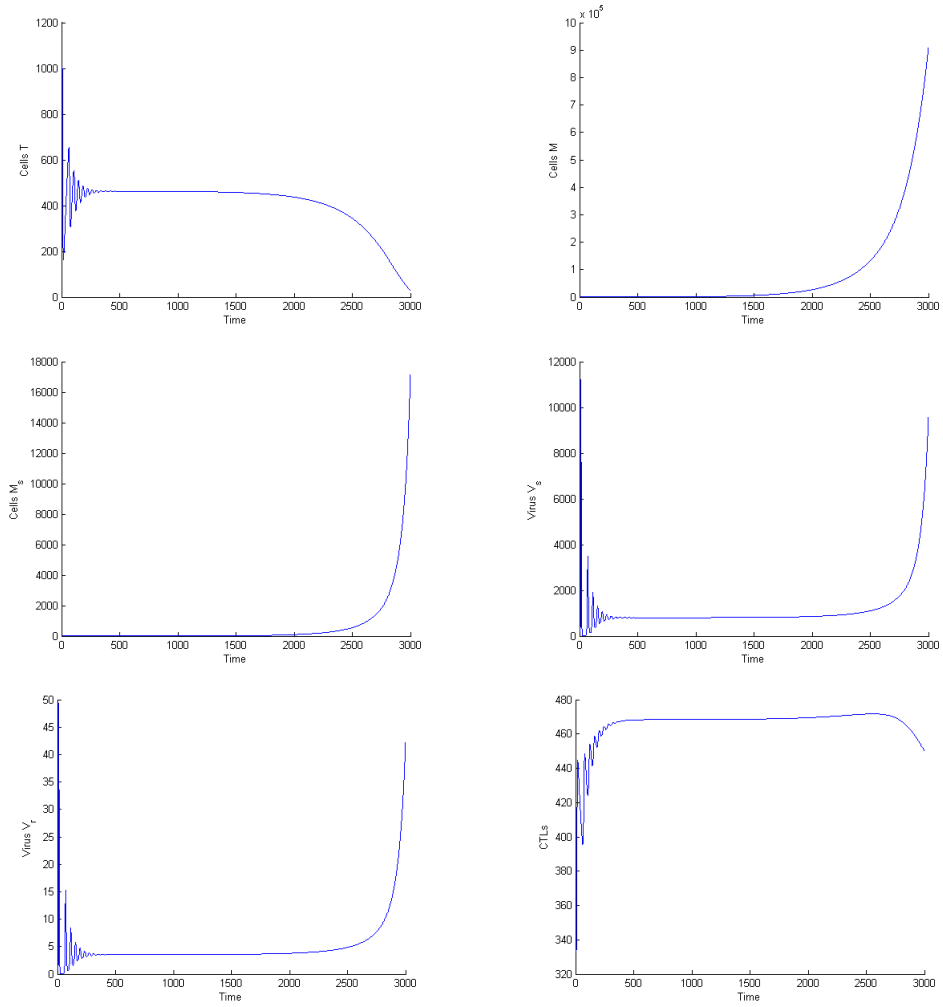

Figure 3.3: Rapid progressors (RP) of the model (3.1).

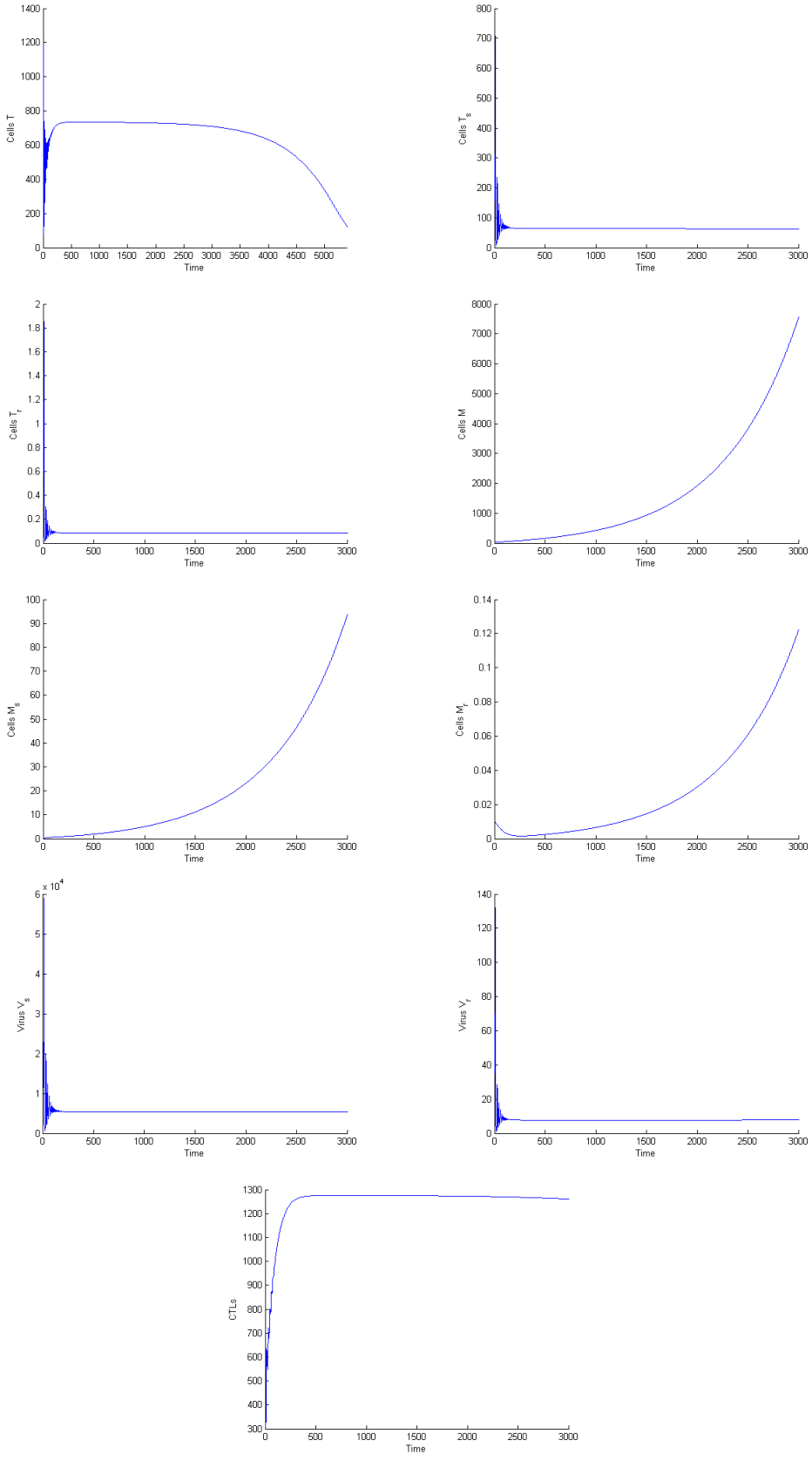

Figure 3.4: Long-term non progressors (LTNP) of the model (3.1).

Figure 3.5 depicts the dynamics of CD4^+ T cells, sensitive and drug-resistant virus for distinct treatment regimes, but equal efficacies of RTIs and PIs. Namely, it is considered $t_1 = t_2 = 0.1$, $t_1 = t_2 = 0.4$, and $t_1 = t_2 = 0.7$. It is observed that at very low drug efficacy ($t_1 = t_2 = 0.1$), the drug-sensitive virus are not supressed which leads to faster progression to AIDS. At higher drug efficacies ($t_1 = t_2 = 0.7$) it is observed an expressive depletion of drug-sensitive virus and an increase of drug-resistant virus. The later may be explained by the high level of CD4^+ T cells at higher drug efficacies. A larger number of helper cells are infected by the virus, promoting the earlier appearance of drug-resistant virus. The results from low and higher drug efficacies seem to allude to an optimal treatment regime that can reduce drug-sensitive virus and at the same time delay the appearance of drug-resistance.

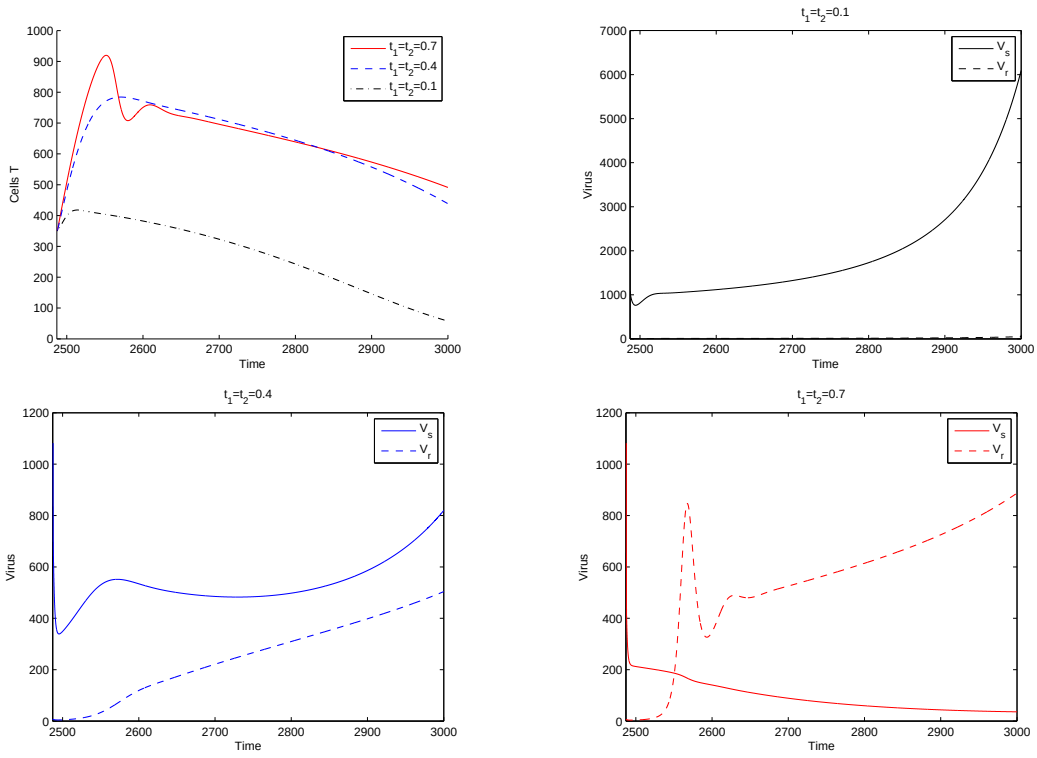

Figure 3.5: Effect of three distinct values of RTI and PI drug efficacy in the patterns of uninfected T cells, drug-sensitive virus and drug-resistant virus, for a typical untreated HIV patient. Presumed $t_1 = t_2 = 0.1$, $t_1 = t_2 = 0.4$, and $t_1 = t_2 = 0.7$.

Bearing this in mind, in Figure 3.6, distinct efficacies are assumed for RTIs and PIs. The RTI-based treatment is characterized by a significantly greater efficacy of RTIs when compared to PIs ($t_1 = 0.7,\ t_2 = 0.1$). On the contrary, the PI-based drug regime assumes a greater efficacy for PIs ($t_1 = 0.1,\ t_2 = 0.7$). From observation of the figure, it seems that PI-based therapeutics produce better results, in terms of delaying disease

progression. In fact, PI-based regime promotes an increase in the T cells, reduces the drug-sensitive virus and delays the appearance of drug-resistant virus. In what concerns the RTI-based treatment, it is observed a faster emergence of drug-resistant virus, associated to a sharper increase in the T cells. Moreover, RTI-based drugs do not reduce drug-sensitive virus to the same extent as PI drugs do [12, 48].

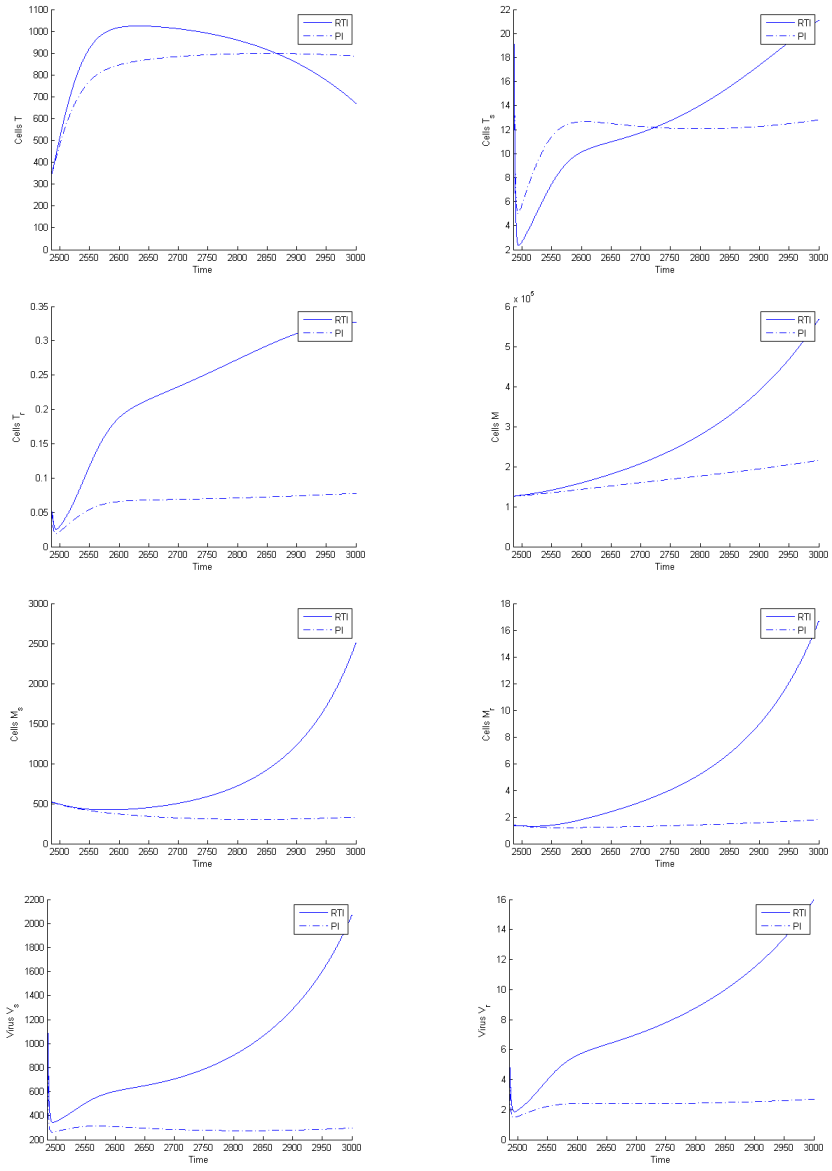

Figure 3.6: RTI-based ($t_1 = 0.7,\ t_2 = 0.1$) and PI-based ($t_1 = 0.1,\ t_2 = 0.7$) treatment, initiated at a CD4^+ T cell count lower than 350 cells mm^{-3} of the model (3.1).

3.1.5 Conclusions

Model I presents the emergence of drug-resistance in a model for HIV epidemics, under distinct HAART regimes. Numerical simulations of the model for different therapy regimes, namely equal RTI and PI efficacies, as opposed to distinct RTI and PI efficacies, are performed. The results of applying equal drug efficacy therapies points to an optimal treatment, able to reduce drug-sensitive virus and prolonging the emergence of resistance. In this sense, RTI-based and PI-based regimes are simulated. The RTI-based drugs identify higher efficacy RTI drugs, and the later define higher efficacy PI drugs. It is observed that PI-based treatments seem to produce better results in terms of disease progression, than RTI-based ones. This agrees with previous results in the literature.

3.2 Model II

Ana R.M. Carvalho and Carla M.A. Pinto, New developments on AIDS-related cancers: the role of the delay and treatment options, Mathematical Methods in the Applied Sciences, 1–14, DOI: 10.1002/mma.4657, 2017.

A simple delay mathematical model for the dynamics of AIDS-related cancers is proposed, in which HAART and chemotherapy are considered. The model is simple with only 4 cells' populations; nevertheless, it provides biologically reasonable results and important inferences are drawn. The main goals are to determine how the intracellular delay affects the overall cancer growth and how HAART and chemotherapy influence cancer development. Initially, the model is defined and the properties of the model are studied, namely, equilibria and positiveness of solutions. The outcomes of the numerical simulations are discussed.

3.2.1 Description of the model

The model is composed by four populations of cells: cancer cells, C, healthy CD4$^+$ T cells, T, infected CD4$^+$ T cells, I, and HIV, V.

The cancer cells growth follows a 'universal law', i.e., the total number of cancer cells', C, grows with a rate $r_1\left(1-\left(\frac{C}{C_0}\right)^{1-q}\right)C^q$, where r_1 is the growth rate and C_0 is the maximum size of the cancer cell population. Previous studies show that cancer tissue

growth can be described with an exponent q ranging from $2/3$ to 1, depending on the growth conditions and the fractal topology of the neoplastic vascular system. It is considered $q = 3/4$ [72]. Cancer cells are killed by the immune system at rate k_1.

Healthy cells are produced at a rate s_2 and die by apoptosis at a rate μ_1. They also die due to the effect of the cancer cells at rate p, and are infected by HIV at rate k_2. Following infection of HIV, there is a period of 1 day, known as the eclipse phase, before viral RNA is produced. This 'incubation period' is modeled by τ. RTI-based treatment efficacy is included in the CD4$^+$ T cells equations using the parameter $0 \leq \epsilon_{RT} \leq 1$. A value of 1 means 100% treatment efficacy. The infected cells die at a rate μ_I. The virus are produced by the infected CD4$^+$ T cells, with bursting size N. However, this number will be decreased by a factor $(1 - \epsilon_P)$, where $(0 \leq \epsilon_P \leq 1)$ is the PI drug efficacy. The virus die at a rate c.

The nonlinear system of delay differential equations describing the dynamics of the model is:

$$\begin{aligned}
\dot{C}(t) &= r_1 \left(1 - \left(\tfrac{C(t)}{C_0}\right)^{1/4}\right) C(t)^{3/4} - k_1 T(t) C(t) \\
\dot{T}(t) &= s_2 + T(t)\left[r_2\left(1 - \tfrac{C(t)+T(t)+I(t)}{m}\right) - \mu_1 - p k_1 C(t) - (1-\epsilon_{RT}) k_2 V(t)\right] \\
\dot{I}(t) &= (1-\epsilon_{RT}) k_2 T(t-\tau) V(t-\tau) - \mu_I I(t) \\
\dot{V}(t) &= (1-\epsilon_P) N \mu_I I(t) - c V(t)
\end{aligned} \tag{3.17}$$

The proposed model is extended to include the effects of the chemotherapy, $D(t)$, in cancer cell growth. It is assumed that the drugs are effective only at certain phases of the cell cycle and that their effectiveness is bounded. As such, the saturation term $(1 - e^{-D})$, represents the fraction of the cells killed by a dose D of chemotherapy. Cell dose response terms are included in the equations of the cancer, healthy and infected cells, in particular, $P_C(1 - e^{-D})$ and $P_T(1 - e^{-D})$. Function $u(t)$ describes the amount of drug influx into the system and the injection time, assuming intravenous administration [53]. Constant d_D represents the drug elimination rate. It is assumed an instantaneous drug distribution in all body parts. The extended system is thus:

$$
\begin{aligned}
\dot{C}(t) &= r_1\left(1-\left(\tfrac{C(t)}{C_0}\right)^{1/4}\right)C(t)^{3/4} - k_1T(t)C(t) - P_C\left(1-e^{-D(t)}\right)C(t)\\
\dot{T}(t) &= s_2 + T(t)\left[r_2\left(1-\tfrac{C(t)+T(t)+I(t)}{m}\right) - \mu_1 - pk_1C(t) - (1-\epsilon_{RT})k_2V(t) - \right.\\
&\quad \left. -P_T\left(1-e^{-D(t)}\right)\right]\\
\dot{I}(t) &= (1-\epsilon_{RT})k_2T(t-\tau)V(t-\tau) - \mu_II(t) - P_T\left(1-e^{-D(t)}\right)I(t)\\
\dot{V}(t) &= (1-\epsilon_P)N\mu_II(t) - cV(t)\\
\dot{D}(t) &= u(t) - d_DD(t)
\end{aligned}
\tag{3.18}
$$

where

$$
u(t) = \begin{cases} 2.3869, & t = 21n, \qquad n = 1, 2, ... \\ 0, & otherwise \end{cases}
$$

3.2.2 Model properties

Let $X = C([-\tau, 0], \mathbb{R})$ be the Banach space of continuous mapping from $[-\tau, 0]$ to $\mathbb{R}$ equipped with the sup-norm. The initial conditions for system (3.17) are given as follows:

$$
C(\theta) \geq 0, \qquad T(\theta) \geq 0, \qquad I(\theta) \geq 0, \qquad V(\theta) \geq 0, \qquad \theta \in [-\tau, 0] \tag{3.19}
$$

Lema 3.2.1 *Given the initial conditions (3.19), the solutions of* $C(t)$, $T(t)$, $I(t)$, *and* $V(t)$ *remain positive for all* $t \geq 0$.

Proof Considering the CD4^+ T cells, one derives:

$$
T(t) \geq T(0)e^{-\int_0^t(\Theta(\epsilon))d\epsilon} + \int_0^t s_2e^{-\int_\nu^t(\Theta(\epsilon))d\epsilon}d\nu \geq 0 \tag{3.20}
$$

$\Theta(t) = \mu_1 + pk_1C(t) + (1-\epsilon_{RT})k_2V(t)$.

Similarly, for the infected cells:

$$\begin{aligned} I(t) &= I(0)e^{-\int_0^t \mu_I d\epsilon} + \\ &\quad + \int_0^t (1-\epsilon_{RT})k_2 T(\nu-\tau)V(\nu-\tau)e^{-\int_\nu^t \mu_I d\epsilon} d\nu \\ I(t) &\geq I(0)e^{-\int_0^t \mu_I d\epsilon} \geq 0 \end{aligned} \tag{3.21}$$

For the virus population, it is obtained:

$$\begin{aligned} V(t) &= V(0)e^{-ct} + \int_0^t (1-\epsilon_P)N\mu_I I(\nu)e^{-c(t-\nu)}d\nu \\ V(t) &\geq V(0)e^{-ct} \geq 0 \end{aligned} \tag{3.22}$$

For the cancer cell population:

$$C(t) \geq C(0)e^{-\int_0^t k_1 T(\epsilon)d\epsilon} \geq 0 \tag{3.23}$$

this implies that all state variables are non-negative and the solutions of model (3.17) remain positive for all $t \geq 0$.

■

Lema 3.2.2 *The solutions of model (3.17) with initial conditions* $C \geq 0$, $T \geq 0$, $I \geq 0$, *and* $V \geq 0$ *are bounded for all* $t \geq 0$ *in the biologically feasible region defined by the set*

$$\Omega = \left\{ (C,T,I,V) \in \mathcal{R}_+^4 : T, I \leq T^0, V \leq \frac{(1-\epsilon_P)N\mu_I T^0}{c}, C \leq \left(\frac{r_1 C_0^{1/4}}{r_1 + k_1 T^0 C_0^{1/4}} \right)^4 \right\}$$

Proof It is now shown that all feasible solutions are uniformly bounded in Ω. From the CD4$^+$ T cells equation of system (3.17), it is known $T(t) \leq T^0$, where

$$T^0 = \frac{m}{2r_2}\left(r_2 - \mu_1 + \sqrt{(r_2-\mu_1)^2 + \frac{4r_2 s_2}{m}} \right).$$

Moreover, adding the equation of the infected cells, gives:

$$\begin{aligned} \tfrac{dT_{total}}{dt} &= s_2 + T\left[r_2\left(1 - \tfrac{C+T+I}{m}\right) - \mu_1 - pk_1 C \right] - \mu_I I T_{total} \\ &\leq s_2 + T^0 r_2 - \left(\tfrac{T_0}{m} + \mu_1 \right) T_{total} \end{aligned} \tag{3.24}$$

Through integration, it is obtained:

$$T_{total} \leq \frac{K}{A} + \left(T_{Total}(0) - \frac{K}{A} \right) e^{-At} \tag{3.25}$$

where $K = s_2 + T^0 r_2$ and $A = \frac{T_0}{m} + \mu_1$ therefore:

$$\limsup_{t\to\infty} T_{total}(t) \leq \frac{K}{A} \tag{3.26}$$

and T_{total} is bounded. Considering the virus population:

$$\frac{dV}{dt} \leq (1-\epsilon_P) N \mu_I T^0 - cV \tag{3.27}$$

Integration gives:

$$V(t) \leq \frac{(1-\epsilon_P) N \mu_I T^0}{c} + \left(V(0) - \frac{(1-\epsilon_P) N \mu_I T^0}{c} \right) e^{-ct} \tag{3.28}$$

and:

$$\limsup_{t\to\infty} V(t) \leq \frac{(1-\epsilon_P) N \mu_I T^0}{c} \tag{3.29}$$

hence $V(t)$ is bounded. From the equation of the cancer cells of system (3.17), one gets:

$$\frac{dC}{dt} \leq C \left[r_1 C^{-1/4} \left(1 - \left(\frac{C}{C_0} \right)^{1/4} \right) - k_1 T^0 \right] = \frac{C \left[r_1 C_0^{1/4} - r_1 C^{1/4} - k_1 T^0 C_0^{1/4} C^{1/4} \right]}{C_0^{1/4} C^{1/4}} \tag{3.30}$$

Integration gives:

$$C(t) \leq \left(\frac{r_1 C_0^{1/4} - \exp\left(\left(-\frac{r_1 + k_1 T^0 C_0^{1/4}}{4 C_0^{1/4}} \right) t \right)}{r_1 + k_1 T^0 C_0^{1/4}} \right)^4 \tag{3.31}$$

thus,

$$\limsup_{t\to\infty} C(t) \leq \left(\frac{r_1 C_0^{1/4}}{r_1 + k_1 T^0 C_0^{1/4}} \right)^4 \tag{3.32}$$

therefore $C(t)$ is also bounded.

Our invariant region is therefore defined by Ω. Hence, any solution of system (3.17) that starts in the positive orthant $\mathcal{R}^4_+$ at $t \geq 0$ will approach it asymptomatically. Hence, Ω is positively invariant and attracting with respect to model (3.17).

■

Next, the equilibria of model (3.17) are calculated. It is assumed a quasi-steady state for the viral population, obtaining:

$$V^\star = \frac{(1-\epsilon_P)N\mu_I I^\star}{c} \tag{3.33}$$

Substituting $V^\star$ in the equation of the I cells in model (3.17), one gets:

$$I^\star \left[\frac{(1-\epsilon_{RT})k_2(1-\epsilon_P)N\mu_I T^\star}{c} - \mu_I \right] = 0 \tag{3.34}$$

which implies:

$$I^\star = 0 \qquad or \qquad T^\star = \frac{c\mu_I}{(1-\epsilon_{RT})k_2(1-\epsilon_P)N\mu_I} \tag{3.35}$$

For $I^\star = 0$, the system (3.17) is at an HIV-free cancer equilibrium state. The full endemic state is of the form $P = (C^\star, T^\star, I^\star, V^\star)$, in which HIV and cancer are simultaneously present in the organism.

First, the solution $T^\star$ was replaced in the equation of the T cells in model (3.17). From this equation can derive the value of V at equilibrium, obtaining:

$$V^\star = \frac{s_2 + T^\star \left[r_2 \left(1 - \frac{C^\star + T^\star + I^\star}{m} \right) - \mu_1 - pk_1 C^\star \right]}{(1-\epsilon_{RT})k_2 T^\star} \tag{3.36}$$

Now, from equation (3.33):

$$I^\star = cm \left[\frac{s_2 + T^\star \left[r_2 \left(1 - \frac{C^\star + T^\star}{m} \right) - \mu_1 - pk_1 C^\star \right]}{m(1-\epsilon_{RT})k_2 T^\star (1-\epsilon_P)N\mu_I + cr_2 T^\star} \right] \tag{3.37}$$

Now, it turns to the cancer cells' equation in model (3.17).

$$g(C) = C \left[r_1 C^{-1/4} \left(1 - \left(\frac{C}{C_0} \right)^{1/4} \right) - k_1 T^\star \right] = 0 \tag{3.38}$$

whose solutions are:

$$C^\star = 0 \qquad or \qquad r_1 C^{-1/4}\left(1-\left(\frac{C}{C_0}\right)^{1/4}\right) - k_1 T^\star = 0 \tag{3.39}$$

Now, $g(C)$ is defined at equilibrium, getting:

$$g(C^\star) = r_1 C^{-1/4}\left(1-\left(\frac{C}{C_0}\right)^{1/4}\right) - k_1 T^\star \tag{3.40}$$

It should be noted that only the cancer-free equilibrium point is explicitly obtained. Thus, the disease-free equilibrium is given by $P_0 = (C_0, T_0, I_0, V_0) = (0, T_0, 0, 0)$, where $T_0 = \frac{m}{2r_2}\left(B + \sqrt{B^2 + \frac{2r_2 s_2}{m}}\right)$ and $B = r_2 - \mu_1$.

The cancer-free equilibrium is written as: $P_1 = (0, T_1, I_1, V_1)$, where

$T_1 = \frac{c\mu_I}{(1-\epsilon_{RT})k_2(1-\epsilon_P)N\mu_I}$, $I_1 = cm\left(\frac{s_2+T_1\left[r_2\left(1-\frac{T_1}{m}\right)-\mu_1\right]}{m(1-\epsilon_{RT})k_2T_1(1-\epsilon_P)N\mu_I+cr_2T_1}\right)$ and

$V_1 = \frac{s_2+T_1\left[r_1\left(1-\frac{T_1+I_1}{m}\right)-\mu_1\right]}{(1-\epsilon_{RT})k_2T_1}$.

3.2.3 Numerical results

In this section, models (3.17) and (3.18) are simulated. The parameters used in the simulations are given in Table 3.2 and the initial conditions are set to $C(0) = 100$ mL^{-1}, $T(0) = 5 \times 10^5$ mL^{-1}, $I(0) = 100$ mL^{-1} and $V(0) = 1000$ mL^{-1}.

Parameter	Value	Units	Reference
r_1	0.18	day^{-1}	[69]
m	1500×10^3	mL^{-1}	[69]
k_1	10^{-8}	mL^{-1} day^{-1}	[69]
r_2	0.03	day^{-1}	[69]
p	0.1		[69]
k_2	2.4×10^{-7}	mL^{-1} day^{-1}	[31]
μ_I	0.3	day^{-1}	[69]
N	1000	mL^{-1}	[33]
c	3	day^{-1}	[30]
τ	varied		
P_C	0.9	day^{-1}	[35]
P_T	0.6	day^{-1}	[35]
d_D	0.9	day^{-1}	[35]
ϵ_{RT}	$[0, 1]$		
ϵ_P	$[0, 1]$		
C_0	10^6	day^{-1}	[72]
s_2	10000	mL^{-1} day^{-1}	[30]
μ_1	0.02	day^{-1}	[30]

Table 3.2: Parameters used in the numerical simulations of models (3.17) and (3.18).

Results with no chemotherapeutic drug

The numerical results of model (3.17) are presented. Figures 3.7-3.8 depict the density of the cancer cells and of HIV at days 350, 1000 and 2000, for several combinations of HAART efficacies, ϵ_{RT} and ϵ_P, and $\tau = 1$. One can observe that the number of cancer cells decreases for a combination of RTI and PI with efficacies above 0.85. HIV has a slight different pattern, in which more severity is seen for smaller values of ϵ_{RT} and $\epsilon_P < 0.92$. As ϵ_{RT} increases and for $\epsilon_P > 0.9$, HAART is more effective. Moreover, the number of CD4$^+$ T cells increases for higher values of ϵ_{RT} and ϵ_P, whereas the infected T cells decrease. These results are epidemiologically valid.

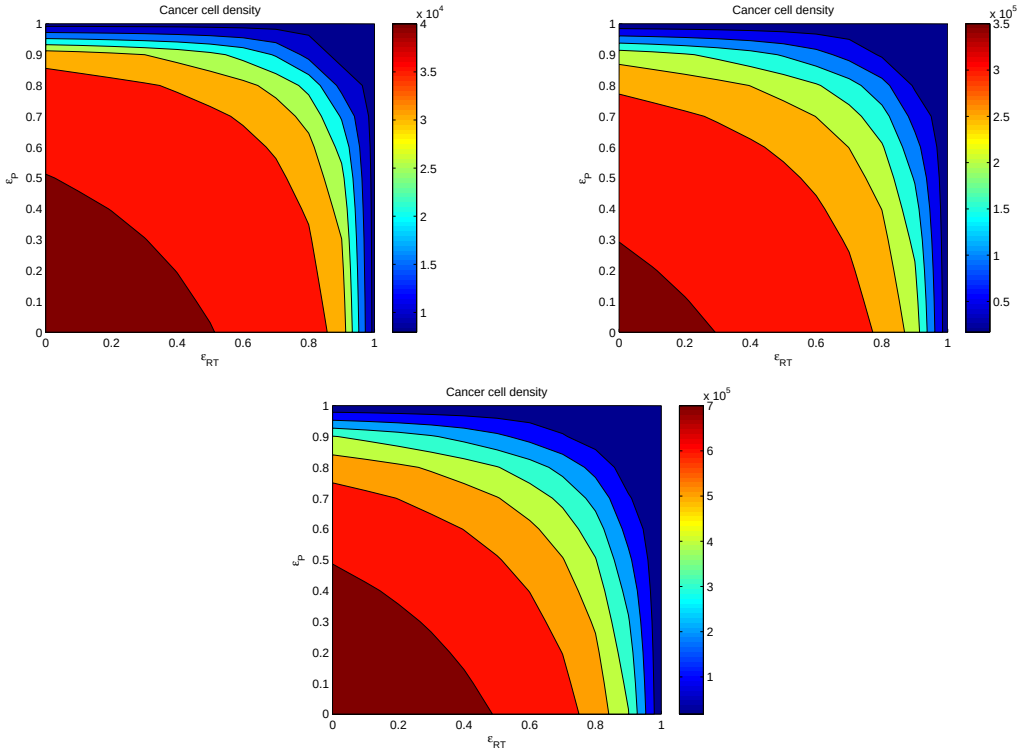

Figure 3.7: Contour plot showing cancer cells after 350, 1000 and 2000 days, for various combinations of RTI and PI treatments, and $\tau = 1$. For more information, see text.

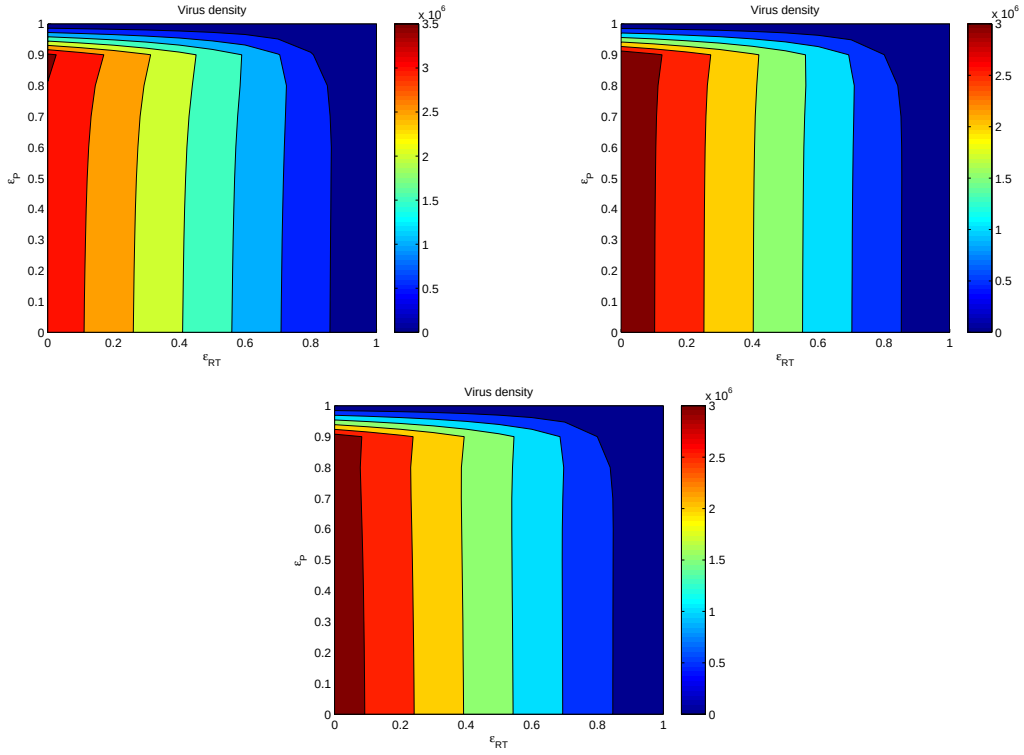

Figure 3.8: Contour plot showing virus density after 350, 1000 and 2000 days, for various combinations of RTI and PI treatments, and $\tau = 1$. For more information, see text.

Figures 3.9-3.10 depict the densities of the cancer cells and of virus for distinct combination therapies and different values of τ. There is not a substantial variation on the patterns of the cancer cells and of virus for $\tau > 0$. For $\tau = 0$, the coinfection is less endemic, namely, the number of cancer cells and of HIV is small. The behaviour seen for HIV when $\tau = 0$ agrees with previous works on the efficacies of HAART. PI-based treatments appear to be more effective in fighting HIV [22, 48]. Nevertheless, this was observed in non-delay models. Since there is an eclipse phase [78, 57], the delay exists and as can be observed from the numerical simulations, it is considerably important in the dynamics of the cancer growth and of HIV infection.

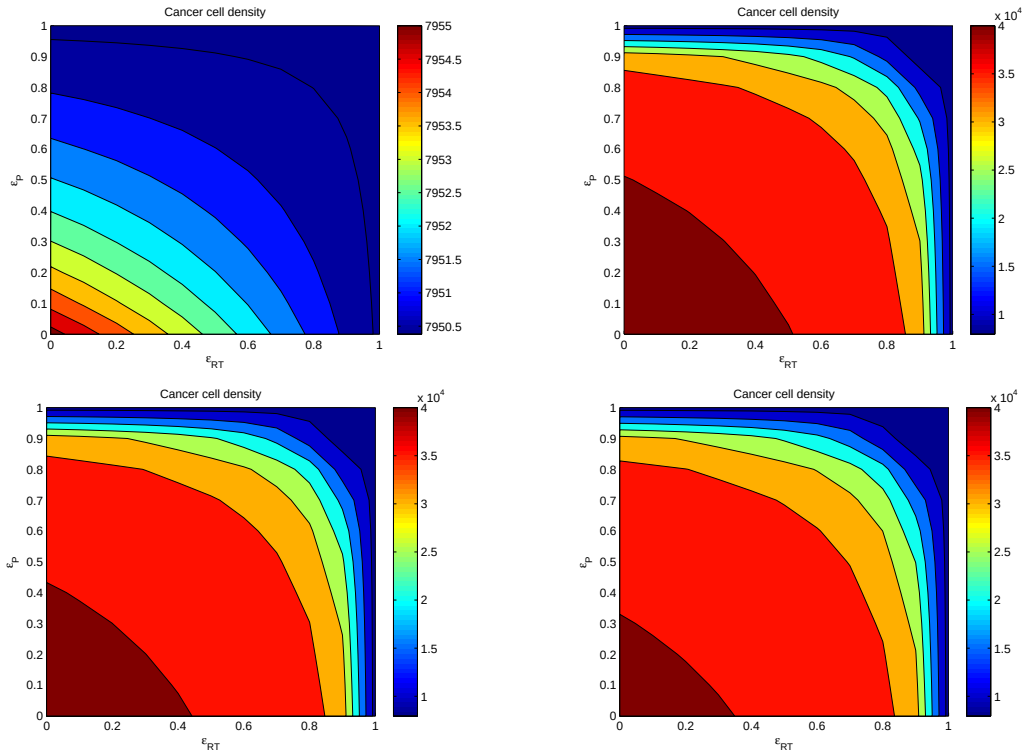

Figure 3.9: Contour plot showing cancer cells after 350 days for distinct values of τ (Top left - $\tau = 0$, Top right - $\tau = 1$, Bottom left - $\tau = 5$, Bottom right - $\tau = 10$). For more information, see text.

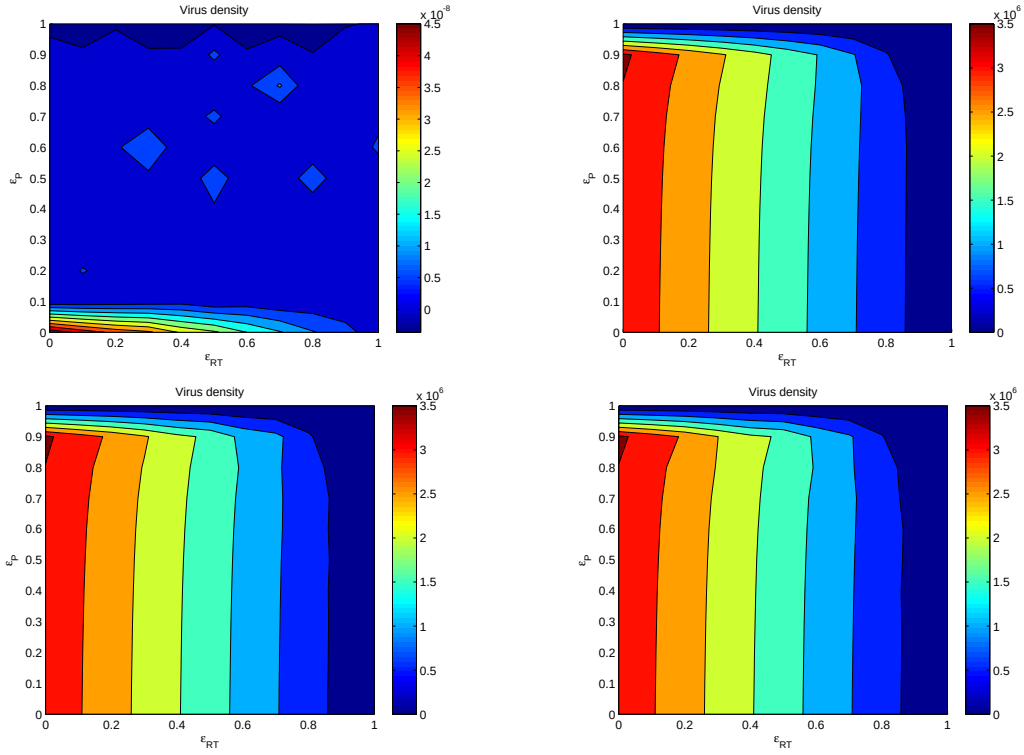

Figure 3.10: Contour plot showing virus after 350 days for distinct values of the τ (Top left - $\tau = 0$, Top right - $\tau = 1$, Bottom left - $\tau = 5$, Bottom right - $\tau = 10$). For more information, see text.

Figure 3.11 depicts the time series of the variables of model (3.17) for different values of the delay, τ, and in the presence of HAART. It can be seen that the model bifurcates from a disease-free state to an endemic state as the delay, τ, increases from 0. Moreover, the severity of the endemic state reduces with τ. In particular, for $\tau = 10$, the number of infected T cells and of virus is significantly smaller on the transient, than for $\tau = 1,\ 5$, though the asymptotic value is the same. With respect to cancer cells, there is a slight decrease for $\tau = 10$, in comparison to $\tau = 1,\ 5$. It is worth noting that higher values of HIV peaks induce lower immune responses and heavier and difficult to treat HIV-related illnesses and co-morbidities.

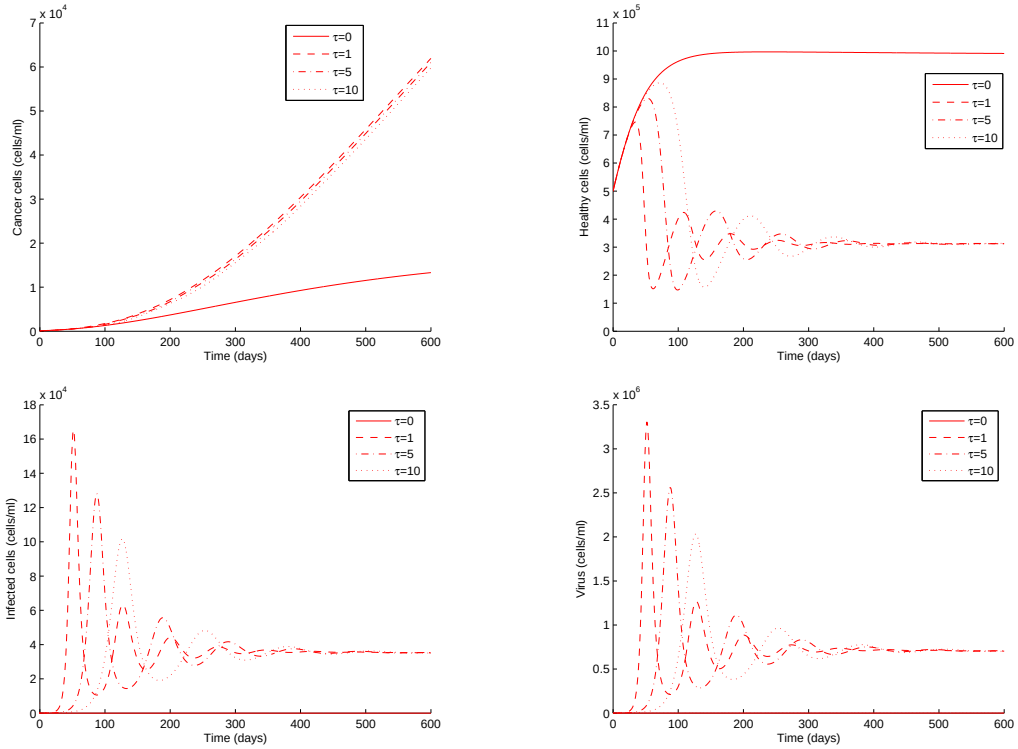

Figure 3.11: Time series of the variables of system (3.17) for different values of τ. Parameter values and initial conditions are given in the text, except $\epsilon_{RT} = \epsilon_P = 0.8$.

Figure 3.12 shows the reduction curves representing the cancer cells after time $t = 350,\ 1000,\ 2000$ days, for various values of HAART efficacy, $\epsilon_{RT} = \epsilon_P$. This figure suggests that early HAART initiation is preferred, since a decline of the cancer cells' number is achieved for higher values of the treatment efficacy.

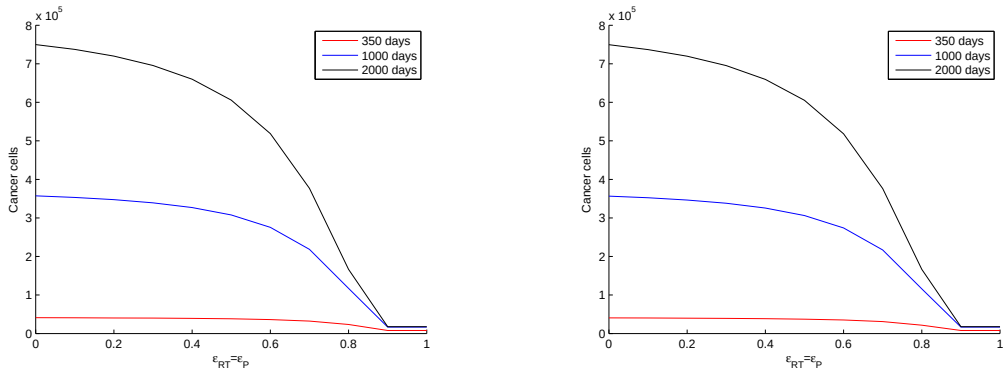

Figure 3.12: Variation of the number of the cancer cells after time $t = 350,\ 1000, 2000$ days, for $\epsilon_{RT} = \epsilon_P \in [0, 1]$ and $\tau = 1$ (Left) and $\tau = 10$ (Right). Parameter values and initial conditions are given in the text.

Figure 3.13 shows the time series of the variables of model (3.17) for distinct values of $\epsilon_{RT} = \epsilon_P$. As the efficacy increases, the concentration of cancer cells, infected cells and virus decrease. On the other hand, the concentration of healthy cells increases. In Figure 3.14, a similar analysis is done for $\epsilon_{RT} + \epsilon_P = 0.9$. Results reveal that if one of the drugs (ϵ_{RT} or ϵ_P) is high enough then lower number of cancer cells and higher CD4$^+$ T cells concentrations are obtained, despite higher viral loads. Designing of new chemotherapies and HAART in HIV-infected patients with AIDS-related cancers, may also take into account this valuable information. A compromise between cancer cells' declining and smaller viral loads must be achieved.

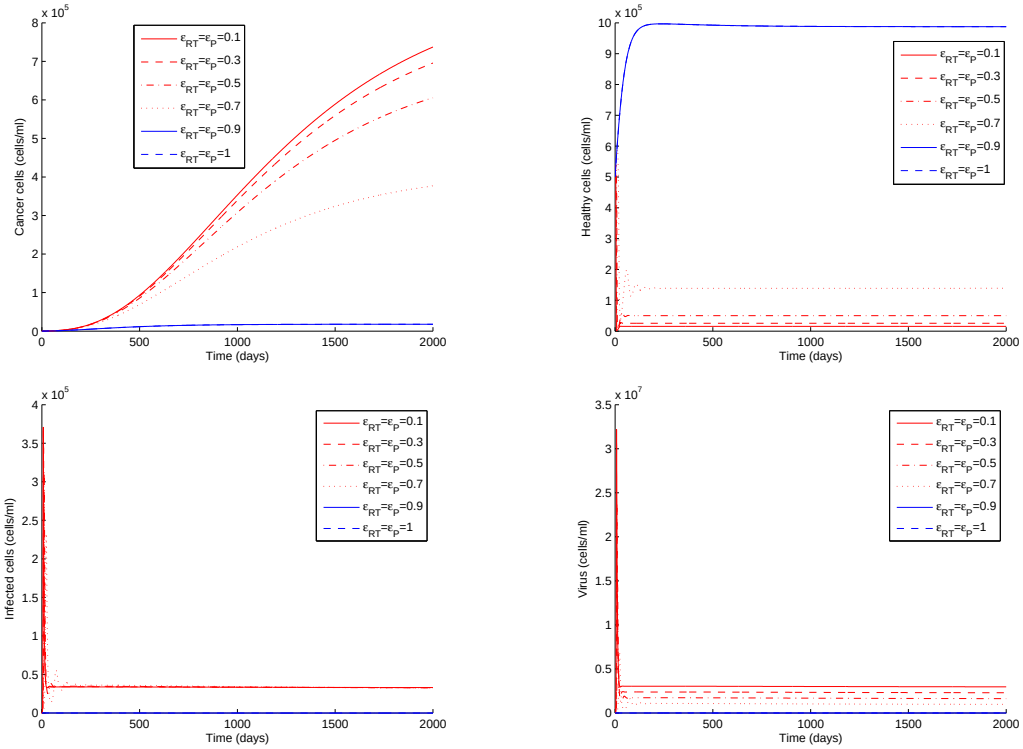

Figure 3.13: Dynamics of the variables of system (3.17) for different values of $\epsilon_{RT} = \epsilon_P$. Parameter values and initial conditions are given in the text, except $\tau = 1$.

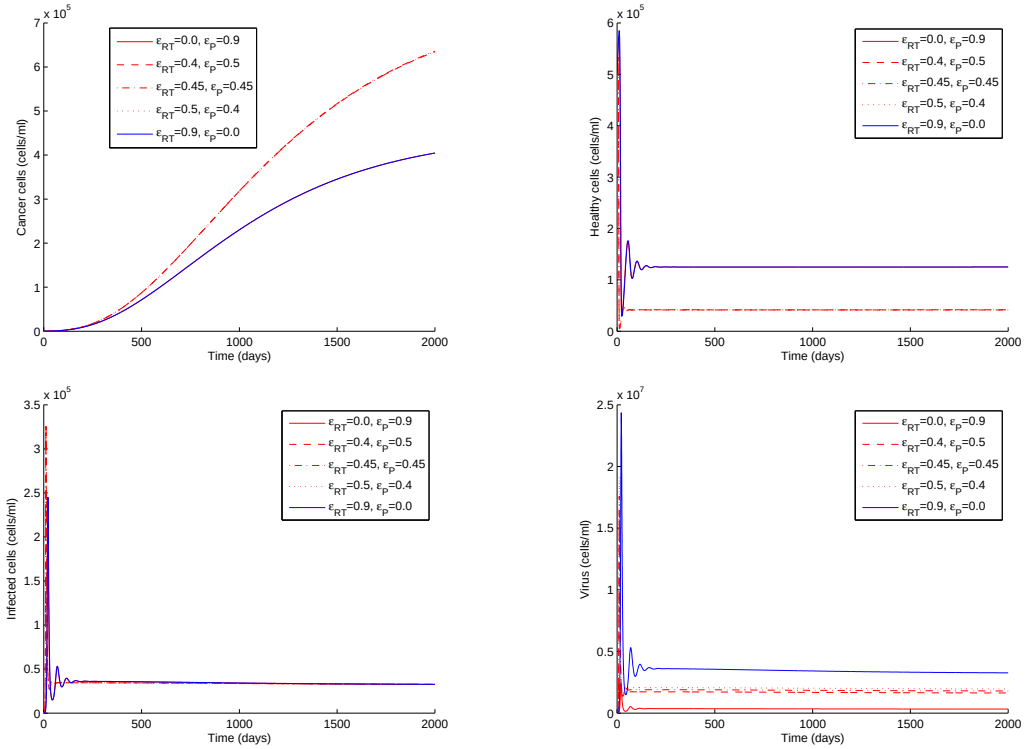

Figure 3.14: Dynamics of the variables of system (3.17) for different values of $\epsilon_{RT}+\epsilon_P = 0.9$. Parameter values and initial conditions are given in the text, except $\tau = 1$.

Figure 3.15 clearly suggests that in the presence of smaller HIV infection rates, HAART reduces cancer growth, even when HAART efficacy is only 50%. Whereas for higher HIV infection rates, higher values of ϵ_{RT} and ϵ_P are needed to prevent cancer development. Nowadays, HAART efficacies are high. In particular, the efficacy of an integrase inhibitor, named Raltegravir, was estimated to 0.94, when combined with emtricitabine and tenofovir disoproxil fumarate, and 0.997 during monotherapy [31]. Thus, HIV-infected patients with AIDS-related cancers surely benefit from full adherence to HAART treatment protocol.

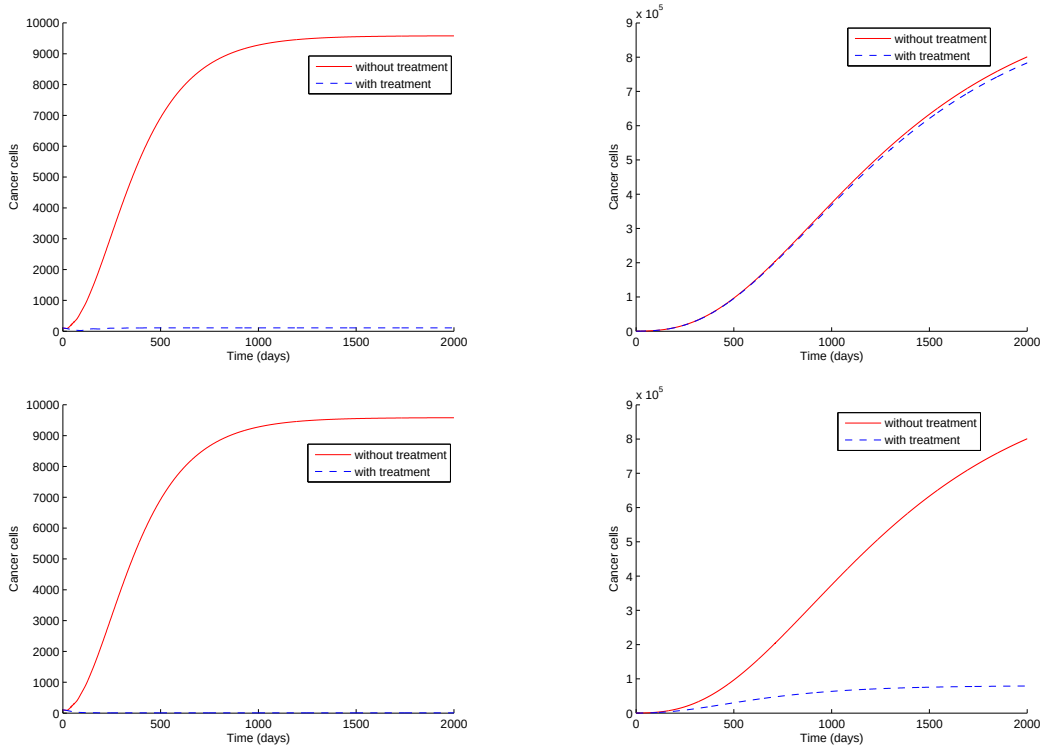

Figure 3.15: Dynamics of the cancer cells of system (3.17) for two values of the HIV infection rate, (Left - $k_2 = 2.4 \times 10^{-8}$, Right - $k_2 = 2.4 \times 10^{-5}$) . Two cases were considered: HAART with two efficacies $\epsilon_{RT} = \epsilon_P = 0.5$ (Top) and $\epsilon_{RT} = \epsilon_P = 0.95$ (Bottom), and without HAART ($\epsilon_{RT} = \epsilon_P = 0$). Parameter values and initial conditions are given in the text, except $\tau = 1$.

Figure 3.16 shows several plots of the function $g(C)$ as a function of C, for distinct values of the cancer killing rate, k_1. Each trajectory represents different values of k_1, which increase from top to bottom trajectory/line. The values considered were in the range 1×10^{-9} to 2×10^{-8} and the step size was 1×10^{-9}, for the two cases considered: with and without HAART. HAART is a key factor in cancer growth control, as can be seen by the magnitude of the values of C that zeroes the function $g(C)$. Smaller $C^\star$ are obtained when treatment is considered, thus lowering the values of $V^\star$ (3.36) and $I^\star$ (3.37).

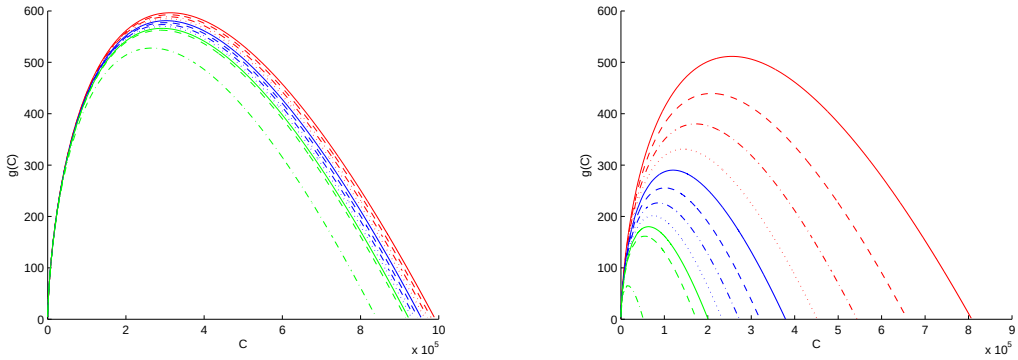

Figure 3.16: Plot of the function $g(C)$ for different values of k_1, the rate of cancer cells loss, without HAART (Left - $\epsilon_{RT} = \epsilon_P = 0$) and with HAART (Right - $\epsilon_{RT} = \epsilon_P = 0.8$). Parameter values and initial conditions are given in the text, except $\tau = 1$.)

Results with chemotherapeutic drug

The results of the simulations of model (3.18) are discussed. Figures 3.17 show the chemotherapeutic drug administration pattern, for distinct values of d_D.

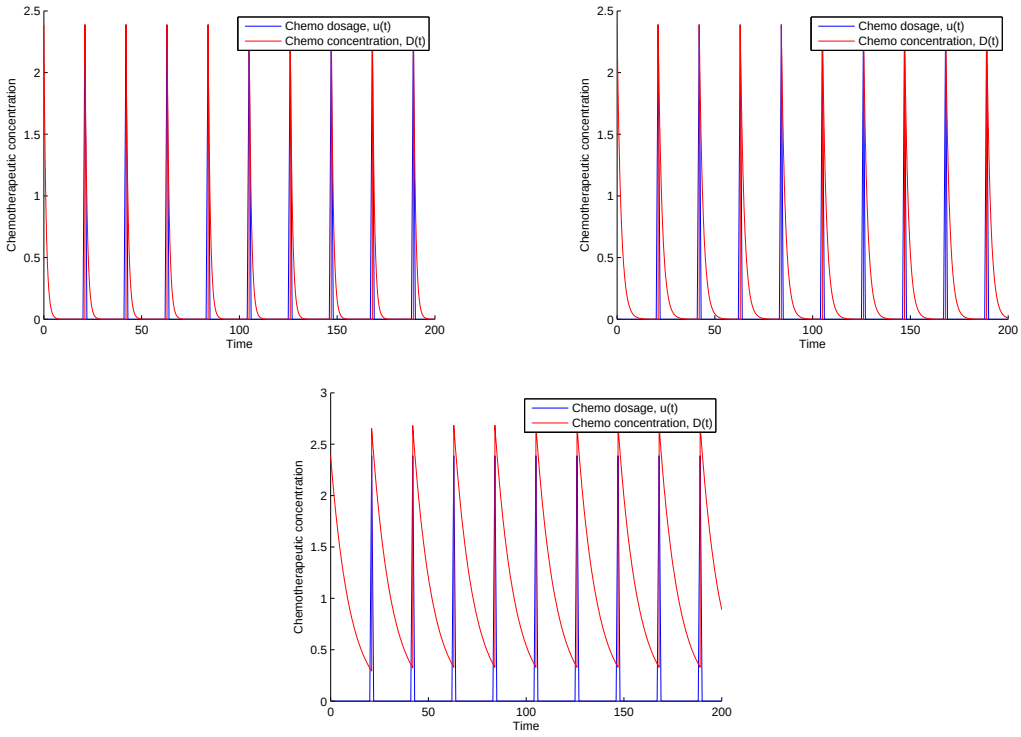

Figure 3.17: Chemotherapeutic drug dose concentration for $\tau = 1$ and different values of d_D, the drug elimination rate (Top left - $d_D = 0.9$, Top right - $d_D = 0.5$, Bottom - $d_D = 0.1$). Parameter values are given in the text, except $\epsilon_{RT} = \epsilon_P = 0.8$. The initial conditions are set to $C(0) = 10^5$ mL^{-1}, $T(0) = 3 \times 10^5$ mL^{-1}, $I(0) = 10^3$ mL^{-1} and $V(0) = 4 \times 10^3$ mL^{-1}.

The concentration of the cancer cells for various values of d_D is given in Fig. 3.18. The chemotherapy effectiveness is highly dependable on the values of the drug decay rates. The simulations of the model suggest that the administration of the same therapeutic dosage is followed by distinct outcomes, with respect to cancer growth, when various decay rates are considered. Smaller decay rates promote higher elimination of cancer cells. Future chemotherapeutic protocols should take this into consideration.

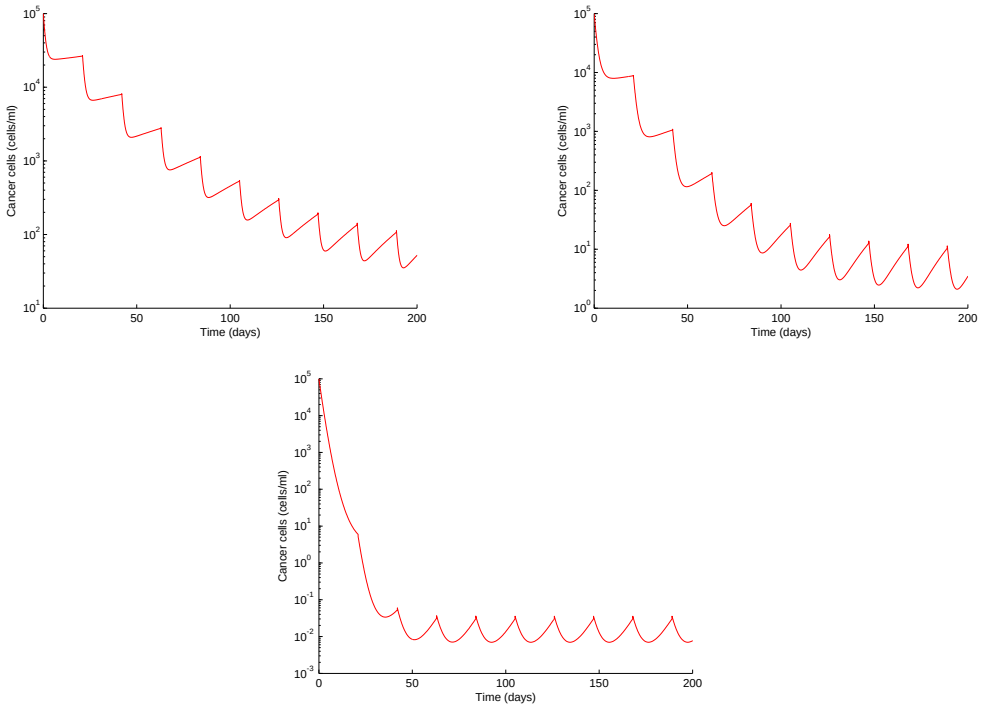

Figure 3.18: Variation of the cancer cells for $\tau = 1$ and distinct values of the d_D (Top left - $d_D = 0.9$, Top right - $d_D = 0.5$, Bottom - $d_D = 0.1$). Parameter values are given in the text, except $\epsilon_{RT} = \epsilon_P = 0.8$. Initial conditions are set to $C(0) = 10^5$ mL^{-1}, $T(0) = 3 \times 10^5$ mL^{-1}, $I(0) = 10^3$ mL^{-1} and $V(0) = 4 \times 10^3$ mL^{-1}.

3.2.4 Conclusions

Model II proposes a simple delay mathematical model for the dynamics of AIDS-related cancer in the presence of HAART and chemotherapy. The equilibria of the model are computed. The model is simulated for relevant parameters and its behaviour is scrutinized in the presence and absence of HAART and chemotherapy. Results show that HAART may benefit HIV-infected patients not only by reducing HIV viral load but by controlling cancer cell growth. Moreover, the chemotherapy effectiveness is highly dependable on the values of the drug decay rates. Smaller decay rates promote higher elimination of cancer cells. The delay is also a principal actor in cancer cells growth, influencing the immune response to cancer development. Similarly to every mathematical model, the current one could be a simplified version of a much more complex model of the biological mechanisms, behind AIDS-related cancers growth. Relevant factors to include in such a model would be, for e.g., the contribution of the spatial dynamics of the tumour in growth control.

Chapter 4

Models for coinfection of HIV and HCV

4.1 Model III

A.R.M. Carvalho and C.M.A. Pinto, A coinfection model for HIV and HCV, BioSystems 124, 46–60, 2014.

A mathematical model for the dynamics of HIV and HCV coinfection is proposed. This model intends to study the effect of the treatment for both diseases and vertical transmission from mother to child, in the case of HIV. HIV and HCV share several transmission routes, nevertheless, here only it is considered sexual transmission for HIV and HCV and vertical transmission for HIV. The reproduction numbers and the local and global stability of the disease free equilibrium are computed. Bifurcation diagrams are presented that reveal the dynamical behavior of the model for variation of relevant parameters. Simulation results of the full model are presented.

4.1.1 Description of the model

The population of the model includes nine classes, namely, the susceptible individuals, S, the individuals infected with HIV, I_a, the individuals showing symptoms of AIDS, A_a, the individuals infected with HCV, I_c, the individuals infected with chronic HCV, C_c, the individuals coinfected with HIV and HCV, I_aI_c, the individuals coinfected with HIV and with chronic HCV, I_aC_c, the individuals showing symptoms of AIDS and coinfected with HCV, A_aI_c, and the individuals showing symptoms of AIDS and with chronic HCV coinfection, A_aC_c.

In Figure 4.1 it is presented the flow chart of the model. It represents schematically the epidemiology of HIV and HCV coinfection. The different disease stages are reproduced by the different compartments (rectangles) and the arrows indicate the way individuals progress from one stage to the other.

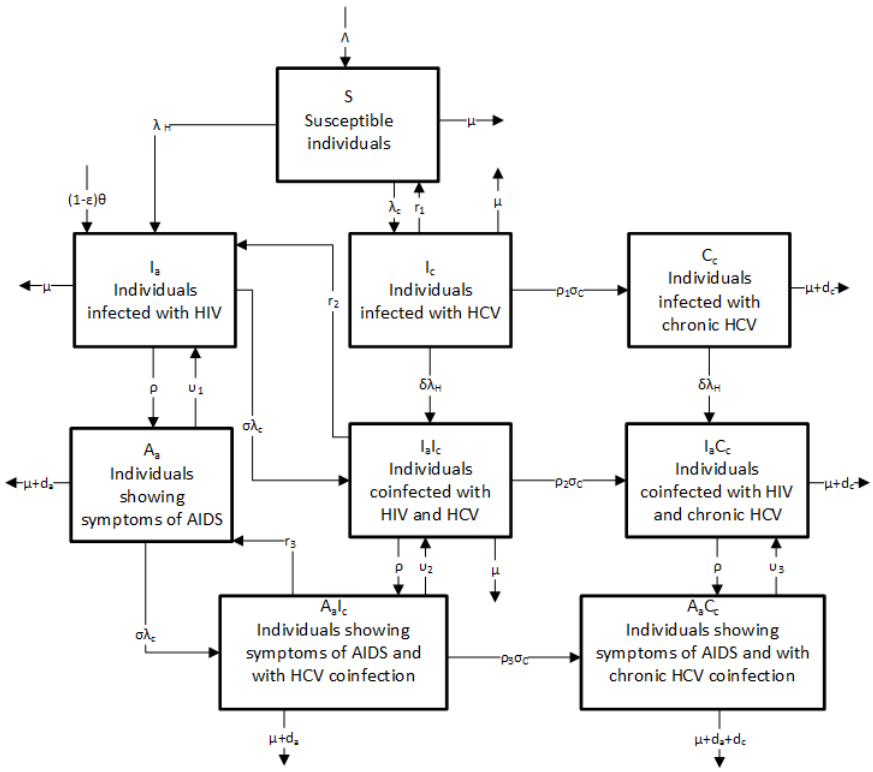

Figure 4.1: Flow chart of the model.

At time t, the population of size $N(t)$, has constant inflow of susceptible individuals, S, at a rate Λ. For all classes, the natural mortality rate is μ. Susceptible individuals, S, exposed to HIV, move to class I_a, at a rate λ_H, given by:

$$\lambda_H = \frac{cb_h(I_a + A_a + \sigma_3(I_aI_c + I_aC_C))}{N}$$

Parameter b_h is the effective sexual contact rate for HIV infection to occur, and c is the average number of sexual partners per unit of time. On the other hand, when in contact with HCV patients, susceptible individuals, S, move to class I_c, at a rate:

$$\lambda_C = \frac{cb_c(I_c + C_c + \eta_1 I_aI_c + \eta_2 I_aC_c)}{N}$$

where parameter b_c is the effective contact rate for HCV infection to occur. Parameters $\eta_1, \eta_2, \sigma_3 > 1$ model the fact that dually infected individuals are more infectious than their corresponding counterparts.

A fraction of newborns are infected with HIV during birth and hence are directly recruited into the infectious class, I_a, at a rate $(1-\epsilon)\theta$. Other children die at birth $(0 \leq \epsilon \leq 1)$, where ϵ is the fraction of newborns infected with HIV that die immediately after birth, and θ is the rate of newborns infected with HIV. The individuals infected with HIV, I_a, move at a rate ρ to the AIDS class, A_a. Individuals showing symptoms of AIDS are treated at a rate υ_1, and die because of AIDS at a rate d_a.

The individuals infected with HCV, I_c move to the susceptible class, S, after treatment at a rate r_1. They can progress to a chronic stage, C_c, at a rate $\rho_1\sigma_C$, where ρ_1 is the proportion of infected individuals who are chronic carriers and $\frac{1}{\sigma_C}$ is the average time that an individual infected with HCV remains in a state of acute infection. The individuals with chronic HCV infection, C_c, die because of HCV at a rate d_c.

Now the dynamics of the coinfection are defined. The individuals infected with HIV, I_a, are infected with HCV at a rate $\sigma\lambda_C$ and move to class I_aI_c. Modification parameter $\sigma > 1$ accounts for the fact that there is an increased risk of getting HCV for someone already infected with HIV, due to the vulnerability of the immune system. Reciprocally, the individuals infected with HCV, I_c are infected with HIV at a rate $\delta\lambda_H$ and move to the class I_aI_c. Parameter $\delta > 1$ accounts for the increased susceptibility to HIV infection for HCV infected people, since HCV accelerates the decline of the immune function. Dually infected individuals, I_aI_c, recover from HCV infection at a rate r_2 and move to class I_a. On the other hand, they can progress to AIDS at a rate ρ and move to class A_aI_c. Moreover, I_aI_c individuals may become HCV chronic carriers, at a rate $\rho_2\sigma_C$, and move to class I_aC_c. Parameter ρ_2 is the proportion of dually infected individuals who are chronic carriers. Dually HIV and chronic HCV infected individuals, I_aC_c, may progress to AIDS at a rate ρ and move to class A_aC_c.

Individuals showing symptoms of AIDS, A_a, are infected with HCV at a rate $\sigma\lambda_C$ and move to class A_aI_c. The individuals in class A_aI_c are treated and recover from HCV infection at a rate r_3 and move to class A_a or are treated and recover from AIDS stage at a rate υ_2 and move to class I_aI_c. The individuals in class A_aI_c become HCV chronic carriers at a rate $\rho_3\sigma_C$ and move to class A_aC_c. Parameter ρ_3 is the proportion of individuals in A_aI_c class who are chronic carriers. Individuals showing symptoms of AIDS and with chronic HCV coinfection, A_aC_c, are treated for HIV at a rate υ_3, and move to I_aC_c.

The following nonlinear system of ordinary differential equations summarizes the description of the model:

$$
\begin{aligned}
\tfrac{dS}{dt} &= \Lambda - \lambda_H S - \lambda_C S + r_1 I_c - \mu S \\
\tfrac{dI_a}{dt} &= \lambda_H S - (\rho + \sigma\lambda_C + \mu) I_a + (1-\epsilon)\theta I_a + r_2 I_a I_c + \upsilon_1 A_a \\
\tfrac{dA_a}{dt} &= \rho I_a - (\upsilon_1 + d_a + \mu) A_a + r_3 A_a I_c - \sigma\lambda_C A_a \\
\tfrac{dI_c}{dt} &= \lambda_C S - (r_1 + \delta\lambda_H + \rho_1\sigma_C + \mu) I_c \\
\tfrac{dC_c}{dt} &= \rho_1\sigma_C I_c - (\delta\lambda_H + \mu + d_c) C_c \\
\tfrac{dI_a I_c}{dt} &= \delta\lambda_H I_c + \sigma\lambda_C I_a + \upsilon_2 A_a I_c - (r_2 + \rho + \rho_2\sigma_C + \mu) I_a I_c \\
\tfrac{dI_a C_c}{dt} &= \rho_2\sigma_C I_a I_c + \delta\lambda_H C_c + \upsilon_3 A_a C_c - (\rho + \mu + d_c) I_a C_c \\
\tfrac{dA_a I_c}{dt} &= \sigma\lambda_C A_a + \rho I_a I_c - (r_3 + \upsilon_2 + \rho_3\sigma_C + \mu + d_a) A_a I_c \\
\tfrac{dA_a C_c}{dt} &= \rho_3\sigma_C A_a I_c + \rho I_a C_c - (\upsilon_3 + \mu + d_a + d_c) A_a C_c
\end{aligned}
\tag{4.1}
$$

The dynamics of the total population $N(t) = S(t) + I_a(t) + A_a(t) + I_c(t) + C_c(t) + I_a I_c(t) + I_a C_c(t) + A_a I_c(t) + A_a C_c(t)$ is given by:

$$\tfrac{dN}{dt} = \Lambda + (1-\epsilon)\theta I_a - \mu N - d_a(A_a + A_a I_c + A_a C_c) - d_c(C_c + I_a C_c + A_a C_c)$$

In Table 4.1, it summarizes the parameters and the variables of model (4.1).

Variable/Parameter	Description
S	Susceptible individuals
I_a	Individuals infected with HIV
A_a	Individuals showing symptoms of AIDS
I_c	Individuals infected with HCV
C_c	Individuals infected with chronic HCV
I_aI_c	Individuals coinfected with HIV and HCV
I_aC_c	Individuals coinfected with HIV and chronic HCV
A_aI_c	Individuals showing symptoms of AIDS and with HCV coinfection
A_aC_c	Individuals showing symptoms of AIDS and with chronic HCV coinfection
Λ	Recruitment rate
μ	Natural mortality rate
c	Average number of sexual partners
b_h	Effective sexual contact rate for HIV transmission to occur
b_c	Effective sexual contact rate for HCV transmission to occur
σ_3	Modification parameter
$\eta_i, = 1, 2$	Modification parameter
$r_i\ i = 1, 2, 3$	HCV treatment rates
$\rho_i, i = 1, 2, 3$	Proportion of infected individuals who are chronic carries
d_c	Mortality due to HCV
ϵ	Fraction of newborns infected with HIV that die immediately after birth
θ	Rate of newborns infected with HIV
ρ	Rate of progression to AIDS
$\upsilon_i, i = 1, 2, 3$	HIV treatment rate
d_a	Mortality due to HIV
σ	Modification parameter
δ	Modification parameter
$\frac{1}{\sigma_C}$	Average time that an individual infected with HCV remains in a state of acute infection

Table 4.1: Description of the variables and the parameters of model (4.1).

4.1.2 Reproduction numbers and stability of disease-free equilibria

In this subsection, the reproduction number of model (4.1), R_0, is calculated. The basic reproduction number is defined as the number of secondary infections due to a single infection in a completely susceptible population [150].

Initially two sub-models of model (4.1) are considered. Model (4.2) is obtained from

model (4.1) by setting the variables concerning HCV dynamics (I_c, C_c, I_aI_c, I_aC_c, A_aI_c and A_aC_c) to zero, and model (4.4) follows from model (4.1) by setting the variables concerning HIV dynamics (I_a, A_a, I_aI_c, I_aC_c, A_aI_c and A_aC_c) to zero.

It starts by computing the reproduction number of the system (4.2), R_{HIV}. The next generation method [150] is used.

$$\begin{aligned} \frac{dS}{dt} &= \Lambda - \lambda_H S - \mu S \\ \frac{dI_a}{dt} &= \lambda_H S - (\rho + \mu) I_a + (1-\epsilon)\theta I_a + \upsilon_1 A_a \\ \frac{dA_a}{dt} &= \rho I_a - (\upsilon_1 + d_a + \mu) A_a \end{aligned} \tag{4.2}$$

where $\lambda_H = \frac{cb_h(I_a + A_a)}{N}$

The disease free equilibrium of model (4.2) is given by:

$$P_0^1 = \left(S_0^1, I_{a0}^1, A_{a0}^1,\right) = \left(\frac{\Lambda}{\mu}, 0, 0\right)$$

Using the notation in [150] on system (4.2), matrices for the new infection terms, F, and the other terms, V, are given by:

$$F = \begin{bmatrix} cb_h & cb_h \\ 0 & 0 \end{bmatrix}$$

$$V = \begin{bmatrix} \rho + \mu - (1-\epsilon)\theta & -\upsilon_1 \\ -\rho & \upsilon_1 + d_a + \mu \end{bmatrix}$$

The associative basic reproduction number is given by:

$$R_{HIV} = \rho(FV^{-1}) = \frac{b_h c(\upsilon_1 + d_a + \mu + \rho)}{\rho(d_a + \mu) + (\mu - (1-\epsilon)\theta)(\upsilon_1 + d_a + \mu)} \tag{4.3}$$

where ρ indicates the spectral radius of FV^{-1}. By Theorem 2 in [150], the following lemma is obtained.

Lema 4.1.1 *The disease free equilibrium P_0^1 is locally asymptotically stable if $R_{HIV} < 1$ and unstable if $R_{HIV} > 1$.*

The computation of the reproduction number of submodel (4.4) below, R_{HCV}, follows.

$$\begin{aligned} \frac{dS}{dt} &= \Lambda - \lambda_C S + r_1 I_c - \mu S \\ \frac{dI_c}{dt} &= \lambda_C S - (r_1 + \rho_1 \sigma_C + \mu) I_c \\ \frac{dC_c}{dt} &= \rho_1 \sigma_C I_c - (\mu + d_c) C_c \end{aligned} \tag{4.4}$$

where $\lambda_C = \frac{cb_c(I_c+C_c)}{N}$.

The disease free equilibrium state P_0^2 of model (4.4) is given by:

$$P_0^2 = (S_0^2, I_{c0}^2, C_{c0}^2) = \left(\frac{\Lambda}{\mu}, 0, 0\right)$$

Using the notation in [150] on system (4.4), matrices for the new infection terms, F, and the other terms, V, are given by:

$$F = \begin{bmatrix} cb_c & cb_c \\ 0 & 0 \end{bmatrix}$$

$$V = \begin{bmatrix} r_1 + \rho_1 \sigma_C + \mu & 0 \\ -\rho_1 \sigma_C & d_c + \mu \end{bmatrix}$$

The associative basic reproduction number is given by:

$$R_{HCV} = \rho(FV^{-1}) = \frac{cb_c(d_c + \mu + \rho_1 \sigma_C)}{(d_c + \mu)(r_1 + \rho_1 \sigma_C + \mu)} \tag{4.5}$$

where ρ indicates the spectral radius of FV^{-1}. By Theorem 2 in [150], the following result is obtained.

Lema 4.1.2 *The disease free equilibrium P_0^2 is locally asymptotically stable if $R_{HCV} < 1$ and unstable if $R_{HCV} > 1$.*

Now the calculation of the reproduction number of the full model (4.1), R_0, is continued. The disease free equilibrium state, P_0, of model (4.1) is given by:

$$\begin{aligned} P_0 &= (S^0, I_a^0, A_a^0, I_c^0, C_c^0, I_a I_c^0, I_a C_c^0, A_a I_c^0, A_a C_c^0) \\ &= \left(\tfrac{\Lambda}{\mu}, 0, 0, 0, 0, 0, 0, 0, 0\right) \end{aligned} \tag{4.6}$$

Using the notation in [150] on system (4.1), matrices for the new infection terms, F, and the other terms, V, are given by:

$$F = \begin{pmatrix} cb_h & cb_h & 0 & 0 & cb_h\sigma_3 & cb_h\sigma_3 & 0 & 0 \\ 0 & 0 & 0 & 0 & 0 & 0 & 0 & 0 \\ 0 & 0 & cb_c & cb_c & cb_c\eta_1 & cb_c\eta_2 & 0 & 0 \\ 0 & 0 & 0 & 0 & 0 & 0 & 0 & 0 \\ 0 & 0 & 0 & 0 & 0 & 0 & 0 & 0 \\ 0 & 0 & 0 & 0 & 0 & 0 & 0 & 0 \\ 0 & 0 & 0 & 0 & 0 & 0 & 0 & 0 \\ 0 & 0 & 0 & 0 & 0 & 0 & 0 & 0 \end{pmatrix}$$

$$V = \begin{pmatrix} \rho+\mu-(1-\epsilon)\theta & -\upsilon_1 & 0 & 0 & -r_2 & 0 & 0 & 0 \\ -\rho & \upsilon_1+d_a+\mu & 0 & 0 & 0 & 0 & -r_3 & 0 \\ 0 & 0 & r_1+\rho_1\sigma_C+\mu & 0 & 0 & 0 & 0 & 0 \\ 0 & 0 & -\rho_1\sigma_C & d_c+\mu & 0 & 0 & 0 & 0 \\ 0 & 0 & 0 & 0 & r_2+\rho+\rho_2\sigma_C+\mu & 0 & -\upsilon_2 & 0 \\ 0 & 0 & 0 & 0 & -\rho_2\sigma_C & \rho+d_c+\mu & 0 & -\upsilon_3 \\ 0 & 0 & 0 & 0 & -\rho & 0 & r_3+\upsilon_2+\rho_3\sigma_C+d_a+\mu & 0 \\ 0 & 0 & 0 & 0 & 0 & -\rho & -\rho_3\sigma_C & \upsilon_3+\mu+d_a+d_c \end{pmatrix}$$

The associative basic reproduction number of the full model is computed to be:

$$R_0 = \rho(FV^{-1}) = \max\{R_{HIV}, R_{HCV}\} \tag{4.7}$$

where ρ indicates the spectral radius of FV^{-1}. By Theorem 2 [150], the following lemma is derived.

Lema 4.1.3 *The disease free equilibrium P_0 is locally asymptotically stable if $R_0 < 1$ and unstable if $R_0 > 1$.*

4.1.3 Global stability of the disease-free equilibria

In this subsection, the global stability of the disease free equilibrium of the full model (4.1) is calculated. The stability of the disease free equilibria of the two submodels (4.2) and (4.4) is ptoven.

Lema 4.1.4 *For model (4.2), the disease free equilibrium P_0^1 is globally asymptotically stable if $R_{HIV} < 1$.*

Proof The comparison theorem is used to prove the global stability of the disease free equilibrium of submodel (4.2). The rate of change of the variables (I_a, A_a) of system (4.2) can be rewritten as follows.

$$\begin{pmatrix} \dot{I}_a \\ \dot{A}_a \end{pmatrix} = (F - V) \begin{pmatrix} I_a \\ A_a \end{pmatrix} - \left(1 - \frac{S}{N}\right) F \begin{pmatrix} I_a \\ A_a \end{pmatrix} \tag{4.8}$$

where F and V are as defined above for system (4.2). Since $S \leq N$ for all $t \geq 0$, then:

$$\begin{pmatrix} \dot{I}_a \\ \dot{A}_a \end{pmatrix} \leq (F - V) \begin{pmatrix} I_a \\ A_a \end{pmatrix} \tag{4.9}$$

If $R_{HIV} < 1$, then $\rho(FV^{-1}) < 1$, which is equivalent to say that the matrix $F - V$ has all eigenvalues in the left-half plane [150]. It follows that the linear system given by equality (4.9) is stable whenever $R_{HIV} < 1$, and hence $(I_a(t), A_a(t)) \to (0, 0)$ as $t \to \infty$ for this linear ordinary differential equation (ODE) system. Consequently, after using a standard comparison theorem [63, 133], one obtains $(I_a(t), A_a(t)) \to (0, 0)$, for the nonlinear system given by the last two equations of system (4.2). Returning now to the first equation of model (4.2) and substituting $I_a = A_a = 0$, one gets a linear system with $S(t) \to \frac{\Lambda}{\mu}$. Thus, $(S(t), I_a(t), A_a(t)) \to (\frac{\Lambda}{\mu}, 0, 0)$ as $t \to \infty$ for $R_{HIV} < 1$, so that P_0^1 is globally asymptotically stable if $R_{HIV} < 1$.

■

Now it's repeated the same procedure for the computation of the global stability of the disease free equilibrium of submodel (4.4).

Lema 4.1.5 *For the submodel (4.4), the disease free equilibrium P_0^2 is globally asymptotically stable if $R_{HCV} < 1$.*

Proof The comparison theorem is used to prove the global stability of the disease free equilibrium of submodel (4.4). The rate of change of the variables (I_c, C_c) of system (4.4) can be rewritten as:

$$\begin{pmatrix} \dot{I}_c \\ \dot{C}_c \end{pmatrix} = (F - V) \begin{pmatrix} I_c \\ C_c \end{pmatrix} - \left(1 - \frac{S}{N}\right) F \begin{pmatrix} I_c \\ C_c \end{pmatrix} \tag{4.10}$$

where F and V are as defined above for system (4.4). Since $S \leq N$ for all $t \geq 0$, then:

$$\begin{pmatrix} \dot{I}_c \\ \dot{C}_c \end{pmatrix} \leq (F - V) \begin{pmatrix} I_c \\ C_c \end{pmatrix} \tag{4.11}$$

If $R_{HCV} < 1$, then $\rho(FV^{-1}) < 1$, which is equivalent to say that the matrix $F - V$ has all eigenvalues in the left-half plane [150]. It follows that the linear system given by the equality (4.11) is stable whenever $R_{HCV} < 1$, and hence $(I_c(t), C_c(t)) \to (0, 0)$ as $t \to \infty$ for this linear ODE system. Consequently, a standard comparison theorem [63, 133] is used, to obtain $(I_c(t), C_c(t)) \to (0, 0)$ for the nonlinear system, given by the last two equations of (4.4). Returning now to the first equation of submodel (4.4) and substituting $I_c = C_c = 0$ gives a linear system with $S(t) \to \frac{\Lambda}{\mu}$. Thus, $(S(t), I_c(t), C_c(t)) \to (\frac{\Lambda}{\mu}, 0, 0)$ as $t \to \infty$ for $R_{HCV} < 1$, so that P_0^2 is globally asymptotically stable if $R_{HCV} < 1$.

■

The global stability of the disease free equilibrium of model (4.1), can only be achieved in very specific conditions, namely, when new coinfection cases are prevented from occurring. Patients infected with HIV or HCV could not become coinfected in such conditions. As this condition is somewhat unrealistic it is not included here. New techniques will be applied in future work in order to try to prove the global stability of the disease free equilibrium.

4.1.4 Bifurcation analysis of the model

In this section, XPPAUT [40] is used to draw schematic bifurcation diagrams for six relevant parameters of the model (4.1). Changing colors indicates a change in the stability of the equilibria.

Figure 4.2 is a sketch of the bifurcation diagram of model (4.1) for the variation of parameter b_h, the effective sexual contact rate for a HIV infection to occur. It starts from a disease-free equilibrium at $b_h = 0$. At $b_h = 0.0456$, there is a bifurcation point (1), at which the model bifurcates to the stable HIV endemic equilibrium. The color green

means that the disease-free equilibrium is stable and the color red means that it has lost stability, and now is the HIV endemic equilibrium that it is stable. Thus, increasing the effective sexual contact rate for HIV infection to occur will translate in new cases of HIV infections.

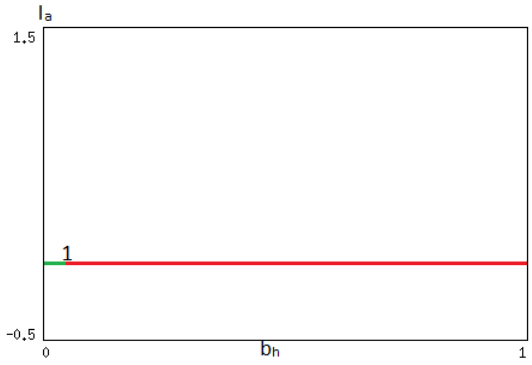

Figure 4.2: Sketch of the bifurcation diagram of model (4.1), for different values of b_h, the effective sexual contact rate for a HIV infection to occur. Remaining parameter values are given in Table 4.2. Green - stable disease-free equilibrium, red - stable HIV endemic equilibrium. For more information, see text.

Figure 4.3 depicts the sketch of the bifurcation diagram of model (4.1), for different values of b_c, the effective contact rate for HCV infection to occur. It starts from a stable disease-free equilibrium at $b_c = 0$. At $b_c = 0.2758$, there is a bifurcation point (1), where the model bifurcates to the stable HCV endemic equilibrium. This means that increasing the effective contact rate for HCV infection to occur will promote the appearance of new cases of HCV.

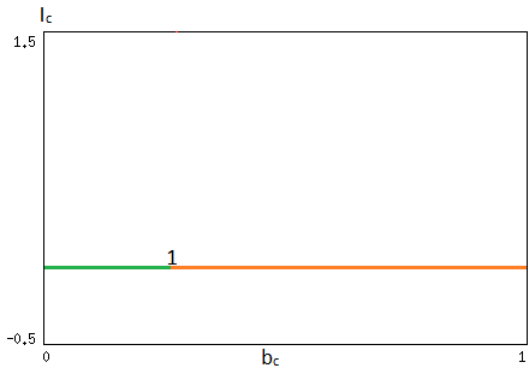

Figure 4.3: Schematic bifurcation diagram of model (4.1), for different values of b_c, the effective contact rate for HCV infection to occur. Remaining parameter values are given in Table 4.2. Green - stable disease-free equilibrium, orange - stable HCV endemic equilibrium. For more information, see text.

In Figure 4.4 a sketch of the bifurcation diagram of model (4.1) is drawn, for variation of parameter c, the average number of sexual partners. It starts from a disease-free equilibrium at $c = 0$. At $c = 1.267$, there is a bifurcation point (1), at which the model bifurcates to the stable HIV endemic equilibrium. This means that increasing the average number of sexual partners of susceptible individuals will, as expected, translate in new cases of HIV infections. Increasing further c, a secondary bifurcation occurs at $c = 8.651$ (2), at which the model changes the dynamical behavior to a stable full endemic equilibrium. Biologically this implies that increasing the average number of sexual partners will burst coinfection cases. Note that as both diseases, HIV and HCV share the same transmission route, in this case, by sexual contact, increasing the average number of sexual partners affects both diseases. Moreover, as HCV is more difficult to be transmitted through sexual intercourse, it is reasonable that for HCV to occur a larger number of sexual partners is needed.

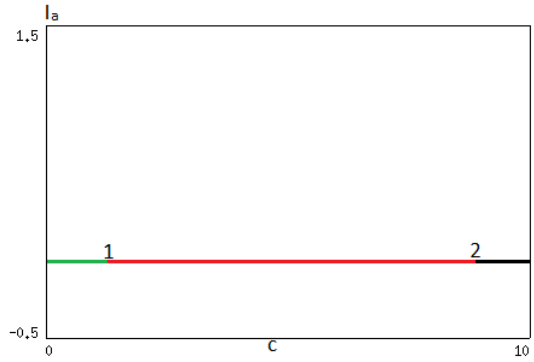

Figure 4.4: Sketch of the bifurcation diagram of model (4.1), for different values of c, the average number of sexual partners. Remaining parameter values are given in Table 4.2. Green - stable disease-free equilibrium, red - stable HIV endemic equilibrium, black - stable full endemic equilibrium. For more information, see text.

In Figure 4.5, a schematic bifurcation diagram of model (4.1) is described, for different values of θ, the fraction of newborns infected with HIV during birth. It starts from a stable HIV endemic equilibrium at $\theta = 0.1$. At $\theta = 0.0084$ there is a bifurcation point (1), at which the model bifurcates to the stable disease-free equilibrium. The model predicts, in this case, that decreasing the number of infected newborns will decrease the number of HIV infected individuals.

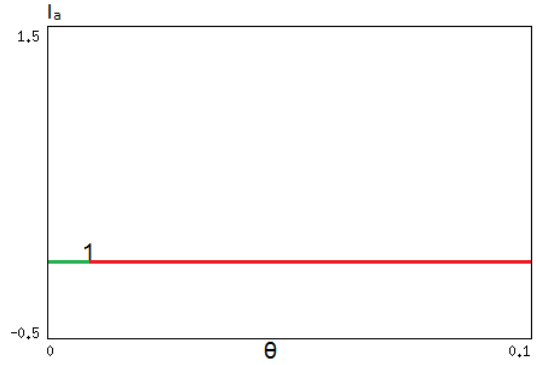

Figure 4.5: Sketch of the bifurcation diagram of model (4.1), for different values of θ, the fraction of newborns infected with HIV during birth. Remaining parameter values are given in Table 4.2. Red - stable HIV endemic equilibrium, green - stable disease-free equilibrium. For more information, see text.

Figure 4.6 shows the sketch of the bifurcation diagram for different values of r_1, the treatment rate for individuals solely infected with HCV. It starts from a stable HCV

endemic equilibrium at $r_1 = 0$. At $r_1 = 0.5277$, there is a bifurcation point (1), at which the model bifurcates to the disease-free equilibrium. This means that increasing the treatment rate for individuals solely infected with HCV is a successful strategy, since patients recover from HCV infection.

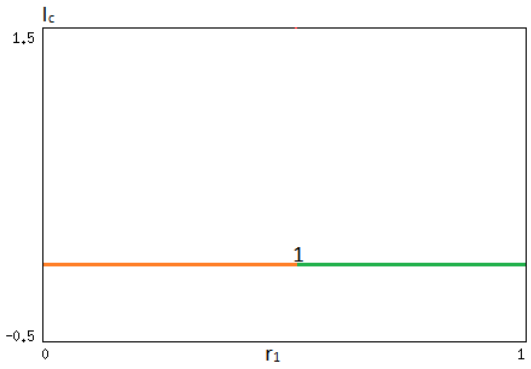

Figure 4.6: Bifurcation diagram of model (4.1), for different values of r_1, the treatment rate for individuals solely infected with HCV. Remaining parameter values are given in Table 4.2, except for $b_c = 0.5$. Orange - stable HCV endemic equilibrium, green - stable disease-free equilibrium. For more information, see text.

In Figure 4.7 a schematic bifurcation diagram of model (4.1) is drawn, for different values of r_2, the treatment rate for HCV, of individuals dually infected with HIV and HCV. It starts from a stable two disease endemic equilibrium. At $r_2 = 0.4203$ there is a bifurcation point (1), at which the model bifurcates to the stable HIV endemic equilibrium. Biologically, this means that increasing the treatment rate for HCV of individuals dually infected with HIV and HCV leads to a recovery from the HCV infection. The individual returns to the stage of HIV solely infection.

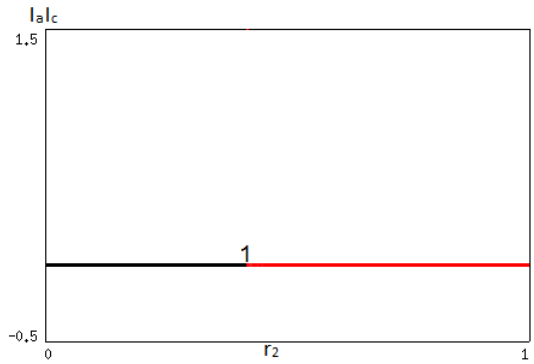

Figure 4.7: Sketch of the bifurcation diagram of model (4.1), for different values of r_2, the treatment rate for HCV of individuals dually infected with HIV and HCV. Remaining parameter values are given in Table 4.2, except for $b_h = 0.15$, $b_c = 0.5$ and $\sigma_C = 0.43$. Black - stable two disease endemic equilibrium, red - stable HIV endemic equilibrium. For more information, see text.

In the next section, numerical simulations are presented where bifurcation between distinct equilibria can be observed, for variation of the parameters considered above.

4.1.5 Numerical results

The numerical simulations of model (4.1) are presented. The parameter values used in the simulations can be found in Table 4.2 and the following initial conditions $S(0) = 500$, $I_a(0) = 10 = I_aI_c(0)$, $A_a(0) = 5$, $C_c(0) = 5$, $I_c(0) = 15$, $I_aC_c(0) = 10$, $A_aI_c(0) = 3$, $A_aC_c(0) = 1$ are used.

Parameter	Value	Reference
c	1	Estimated
b_h	0.036	[54]
σ_3	1.0002	Estimated
b_c	0.05	[149]
η_1	1.0002	[16]
η_2	1.002	Estimated
Λ	12	Estimated
μ	0.02	[16]
r_1	0.25	[16]
r_2	0.2	Estimated
r_3	0.15	Estimated
ρ	0.1908	[85]
σ	1.001	[16]
ϵ	0.2	[157]
θ	0.1	Estimated
υ_1	0.2	[16]
υ_2	0.2	Estimated
υ_3	0.15	Estimated
d_a	0.33	[16]
d_c	0.2801	[16]
δ	1.001	[16]
ρ_1	0.43	[123]
ρ_2	0.45	Estimated
ρ_3	0.47	Estimated
σ_C	0.1667	[123]

Table 4.2: Parameters used in the numerical simulations of model (4.1). Where appropriate the units are yr^{-1}.

In Figure 4.8, the dynamics of the relevant variables of system (4.1) are plotted. It is observed that, for the given parameter values and initial conditions, the model approaches asymptotically the stable disease-free equilibrium.

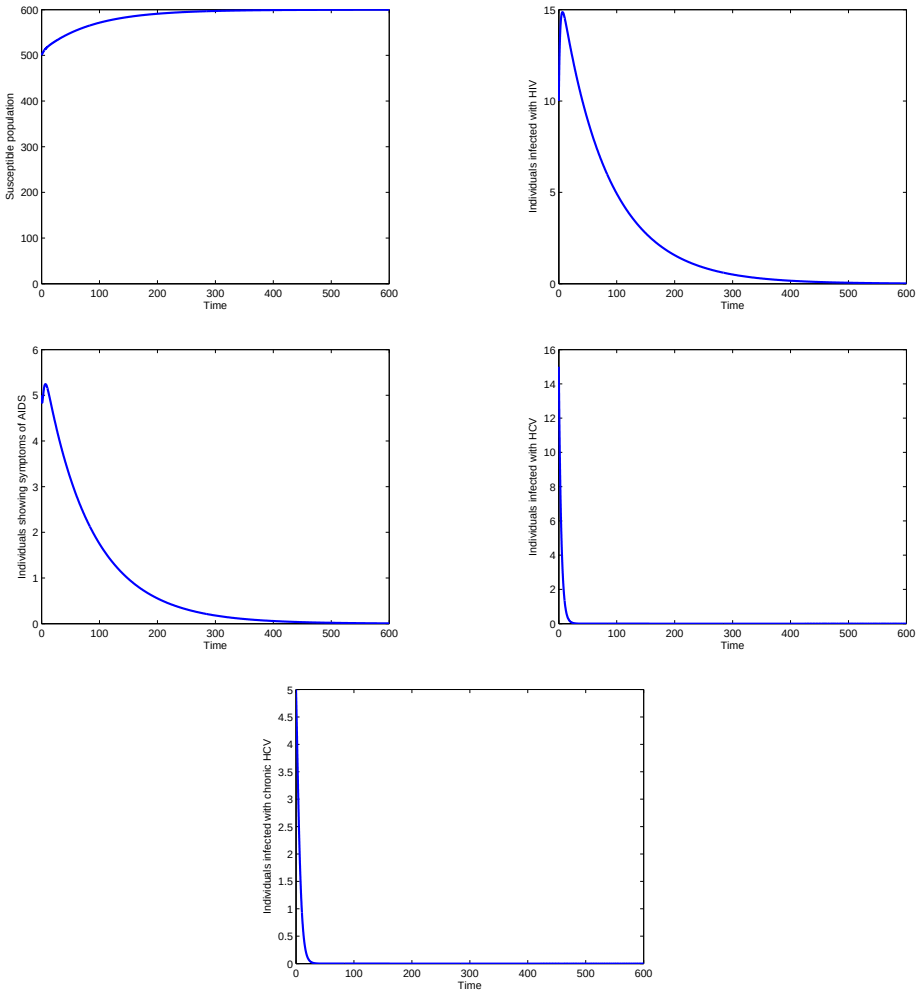

Figure 4.8: Disease-free equilibrium of system (4.1) for parameter values given in Table 4.2 and initial conditions ($R_{HIV} = 0.1813$, $R_{HCV} = 0.7895$, $R_0 = 0.7895$). Remaining variables tend asymptotically to zero.

In Figure 4.9, it is observed that the model approaches asymptotically the stable endemic HIV equilibrium.

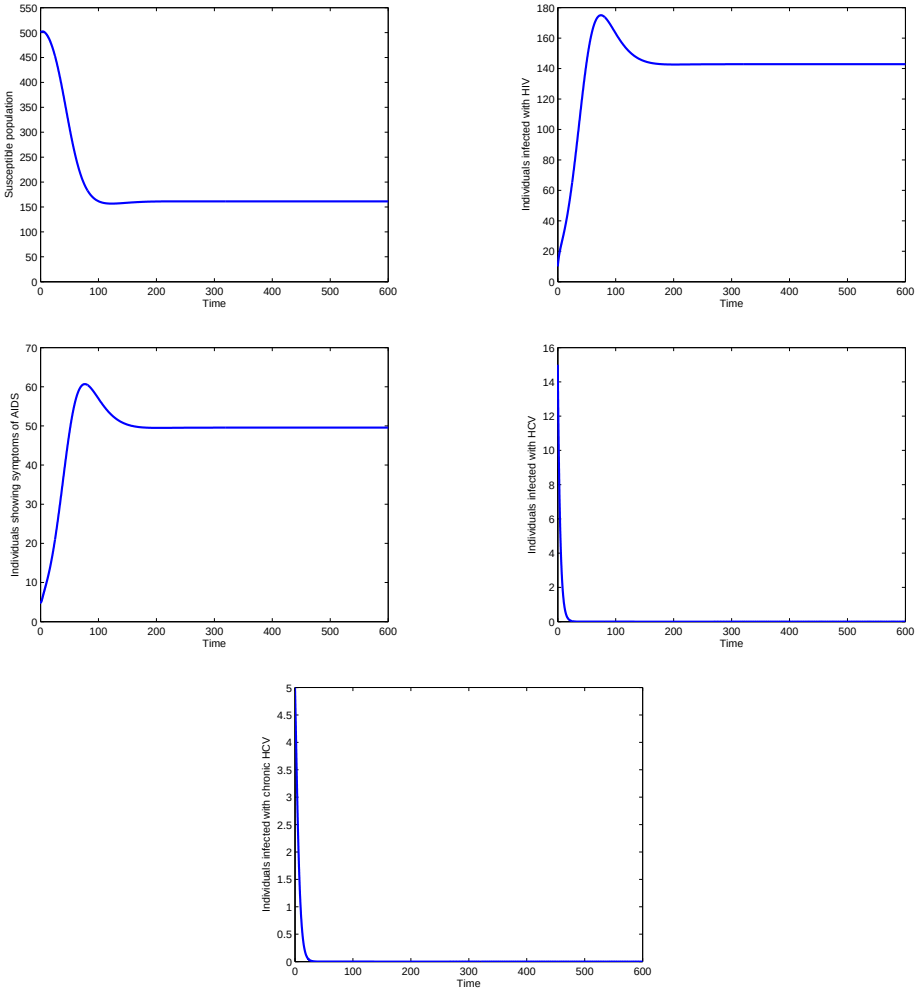

Figure 4.9: Stable endemic HIV equilibrium of system (4.1) for given parameter values in Table 4.2, except $b_h = 0.1$, and initial conditions ($R_{HIV} = 2.1930$, $R_{HCV} = 0.1813$, $R_0 = 2.1930$). Remaining variables go asymptotically to zero.

Figure 4.10 shows the stable endemic HCV equilibrium for system (4.1).

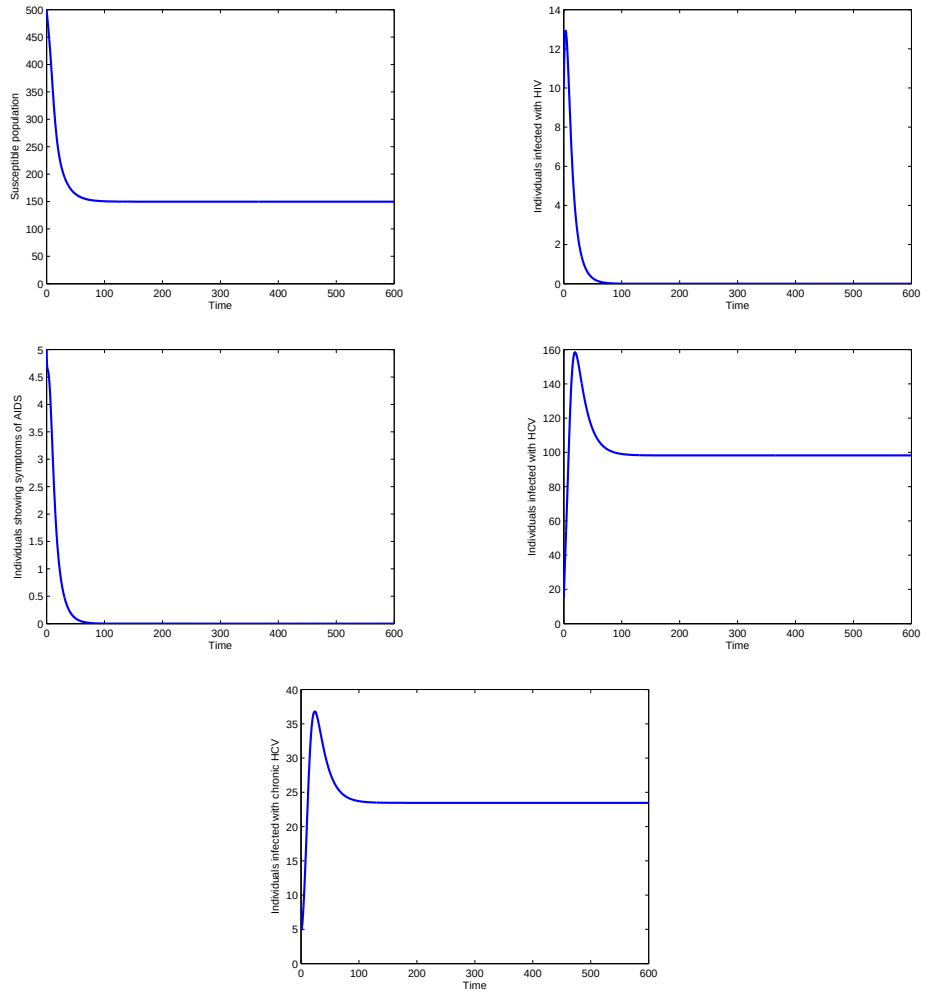

Figure 4.10: Stable HCV endemic equilibrium of system (4.1) for parameter values given in Table 4.2, except $b_c = 0.5$, and initial conditions ($R_{HIV} = 0.7895$, $R_{HCV} = 1.8129$, $R_0 = 1.8129$). Remaining variables tend asymptotically to zero.

Figure 4.11 describes the dynamics of the variables of system (4.1). It is observed that, for the given parameter values and initial conditions, the model approaches asymptotically the stable two disease endemic equilibrium.

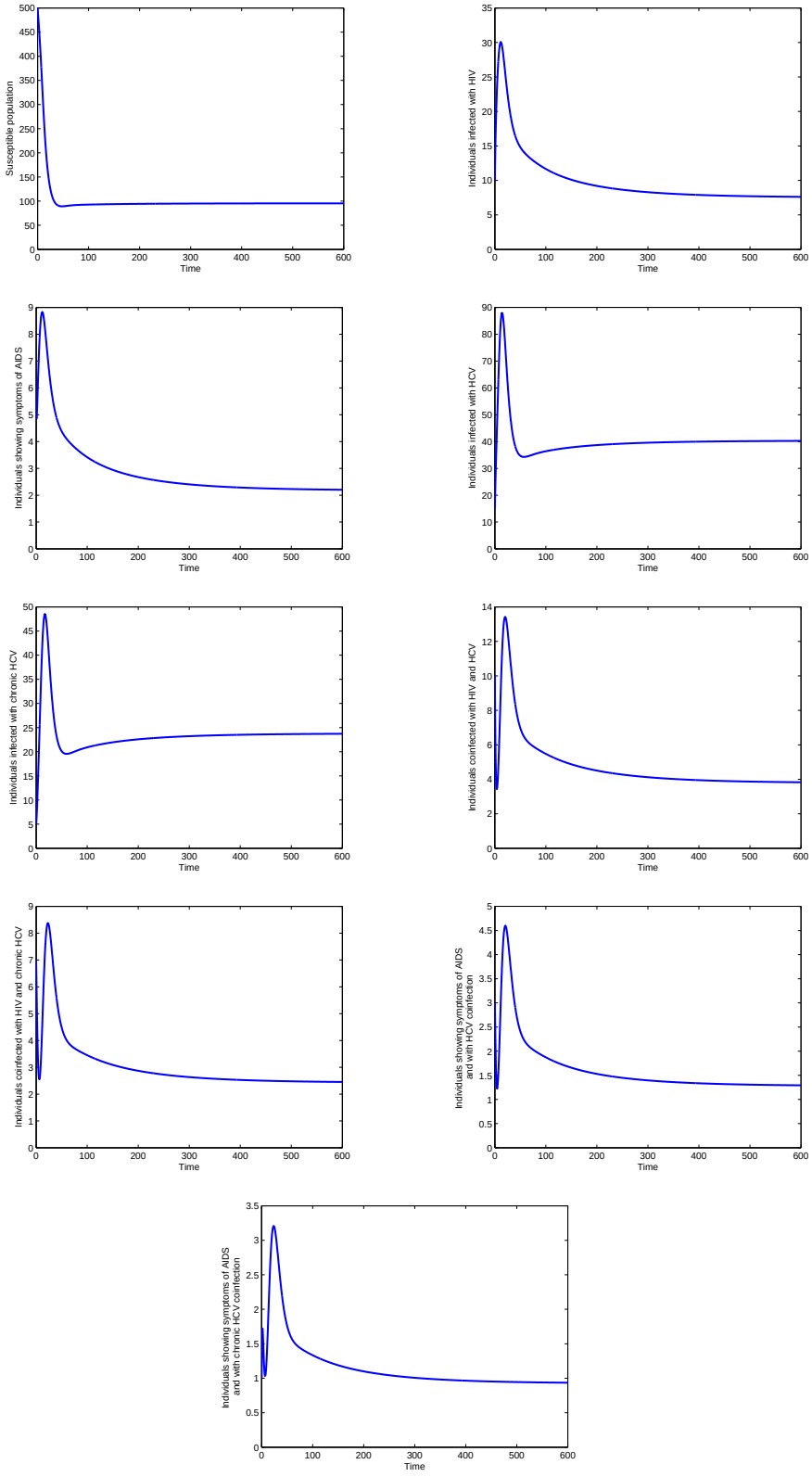

Figure 4.11: Stable two disease endemic equilibrium of system (4.1) for given parameter values in Table 4.2, except for $b_h = 0.15$, $\sigma_C = 0.43$ and $b_c = 0.5$, and initial conditions ($R_{HIV} = 3.2895$, $R_{HCV} = 1.7764$, $R_0 = 3.2895$).

Figure 4.12 shows the dynamics of the variables of system (4.1) for different values of b_h, the effective contact rate for HIV infection to occur. It is observed that as b_h increases the system (4.1) bifurcates from the stable disease-free equilibrium to the stable HIV endemic equilibrium. Realistically, augmenting the sexual contact rate between individuals is followed by a burst of HIV infection.

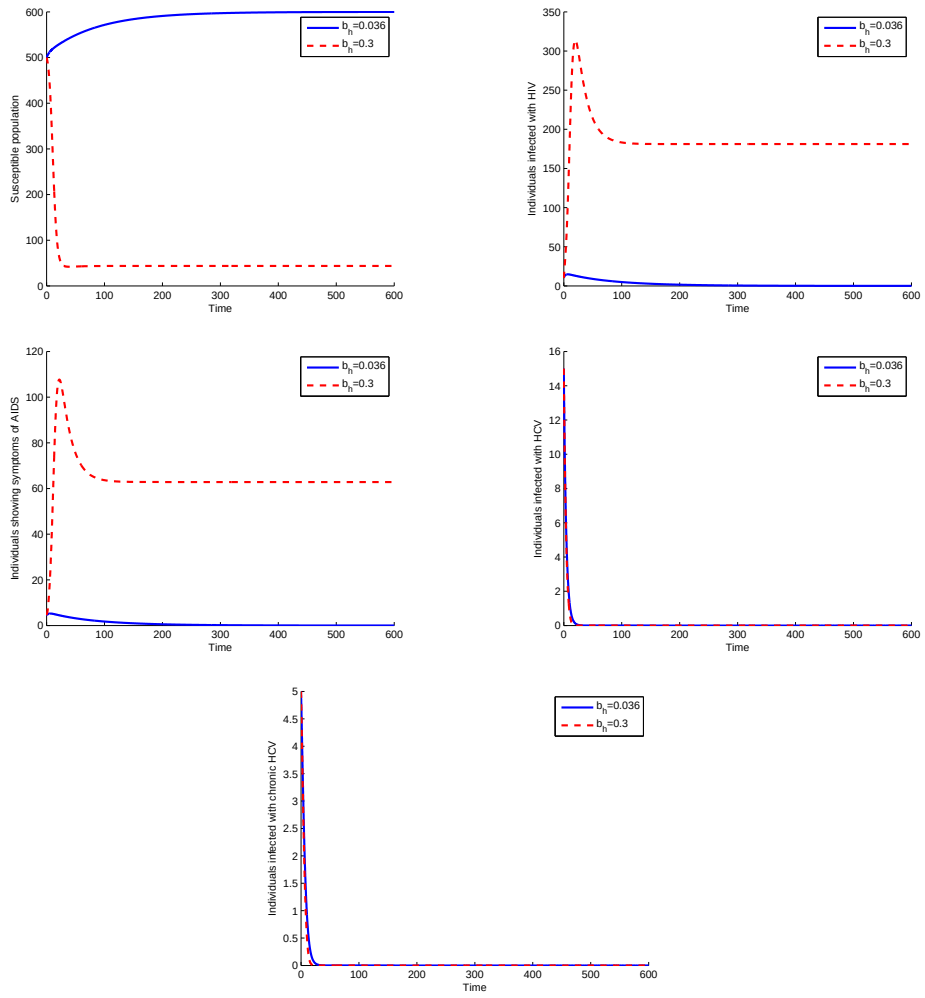

Figure 4.12: Dynamics of the relevant variables of system (4.1) for different values of b_h, the effective sexual contact rate for HIV transmission to occur, for given parameter values in Table 4.2 and initial conditions. For more information, see text.

In Figure 4.13, it is shown the dynamics of the variables of system (4.1) for different values of b_c, the effective contact rate for HCV infection to occur. It is observed that as b_c increases the system (4.1) bifurcates from the stable disease-free equilibrium to the stable HCV endemic equilibrium. This behavior translates, biologically, in new cases of HCV for higher values of b_c.

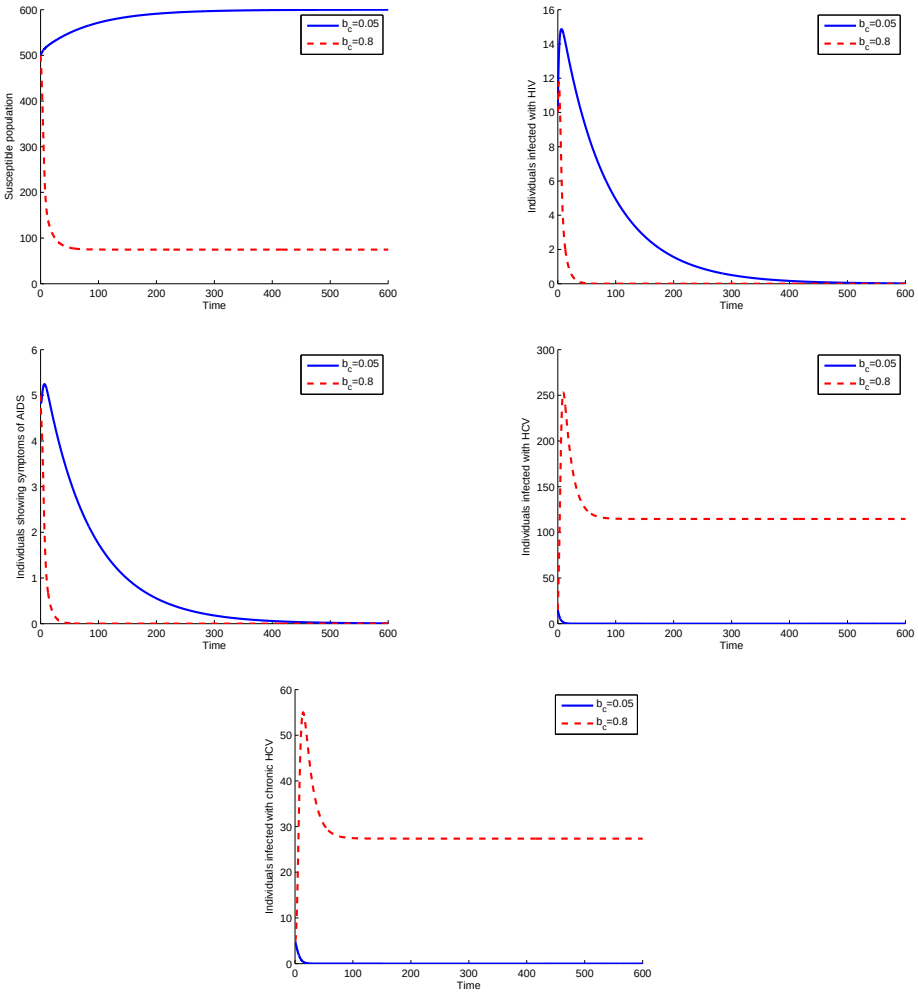

Figure 4.13: Dynamics of the relevant variables of system (4.1) for different values of b_c, the effective contact rate for HCV infection to occur. Parameter values are in Table 4.2 and initial conditions in the text. For more information, see text.

Figure 4.14 depicts the behavior of system (4.1) for different values of c, the average number of sexual partners per unit of time. It is observed that as c increases the system (4.1) bifurcates from the stable disease-free equilibrium to the stable HIV endemic equilibrium and then, increasing further the value of c, there is another bifurcation to the full endemic equilibrium. Biologically, this means that augmenting the average number of sexual partners fuels the appearance of new cases of HIV infection, and, after some value, it even promotes the appearance of coinfection cases.

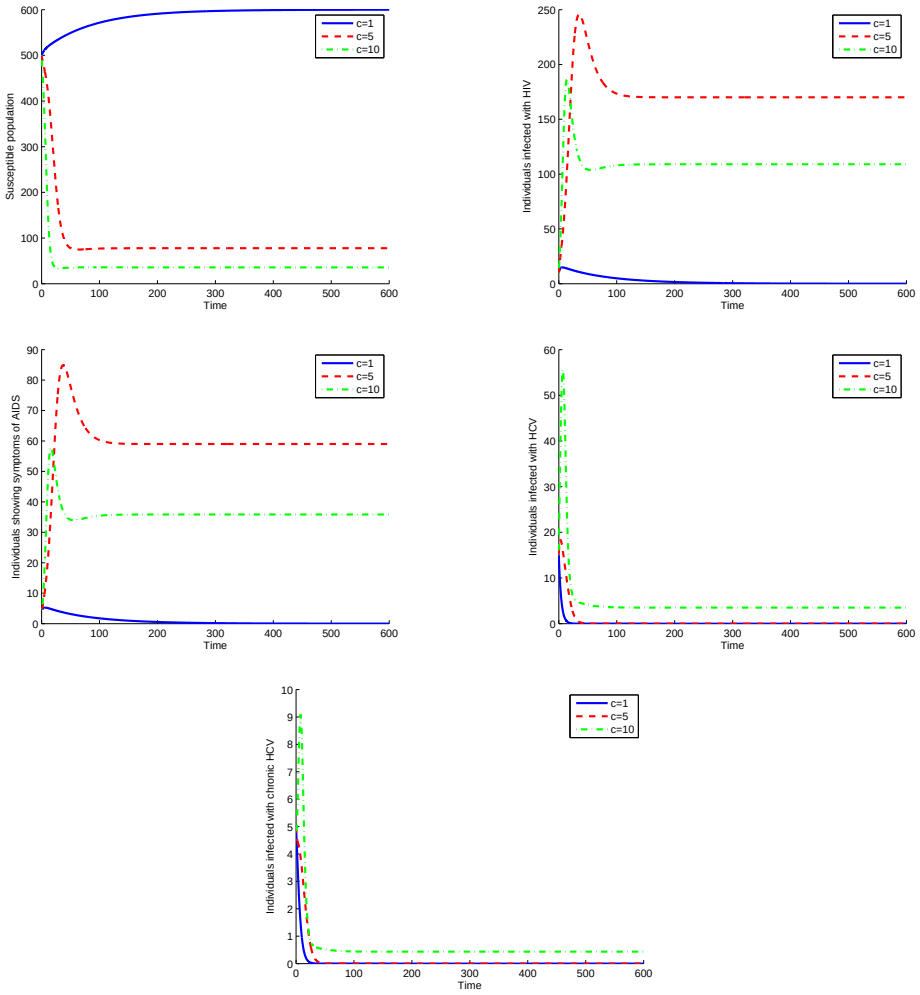

Figure 4.14: Dynamics of the relevant variables of system (4.1) for different values of c, the average number of sexual partners per unit of time, for given parameter values in Table 4.2 and initial conditions. For more information, see text.

In Figure 4.15 are depicted the dynamics of the variables of system (4.1) for different values of θ, the fraction of newborns infected with HIV during birth. It is observed that as θ increases the system (4.1) bifurcates from the stable disease-free equilibrium to the stable HIV endemic equilibrium.

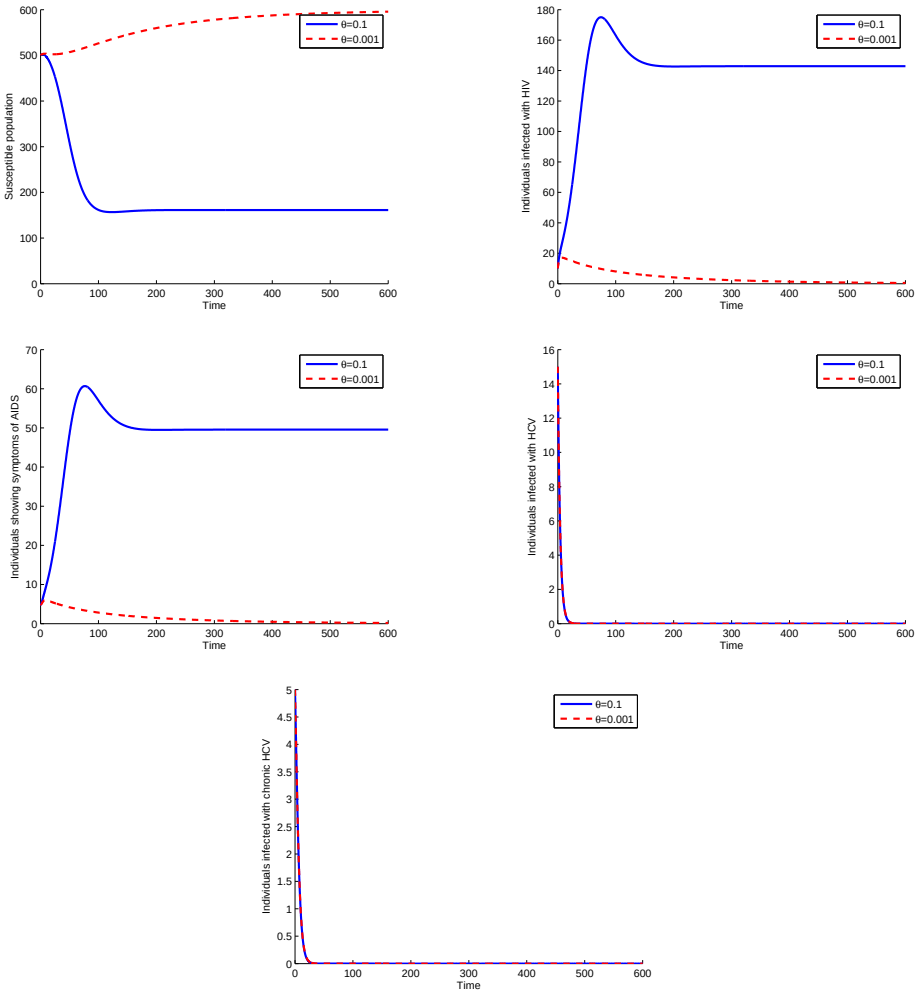

Figure 4.15: Dynamics of the relevant variables of system (4.1) for different values of θ, the fraction of newborns infected with HIV during birth, for given parameter values in Table 4.2, except for $b_h = 0.1$, and initial conditions. For more information, see text.

In Figure 4.16 the behavior of system (4.1) is drawn for different values of r_1, the treatment rate for individuals solely infected with HCV. It is observed that as r_1 increases the stable HCV endemic state gives rise to the stable disease-free equilibrium. This means that the treatment was successful and patients recovered from HCV.

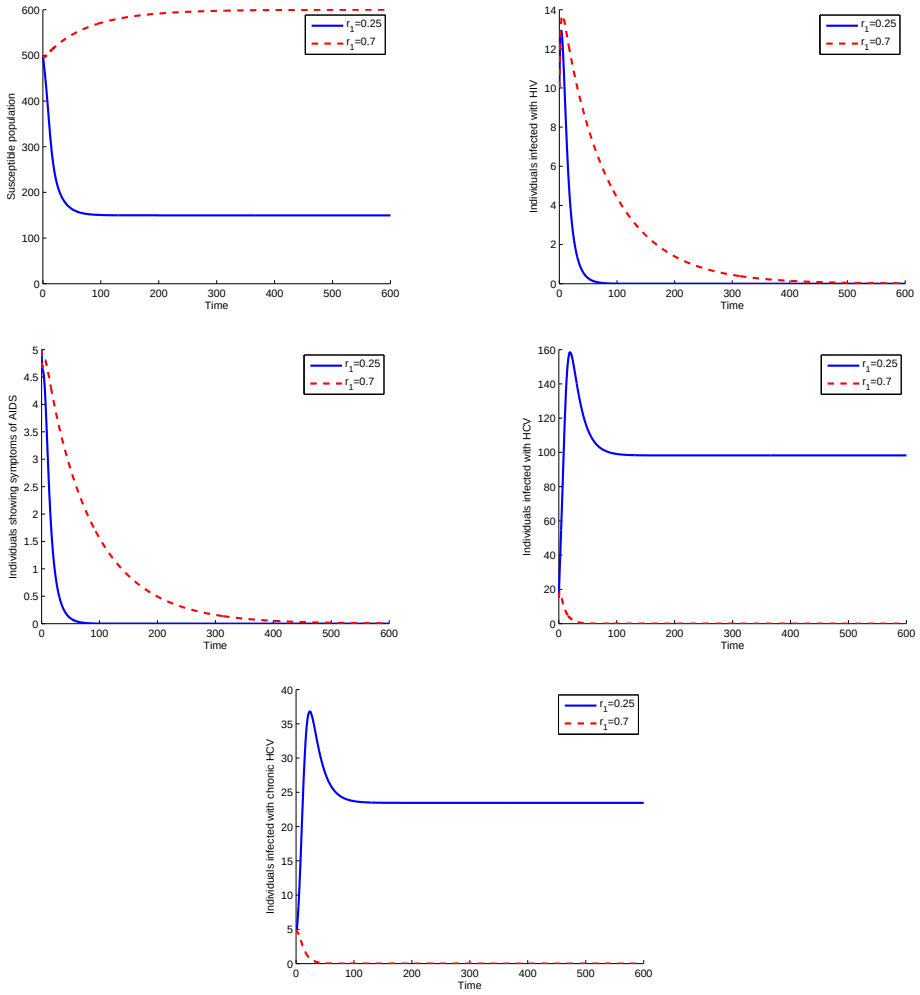

Figure 4.16: Dynamics of the relevant variables of system (4.1) for different values of r_1, the treatment rate for individuals solely infected with HCV, for given parameter values in Table 4.2, except for $b_c = 0.5$, and initial conditions. For more information, see text.

In Figure 4.17, the effects on the dynamics of model (4.1) are observed, for variation of r_2, the treatment rate for individuals dually infected with HIV and HCV. As r_2 increases the system (4.1) bifurcates from the stable full endemic equilibrium to the stable HIV endemic equilibrium. Thus, patients recover from HCV infection.

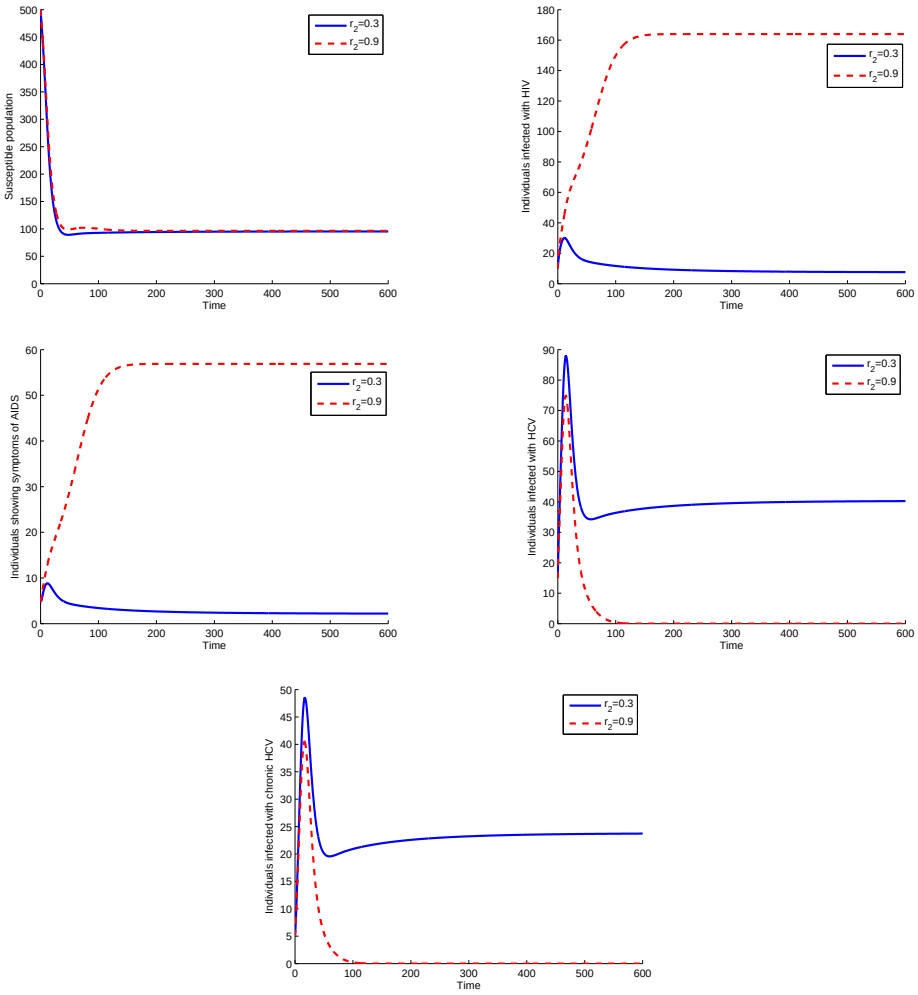

Figure 4.17: Dynamics of the relevant variables of system (4.1) for different values of r_2, the treatment rate for HCV in individuals dually infected with HIV and HCV, for given parameter values in Table 4.2, except for $b_h = 0.15$, $b_c = 0.5$, and $\sigma_C = 0.43$, and initial conditions. For more information, see text.

4.1.6 Conclusions

Model III includes treatment for both diseases, and vertical transmission in the case of HIV. The local stability of the disease-free equilibria for the full model and the global stability of the disease-free equilibria for the two submodels (HCV only and HIV only submodels) are studied. XPPAUT is used to sketch bifurcation diagrams, for relevant parameters, e.g., the mean number of sexual partners, the sexual contact rates, and the treatment rates. Numerical results illustrate the change on the dynamical behavior of the

model for these parameters. The outcomes suggest that specific measures should be considered, by the policy makers, in order to reduce HIV infection, such as: distributing more condoms to individuals; develop campaigns in order to warn individuals about the consequences of having many sexual partners; continuing treatment for AIDS and pursuing the investigation of new and better drugs to combat HIV, treat newborns infected with HIV and advise pregnant women for the benefits of HIV treatment. Considering HCV infection, treatment is highly recommended as well as other measures (e.g., more informational campaigns about the disease, its transmission routes, amongst others) in order to decrease the number of infectious and of chronic carriers. Future work will focus on the study of regular screening for HIV and of condom use, of the effects of needle sharing, as well as an application/validation of the model to real portuguese data, with corresponding estimation of parameter values.

4.2 Model IV

C.M.A. Pinto and A.R.M. Carvalho, Effects of treatment, awareness and condom use in a coinfection model for HIV and HCV in MSM, Journal of Biological Systems 23(2), 165–193, 2015.

A HIV and HCV coinfection model is described, with the objective of studying the effectc of treatment for both diseases, screening, unawareness and awareness of HIV infection, and the use of condom. The reproduction numbers of the full model, and of the two submodels (HIV only and HCV only models) are computed. The local stability of the disease-free equilibria is studied. The sensitivity indices of the reproduction number to relevant parameters of the model are computed. Bifurcation diagrams are presented, built with the help of XPPAUT, to better understand the dynamics of the proposed model. Finally, simulation results of the full model are presented.

4.2.1 Description of the model

The total population, $N(t)$ is divided in the following sixteen classes: the unscreened susceptible individuals, $S_{\tilde{s}}(t)$, the screened susceptible individuals, $S_s(t)$, the HIV unaware infected individuals, $I_{\tilde{a}}(t)$, the HIV aware infected individuals, $I_a(t)$, the unaware individuals showing symptoms of AIDS, $A_{\tilde{a}}(t)$, the aware individuals that developed AIDS, $A_a(t)$, the HCV infected individuals screened for HIV, $I_c(t)$, the HCV infected individuals unscreened for HIV, $I_{\tilde{c}}(t)$, the chronic HCV infected individuals unscreened

for HIV, $C_{\tilde{s}}(t)$, the chronic HCV infected individuals screened for HIV, $C_s(t)$, the HCV and HIV unaware coinfected individuals, $I_cI_{\tilde{a}}(t)$, the HCV and HIV aware coinfected individuals, $I_cI_a(t)$, the chronic HCV and HIV unaware coinfected individuals, $CI_{\tilde{a}}(t)$, the chronic HCV and HIV aware coinfected individuals, $CI_a(t)$, the HCV and AIDS dually infected individuals, $I_cA(t)$, and the chronic HCV and AIDS coinfected individuals, $CA(t)$.

The schematic diagram of the model is given in Figure 4.18.

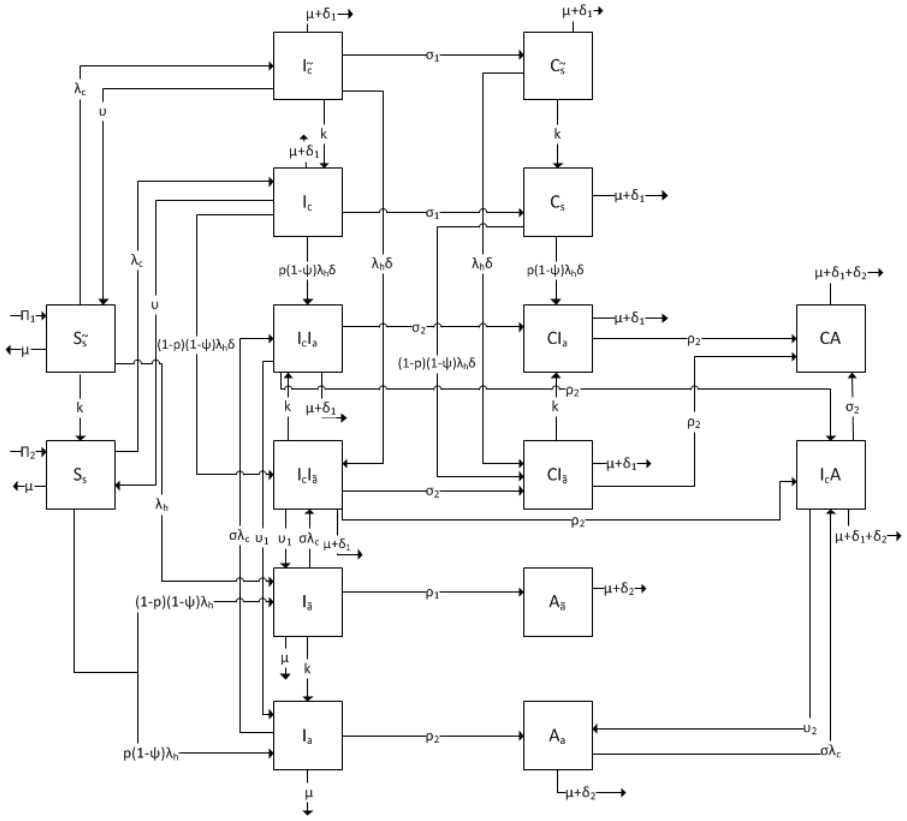

Figure 4.18: Flow chart of the model.

The population of size $N(t)$, at time t, has constant inflow of susceptibles $S_{\tilde{s}}(t)$ and $S_s(t)$, $\Lambda = \Lambda_1 + \Lambda_2$. The natural mortality rate is μ in all classes. Susceptible unscreened individuals, $S_{\tilde{s}}(t)$, get infected with HIV at a rate λ_h, where:

$$\lambda_h = c(1-\theta)b_h \frac{I_a(t) + I_{\tilde{a}}(t) + \eta_1(I_cI_{\tilde{a}}(t) + I_cI_a(t))}{N(t)}$$

Parameter b_h is the probability that a contact will result in an HIV infection and c is the mean number sexual parterns that a susceptible individual acquires, annually. To model

the impact of condom use as a primary prevention tool, it is assumed that the level of protection by condoms is given by $\theta \in [0, 1]$. If $\theta = 0$ then condoms do not offer any protection, whereas $\theta = 1$ implies perfect protection [84]. Parameter $\eta_1 > 1$ models the fact that dually infected individuals are more infectious than their corresponding counterparts [19, 34, 16]. Unscreened individuals are screened at a rate k and move to the class of screened susceptible individuals, $S_s(t)$.

Screened susceptible individuals, $S_s(t)$ are infected with HIV at a rate $(1 - \psi)\lambda_h$, where $0 \leq \psi \leq 1$ measures the efficacy of screening in reducing disease transmission. If $\psi = 0$, then the screening has no effect on the behavior of individuals, on the contrary, if $\psi = 1$ then screening is 100% effective in preventing HIV transmission. It is considered that screened susceptible individuals can be infected. Routine testing serves only one individual knowing his or her HIV status and accessing care if he or she needs it. A proportion p of screened individuals enter the infected class of individuals who are aware of their condition, $I_a(t)$. A proportion $(1 - p)$ of infected individuals that are not routinely screened go to the class $I_{\tilde{a}}(t)$ and are unaware of their infectious state. These unscreened individuals are screened after some time at a rate k and move to class $I_a(t)$. Individuals at class $I_a(t)$ receive HAART treatment, nevertheless there are some that develop AIDS at a rate ρ_2. Individuals in class $I_{\tilde{a}}(t)$ may also develop AIDS at a rate ρ_1. It is assumed $\rho_1 \geq \rho_2$, since individuals at class $I_{\tilde{a}}(t)$ do not receive HAART treatment, due to their unawareness of the disease condition. AIDS induced death rate is δ_2.

Considering now HCV infection, susceptible unscreened individuals, $S_{\tilde{s}}(t)$ are infected with HCV at a rate λ_c, and move to class $I_{\tilde{c}}$, where:

$$\lambda_c = c(1 - \theta)b_c \frac{I_c(t) + I_{\tilde{c}}(t) + \eta_2(I_c I_{\tilde{a}}(t) + I_c I_a(t))}{N(t)}$$

Parameter b_c is the probability that a contact will result in an HCV infection, $\eta_2 > 1$ models the fact that dually infected individuals are more infectious than their corresponding counterparts [19, 34, 16]. The HCV, unscreened for HIV, infected individuals, $I_{\tilde{c}}(t)$, recover spontaneously (or from treatment), at a rate υ, and return to class $S_{\tilde{s}}(t)$. They can also progress to a chronic stage, $C_{\tilde{s}}(t)$, at a rate σ_1. Or they can be screened at a rate k and move to class $I_c(t)$. These individuals are infected with HIV at a rate $\delta\lambda_h$, where δ accounts for the susceptibility to HIV infection for HCV infected people [16, 114].

The screened susceptible individuals, $S_s(t)$ are infected with HCV at a rate λ_c and move to class $I_c(t)$. The screened HCV infected individuals are infected with HIV at a rate $(1 - \psi)\lambda_h\delta$, recover at a rate υ and move back to class $S_s(t)$, or progress to a chronic

phase at a rate σ_1 and move to class $C_s(t)$.

The chronic HCV infected individuals, unscreened for HIV, $C_{\tilde{s}(t)}$, are infected with HIV at a rate $\delta\lambda_h$ and move to the class $CI_{\tilde{a}}(t)$, and are screened at a rate k and move to class $C_s(t)$. The chronic HCV infected individuals, screened for HIV, $C_s(t)$, are infected with HIV at a rate $(1-\psi)\delta\lambda_h$.

The HIV unaware infected individuals, $I_{\tilde{a}}(t)$, are infected with HCV at a rate $\sigma\lambda_c$, and move to class $I_cI_{\tilde{a}}(t)$, where $\sigma > 1$ is the modification parameter modeling the increased risk of being infected with HCV when a person is already infected with HIV [149, 34, 16]. Reciprocally, the HCV infected indiviuals, screened for HIV, $I_c(t)$, are infected with HIV at a rate $(1-p)(1-\psi)\delta\lambda_h$ and also move to class $I_cI_{\tilde{a}}(t)$. Individuals in class $I_cI_{\tilde{a}}(t)$ spontaneously recover from HCV infection, at a rate υ_1, and move to class $I_{\tilde{a}}(t)$, or progress to AIDS at a rate ρ_2 and move to class $I_cA(t)$. They can also be screened for HIV and move to class $I_cI_a(t)$. Finally individuals in class $I_cI_{\tilde{a}}(t)$ can become chronic carriers at a rate σ_2 and move to class $CI_{\tilde{a}}(t)$.

The HIV aware infected individuals, $I_a(t)$, are infected with HCV at a rate $\sigma\lambda_c$, and move to class $I_cI_a(t)$. Reciprocally, the HCV infected individuals, $I_c(t)$, are infected with HIV at a rate $\delta(1-\psi)\lambda_h$. Individuals in class $I_cI_a(t)$ spontaneously recover from HCV infection at a rate υ_1 and move to the class $I_a(t)$. They progress to AIDS at a rate ρ_2, and move to class $I_cA(t)$. Or they may become HCV chronic carriers, at a rate σ_2, and move to class $CI_a(t)$.

The individuals with chronic HCV infection, and unscreened for HIV, $C_{\tilde{s}}(t)$, are infected with HIV at a rate $\delta\lambda_h$ and move to class $CI_{\tilde{a}}(t)$. Individuals in this class are screened at a rate k and move to class CI_a or progress to AIDS at a rate ρ_2. HCV induced death is δ_1 in all HCV classes.

The HCV infected individuals at chronic phase, screened for HIV, $C_s(t)$, are infected with HIV at a rate $(1-\psi)\delta\lambda_h$. The chronic HCV carriers and HIV aware dually infected individuals, $CI_a(t)$ progress to AIDS at a rate ρ_2 and move to class $CA(t)$.

AIDS aware individuals, $A_s(t)$, are infected with HCV at a rate $\sigma\lambda_c$ and move to class $I_cA(t)$. The individuals in class $I_cA(t)$ are treated for HCV infection at a rate υ_2 and move to class A_s. The individuals in class $I_cA(t)$ become HCV chronic carriers at a rate σ_2 and move to class $CA(t)$.

The parameters and variables of the model are summarized in Table 4.3.

Variable/Parameter	Description
$S_s(t)$	susceptible screened individuals
$S_{\tilde{s}}(t)$	susceptible unscreened individuals
$I_a(t)$	HIV infected aware individuals
$I_{\tilde{a}}(t)$	HIV infected unaware individuals
$A_a(t)$	aware individuals showing symptoms of AIDS
$A_{\tilde{a}}(t)$	unaware individuals showing symptoms of AIDS
$I_c(t)$	screened for HIV, HCV infected individuals
$I_{\tilde{c}}(t)$	unscreened for HIV, HCV infected individuals
$C_s(t)$	screened for HIV, chronic HCV infected individuals
$C_{\tilde{s}}(t)$	unscreened for HIV, chronic HCV infected individuals
$I_cI_a(t)$	HCV and HIV aware coinfected individuals
$I_cI_{\tilde{a}}(t)$	HCV and HIV unaware coinfected individuals
$CI_a(t)$	HIV aware and chronic HCV dually infected individuals
$CI_{\tilde{a}}(t)$	HIV unaware and chronic HCV coinfected individuals
$I_cA(t)$	HCV and AIDS coinfected individuals
$CA(t)$	chronic HCV and AIDS coinfected individuals
Λ_1	recruitment rate of unscreened individuals
Λ_2	recruitment rate of screened individuals
μ	natural mortality rate
b_h	probability that a contact will result in an HIV infection
b_c	probability that a contact will result in an HCV infection
c	mean number sexual parterns a susceptible individual acquires
θ	level of protection by condoms
p	proportion of screened individuals aware of their HIV status
ψ	efficacy of screening in reducing HIV transmission
υ, υ_i, $i = 1, 2$	recovery rate of treated for HCV
σ_i, $i = 1, 2$	rate of progression to chronic phase of HCV
δ_1	mortality due to HCV
ρ_i, $i = 1, 2$	rate of progression to AIDS
k	awareness of unscreened HIV infected individuals after being screened
δ_2	mortality due to HIV
η_i, $i =, 1, 2$	modification parameter
σ	modification parameter
δ	modification parameter

Table 4.3: Definition of parameters and variables of model (4.12).

The system of nonlinear ordinary differential equations for the proposed model is given by:

$$
\begin{aligned}
\tfrac{dS_{\tilde{s}}}{dt} &= \Lambda_1 + \upsilon I_{\tilde{c}} - \lambda_h S_{\tilde{s}} - \lambda_c S_{\tilde{s}} - kS_{\tilde{s}} - \mu S_{\tilde{s}} \\
\tfrac{dS_s}{dt} &= \Lambda_2 + kS_{\tilde{s}} - (1-\psi)\lambda_h S_s - \lambda_c S_s + \upsilon I_c - \mu S_s \\
\tfrac{dI_{\tilde{a}}}{dt} &= (1-p)(1-\psi)\lambda_h S_s + \lambda_h S_{\tilde{s}} + \upsilon_1 I_c I_{\tilde{a}} - (k + \rho_1 + \sigma\lambda_c + \mu) I_{\tilde{a}} \\
\tfrac{dI_a}{dt} &= p(1-\psi)\lambda_h S_s + kI_{\tilde{a}} + \upsilon_1 I_c I_a - (\sigma\lambda_c + \rho_2 + \mu) I_a \\
\tfrac{dA_{\tilde{a}}}{dt} &= \rho_1 I_{\tilde{a}} - (\mu + \delta_2) A_{\tilde{a}} \\
\tfrac{dA_a}{dt} &= \rho_2 I_a + \upsilon_2 I_c A - (\sigma\lambda_c + \mu + \delta_2) A_a \\
\tfrac{dI_{\tilde{c}}}{dt} &= \lambda_c S_{\tilde{s}} - (k + \upsilon + \sigma_1 + \delta\lambda_h + \mu + \delta_1) I_{\tilde{c}} \\
\tfrac{dI_c}{dt} &= \lambda_c S_s + kI_{\tilde{c}} - (\upsilon + \sigma_1 + (1-\psi)\delta\lambda_h + \mu + \delta_1) I_c \\
\tfrac{dC_{\tilde{s}}}{dt} &= \sigma_1 I_{\tilde{c}} - (k + \delta\lambda_h + \mu + \delta_1) C_{\tilde{s}} \qquad (4.12) \\
\tfrac{dC_s}{dt} &= \sigma_1 I_c + kC_{\tilde{s}} - ((1-\psi)\delta\lambda_h + \mu + \delta_1) C_s \\
\tfrac{dI_c I_{\tilde{a}}}{dt} &= (1-p)(1-\psi)\delta\lambda_h I_c + \delta\lambda_h I_{\tilde{c}} + \sigma\lambda_c I_{\tilde{a}} - \\
&\quad -(k + \sigma_2 + \rho_2 + \upsilon_1 + \mu + \delta_1) I_c I_{\tilde{a}} \\
\tfrac{dI_c I_a}{dt} &= p(1-\psi)\delta\lambda_h I_c + \sigma\lambda_c I_a + kI_c I_{\tilde{a}} - (\upsilon_1 + \rho_2 + \sigma_2 + \mu + \delta_1) I_c I_a \\
\tfrac{dCI_{\tilde{a}}}{dt} &= (1-p)(1-\psi)\lambda_h \delta C_s + \delta\lambda_h C_{\tilde{s}} + \sigma_2 I_c I_{\tilde{a}} - (k + \rho_2 + \mu + \delta_1) CI_{\tilde{a}} \\
\tfrac{dCI_a}{dt} &= p(1-\psi)\delta\lambda_h C_s + \sigma_2 I_c I_a + kCI_{\tilde{a}} - (\rho_2 + \mu + \delta_1) CI_a \\
\tfrac{dI_c A}{dt} &= \sigma\lambda_c A_a + \rho_2 I_c I_{\tilde{a}} + \rho_2 I_c I_a - (\upsilon_2 + \sigma_2 + \mu + \delta_1 + \delta_2) I_c A \\
\tfrac{dCA}{dt} &= \rho_2 CI_{\tilde{a}} + \rho_2 CI_a + \sigma_2 I_c A - (\mu + \delta_1 + \delta_2) CA
\end{aligned}
$$

with non-negative initial conditions given by:

$$\begin{array}{l} S_s(0) = S_{s0},\ S_{\tilde{s}} = S_{\tilde{s}0},\ I_{\tilde{a}}(0) = I_{\tilde{a}0},\ I_a = I_{a0},\ A_a(0) = A_{a0},\ A_{\tilde{a}} = A_{\tilde{a}0}, \\ I_c(0) = I_{c0},\ I_{\tilde{c}} = I_{\tilde{c}0},\ C_s(0) = C_{s0},\ C_{\tilde{s}} = C_{\tilde{s}0} I_c I_{\tilde{a}} = I_c I_{\tilde{a}0}, \\ I_c I_a(0) = I_c I_{a0},\ CI_{\tilde{a}}(0) = CI_{\tilde{a}0},\ CI_a(0) = CI_{a0}, I_c A(0) = I_c A_0, \\ CA(0) = CA_0 \end{array} \tag{4.13}$$

Model (4.12) will be analyzed in the domain $\Omega \subset \mathbb{R}^{16}_{+0}$, given by:

$$\begin{array}{l} \Omega = \{(S_s, S_{\tilde{s}}, I_a, I_{\tilde{a}}, A_a, A_{\tilde{a}}, \\ I_c, I_{\tilde{c}}, C_s, C_{\tilde{s}} m, I_c I_a, CI_a, I_c I_{\tilde{a}}, CI_a, CI_{\tilde{a}}, I_c A, CA) \in \mathbb{R}^{16}_{+} : 0 \leq N \leq \frac{\Lambda_1 + \Lambda_2}{\mu}\} \end{array}$$

Theorem 4.2.1 *The solutions of system (4.12) with initial conditions (4.13) satisfy* $S_{\tilde{s}}(t) \geq 0$, $S_s(t) \geq 0$, $I_{\tilde{a}}(t) \geq 0$, $I_a(t) \geq 0$, $A_{\tilde{a}}(t) \geq 0$, $A_a(t) \geq 0$, $I_{\tilde{c}}(t) \geq 0$, $I_c(t) \geq 0$, $C_{\tilde{s}}(t) \geq 0$, $C_s(t) \geq 0$, $I_c I_{\tilde{a}}(t) \geq 0$, $I_c I_a(t) \geq 0$, $CI_{\tilde{a}}(t) \geq 0$, $CI_a(t) \geq 0$, $I_c A(t) \geq 0$, $CA(t) \geq 0$ *for all* $t > 0$. *The region* $\Omega \in \mathbb{R}^{16}_{+0}$ *is positively invariant and attracting with respect to system (4.12).*

Proof From the first equation of model (4.12) has:

$$\dot{S}_{\tilde{s}} \geq -\left[\lambda_h + \lambda_c + k + \mu\right] S$$

thus:

$$S_{\tilde{s}}(t) \geq S_{\tilde{s}}(0) e^{\left[-\int_0^t [\lambda_h(s) + \lambda_c(s) + k + \mu] ds\right]} > 0$$

Similarly for the second equation of system (4.12):

$$S_s \geq S_s(0) e^{\left[-\int_0^t ((1-\psi) + \lambda_c + \mu)\right]} > 0$$

In an analogous fashion, this can easily be shown $I_a(t)$, $I_{\tilde{a}}$, $A_a(t)$, $A_{\tilde{a}}$, $I_c(t)$, $I_{\tilde{c}}$, $C_s(t)$, $C_{\tilde{s}}$, $I_c I_{\tilde{a}}(t)$, $I_c I_a(t)$, $CI_{\tilde{a}}(t)$, $CI_a(t)$, $I_c A(t)$, and $CA(t)$ are all positive for all $t > 0$.

It is now shown that all feasible solutions are uniformly bounded in Ω. Adding all equations of system (4.12) gets:

$$\begin{array}{rcl} \dot{N} & = & \Lambda_1 + \Lambda_2 - \mu N - \delta_2(A_a + A_{\tilde{a}} + I_c A + CA) - \delta_1(I_c + I_{\tilde{c}} + C_s + C_{\tilde{s}} + I_c I_{\tilde{a}} + I_c I_a + CI_{\tilde{a}} + CI_a), \\ \dot{N} & \leq & \Lambda_1 + \Lambda_2 - \mu N \end{array}$$

This differential equation is solved by observing that:

$$0 \leq N \leq \frac{\Lambda}{\mu} + N(0)e^{-\mu t}$$

where $\Lambda = \Lambda_1 + \Lambda_2$, $N(0)$ represents the initial value of the model's variables. Then $0 \leq N \leq \frac{\Lambda}{\mu}$, as $t \to \infty$. Therefore, $\frac{\Lambda}{\mu}$ is an upper bound of N provided that $N(0) \leq \frac{\Lambda}{\mu}$. If $N(0) > \frac{\Lambda}{\mu}$, then $N(t)$ will decrease to this level. Thus, all feasible solutions of the system enter or remain in the region Ω. Hence, the region of biological interest Ω is positively invariant under the flow induced by system (4.12).

■

4.2.2 Reproduction numbers and stability of disease-free equilibria

In this subsection, the reproduction number, R_0, of model (4.12) is calculated. The basic reproduction number is defined as the number of secondary infections due to a single infection in a completely susceptible population.

The following two sub-models of model (4.12) are considered. Model (4.14) is derived from model (4.12) by setting the variables concerning HIV dynamics ($I_{\tilde{a}}$, I_a, $A_{\tilde{s}}$, A_s, $I_cI_{\tilde{a}}$, I_cI_a, $CI_{\tilde{a}}$, CI_a, I_cA and CA) to zero, and model (4.16) follows from model (4.12) by setting the variables concerning HCV dynamics ($I_{\tilde{c}}$, I_c, $C_{\tilde{s}}$, C_s, $I_cI_{\tilde{a}}$, I_cI_a, $CI_{\tilde{a}}$, CI_a, I_cA and CA) to zero.

The reproduction number, R_{HCV}, of system (4.14) is calculated. The next generation method [150] is used.

$$\begin{aligned}
\tfrac{dS_{\tilde{s}}}{dt} &= \Lambda_1 + \upsilon I_{\tilde{c}} - \lambda_c S_{\tilde{s}} - kS_{\tilde{s}} - \mu S_{\tilde{s}} \\
\tfrac{dS}{dt} &= \Lambda_2 + kS_{\tilde{s}} - \lambda_c S_s + \upsilon I_c - \mu S_s \\
\tfrac{dI_{\tilde{c}}}{dt} &= \lambda_c S_{\tilde{s}} - (k + \upsilon + \sigma_1 + \mu + \delta_1) I_{\tilde{c}} \\
\tfrac{dI_c}{dt} &= \lambda_c S_s - (\upsilon + \sigma_1 + \mu + \delta_1) I_c \\
\tfrac{dC_{\tilde{s}}}{dt} &= \sigma_1 I_{\tilde{c}} - (k + \mu + \delta_1) C_{\tilde{s}} \\
\tfrac{dC_s}{dt} &= \sigma_1 I_c + kC_{\tilde{s}} - (\mu + \delta_1) C_s
\end{aligned} \tag{4.14}$$

where $\lambda_c = c(1-\theta)b_c \frac{I_c + I_{\tilde{c}}}{N}$.

The disease-free equilibrium of model (4.14) is given by:

$$P_0^1 = \left(\frac{\Lambda_1}{k+\mu}, \frac{\Lambda_2}{\mu} + \frac{k\Lambda_1}{\mu(k+\mu)}, 0, 0, 0, 0\right)$$

Using the notation of [150], matrices for the new infection terms, F, and the other terms, V, are given by:

$$F = \begin{bmatrix} c(1-\theta)b_c\frac{\Lambda_1\mu}{\Lambda_1(\mu+1)+\Lambda_2(k+\mu)} & c(1-\theta)b_c\frac{\Lambda_1\mu}{\Lambda_1(\mu+1)+\Lambda_2(k+\mu)} & 0 & 0 \\ c(1-\theta)b_c\frac{\Lambda_1\mu+\Lambda_2(k+\mu)}{\Lambda_1(\mu+1)+\Lambda_2(k+\mu)} & c(1-\theta)b_c\frac{\Lambda_1\mu+\Lambda_2(k+\mu)}{\Lambda_1(\mu+1)+\Lambda_2(k+\mu)} & 0 & 0 \\ 0 & 0 & 0 & 0 \\ 0 & 0 & 0 & 0 \end{bmatrix}$$

$$V = \begin{bmatrix} k+\upsilon+\sigma_1+\mu+\delta_1 & 0 & 0 & 0 \\ -k & \upsilon+\sigma_1+\mu+\delta_1 & 0 & 0 \\ -\sigma_1 & 0 & k+\mu+\delta_1 & 0 \\ 0 & -\sigma_1 & -k & \mu+\delta_1 \end{bmatrix}$$

The associative basic reproduction number is thus:

$$R_{HCV} = \rho(FV^{-1}) = \frac{c(1-\theta)b_c}{\upsilon+\sigma_1+\mu+\delta_1} \tag{4.15}$$

where ρ indicates the spectral radius of FV^{-1}. By Theorem 2 [150], the following lemma is obtained.

Lema 4.2.2 *The disease-free equilibrium P_0^1 is locally asymptotically stable if $R_{HCV} < 1$ and unstable if $R_{HCV} > 1$.*

This is followed by the calculation of the reproduction number, R_{HIV}, of model (4.16).

$$\begin{aligned}
\frac{dS_{\tilde{s}}}{dt} &= \Lambda_1 - \lambda_h S_{\tilde{s}} - kS_{\tilde{s}} - \mu S_{\tilde{s}} \\
\frac{dS_s}{dt} &= \Lambda_2 + kS_{\tilde{s}} - (1-\psi)\lambda_h S_s - \mu S_s \\
\frac{dI_{\tilde{a}}}{dt} &= (1-p)(1-\psi)\lambda_h S_s + \lambda_h S_{\tilde{s}} - (k+\rho_1+\mu)I_{\tilde{a}} \\
\frac{dI_a}{dt} &= p(1-\psi)\lambda_h S_s + kI_{\tilde{a}} - (\rho_2+\mu)I_k \\
\frac{dA_{\tilde{s}}}{dt} &= \rho_1 I_{\tilde{a}} - (\mu+\delta_2)A_{\tilde{a}} \\
\frac{dA}{dt} &= \rho_2 I_a - (\mu+\delta_2)A
\end{aligned} \tag{4.16}$$

where $\lambda_h = c(1-\theta)b_h\frac{I_{\tilde{a}}+I_a}{N}$.

The disease-free equilibrium state P_0^2 of model (4.16) is given by:

$$P_0^2 = \left(\frac{\Lambda_1}{k+\mu}, \frac{\Lambda_2}{\mu} + \frac{k\Lambda_1}{\mu(k+\mu)}, 0, 0, 0, 0\right)$$

Using the notation of [150], matrices for the new infection terms, F, and the other terms, V, are the following:

$$F = \begin{bmatrix}
\frac{c(1-\theta)b_h}{(\Lambda_1+\Lambda_2)(\mu+k)}\left[(1-p)(1-\psi)(k\Lambda_1+\Lambda_2(k+\mu))+\Lambda_1\mu\right] & \frac{c(1-\theta)b_h}{(\Lambda_1+\Lambda_2)(\mu+k)}\left[(1-p)(1-\psi)(k\Lambda_1+\Lambda_2(k+\mu))+\Lambda_1\mu\right] & 0 & 0 \\
p(1-\psi)c(1-\theta)b_h\frac{k\Lambda_1+\Lambda_2(k+\mu)}{(\Lambda_1+\Lambda_2)(\mu+k)} & p(1-\psi)c(1-\theta)b_h\frac{k\Lambda_1+\Lambda_2(k+\mu)}{(\Lambda_1+\Lambda_2)(\mu+k)} & 0 & 0 \\
0 & 0 & 0 & 0 \\
0 & 0 & 0 & 0
\end{bmatrix}$$

$$V = \begin{bmatrix}
k+\rho_1+\mu & 0 & 0 & 0 \\
-k & \rho_2+\mu & 0 & 0 \\
-\rho_1 & 0 & \mu+\delta_2 & 0 \\
0 & -\rho_2 & 0 & \mu+\delta_2
\end{bmatrix}$$

The associative basic reproduction number is given by:

$$\begin{aligned}
R_{HIV} &= \rho(FV^{-1}) \\
&= \frac{c(1-\theta)b_h}{(k+\mu+\rho_1)(\rho_2+\mu)(\Lambda_1+\Lambda_2)(\mu+k)}\left[(1-\psi)(k\Lambda_1+\Lambda_2(k+\mu))(k+\mu+\rho_2+p(\rho_1-\rho_2))+\Lambda_1\mu(k+\mu+\rho_2)\right]
\end{aligned} \tag{4.17}$$

where ρ indicates the spectral radius of FV^{-1}. By Theorem 2 [150], the following lemma is obtained.

Lema 4.2.3 *The disease-free equilibrium P_0^2 is locally asymptotically stable if $R_{HIV} < 1$ and unstable if $R_{HIV} > 1$.*

The calculation of the reproduction number, R_0, of the full model (4.12) follows. The disease-free equilibrium state P_0 of model (4.12) is given by:

$$P_0 = \left(\frac{\Lambda_1}{k+\mu}, \frac{\Lambda_2}{\mu} + \frac{k\Lambda_1}{\mu(k+\mu)}, 0, 0, 0, 0, 0, 0, 0, 0, 0, 0, 0, 0, 0, 0, 0, 0\right)$$

Using the notation in [150] on system (4.12), the matrices for the new infection terms, F, and the other terms, V, and the matrix FV^{-1} are calculated. Then, the reproduction number is the spectral radius of FV^{-1}.

$$F = \begin{pmatrix}
\frac{c(1-\theta)b_h}{(\Lambda_1+\Lambda_2)(\mu+k)}[(1-p)(1-\psi)(k\Lambda_1+\Lambda_2(k+\mu))+\Lambda_1\mu] & \frac{c(1-\theta)b_h}{(\Lambda_1+\Lambda_2)(\mu+k)}[(1-p)(1-\psi)(k\Lambda_1+\Lambda_2(k+\mu))+\Lambda_1\mu] & 0 & 0 & 0 & 0 & 0 & 0 & \frac{c(1-\theta)b_h}{(\Lambda_1+\Lambda_2)(\mu+k)}[(1-p)(1-\psi)(k\Lambda_1+\Lambda_2(k+\mu))+\Lambda_1\mu] & \frac{c(1-\theta)b_h}{(\Lambda_1+\Lambda_2)(\mu+k)}[(1-p)(1-\psi)(k\Lambda_1+\Lambda_2(k+\mu))+\Lambda_1\mu] & 0 & 0 & 0 & 0 \\
p(1-\psi)c(1-\theta)b_h\frac{k\Lambda_1+\Lambda_2(k+\mu)}{(\Lambda_1+\Lambda_2)(\mu+k)} & p(1-\psi)c(1-\theta)b_h\frac{k\Lambda_1+\Lambda_2(k+\mu)}{(\Lambda_1+\Lambda_2)(\mu+k)} & 0 & 0 & 0 & 0 & 0 & 0 & p(1-\psi)c(1-\theta)b_h\frac{k\Lambda_1+\Lambda_2(k+\mu)}{(\Lambda_1+\Lambda_2)(\mu+k)} & p(1-\psi)c(1-\theta)b_h\frac{k\Lambda_1+\Lambda_2(k+\mu)}{(\Lambda_1+\Lambda_2)(\mu+k)} & 0 & 0 & 0 & 0 \\
0 & 0 & 0 & 0 & 0 & 0 & 0 & 0 & 0 & 0 & 0 & 0 & 0 & 0 \\
0 & 0 & 0 & 0 & 0 & 0 & 0 & 0 & 0 & 0 & 0 & 0 & 0 & 0 \\
0 & 0 & 0 & 0 & c(1-\theta)b_c\frac{\Lambda_1\mu}{(\Lambda_1+\Lambda_2)(\mu+k)} & c(1-\theta)b_c\frac{\Lambda_1\mu}{(\Lambda_1+\Lambda_2)(\mu+k)} & 0 & 0 & c(1-\theta)b_c\frac{\Lambda_1\mu}{(\Lambda_1+\Lambda_2)(\mu+k)} & c(1-\theta)b_c\frac{\Lambda_1\mu}{(\Lambda_1+\Lambda_2)(\mu+k)} & 0 & 0 & 0 & 0 \\
0 & 0 & 0 & 0 & c(1-\theta)b_c\frac{k\Lambda_1+\Lambda_2(k+\mu)}{(\Lambda_1+\Lambda_2)(\mu+k)} & c(1-\theta)b_c\frac{k\Lambda_1+\Lambda_2(k+\mu)}{(\Lambda_1+\Lambda_2)(\mu+k)} & 0 & 0 & c(1-\theta)b_c\frac{k\Lambda_1+\Lambda_2(k+\mu)}{(\Lambda_1+\Lambda_2)(\mu+k)} & c(1-\theta)b_c\frac{k\Lambda_1+\Lambda_2(k+\mu)}{(\Lambda_1+\Lambda_2)(\mu+k)} & 0 & 0 & 0 & 0 \\
0 & 0 & 0 & 0 & 0 & 0 & 0 & 0 & 0 & 0 & 0 & 0 & 0 & 0 \\
0 & 0 & 0 & 0 & 0 & 0 & 0 & 0 & 0 & 0 & 0 & 0 & 0 & 0 \\
0 & 0 & 0 & 0 & 0 & 0 & 0 & 0 & 0 & 0 & 0 & 0 & 0 & 0 \\
0 & 0 & 0 & 0 & 0 & 0 & 0 & 0 & 0 & 0 & 0 & 0 & 0 & 0 \\
0 & 0 & 0 & 0 & 0 & 0 & 0 & 0 & 0 & 0 & 0 & 0 & 0 & 0 \\
0 & 0 & 0 & 0 & 0 & 0 & 0 & 0 & 0 & 0 & 0 & 0 & 0 & 0 \\
0 & 0 & 0 & 0 & 0 & 0 & 0 & 0 & 0 & 0 & 0 & 0 & 0 & 0 \\
0 & 0 & 0 & 0 & 0 & 0 & 0 & 0 & 0 & 0 & 0 & 0 & 0 & 0
\end{pmatrix}$$

$$V = \begin{pmatrix}
k+\rho_1+\mu & 0 & 0 & 0 & 0 & 0 & 0 & 0 & -\upsilon_1 & 0 & 0 & 0 & 0 & 0 \\
-k & \rho_2+\mu & 0 & 0 & 0 & 0 & 0 & 0 & 0 & -\upsilon_1 & 0 & 0 & 0 & 0 \\
-\rho_1 & 0 & \mu+\delta_2 & 0 & 0 & 0 & 0 & 0 & 0 & 0 & 0 & 0 & 0 & 0 \\
0 & -\rho_2 & 0 & \mu+\delta_2 & 0 & 0 & 0 & 0 & 0 & 0 & 0 & 0 & -\upsilon_2 & 0 \\
0 & 0 & 0 & 0 & k+\upsilon+\sigma_1\mu+\delta_1 & 0 & 0 & 0 & 0 & 0 & 0 & 0 & 0 & 0 \\
0 & 0 & 0 & 0 & -k & \upsilon+\sigma_1+\mu+\delta_1 & 0 & 0 & 0 & 0 & 0 & 0 & 0 & 0 \\
0 & 0 & 0 & 0 & -\sigma_1 & 0 & k+\mu+\delta_1 & 0 & 0 & 0 & 0 & 0 & 0 & 0 \\
0 & 0 & 0 & 0 & 0 & -\sigma_1 & -k & \mu+\delta_1 & 0 & 0 & 0 & 0 & 0 & 0 \\
0 & 0 & 0 & 0 & 0 & 0 & 0 & 0 & k+\sigma_2+rho_2+\upsilon_1+\mu+\delta_1 & 0 & 0 & 0 & 0 & 0 \\
0 & 0 & 0 & 0 & 0 & 0 & 0 & 0 & -k & \upsilon_1+\rho_2+\mu+\delta_1 & 0 & 0 & 0 & 0 \\
0 & 0 & 0 & 0 & 0 & 0 & 0 & 0 & -\sigma_2 & 0 & k+\rho_2+\mu+\delta_1 & 0 & 0 & 0 \\
0 & 0 & 0 & 0 & 0 & 0 & 0 & 0 & 0 & -\sigma_2 & -k & \rho_2+\mu+\delta_1 & 0 & 0 \\
0 & 0 & 0 & 0 & 0 & 0 & 0 & 0 & -\rho_2 & -\rho_2 & 0 & 0 & \upsilon_2+\sigma_2+\mu+\delta_1+\delta_2 & 0 \\
0 & 0 & 0 & 0 & 0 & 0 & 0 & 0 & 0 & 0 & -\rho_2 & -\rho_2 & -\sigma_2 & \mu+\delta_1+\delta_2
\end{pmatrix}$$

$$FV^{-1} = \begin{pmatrix}
\frac{A}{k+\mu+\rho_1}+\frac{Ak}{(k+\mu+\rho_1)(\mu+\rho_2)} & \frac{A}{\mu+\rho_2} & 0 & 0 & 0 & 0 & 0 & 0 & 0 & \star & \star & 0 & 0 & 0 & 0 \\
\frac{B}{k+\mu+\rho_1}+\frac{Bk}{(k+\mu+\rho_1)(\mu+\rho_2)} & \frac{B}{\mu+\rho_2} & 0 & 0 & 0 & 0 & 0 & 0 & 0 & \star & \star & 0 & 0 & 0 & 0 \\
0 & 0 & 0 & 0 & 0 & 0 & 0 & 0 & 0 & 0 & 0 & 0 & 0 & 0 & 0 \\
0 & 0 & 0 & 0 & 0 & 0 & 0 & 0 & 0 & 0 & 0 & 0 & 0 & 0 & 0 \\
0 & 0 & 0 & 0 & \frac{C}{\delta_1+k+\mu+\sigma_1+\upsilon}+\frac{Ck}{(\delta_1+\mu+\sigma_1+\upsilon)(\delta_1+k+\mu+\sigma_1+\upsilon)} & \frac{C}{(\delta_1+\mu+\sigma_1+\upsilon)} & 0 & 0 & \star & \star & 0 & 0 & 0 & 0 \\
0 & 0 & 0 & 0 & \frac{D}{\delta_1+k+\mu+\sigma_1+\upsilon}+\frac{Dk}{(\delta_1+\mu+\sigma_1+\upsilon)(\delta_1+k+\mu+\sigma_1+\upsilon)} & \frac{D}{(\delta_1+\mu+\sigma_1+\upsilon)} & 0 & 0 & \star & \star & 0 & 0 & 0 & 0 \\
0 & 0 & 0 & 0 & 0 & 0 & 0 & 0 & 0 & 0 & 0 & 0 & 0 & 0 & 0 \\
0 & 0 & 0 & 0 & 0 & 0 & 0 & 0 & 0 & 0 & 0 & 0 & 0 & 0 & 0 \\
0 & 0 & 0 & 0 & 0 & 0 & 0 & 0 & 0 & 0 & 0 & 0 & 0 & 0 & 0 \\
0 & 0 & 0 & 0 & 0 & 0 & 0 & 0 & 0 & 0 & 0 & 0 & 0 & 0 & 0 \\
0 & 0 & 0 & 0 & 0 & 0 & 0 & 0 & 0 & 0 & 0 & 0 & 0 & 0 & 0 \\
0 & 0 & 0 & 0 & 0 & 0 & 0 & 0 & 0 & 0 & 0 & 0 & 0 & 0 & 0 \\
0 & 0 & 0 & 0 & 0 & 0 & 0 & 0 & 0 & 0 & 0 & 0 & 0 & 0 & 0 \\
0 & 0 & 0 & 0 & 0 & 0 & 0 & 0 & 0 & 0 & 0 & 0 & 0 & 0 & 0
\end{pmatrix}$$

where $A = \frac{c(1-\theta)b_h}{(\Lambda_1+\Lambda_2)(\mu+k)}\left[(1-p)(1-\psi)(k\Lambda_1+\Lambda_2(k+\mu))+\Lambda_1\mu\right]$, $B = p(1-\psi)c(1-\theta)b_h\frac{k\Lambda_1+\Lambda_2(k+\mu)}{(\Lambda_1+\Lambda_2)(\mu+k)}$, $C = c(1-\theta)b_c\frac{\Lambda_1\mu}{(\Lambda_1+\Lambda_2)(\mu+k)}$, and $D = c(1-\theta)b_c\frac{k\Lambda_1+\Lambda_2(k+\mu)}{(\Lambda_1+\Lambda_2)(\mu+k)}$. The formulas represented by $\star$ are irrelevant to compute the eigenvalues, so, for the sake of simplicity, it was decided not to include those here.

In order to compute R_0, the basic reproduction number for the whole model (4.12), it is necessary to compute the eigenvalues of the matrix FV^{-1}, since R_0 is the spectral radius of FV^{-1}, i.e., it is the dominant eigenvalue of this matrix.

Let's now proceed with the computation of the eigenvalues by calculating the determinant below:

$$FV^{-1} = \begin{pmatrix} \frac{A}{k+\mu+\rho_1}+\frac{Ak}{(k+\mu+\rho_1)(\mu+\rho_2)}-\lambda & \frac{A}{\mu+\rho_2} & 0 & 0 \\ \frac{B}{k+\mu+\rho_1}+\frac{Bk}{(k+\mu+\rho_1)(\mu+\rho_2)} & \frac{B}{\mu+\rho_2}-\lambda & 0 & 0 \\ 0 & 0 & \frac{C}{\delta_1+k+\mu+\sigma_1+\upsilon}+\frac{Ck}{(\delta_1+\mu+\sigma_1+\upsilon)(\delta_1+k+\mu+\sigma_1+\upsilon)}-\lambda & \frac{C}{(\delta_1+\mu+\sigma_1+\upsilon)} \\ 0 & 0 & \frac{D}{\delta_1+k+\mu+\sigma_1+\upsilon}+\frac{Dk}{(\delta_1+\mu+\sigma_1+\upsilon)(\delta_1+k+\mu+\sigma_1+\upsilon)} & \frac{D}{(\delta_1+\mu+\sigma_1+\upsilon)}-\lambda \end{pmatrix}$$

As FV^{-1} is a matrix of the form: $\begin{bmatrix} U_1 & 0 \\ 0 & U_2 \end{bmatrix}$, then its eigenvalues are the ones of matrices U and V, where:

$$U_1 = \begin{pmatrix} \frac{A}{k+\mu+\rho_1}+\frac{Ak}{(k+\mu+\rho_1)(\mu+\rho_2)}-\lambda & \frac{A}{\mu+\rho_2} \\ \frac{B}{k+\mu+\rho_1}+\frac{Bk}{(k+\mu+\rho_1)(\mu+\rho_2)} & \frac{B}{\mu+\rho_2}-\lambda \end{pmatrix};$$

$$U_2 = \begin{pmatrix} \frac{C}{\delta_1+k+\mu+\sigma_1+\upsilon}+\frac{Ck}{(\delta_1+\mu+\sigma_1+\upsilon)(\delta_1+k+\mu+\sigma_1+\upsilon)}-\lambda & \frac{C}{(\delta_1+\mu+\sigma_1+\upsilon)} \\ \frac{D}{\delta_1+k+\mu+\sigma_1+\upsilon}+\frac{Dk}{(\delta_1+\mu+\sigma_1+\upsilon)(\delta_1+k+\mu+\sigma_1+\upsilon)} & \frac{D}{(\delta_1+\mu+\sigma_1+\upsilon)}-\lambda \end{pmatrix}$$

After some algebra manipulation R_0 is given by:

$$R_0 = \rho(FV^{-1}) = \max\{R_{HIV}, R_{HCV}\} \tag{4.18}$$

By Theorem 2 [150], the following lemma is obtained.

Lema 4.2.4 *The disease-free equilibrium P_0 is locally asymptotically stable if $R_0 < 1$ and unstable if $R_0 > 1$.*

4.2.3 Bifurcation analysis

In this section, XPPAUT [40] is used to build bifurcation diagrams for distinct parameters of model (4.12).

Figure 4.19 shows the sketch of the bifurcation diagram for different values of β_c, the probability that a contact will result in an HCV infection. Increasing β_c, at $\beta_c = 0.2031$, there is a bifurcation point (1), at which the model bifurcates from a stable disease-free equilibrium to a stable HCV endemic equilibrium. This means that increasing the probability that a contact will result in an HCV infection originates new cases of HCV infections. This is a realistic prediction.

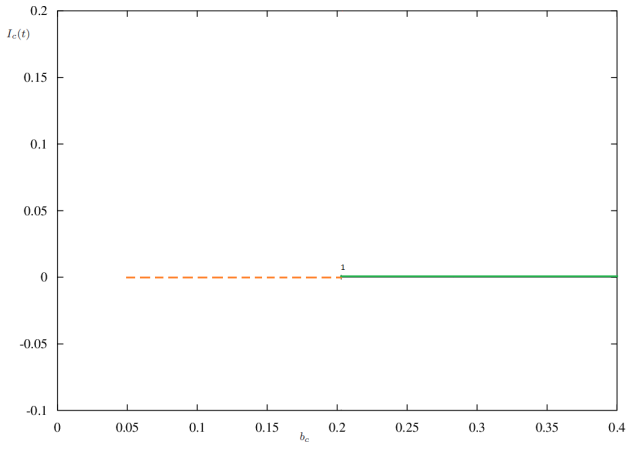

Figure 4.19: Sketch of the bifurcation diagram for different values of β_c, the probability that a contact will result in HCV transmission. Remaining parameter values are given in Table 4.5, except for $\beta_h = 0.032$. At the bifurcation point (1) $\beta_c \simeq 0.2031$. Orange dashed line - stable disease-free equilibrium, green filled line - stable HCV endemic equilibrium. For more information, see text.

Figure 4.20 depicts the bifurcation diagram for different values of β_h, the probability that a contact will result in an HIV infection. Beginning from a disease-free equilibrium and increasing β_h, at $\beta_h = 0.034$, there is a bifurcation point (1), at which the model bifurcates to the stable HIV endemic equilibrium. This means that increasing the probability that a contact will result in an HIV infection promotes the appearance of new cases of HIV infections, as biologically expected.

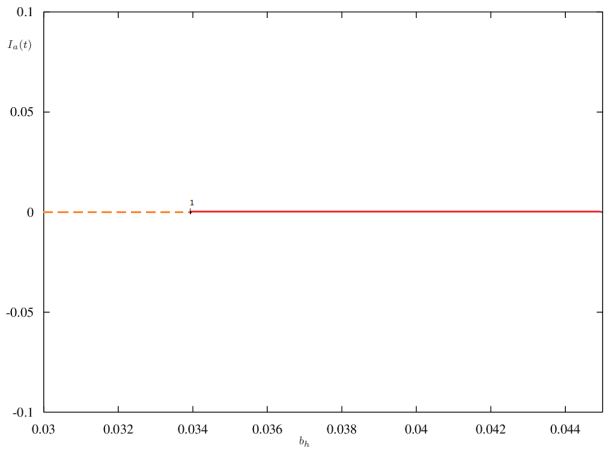

Figure 4.20: Drawing of the bifurcation diagram for different values of β_h, the probability that a contact will result in HIV transmission. Remaining parameter values are given in Table 4.5. At the bifurcation point (1) $\beta_h \simeq 0.034$. Orange dashed line - stable disease-free equilibrium, red filled line - stable HIV endemic equilibrium. For more information, see text.

Figure 4.21 depicts the bifurcation diagram for different values of β_c, the probability that a contact will result in an HCV infection. Beginning from an HIV endemic equilibrium and increasing β_c, at $\beta_c = 0.2503$, there is a bifurcation point (1), at which the model bifurcates to the stable two endemic equilibrium. This means that in a population already infected with HIV, with lowered defense mechanisms, increasing the probability of a contact resulting in HCV infection will set off new coinfection cases.

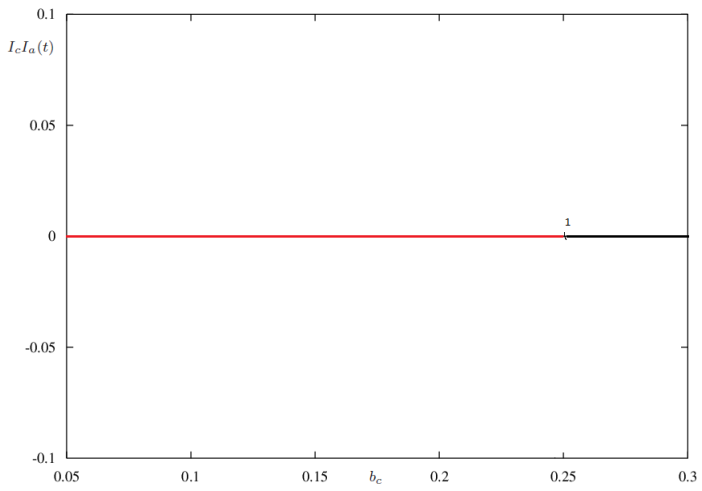

Figure 4.21: Sketch of the bifurcation diagram for different values of β_c, the probability that a contact will result in an HCV infection. Remaining parameter values are given in Table 4.5. At the bifurcation point (1) $\beta_c = 0.2503$. Red filled line - stable HIV endemic equilibrium, black filled line - stable two endemic equilibrium. For more information, see text.

Figure 4.22 depicts the bifurcation diagram for different values of β_h, the probability that a contact will result in an HIV infection. Beginning from an HCV endemic equilibrium and increasing β_h, at $\beta_h = 0.0503$, there is a bifurcation point (1), at which the model bifurcates to the stable two endemic equilibrium. This means that in a population with impaired immune system due to infection with HCV, increasing the probability of a contact resulting in HIV infection will trigger new coinfection cases.

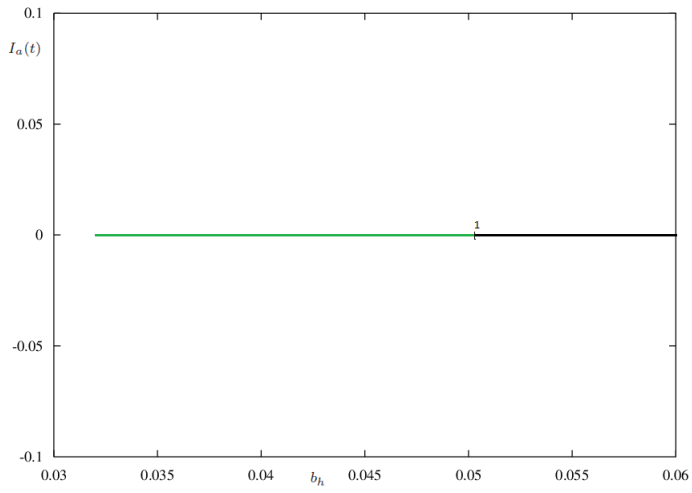

Figure 4.22: Sketch of the bifurcation diagram for different values of β_h, the probability that a contact will result in an HIV infection. Remaining parameter values are given in Table 4.5. At the bifurcation point (1) $\beta_h = 0.0503$. Green filled line - stable HCV endemic equilibrium, black filled line - stable two endemic equilibrium. For more information, see text.

4.2.4 Sensitivity analysis

In this section, the sensitivity indices of the reproduction number, R_0, to relevant parameters of model (4.12) are performed. The procedure developed in [27] follows. The sensitivity analysis is used to measure the relative change in a state variable when a given parameter is varied. Measuring the R_0 sensitivity indices is extremely important since the value of R_0 determines the spread or the eradication of the disease.

The sensitivity index of $R_0 = max\{R_{HIV}, R_{HCV}\}$ with respect to parameter $\beta_c = c(1-\theta)b_c$ is given by:

$$\frac{\partial R_0}{\partial \beta_c} \times \frac{\beta_c}{R_0} = 1$$

The sensitivity index of R_0 with respect to parameter $\beta_h = c(1-\theta)b_h$ is given by:

$$\frac{\partial R_0}{\partial \beta_h} \times \frac{\beta_h}{R_0} = 1$$

These values for this sensitivity index mean that the probability of HCV or HIV transmission has strong influence in HCV and HIV control and management. Similar expressions

may be obtained for the other parameters of R_0. Nevertheless, most of the expressions for the sensitivity indices are complex with little obvious structure. Therefore, the corresponding values for the parameter values given in Table 4.5 are computed. The signs of the sensitivity indices may be found in Table 4.4. A positive sign implies that increases in the corresponding parameter values translate in an increase in the value of R_0. Inversely for a negative sign, a negative index means than an increase in the parameter value implies a decrease in the value of R_0. For example, an increase of 5% in the values of β_h or β_c augments 5% the value of R_0. Similar inferences may be performed for the other indices.

Parameter	Sensitivity index sign
β_c	+
β_h	+
θ	-
ν	-
σ_1	-
σ_2	-
p	+
k	+
ρ_2	-
ρ_1	-

Table 4.4: Sensitivity indexes for relevant parameters of model (4.12).

4.2.5 Numerical results

In this section, the numerical simulations of model (4.12) are presented. The parameter values used in the simulations can be found in Table 4.5 and the following initial conditions: $S_{\tilde{s}}(0) = 500$, $S_s(t) = 0$ (assume that no individuals were screened initially), $I_{\tilde{a}}(0) = 80$, $I_a(0) = 0$, $A_a(t) = 0$, $A_{\tilde{a}} = 15$, $I_c(t) = 0$, $I_{\tilde{c}} = 20$, $C_s(0) = 0$, $C_{\tilde{s}} = 5$, $I_cI_a(0) = I_cI_{\tilde{a}} = CI_a = CI_{\tilde{a}} = I_cA = CA = 0$ are used.

Parameter	Value	Reference
Λ_1	8	Assume
Λ_2	4	Assume
c	8	Assume
θ	0.20	[2]
b_h	0.036	[54]
b_c	0.05	[149]
η_1	1.0002	[16]
η_2	1.0002	[16]
υ	0.25	[149]
υ_1	0.27	Assume
υ_2	0.25	Assume
μ	0.020	[16]
p	0.0367	[85]
ψ	0.0288	[85]
k	0.00388	[85]
ρ_1	0.1908	[85]
ρ_2	0.1511	[85]
δ_1	0.2801	Assume
δ_2	0.2801	[85]
δ	1.0001	[16]
σ	1.001	[16]
σ_1	0.75	[87]
σ_2	0.75	[87]

Table 4.5: Parameters used in the numerical simulations of model (4.12), where appropriate units are yr^{-1}.

In Figures 4.23, it is observed that the model approaches asymptotically the stable HIV endemic equilibrium.

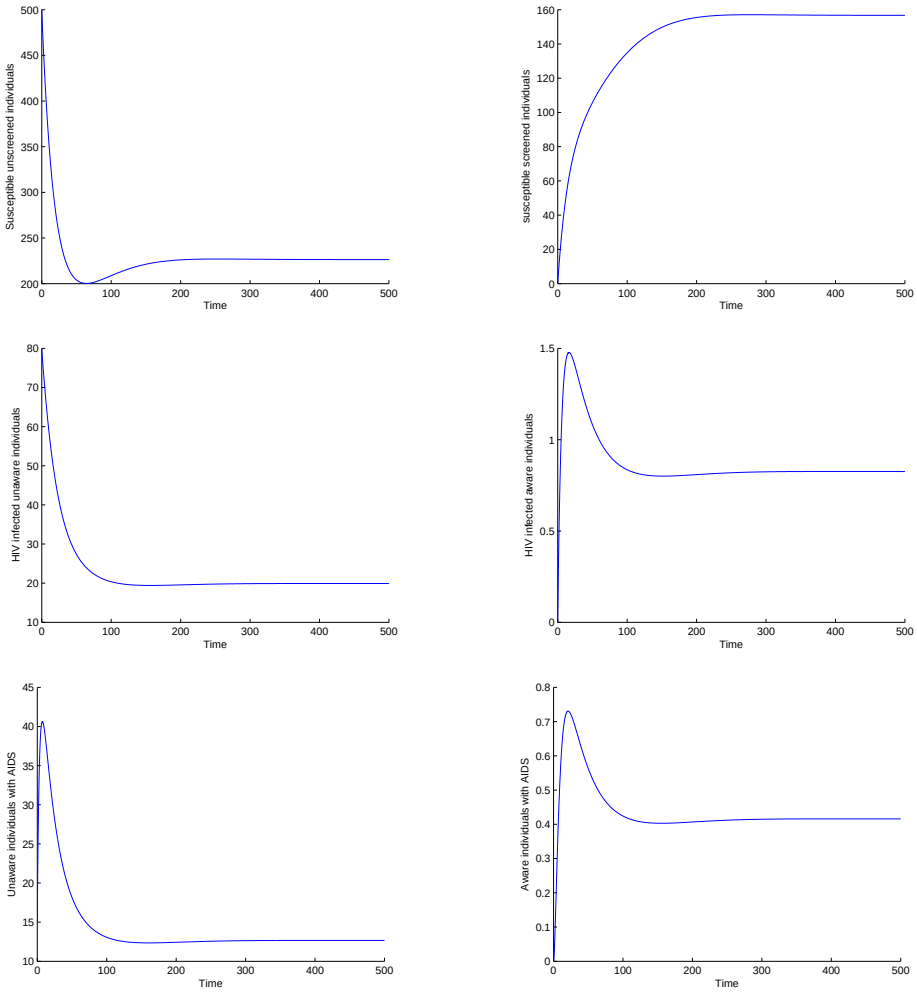

Figure 4.23: Stable HIV endemic equilibrium of system (4.12) for given parameter values in Table 4.5, and given initial conditions ($R_{HIV} = 1.0875$, $R_{HCV} = 0.2461$, $R_0 = 1.0875$). The remaining variables go asymptotically to 0. For more information, see text.

Figure 4.24 shows the stable HCV endemic equilibrium for system (4.12).

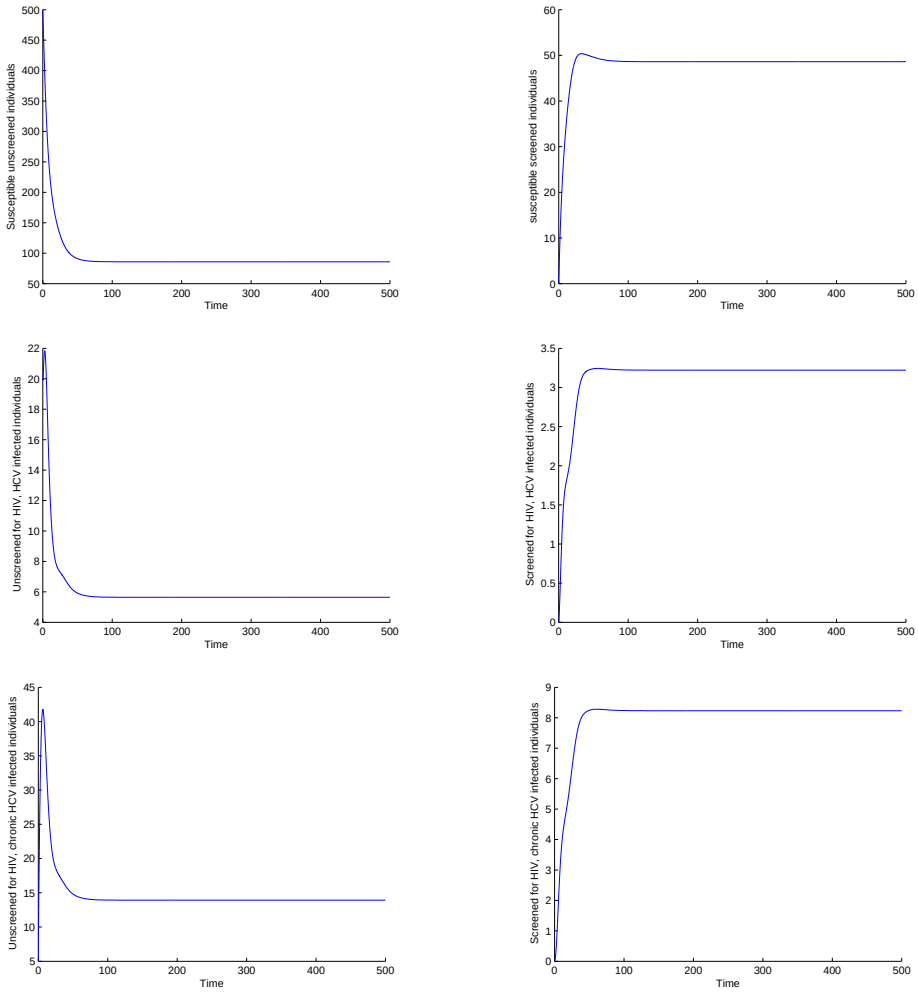

Figure 4.24: Stable HCV endemic equilibrium of system (4.12) for parameter values given in Table 4.5, except $\beta_c = 0.25$ and $\beta_h = 0.032$, and given initial conditions ($R_{HIV} = 0.9667$, $R_{HCV} = 1.2307$, $R_0 = 1.2307$). The remaining variables go asymptotically to 0. For more information, see text.

In Figure 4.25, the dynamics of the variables of system (4.12)is drawn. It is observed that, for the given parameters values and initial conditions, the model approaches asymptotically the stable two disease endemic equilibrium.

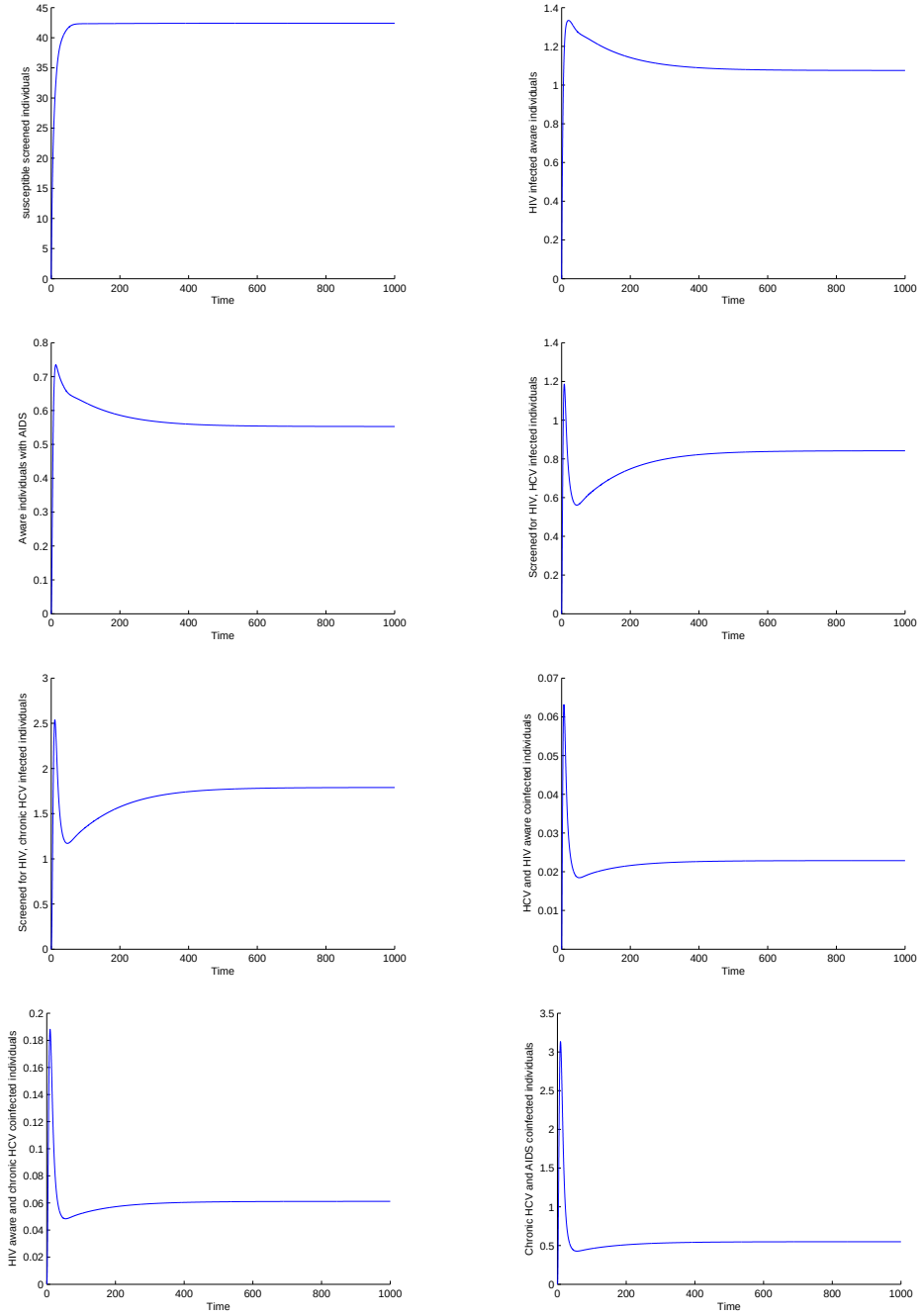

Figure 4.25: Stable two disease endemic equilibrium of system (4.12) for given parameter values in Table 4.5, except for $b_h = 0.054$, $b_c = 0.25$, and given initial conditions ($R_{HIV} = 1.6313$, $R_{HCV} = 1.2307$, $R_0 = 1.6313$) (relevant variables). For more information, see text.

In Figure 4.26, it plots the dynamics of the relevant variables of system (4.12) for different values of θ, the level of protection against HIV and HCV by condom use. It

is observed that as θ decreases the system (4.12) bifurcates from the stable disease-free equilibrium to the stable HIV endemic equilibrium. This suggests that individuals should, as expected, use condom, to prevent being infected with HIV.

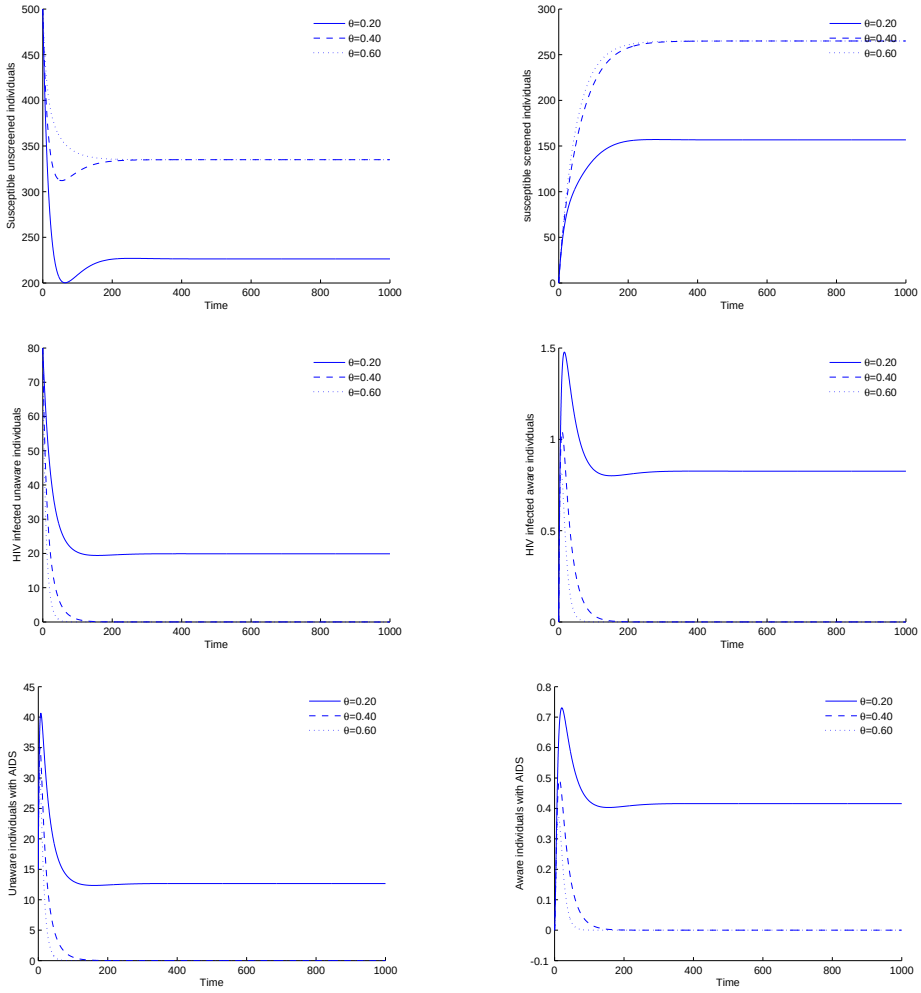

Figure 4.26: Dynamics of the relevant variables of the system (4.12) for different values of θ, the level of protection against HIV and HCV by condom use. Parameter values are given in Table 4.5 and initial conditions are in the text. The remaining variables go asymptotically to zero. For more information, see text.

Figure 4.27 shows the dynamics of the relevant variables of system (4.12) for diferent values of β_h, the probability that a contact will result in an HIV infection. It is observed that increasing the system (4.12) has a bifurcation point as β_h increases from 0.030 till 0.1. The system bifurcates from a stable disease-free equilibrium to a stable HIV endemic equilibrium. This was a predictable outcome and suggests that measures that reduce this probability β_h should be taken under consideration in order to reduce HIV

transmission.

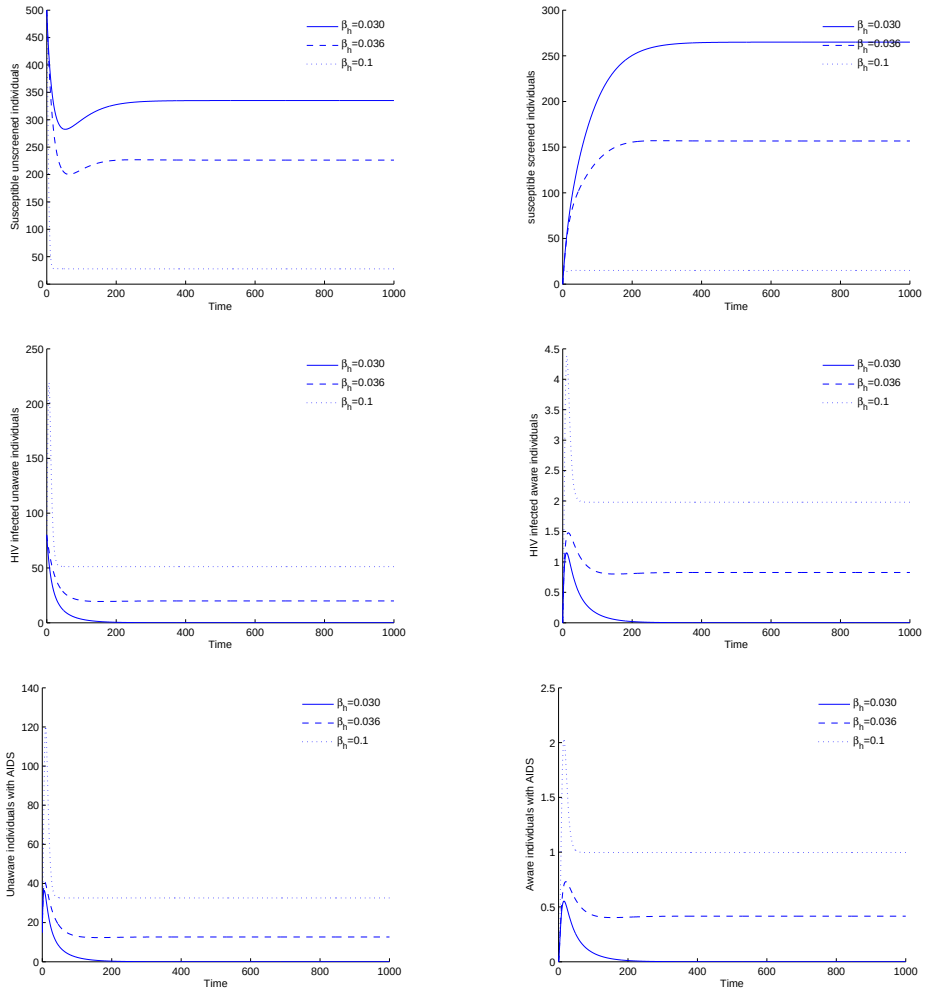

Figure 4.27: Dynamics of the relevant variables of the system (4.12) for diferent values β_h, the probability that a contact will result in an HIV infection. Parameter values are given in Table 4.5 and initial conditions are in the text. The remaining variables go asymptotically to zero. For more information see text.

In Figure 4.28, the dynamics of the relevant variables of system (4.12) are plotted for different values of β_c, the probability that a contact will result in an HCV infection. It is observed that as β_c increases from 0.05 to 0.25 there is a bifurcation from a state without disease to a state with HCV infection that persists with the continuous increase of β_c. The number of chronic carriers also increases. Biologically this is a reasonable outcome, one would expect an augment in the number of new disease cases as the probability of transmission increases.

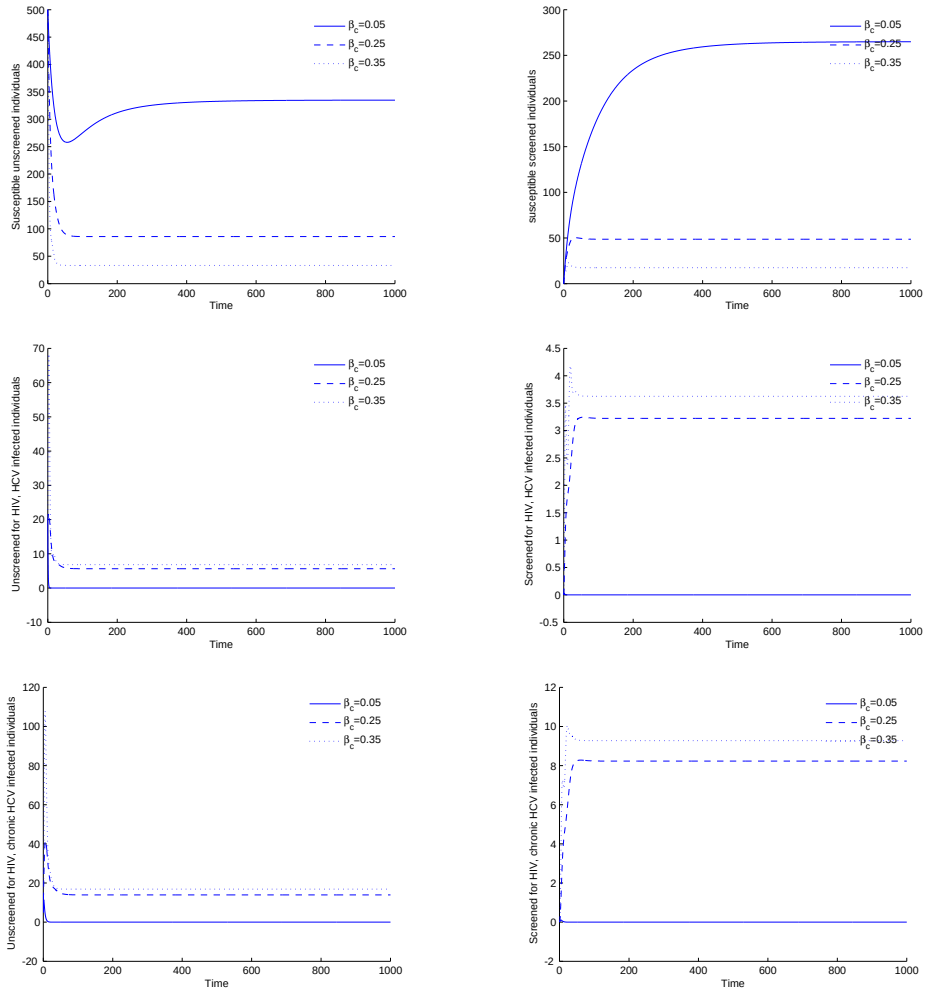

Figure 4.28: Dynamics of the relevant variables of the system (4.12) for different values of β_c, the probability that a contact will result in an HCV infection. Parameter values are given in Table 4.5, except $b_h = 0.032$ and initial conditions are in the text. For more information, see text.

In Figure 4.29, the dynamics of the relevant variables of system (4.12) are plotted for different values of ψ, the parameter that measures the efficacy of screening in reducing HIV transmission. It is observed that as ψ increases the number of individuals infected with HIV and suffering from AIDS decreases, in fact, the system (4.12) is initially at a stable HIV endemic equilibrium and changes its qualitative behavior to a stable disease-free equilibrium. In real life, this means that individuals that are screened should change their behavior in order to prevent transmission of the disease. In fact, there are some studies that show that screened HIV infectives tend to change their behavior and those whose test is negative don't [160]. Nevertheless, the tests are meant to promote

behavior change and to access to health care for all screened individuals.

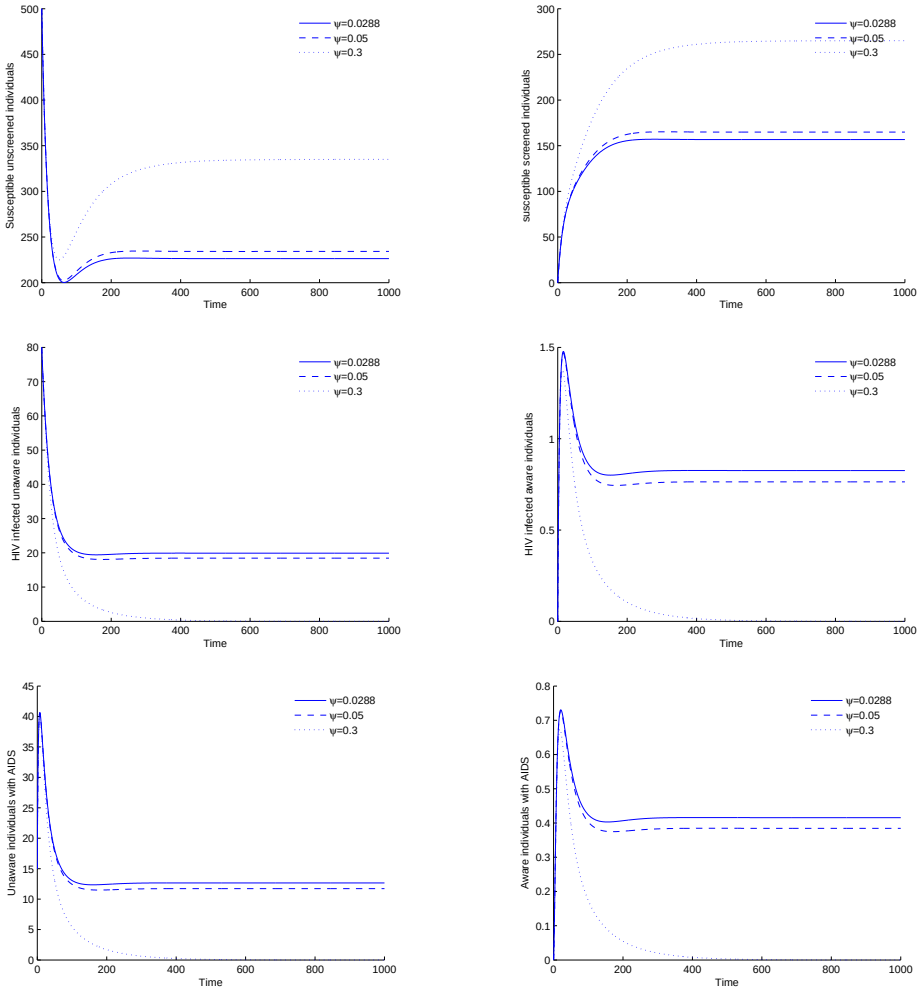

Figure 4.29: Dynamics of the relevant variables of the system (4.12) for different values of ψ, the parameter that measures the efficacy of screening in reducing HIV transmission. Parameter values are given in Table 4.5 and initial conditions are in the text. Remaining variables go asymptotically to zero. For more information, see text.

4.2.6 Conclusions

Model IV is a coinfection model for HCV and HIV infections, that includes treatment for both diseases, unawareness and awareness if HIV infection, and the use of condom. The local stability of the disease-free equilibria for the full model and for the two submodels (HCV only and HIV only submodels) are studied. Bifurcation diagrams are sketched

for relevant parameters, such as the probabilities that a contact will result in a HIV or an HCV infection. Numerical examples are used to illustrate the change of the dynamical behavior of certain relevant parameters. The results obtained suggest that specific measures should be considered in order to reduce HIV infection, such as: distributing more condoms to individuals and try to forward the message that condom should be used during anal intercourse (though this might not be well accepted in MSM population due to unprotected sex negotiation); develop campaigns in order to warn individuals about the consequences of having many sexual partners; continuing treatment for AIDS and pursuing the investigation of new and better drugs to combat the virus; regular screening. Considering HCV infection, treatment is also highly recommended as well as other measures (e.g., more informational campaigns about the disease) in order to decrease the number of infectious and of chronic carriers. MSM population is at risk of HCV reinfection following successful treatment and documented clearance of HCV, they should be warned about this important risk. Future work will consider the effect of needle sharing in the case of HIV and HCV transmission rates, and an application of the model to real Portuguese data, with corresponding estimation of parameter values.

Chapter 5

Models for coinfection of HIV and TB

C.M.A. Pinto and A.R.M. Carvalho, The HIV/TB coinfection severity in the presence of TB multi-drug resistant strains, Ecological Complexity 32, 1–20, 2017.

Based on the previously mentioned research, it is considered a non-integer order model for HIV and TB coinfection, with the objective of studying the presence of drug resistant TB strains and treatment for both diseases. The novelty of this model is the inclusion of the derivation of a fractional order model for the dynamics of the coinfection of HIV and TB in the presence of TB resistant strains. The model is introduced, and the reproduction number and stability of the disease-free equilibrium are studied. It follows the proofs for the global stability of the disease-free equilibria of the two submodels and of the full model. The sensitivity analysis is done. Numerical simulations of the model for distinct values of the order of the fractional derivative and relevant parameters, and discussion of the results, are done.

5.1 Description of the model

The model is composed of 13 classes. In Fig. 5.1, it is depicted the flow chart of the model. It represents schematically the epidemiology of HIV and TB coinfection. The different disease stages are reproduced by the different compartments (rectangles) and the arrows indicate the way individuals progress from one stage to the other.

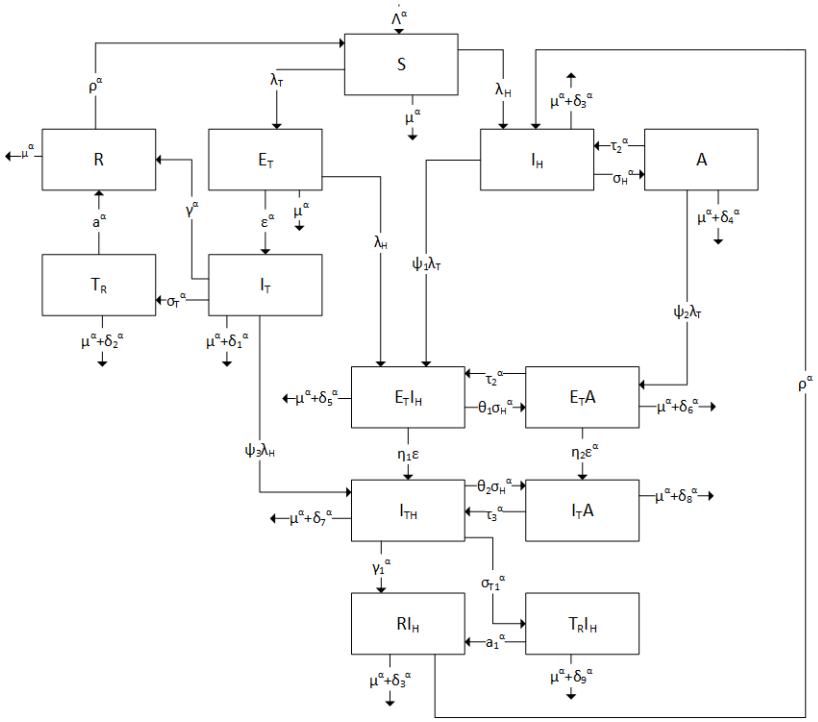

Figure 5.1: Flow chart of the model.

The individuals in the susceptible class, S, are recruited at a rate Λ^α. They are infected by individuals infected with HIV and active TB at rates:

$$\lambda_H = \frac{\beta_H^\alpha (I_H + E_T I_H + R I_H + \eta_H (I_{TH} + T_R I_H))}{N}$$

and

$$\lambda_T = \frac{\beta_T^\alpha (I_T + \eta_T T_R + \eta_{TH} (I_{TH} + T_R I_H))}{N}$$

respectively. Parameters β_H^α and β_T^α are the effective contact rates for HIV and TB infection, respectively. The modification parameters η_H and η_{TH} account for the increased infectiousness of individuals coinfected with HIV and TB, when compared to individuals solely infected with either HIV or TB, respectively. The modification parameter η_T represents the increased infectiousness of the MRD-TB drug-resistant infected individuals when compared to the individuals infected with non-resistant TB strains. It is considered, for simplification, that people showing symptoms of AIDS do not infect others.

The individuals exposed to TB, E_T, develop active TB at rate ϵ^α and move to the class of infected individuals, I_T. The exposed, E_T, may also be infected with HIV at a rate

λ_H and move to the class of individuals exposed to TB and infected with HIV, $E_T I_H$. Individuals I_T may recover from TB at rate γ^α and move to the recovered class, R. They become resistant to the first line of TB treatment at rate σ_T^α, and move to the MDR-TB drug-resistant individuals' class, T_R. I_T individuals are infected with HIV at rate $\psi_3\lambda_H$, where $\psi_3 > 1$ captures the fact that individuals infected with TB are more infectious than the ones only exposed to TB, and move to the dually infected class, I_{TH}. The individuals infected with the MDR-TB strains, T_R, recover from TB at rate a^α. The recovered individuals, R, become susceptible to TB at rate ρ^α, since there is no permanent TB immunity.

The individuals infected with HIV, I_H, develop AIDS at a rate σ_H^α moving to the class of patients showing symptoms of AIDS, A. They are also infected with TB at rate $\psi_1\lambda_T$, where ψ_1 is a modification parameter, and move to class $E_T I_H$. The individuals with AIDS, A, are treated at rate τ_2^α, and move to class I_H. They are infected with TB at rate $\psi_2\lambda_T$, where $\psi_2 > \psi_1$ is modification parameter, and move to the class of individuals exposed to TB and showing symptoms of AIDS, $E_T A$. The inequality $\psi_2 > \psi_1$ represents the fact that the individuals with AIDS are more infectious than those only infected with HIV. The individuals in class $E_T I_H$, and in class $E_T A$, develop active TB at rates $\eta_1\epsilon^\alpha$ and $\eta_2\epsilon^\alpha$, and move to classes I_{TH} and $I_T A$, respectively. The class $I_T A$ are the dually infected individuals with active TB and AIDS. It is noted that $\eta_2 > \eta_1$, since patients with AIDS develop active TB faster than individuals infected only with HIV. The patients in class $E_T I_H$ and in class I_{TH} proceed to AIDS at rates $\theta_1\sigma_H^\alpha$ and $\theta_2\sigma_H^\alpha$, respectively, where $\theta_2 > \theta_1$. The later translates the fact that individuals infected with TB proceed faster to AIDS than the ones exposed to TB. The individuals in class I_{TH} are treated for TB at rate γ_1^α and move to class RI_H (patients recovered from TB and infected with HIV). Moreover, patients in class I_{TH} may develop MDR-TB strains at rate σ_{T1}^α and move to class $T_R I_H$ (individuals dually infected with HIV and MDR-TB strains). The later recover from TB at rate a_1^α. The TB recovered individuals, RI_H move to the HIV solely infected class (I_H) at rate ρ^α. The individuals in class $I_T A$ are treated for HIV and move to class I_{TH} at rate τ_3^α. All individuals die from natural causes at rate μ^α. Depending on the state of infection, individuals die from HIV, or TB, or HIV and TB coinfection, at rates δ_i^α, $i = 1, \cdots, 9$.

The nonlinear system of fractional-order differential equations describing the dynamics of the model is:

$$
\begin{aligned}
\tfrac{d^\alpha S}{dt^\alpha} &= \Lambda^\alpha - \lambda_T S - \lambda_H S + \rho^\alpha R - \mu^\alpha S \\
\tfrac{d^\alpha E_T}{dt^\alpha} &= \lambda_T S - (\lambda_H + \epsilon^\alpha + \mu^\alpha) E_T \\
\tfrac{d^\alpha I_T}{dt^\alpha} &= \epsilon^\alpha E_T - (\psi_3 \lambda_H + \gamma^\alpha + \sigma_T^\alpha + \mu^\alpha + \delta_1^\alpha) I_T \\
\tfrac{d^\alpha R}{dt^\alpha} &= \gamma^\alpha I_T + a^\alpha T_R - (\rho^\alpha + \mu^\alpha) R \\
\tfrac{d^\alpha T_R}{dt^\alpha} &= \sigma_T^\alpha I_T - (a^\alpha + \mu^\alpha + \delta_2^\alpha) T_R \\
\tfrac{d^\alpha I_H}{dt^\alpha} &= \lambda_H S + \tau_2^\alpha A + \rho^\alpha R I_H - (\psi_1 \lambda_T + \sigma_H^\alpha + \mu^\alpha + \delta_3^\alpha) I_H \\
\tfrac{d^\alpha A}{dt^\alpha} &= \sigma_H^\alpha I_H - (\psi_2 \lambda_T + \tau_2^\alpha + \mu^\alpha + \delta_4^\alpha) A \qquad (5.1) \\
\tfrac{d^\alpha E_T I_H}{dt^\alpha} &= \lambda_H E_T + \psi_1 \lambda_T I_H + \tau_2^\alpha E_T A - (\eta_1 \epsilon^\alpha + \theta_1 \sigma_H^\alpha + \mu^\alpha + \delta_5^\alpha) E_T I_H \\
\tfrac{d^\alpha E_T A}{dt^\alpha} &= \theta_1 \sigma_H^\alpha E_T I_H + \psi_2 \lambda_T A - (\eta_2 \epsilon^\alpha + \tau_2^\alpha + \mu^\alpha + \delta_6^\alpha) E_T A \\
\tfrac{d^\alpha I_{TH}}{dt^\alpha} &= \eta_1 \epsilon^\alpha E_T I_H + \psi_3 \lambda_H I_T + \tau_3^\alpha I_T A - (\gamma_1^\alpha + \sigma_{T1}^\alpha + \theta_2 \sigma_H^\alpha + \mu^\alpha + \delta_7^\alpha) I_{TH} \\
\tfrac{d^\alpha I_T A}{dt^\alpha} &= \theta_2 \sigma_H^\alpha I_{TH} + \eta_2 \epsilon^\alpha E_T A - (\tau_3^\alpha + \mu^\alpha + \delta_8^\alpha) I_T A \\
\tfrac{d^\alpha R I_H}{dt^\alpha} &= \gamma_1^\alpha I_{TH} + a_1^\alpha T_R I_H - (\rho^\alpha + \mu^\alpha + \delta_3^\alpha) R I_H \\
\tfrac{d^\alpha T_R I_H}{dt^\alpha} &= \sigma_{T1}^\alpha I_{TH} - (a_1^\alpha + \mu^\alpha + \delta_9^\alpha) T_R I_H
\end{aligned}
$$

where $\alpha \in (0, 1]$ is the order of the fractional derivative. When $\alpha = 1$, then the model is the integer order counterpart. The fractional derivative of the proposed model is used in the Caputo sense, i.e.:

$$\frac{d^\alpha y(t)}{dt^\alpha} = I^{p-\alpha} y^{(p)}(t), \quad t > 0$$

where $p = \lceil \alpha \rceil$ is the value of α rounded up to the nearest integer, $y^{(p)}$ is the p-th derivative of $y(r)$, I^{p_1} is the Riemann-Liouville fractional integral given by:

$$I^{p_1} z(t) = \frac{1}{\Gamma(p_1)} \int_0^t \left(t - t'\right)^{p_1 - 1} z(t') dt'$$

The main advantage using Caputo's fractional derivative is that the classical initial conditions can be used without encountering any problem during solvability.

5.1.1 Non-negative solutions

Denote $R_+^{13} = \{x \in R^{13} \mid x \geq 0\}$ and let

$$x(t) = (S(t), E_T(t), I_T(t), R(t), T_R(t), I_H(t), A(t), E_T I_H(t), E_T A(t), I_{TH}(t), I_T A(t), R I_H(t), T_R I_H(t))^T \tag{5.2}$$

To prove the main theorem, the following Generalized Mean Value Theorem [86] and corollary are needed.

Lema 5.1.1 *[86] Suppose that $f(x) \in C[a,b]$ and $D_a^\alpha f(x) \in C(a,b]$, for $0 < \alpha \leq 1$, then*

$$f(x) = f(a) + \frac{1}{\Gamma(\alpha)}(D_a^\alpha f)(\xi)(x-a)^\alpha$$

with $a \leq \xi \leq x$, $\forall x \in (a,b]$ and $\Gamma(\cdot)$ is the gamma function.

Corollary 5.1.2 *Suppose that $f(x) \in C[a,b]$ and $D_a^\alpha f(x) \in C(a,b]$, for $0 < \alpha \leq 1$. If $D_a^\alpha f(x) \geq 0$, $\forall x \in (a,b)$, then $f(x)$ is non-decreasing for each $x \in [a,b]$. If $D_a^\alpha \leq 0$, $\forall x \in (a,b)$, then $f(x)$ is non-increasing for each $x \in [a,b]$.*

Now the main theorem is proved.

Theorem 5.1.3 *There is a unique solution*

$$x(t) = (S(t), E_T(t), I_T(t), R(t), T_R(t), I_H(t), A(t), E_T I_H(t), E_T A(t), I_{TH}(t), I_T A(t), R I_H(t), T_R I_H(t))^T \tag{5.3}$$

of the model (5.1) on $t \geq 0$ and the solution will remain in R_+^{13}.

Proof From Theorem 3.1 and Remark 3.2 of [67], the solution is known in $(0, +\infty)$ of the initial value problem exists and is unique. It is now proven that the non-negative orthant R_+^{13} is a positively invariant region. To do this, it is necessary to show that on each hyperplane bounding the non-negative orthant, the vector field points to R_+^{13}. From model (5.1):

$$D^\alpha S\mid_{S=0}=\Lambda^\alpha+\rho^\alpha R\geq 0 \qquad D^\alpha E_T\mid_{E_T=0}=\lambda_T S\geq 0 \qquad D^\alpha I_T\mid_{I_T=0}=\epsilon^\alpha E_T\geq 0$$

$$D^\alpha R\mid_{R=0}=\gamma^\alpha I_T+a^\alpha T_R\geq 0 \qquad D^\alpha T_R\mid_{T_R=0}=\sigma_T^\alpha I_T\geq 0$$

$$D^\alpha I_H\mid_{I_H=0}=\lambda_H S+\tau_2^\alpha A+\rho^\alpha R I_H\geq 0 \qquad D^\alpha A\mid_{A=0}=\sigma_H^\alpha I_H\geq 0$$

$$D^\alpha E_T I_H\mid_{E_T I_H=0}=\lambda_H E_T+\psi_1\lambda_T I_H+\tau_2 E_T A\geq 0$$

$$D^\alpha E_T A\mid_{E_T A=0}=\theta_1\sigma_H^\alpha E_T I_H+\psi_2\lambda_T A\geq 0$$

$$D^\alpha I_{TH}\mid_{I_{TH}=0}=\eta_1\epsilon^\alpha E_T I_H+\psi_3\lambda_H I_T\geq 0 \qquad D^\alpha I_T A\mid_{I_T A=0}=\theta_2\sigma_H^\alpha I_{TH}+\eta_2\epsilon^\alpha E_T A\geq 0$$

$$D^\alpha R I_H\mid_{R I_H=0}=\gamma_1^\alpha I_{TH}+a_1^\alpha T_R IH\geq 0 \qquad D^\alpha T_R I_H\mid_{T_R I_H=0}=\sigma_{T1}^\alpha I_{TH}\geq 0$$

Then, by Corollary 2, the solution will remain in R_+^{13}.

■

5.2 Reproduction number

In this section, the reproduction number of model (5.1), R_0, is calculated. The basic reproduction number is defined as the number of secondary infections due to a single infection in a completely susceptible population.

Are considered two sub-models of model (5.1). Model (5.4) arises from model (5.1) by setting the variables concerning HIV/AIDS dynamics (I_H, A, $E_T I_H$, $E_T A$, I_{TH}, $I_T A$, RI_H and $T_R I_H$) to zero, and model (5.8) follows from model (5.1) by setting the variables concerning TB (E_T, I_T, R, T_R, $E_T I_H$, $E_T A$, I_{TH}, $I_T A$, RI_H and $T_R I_H$) to zero.

One starts with the computation of the reproduction number of system (5.4), R_T. The next generation method is used to compute R_T [150].

$$\begin{aligned}
\frac{d^\alpha S}{dt^\alpha} &= \Lambda^\alpha - \lambda_T S + \rho^\alpha R - \mu^\alpha S \\
\frac{d^\alpha E_T}{dt^\alpha} &= \lambda_T S - (\epsilon^\alpha + \mu^\alpha) E_T \\
\frac{d^\alpha I_T}{dt^\alpha} &= \epsilon^\alpha E_T - (\gamma^\alpha + \sigma_T^\alpha + \mu^\alpha + \delta_1^\alpha) I_T \\
\frac{d^\alpha R}{dt^\alpha} &= \gamma^\alpha I_T + a^\alpha T_R - (\rho^\alpha + \mu^\alpha) R \\
\frac{d^\alpha T_R}{dt^\alpha} &= \sigma_T^\alpha I_T - (a^\alpha + \mu^\alpha + \delta_2^\alpha) T_R
\end{aligned} \tag{5.4}$$

where $\lambda_T = \frac{\beta_T^\alpha (I_T + \eta_T T_R)}{N}$. The disease-free equilibrium of model (5.4) is given by:

$$P_0^1 = (S_0, E_{T0}, I_{T0}, R_{T0}, T_{R0}) = \left(\frac{\Lambda^\alpha}{\mu^\alpha}, 0, 0, 0, 0 \right) \tag{5.5}$$

Using the notation in [150] on system (5.4), matrices for the new infection terms, F_T, and the other terms, V_T , are given by:

$$F_T = \begin{pmatrix} 0 & \beta_T^\alpha & \beta_T^\alpha \eta_T \\ 0 & 0 & 0 \\ 0 & 0 & 0 \end{pmatrix}$$

$$V_T = \begin{pmatrix} \epsilon^\alpha + \mu^\alpha & 0 & 0 \\ -\epsilon^\alpha & \gamma^\alpha + \sigma_T^\alpha + \mu^\alpha + \delta_1^\alpha & 0 \\ 0 & -\sigma_T^\alpha & a^\alpha + \mu^\alpha + \delta_2^\alpha \end{pmatrix}$$

The associative basic reproduction number is given by:

$$R_T = \rho(F_T V_T^{-1}) = \frac{\epsilon^\alpha \beta_T^\alpha (\eta_T \sigma_T^\alpha + a^\alpha + \delta_2^\alpha + \mu^\alpha)}{(\epsilon^\alpha + \mu^\alpha)(\gamma^\alpha + \sigma_T^\alpha + \mu^\alpha + \delta_1^\alpha)(a^\alpha + \mu^\alpha + \delta_2^\alpha)} \tag{5.6}$$

where ρ indicates the spectral radius of $F_T V_T^{-1}$.

The linearisation matrix of model (5.4) around the disease-free equilibrium, P_0^1, is:

$$M_1 = \begin{pmatrix} -\mu^\alpha & 0 & -\beta_T^\alpha & \rho^\alpha & -\beta_T^\alpha \eta_T \\ 0 & -(\epsilon^\alpha + \mu^\alpha) & \beta_T^\alpha & 0 & \beta_T^\alpha \eta_T \\ 0 & \epsilon^\alpha & -(\gamma^\alpha + \sigma_T^\alpha + \mu^\alpha + \delta_1^\alpha) & 0 & 0 \\ 0 & 0 & \gamma^\alpha & -(\rho^\alpha + \mu^\alpha) & a^\alpha \\ 0 & 0 & \sigma_T^\alpha & 0 & -(a^\alpha + \mu^\alpha + \delta_2^\alpha) \end{pmatrix}$$

The stability of P_0^1 can be determined using the following lemma:

Lema 5.2.1 *(Theorem 2, [141])*

Let $\alpha \left(= \frac{p}{q}\right)$ *where* $p, q \in \mathrm{Z}^+$ *and gdc*$(p, q) = 1$. *Define* $M = q$, *then the disease-free equilibrium* P_0^1 *of the system (5.4) is asymptotically stable if* $|\arg(\lambda)| > \frac{\pi}{2M}$ *for all roots* λ *of the following equation*

$$\det\left(\mathrm{diag}\left[\lambda^{M\alpha}\lambda^{M\alpha}\lambda^{M\alpha}\lambda^{M\alpha}\lambda^{M\alpha}\right] - M_1\right) = 0$$

Lema 5.2.2 *The disease-free equilibrium* P_0^1 *of the system (5.4) is unstable if* $R_T > 1$.

Proof Expanding, $\det\left(\mathrm{diag}\left[\lambda^{M\alpha}\lambda^{M\alpha}\lambda^{M\alpha}\lambda^{M\alpha}\lambda^{M\alpha}\right] - M_1\right) = 0$, the following equation in terms of λ is obtained:

$$\begin{aligned} &\left(\lambda^{M\alpha} + \mu^\alpha\right)\left(\lambda^{M\alpha} + (\rho^\alpha + \mu^\alpha)\right)\Big[\lambda^{3M\alpha} + (a^\alpha + \delta_2^\alpha + \epsilon^\alpha + \gamma^\alpha + \sigma_T^\alpha + \delta_1^\alpha + 3\mu^\alpha)\lambda^{2M\alpha} \\ &+ [(a^\alpha + \mu^\alpha + \delta_2^\alpha)(\epsilon^\alpha + \gamma^\alpha + \sigma_T^\alpha + \delta_1^\alpha + 2\mu^\alpha) + (\epsilon^\alpha + \mu^\alpha)(\gamma^\alpha + \sigma_T^\alpha + \mu^\alpha + \delta_1^\alpha) \\ &\left(1 - \tfrac{R_T(a^\alpha + \mu^\alpha + \delta_1^\alpha)}{\eta_T \sigma_T^\alpha + a^\alpha + \mu^\alpha + \delta_1^\alpha}\right)\Big]\lambda^{M\alpha} + (\epsilon^\alpha + \mu^\alpha)(\gamma^\alpha + \sigma_T^\alpha + \mu^\alpha + \delta_1^\alpha)(a^\alpha + \mu^\alpha + \delta_2^\alpha)\left(1 - R_T\right)\Big] = 0 \end{aligned} \tag{5.7}$$

Now, the arguments of the roots of the equation, $\lambda^{M\alpha} + \mu^\alpha = 0$, are given by:

$$\arg(\lambda_k) = \frac{\pi}{M\alpha} + k\frac{2\pi}{M\alpha} > \frac{\pi}{M} > \frac{\pi}{2M}$$

where $k = 0, 1, .., (M\alpha - 1)$.

Similarly, the arguments of the roots of the equation, $\lambda^{M\alpha} + (\rho^\alpha + \mu^\alpha) = 0$ are all greater than $\frac{\pi}{2M}$. Thus, using Lemma 5.2.1, it is shown that disease-free equilibrium P_0^1 of the system (5.4) is unstable if there exists at least one root of the polynomial,

$$\begin{aligned} &\lambda^{3M\alpha} + (a^\alpha + \delta_2^\alpha + \epsilon^\alpha + \gamma^\alpha + \sigma_T^\alpha + \delta_1^\alpha + 3\mu^\alpha)\lambda^{2M\alpha} + [(a^\alpha + \mu^\alpha + \delta_2^\alpha)(\epsilon^\alpha + \gamma^\alpha + \sigma_T^\alpha + \delta_1^\alpha + 2\mu^\alpha) \\ &+(\epsilon^\alpha + \mu^\alpha)(\gamma^\alpha + \sigma_T^\alpha + \mu^\alpha + \delta_1^\alpha)\left(1 - \tfrac{R_T(a^\alpha + \mu^\alpha + \delta_1^\alpha)}{\eta_T \sigma_T^\alpha + a^\alpha + \mu^\alpha + \delta_1^\alpha}\right)\Big]\lambda^{M\alpha} \\ &+(\epsilon^\alpha + \mu^\alpha)(\gamma^\alpha + \sigma_T^\alpha + \mu^\alpha + \delta_1^\alpha)(a^\alpha + \mu^\alpha + \delta_2^\alpha)\left(1 - R_T\right) = 0 \end{aligned}$$

having argument less than $\frac{\pi}{2M}$, for $R_T > 1$.

Using Descartes' rule of signs, there is exactly one sign change of the equation:

$$\lambda^{3M\alpha} + (a^\alpha + \delta_2^\alpha + \epsilon^\alpha + \gamma^\alpha + \sigma_T^\alpha + \delta_1^\alpha + 3\mu^\alpha)\lambda^{2M\alpha} + \left[(a^\alpha + \mu^\alpha + \delta_2^\alpha)(\epsilon^\alpha + \gamma^\alpha + \sigma_T^\alpha + \delta_1^\alpha + 2\mu^\alpha)\right.$$
$$\left.+(\epsilon^\alpha + \mu^\alpha)(\gamma^\alpha + \sigma_T^\alpha + \mu^\alpha + \delta_1^\alpha)\left(1 - \frac{R_T(a^\alpha+\mu^\alpha+\delta_1^\alpha)}{\eta_T\sigma_T^\alpha + a^\alpha + \mu^\alpha + \delta_1^\alpha}\right)\right]\lambda^{M\alpha}$$
$$+(\epsilon^\alpha + \mu^\alpha)(\gamma^\alpha + \sigma_T^\alpha + \mu^\alpha + \delta_1^\alpha)(a^\alpha + \mu^\alpha + \delta_2^\alpha)\,(1 - R_T) = 0$$

for $R_T > 1$, thus there is exactly one positive real root of the aforesaid equation, for which the argument is less than $\frac{\pi}{2M}$. Thus, if $R_T > 1$, the disease-free equilibrium, P_0^1, of the system (5.4) is unstable.

■

The computation of the reproduction number of model (5.8) below, R_H, follows.

$$\begin{aligned}
\tfrac{d^\alpha S}{dt^\alpha} &= \Lambda^\alpha - \lambda_H S - \mu^\alpha S \\
\tfrac{d^\alpha I_H}{dt^\alpha} &= \lambda_H S + \tau_2^\alpha A - (\sigma_H^\alpha + \mu^\alpha + \delta_3^\alpha) I_H \\
\tfrac{d^\alpha A}{dt^\alpha} &= \sigma_H^\alpha I_H - (\tau_2^\alpha + \mu^\alpha + \delta_4^\alpha) A
\end{aligned} \tag{5.8}$$

where $\lambda_H = \frac{\beta_H^\alpha I_H}{N}$. The disease-free equilibrium state P_0^2 of model (5.8) is given by:

$$P_0^2 = (S_0^2, I_{H0}^2, A_0^2) = \left(S_0^1, 0, 0\right)$$

Using the notation in [150] on system (5.8), matrices for the new infection terms, F_H, and the other terms, V_H , are given by:

$$F_H = \begin{pmatrix} \beta_H^\alpha & 0 \\ 0 & 0 \end{pmatrix}$$

$$V_H = \begin{pmatrix} \sigma_H^\alpha + \mu^\alpha + \delta_3^\alpha & -\tau_2^\alpha \\ -\sigma_H^\alpha & \tau_2^\alpha + \mu^\alpha + \delta_4^\alpha \end{pmatrix}$$

The associative basic reproduction number is computed to be:

$$R_H = \rho(F_H V_H^{-1}) = \frac{\beta_H^\alpha(\tau_2^\alpha + \mu^\alpha + \delta_4^\alpha)}{(\mu^\alpha + \delta_3^\alpha)(\mu^\alpha + \delta_4^\alpha + \tau_2^\alpha) + \sigma_H^\alpha(\mu^\alpha + \delta_4^\alpha)} \tag{5.9}$$

where ρ indicates the spectral radius of $F_H V_H^{-1}$.

The linearisation matrix of model (5.8) around the disease-free equilibrium, P_0^2, is:

$$M_2 = \begin{pmatrix} -\mu^\alpha & -\beta_H^\alpha & 0 \\ 0 & \beta_H^\alpha - (\sigma_H^\alpha + \mu^\alpha + \delta_3^\alpha) & \tau_2^\alpha \\ 0 & \sigma_H^\alpha & -(\tau_2^\alpha + \mu^\alpha + \delta_4^\alpha) \end{pmatrix}$$

The stability of P_0^2 is derived using the following lemma:

Lema 5.2.3 *(Theorem 2, [141])*

Let $\alpha \left(= \frac{p}{q}\right)$ *where* $p, q \in \mathrm{Z}^+$ *and gdc*$(p, q) = 1$. *Define* $M = q$, *then the disease-free equilibrium* P_0^2 *of the system (5.8) is asymptotically stable if* $|\arg(\lambda)| > \frac{\pi}{2M}$ *for all roots* λ *of the following equation*

$$\det\left(\mathrm{diag}\left[\lambda^{M\alpha}\lambda^{M\alpha}\lambda^{M\alpha}\right] - M_2\right) = 0$$

The next lemma is:

Lema 5.2.4 *The disease-free equilibrium* P_0^2 *of the system (5.8) is unstable if* $R_H > 1$.

Proof Expanding, $\det\left(\mathrm{diag}\left[\lambda^{M\alpha}\lambda^{M\alpha}\lambda^{M\alpha}\right] - M_2\right) = 0$, there is the following equation in terms of λ:

$$\begin{aligned}&\left(\lambda^{M\alpha} + \mu^\alpha\right)\left[\lambda^{2M\alpha} + \left[(\mu^\alpha + \delta_3^\alpha)(1 - R_H) + \sigma_H^\alpha + \tfrac{1}{\tau_2^\alpha + \mu^\alpha + \delta_4^\alpha}\left((\tau_2^\alpha + \mu^\alpha + \delta_4^\alpha)^2 - R_H\sigma_H^\alpha(\mu^\alpha + \delta_4^\alpha)\right)\right]\lambda^{M\alpha}\right. \\ &\left. + (\mu^\alpha + \delta_3^\alpha)(\mu^\alpha + \delta_4^\alpha + \tau_2^\alpha)(1 - R_H) + (\mu^\alpha + \delta_4^\alpha)\sigma_H^\alpha(1 - R_H)\right] = 0\end{aligned} \tag{5.10}$$

The arguments of the roots of the equation, $\lambda^{M\alpha} + \mu^\alpha = 0$, are given by:

$$\arg(\lambda_k) = \frac{\pi}{M\alpha} + k\frac{2\pi}{M\alpha} > \frac{\pi}{M} > \frac{\pi}{2M}$$

where $k = 0, 1, .., (M\alpha - 1)$.

Thus, using Lemma 5.2.3, it is shown that the disease-free equilibrium, P_0^2, of system (5.8) is unstable if there exists at least one root of the polynomial:

$$\lambda^{2M\alpha} + \left[(\mu^\alpha + \delta_3^\alpha)(1 - R_H) + \sigma_H^\alpha + \frac{1}{\tau_2^\alpha + \mu^\alpha + \delta_4^\alpha}\left((\tau_2^\alpha + \mu^\alpha + \delta_4^\alpha)^2 - R_H\sigma_H^\alpha(\mu^\alpha + \delta_4^\alpha)\right)\right]\lambda^{M\alpha}$$
$$+(\mu^\alpha + \delta_3^\alpha)(\mu^\alpha + \delta_4^\alpha + \tau_2^\alpha)(1 - R_H) + (\mu^\alpha + \delta_4^\alpha)\sigma_H^\alpha(1 - R_H) = 0$$

which has argument less than $\frac{\pi}{2M}$, for $R_H > 1$. Using Descartes' rule of signs, there is exactly one sign change of the equation:

$$\lambda^{2M\alpha} + \left[(\mu^\alpha + \delta_3^\alpha)(1 - R_H) + \sigma_H^\alpha + \frac{1}{\tau_2^\alpha + \mu^\alpha + \delta_4^\alpha}\left((\tau_2^\alpha + \mu^\alpha + \delta_4^\alpha)^2 - R_H\sigma_H^\alpha(\mu^\alpha + \delta_4^\alpha)\right)\right]\lambda^{M\alpha}$$
$$+(\mu^\alpha + \delta_3^\alpha)(\mu^\alpha + \delta_4^\alpha + \tau_2^\alpha)(1 - R_H) + (\mu^\alpha + \delta_4^\alpha)\sigma_H^\alpha(1 - R_H) = 0$$

for $R_H > 1$, thus there is exactly one positive real root of the last equation for which the argument is less than $\frac{\pi}{2M}$. Thus, for $R_H > 1$, the disease-free equilibrium P_0^2 of system (5.8) is unstable.

■

The reproduction number of the full model (5.1), R_0, is calculated. The disease-free equilibrium state, P_0, of model (5.1) is given by:

$$\begin{aligned} P_0 &= (S^0, E_T^0, I_T^0, R^0, T_R^0, I_H^0, A^0, E_T I_H^0, E_T A^0, I_{TH}^0, I_T A^0, R I_H^0, T_R I_H^0) \\ &= \left(\tfrac{\Lambda}{\mu}, 0, 0, 0, 0, 0, 0, 0, 0, 0, 0, 0, 0\right) \end{aligned}$$

Using the notation in [150] on system (5.1), matrices for the new infection terms, F, and the other terms, V, are given by:

$$F = \begin{pmatrix} 0 & \beta_T^\alpha & 0 & \beta_T^\alpha \eta_T & 0 & 0 & 0 & 0 & \beta_T^\alpha \eta_{TH} & 0 & 0 & \beta_T^\alpha \eta_{TH} \\ 0 & 0 & 0 & 0 & 0 & 0 & 0 & 0 & 0 & 0 & 0 & 0 \\ 0 & 0 & 0 & 0 & 0 & 0 & 0 & 0 & 0 & 0 & 0 & 0 \\ 0 & 0 & 0 & 0 & 0 & 0 & 0 & 0 & 0 & 0 & 0 & 0 \\ 0 & 0 & 0 & 0 & \beta_H^\alpha & 0 & \beta_H^\alpha & 0 & \beta_H^\alpha \eta_H & 0 & \beta_H^\alpha & \beta_H^\alpha \eta_H \\ 0 & 0 & 0 & 0 & 0 & 0 & 0 & 0 & 0 & 0 & 0 & 0 \\ 0 & 0 & 0 & 0 & 0 & 0 & 0 & 0 & 0 & 0 & 0 & 0 \\ 0 & 0 & 0 & 0 & 0 & 0 & 0 & 0 & 0 & 0 & 0 & 0 \\ 0 & 0 & 0 & 0 & 0 & 0 & 0 & 0 & 0 & 0 & 0 & 0 \\ 0 & 0 & 0 & 0 & 0 & 0 & 0 & 0 & 0 & 0 & 0 & 0 \\ 0 & 0 & 0 & 0 & 0 & 0 & 0 & 0 & 0 & 0 & 0 & 0 \\ 0 & 0 & 0 & 0 & 0 & 0 & 0 & 0 & 0 & 0 & 0 & 0 \end{pmatrix}$$

$$V = \begin{pmatrix} \epsilon^\alpha + \mu^\alpha & 0 & 0 & 0 & 0 & 0 & 0 & 0 & 0 & 0 & 0 & 0 \\ -\epsilon^\alpha & \gamma^\alpha + \sigma_T^\alpha + \mu^\alpha + \delta_1^\alpha & 0 & 0 & 0 & 0 & 0 & 0 & 0 & 0 & 0 & 0 \\ 0 & -\gamma^\alpha & \rho^\alpha + \mu^\alpha & -a^\alpha & 0 & 0 & 0 & 0 & 0 & 0 & 0 & 0 \\ 0 & -\sigma_T^\alpha & 0 & a^\alpha + \mu^\alpha + \delta_2^\alpha & 0 & 0 & 0 & 0 & 0 & 0 & 0 & 0 \\ 0 & 0 & 0 & 0 & \sigma_H^\alpha + \mu^\alpha + \delta_3^\alpha & -\tau_2^\alpha & 0 & 0 & 0 & 0 & -\rho^\alpha & 0 \\ 0 & 0 & 0 & 0 & -\sigma_H^\alpha & \tau_2^\alpha + \mu^\alpha + \delta_4^\alpha & 0 & 0 & 0 & 0 & 0 & 0 \\ 0 & 0 & 0 & 0 & 0 & 0 & \eta_1\epsilon^\alpha + \theta_1\sigma_H^\alpha + \mu^\alpha + \delta_5^\alpha & -\tau_2^\alpha & 0 & 0 & 0 & 0 \\ 0 & 0 & 0 & 0 & 0 & 0 & -\theta_1\sigma_H^\alpha & \eta_2\epsilon^\alpha + \tau_2^\alpha + \mu^\alpha + \delta_6^\alpha & 0 & 0 & 0 & 0 \\ 0 & 0 & 0 & 0 & 0 & 0 & -\eta_1\epsilon^\alpha & 0 & \gamma_1^\alpha + \sigma_{T1}^\alpha + \theta_2\sigma_H^\alpha + \mu^\alpha + \delta_7^\alpha & -\tau_3^\alpha & 0 & 0 \\ 0 & 0 & 0 & 0 & 0 & 0 & 0 & -\eta_2\epsilon^\alpha & -\theta_2\sigma_H^\alpha & \tau_3^\alpha + \mu^\alpha + \delta_8^\alpha & 0 & 0 \\ 0 & 0 & 0 & 0 & 0 & 0 & 0 & 0 & -\gamma_1^\alpha & 0 & \rho^\alpha + \mu^\alpha + \delta_3^\alpha & -a_1^\alpha \\ 0 & 0 & 0 & 0 & 0 & 0 & 0 & 0 & -\sigma_{T1}^\alpha & 0 & 0 & a_1^\alpha + \mu^\alpha + \delta_9^\alpha \end{pmatrix}$$

The associative basic reproduction number is computed to be:

$$R_0 = \rho(FV^{-1}) = \max\{R_T, R_H\} \tag{5.11}$$

where ρ indicates the spectral radius of FV^{-1}.

The matrix of the linearisation of model (5.1) around the disease-free equilibrium, P_0, is:

$$M_3 = \begin{pmatrix}
-\mu^\alpha & 0 & -\beta_T^\alpha & \rho^\alpha & -\beta_T^\alpha\eta_T & -\beta_H^\alpha & 0 & -\beta_H^\alpha & 0 & -\beta_H^\alpha\eta_H - \beta_T^\alpha\eta_{TH} & 0 & -\beta_H^\alpha & -\beta_H^\alpha\eta_H - \beta_T^\alpha\eta_{TH} \\
0 & -(\epsilon^\alpha + \mu^\alpha) & \beta_T^\alpha & 0 & \beta_T^\alpha\eta_T & 0 & 0 & 0 & 0 & \beta_T^\alpha\eta_T & 0 & 0 & \beta_T^\alpha\eta_T \\
0 & \epsilon^\alpha & -(\gamma^\alpha + \sigma_T^\alpha + \mu^\alpha + \delta_1^\alpha) & 0 & 0 & 0 & 0 & 0 & 0 & 0 & 0 & 0 & 0 \\
0 & 0 & \gamma^\alpha & -(\rho^\alpha + \mu^\alpha) & a^\alpha & 0 & 0 & 0 & 0 & 0 & 0 & 0 & 0 \\
0 & 0 & \sigma_T^\alpha & 0 & -(a^\alpha + \mu^\alpha + \delta_2^\alpha) & 0 & 0 & 0 & 0 & 0 & 0 & 0 & 0 \\
0 & 0 & 0 & 0 & 0 & \beta_H^\alpha - (\sigma_H^\alpha + \mu^\alpha + \delta_3^\alpha) & \tau_2^\alpha & \beta_H^\alpha & 0 & \beta_H^\alpha\eta_H & 0 & \beta_H^\alpha + \rho^\alpha & \beta_H^\alpha\eta_H \\
0 & 0 & 0 & 0 & 0 & \sigma_H^\alpha & -(\tau_2^\alpha + \mu^\alpha + \delta_4^\alpha) & 0 & 0 & 0 & 0 & 0 & 0 \\
0 & 0 & 0 & 0 & 0 & 0 & 0 & -(\eta_1\epsilon^\alpha + \theta_1\sigma_H^\alpha + \mu^\alpha + \delta_5^\alpha) & \tau_2^\alpha & 0 & 0 & 0 & 0 \\
0 & 0 & 0 & 0 & 0 & 0 & 0 & \theta_1\sigma_H^\alpha & -(\eta_2\epsilon^\alpha + \tau_2^\alpha + \mu^\alpha + \delta_6^\alpha) & 0 & 0 & 0 & 0 \\
0 & 0 & 0 & 0 & 0 & 0 & 0 & \eta_1\epsilon^\alpha & 0 & -(\gamma_1^\alpha + \sigma_{T1}^\alpha + \theta_2\sigma_H^\alpha + \mu^\alpha + \delta_7^\alpha) & \tau_3^\alpha & 0 & 0 \\
0 & 0 & 0 & 0 & 0 & 0 & 0 & 0 & \eta_2\epsilon^\alpha & \theta_2\sigma_H^\alpha & -(\tau_3^\alpha + \mu^\alpha + \delta_8^\alpha) & 0 & 0 \\
0 & 0 & 0 & 0 & 0 & 0 & 0 & 0 & 0 & \gamma_1^\alpha & 0 & -(\rho^\alpha + \mu^\alpha + \delta_3^\alpha) & a_1^\alpha \\
0 & 0 & 0 & 0 & 0 & 0 & 0 & 0 & 0 & \sigma_{T1}^\alpha & 0 & 0 & -(a_1^\alpha + \mu^\alpha + \delta_9^\alpha)
\end{pmatrix}$$

The stability of P_0 is determined by the next lemma:

Lema 5.2.5 *(Theorem 2, [141])*

Let $\alpha \left(= \frac{p}{q}\right)$ *where* $p, q \in \mathrm{Z}^+$ *and gdc*$(p, q) = 1$. *Define* $M = q$, *then the disease-free equilibrium* P_0 *of the system (5.1) is asymptotically stable if* $|\arg(\lambda)| > \frac{\pi}{2M}$ *for all roots* λ *of the following equation*

$$\det\left(\mathrm{diag}\left[\lambda^{M\alpha}\lambda^{M\alpha}\lambda^{M\alpha}\lambda^{M\alpha}\lambda^{M\alpha}\lambda^{M\alpha}\lambda^{M\alpha}\lambda^{M\alpha}\lambda^{M\alpha}\lambda^{M\alpha}\lambda^{M\alpha}\lambda^{M\alpha}\right] - M_3\right) = 0$$

There is the following lemma:

Lema 5.2.6 *The disease-free equilibrium* P_0 *of the system (5.1) is unstable if* $R_0 > 1$.

Proof Expanding

$$\det\left(\mathrm{diag}\left[\lambda^{M\alpha}\lambda^{M\alpha}\lambda^{M\alpha}\lambda^{M\alpha}\lambda^{M\alpha}\lambda^{M\alpha}\lambda^{M\alpha}\lambda^{M\alpha}\lambda^{M\alpha}\lambda^{M\alpha}\lambda^{M\alpha}\lambda^{M\alpha}\right] - M_3\right) = 0$$

the next equations are obtained in terms of λ:

$$\begin{aligned}
&\left(\lambda^{M\alpha}+\mu^{\alpha}\right)\left(\lambda^{M\alpha}+(\rho^{\alpha}+\mu^{\alpha})\right)\left(\lambda^{M\alpha}+(\rho^{\alpha}+\mu^{\alpha}+\delta_3^{\alpha})\right)\left(\lambda^{M\alpha}+(a_1^{\alpha}+\mu^{\alpha}+\delta_9^{\alpha})\right)\left[\lambda^{2M\alpha}+\right.\\
&\left.+(\gamma_1^{\alpha}+\sigma_{T1}^{\alpha}+\theta_2\sigma_H^{\alpha}+\mu^{\alpha}+\delta_7^{\alpha}+\tau_3^{\alpha}+\mu^{\alpha}+\delta_8^{\alpha}))\,\lambda^{M\alpha}+(\gamma_1^{\alpha}+\sigma_{T1}^{\alpha}+\theta_2\sigma_H^{\alpha}+\mu^{\alpha}+\delta_7^{\alpha})(\mu^{\alpha}+\delta_8^{\alpha})+\tau_3^{\alpha}(\gamma_1^{\alpha}+\sigma_{T1}^{\alpha}+\mu^{\alpha}+\delta_7^{\alpha})\right]\\
&\left[\lambda^{2M\alpha}+(\eta_1\epsilon^{\alpha}+\theta_1\sigma_H^{\alpha}+\mu^{\alpha}+\delta_5^{\alpha}+\eta_2\epsilon^{\alpha}+\tau_2^{\alpha}+\mu^{\alpha}+\delta_6^{\alpha})\,\lambda^{M\alpha}+(\eta_1\epsilon^{\alpha}+\mu^{\alpha}+\delta_5^{\alpha})(\eta_2\epsilon^{\alpha}+\tau_2^{\alpha}+\mu^{\alpha}+\delta_6^{\alpha})+\theta_1\sigma_H^{\alpha}(\eta_2\epsilon^{\alpha}+\mu^{\alpha}+\delta_6^{\alpha})\right]\\
&\left[\lambda^{3M\alpha}+(a^{\alpha}+\delta_2^{\alpha}+\epsilon^{\alpha}+\gamma^{\alpha}+\sigma_T^{\alpha}+\delta_1^{\alpha}+3\mu^{\alpha})\lambda^{2M\alpha}+[(a^{\alpha}+\mu^{\alpha}+\delta_2^{\alpha})(\epsilon^{\alpha}+\gamma^{\alpha}+\sigma_T^{\alpha}+\delta_1^{\alpha}+2\mu^{\alpha})\right.\\
&\left.+(\epsilon^{\alpha}+\mu^{\alpha})(\gamma^{\alpha}+\sigma_T^{\alpha}+\mu^{\alpha}+\delta_1^{\alpha})\left(1-\tfrac{R_T(a^{\alpha}+\mu^{\alpha}+\delta_1^{\alpha})}{\eta_T\sigma_T^{\alpha}+a^{\alpha}+\mu^{\alpha}+\delta_1^{\alpha}}\right)\right]\lambda^{M\alpha}+(\epsilon^{\alpha}+\mu^{\alpha})(\gamma^{\alpha}+\sigma_T^{\alpha}+\mu^{\alpha}+\delta_1^{\alpha})(a^{\alpha}+\mu^{\alpha}+\delta_2^{\alpha})\,(1-R_T)\Big]\\
&\left[\lambda^{2M\alpha}+\left[(\mu^{\alpha}+\delta_3^{\alpha})(1-R_H)+\sigma_H^{\alpha}+\tfrac{1}{\tau_2^{\alpha}+\mu^{\alpha}+\delta_4^{\alpha}}\left((\tau_2^{\alpha}+\mu^{\alpha}+\delta_4^{\alpha})^2-R_H\sigma_H^{\alpha}(\mu^{\alpha}+\delta_4^{\alpha})\right)\right]\lambda^{M\alpha}\right.\\
&\left.+(\mu^{\alpha}+\delta_3^{\alpha})(\mu^{\alpha}+\delta_4^{\alpha}+\tau_2^{\alpha})(1-R_H)+(\mu^{\alpha}+\delta_4^{\alpha})\sigma_H^{\alpha}(1-R_H)\right]=0
\end{aligned} \tag{5.12}$$

Now arguments of the roots of the equation, $\lambda^{M\alpha}+\mu^{\alpha}=0$, are given by: $\arg(\lambda_k) = \frac{\pi}{M\alpha} + k\frac{2\pi}{M\alpha} > \frac{\pi}{M} > \frac{\pi}{2M}$, where $k = 0, 1, .., (M\alpha - 1)$. Similarly, it is proved that the arguments of the next six terms obey $\arg(\lambda_k) > \frac{\pi}{2M}$. By Lemma 5.2.5, it is shown that disease-free equilibrium P_0 of system (5.1) is unstable if there exists at least one root of the polynomials:

$$\lambda^{3M\alpha}+(a^{\alpha}+\delta_2^{\alpha}+\epsilon^{\alpha}+\gamma^{\alpha}+\sigma_T^{\alpha}+\delta_1^{\alpha}+3\mu^{\alpha})\lambda^{2M\alpha}+\left[(a^{\alpha}+\mu^{\alpha}+\delta_2^{\alpha})(\epsilon^{\alpha}+\gamma^{\alpha}+\sigma_T^{\alpha}+\delta_1^{\alpha}+2\mu^{\alpha})\right.$$
$$\left.+(\epsilon^{\alpha}+\mu^{\alpha})(\gamma^{\alpha}+\sigma_T^{\alpha}+\mu^{\alpha}+\delta_1^{\alpha})\left(1-\frac{R_T(a^{\alpha}+\mu^{\alpha}+\delta_1^{\alpha})}{\eta_T\sigma_T^{\alpha}+a^{\alpha}+\mu^{\alpha}+\delta_1^{\alpha}}\right)\right]\lambda^{M\alpha}+(\epsilon^{\alpha}+\mu^{\alpha})(\gamma^{\alpha}+\sigma_T^{\alpha}+\mu^{\alpha}+\delta_1^{\alpha})$$
$$(a^{\alpha}+\mu^{\alpha}+\delta_2^{\alpha})\,(1-R_T)=0$$

or

$$\lambda^{2M\alpha}+\left[(\mu^{\alpha}+\delta_3^{\alpha})(1-R_H)+\sigma_H^{\alpha}+\frac{1}{\tau_2^{\alpha}+\mu^{\alpha}+\delta_4^{\alpha}}\left((\tau_2^{\alpha}+\mu^{\alpha}+\delta_4^{\alpha})^2-R_H\sigma_H^{\alpha}(\mu^{\alpha}+\delta_4^{\alpha})\right)\right]\lambda^{M\alpha}$$
$$+(\mu^{\alpha}+\delta_3^{\alpha})(\mu^{\alpha}+\delta_4^{\alpha}+\tau_2^{\alpha})(1-R_H)+(\mu^{\alpha}+\delta_4^{\alpha})\sigma_H^{\alpha}(1-R_H)=0$$

with arguments less than $\frac{\pi}{2M}$, for $R_T>1$ or $R_H>1$, respectively.

As shown previously, there is exactly one sign change for each polynomial when $R_T>1$ and $R_H>1$, respectively. Since $R_0=\max\{R_T,R_H\}$, then the disease-free equilibrium P_0 of the system (5.1) is unstable for $R_T>1$ and $R_H>1$.

■

5.3 Global stability of the disease-free equilibria

In this section, the global stability of the disease-free equilibrium of the two submodels (5.4) and (5.8) and of the full model (5.1) are calculated.

The proof begins by proving the conditions that guarantee the global stability of the disease-free state for the TB submodel (5.4). The submodel (5.4) is rewritten as:

$$\begin{aligned}\frac{d^{\alpha}X_{TB}}{dt^{\alpha}}&=F_{TB}(X_{TB},Z_{TB})\\ \frac{d^{\alpha}Z_{TB}}{dt^{\alpha}}&=G_{TB}(X_{TB},Z_{TB}),\qquad G_{TB}(X_{TB},0)=0\end{aligned}\tag{5.13}$$

where $X_{TB}=(S,R)$ and $Z_{TB}=(E_T,I_T,T_R)$, with $X_{TB}\in\mathbb{R}_+^2$ denoting the number of uninfected individuals and $Z_{TB}\in\mathbb{R}_+^3$ denoting the number of infected individuals (including the latent, the infectious and the drug-resistant).

The disease-free equilibrium is denoted by $U_{TB}=(X_{TB}^{\star},0)$, where $X_{TB}^{\star}=\left(\frac{\lambda^{\alpha}}{\mu^{\alpha}},0\right)$.

The conditions (H_{11}) and (H_{21}) must be met to guarantee the global asymptotic stability of the disease-free equilibrium of the TB submodel (5.4):

$$\begin{aligned}(H_{11}):&\ \text{For } \tfrac{d^\alpha X_{TB}}{dt^\alpha} = F_{TB}(X_{TB},0),\ \ X^\star_{TB} \qquad \text{is globally asymptotically stable}\\ (H_{21}):&\ G_{TB}(X_{TB},Z_{TB}) = A_{TB}Z_{TB} - \hat{G}_{TB}(X_{TB},Z_{TB}),\ \hat{G}_{TB}\geq 0, \text{for } (X_{TB},Z_{TB})\in \Upsilon_1\end{aligned} \tag{5.14}$$

where $A_{TB} = D_Z G_{TB}(X^\star_{TB},0)$ is a M-matrix (the off-diagonal elements of A_{TB} are non-negative) and Υ_1 is the region where the model makes biological sense. If the system (5.13) satisfies the condition in (5.14) the following theorem holds.

Theorem 5.3.1 *The fixed point $U_{TB} = (X^\star_{TB},0)$ is a globally asymptotically stable equilibrium of the system (5.13) provided that $R_T < 1$ and that the assumptions in (5.14) are satisfied.*

Proof Let

$$F_{TB}(X_{TB},0) = \begin{pmatrix}\lambda^\alpha - \mu^\alpha S\\ 0\end{pmatrix} \tag{5.15}$$

and

$$A_{TB} = \begin{pmatrix}-(\epsilon^\alpha+\mu^\alpha) & \beta^\alpha_T & \beta^\alpha_T\eta_T\\ \epsilon^\alpha & -(\gamma^\alpha+\sigma^\alpha_T+\mu^\alpha+\delta^\alpha_1) & 0\\ 0 & \sigma^\alpha_T & -(a^\alpha+\mu^\alpha+\delta^\alpha_2)\end{pmatrix} \tag{5.16}$$

and

$$\hat{G}_{TB}(X_{TB},Z_{TB}) = \begin{pmatrix}\hat{G}_1(X_{TB},Z_{TB})\\ \hat{G}_2(X_{TB},Z_{TB})\\ \hat{G}_3(X_{TB},Z_{TB})\end{pmatrix} = \begin{pmatrix}\lambda_T N\left(1-\frac{S}{N}\right)\\ 0\\ 0\end{pmatrix} \tag{5.17}$$

Thus $\hat{G}_1(X_{TB},Z_{TB})\geq 0$ and $\hat{G}_2(X_{TB},Z_{TB}) = \hat{G}_3(X_{TB},Z_{TB}) = 0 \Rightarrow \hat{G}_{TB}(X,Z)\geq 0$. Conditions in (5.14) are satisfied, thus the disease-free equilibrium of the TB submodel (5.4) is globally asymptotically stable for $R_T < 1$.

■

Now the same procedure is repeated for the computation of the global stability of the disease-free equilibrium of the HIV submodel (5.8). The later is rewritten as:

$$\begin{aligned} \tfrac{d^\alpha X_A}{dt^\alpha} &= F_A(X_A, Z_A) \\ \tfrac{d^\alpha Z_A}{dt^\alpha} &= G_A(X_A, Z_A), \qquad G_A(X_A, 0) = 0 \end{aligned} \tag{5.18}$$

where $X_A = (S)$ and $Z_A = (I_H, A)$, $X_A \in \mathbb{R}^1_+$ denoting the number of uninfected individuals and $Z_A \in \mathbb{R}^2_+$ denoting the number of infected individuals.

The disease-free equilibrium is given by $U_A = (X_A^\star, 0)$, where $X_A^\star = \left(\frac{\lambda^\alpha}{\mu^\alpha}, 0\right)$.

The conditions (H_{12}) and (H_{22}) must be met to guarantee the global asymptotic stability of the disease-free equilibrium of the HIV submodel (5.8):

$$\begin{aligned} &(H_{12}): \ \text{For } \tfrac{d^\alpha X_A}{dt^\alpha} = F_A(X_A, 0), \ X_A^\star \qquad \text{is globally asymptotic stable} \\ &(H_{22}): \ G_A(X_A, Z_A) = A_A Z_A - \hat{G}_A(X_A, Z_A), \ \hat{G}_A \geq 0, \ \text{for } (X_A, Z_A) \in \Upsilon_2 \end{aligned} \tag{5.19}$$

where $A_A = D_Z G_A(X_A^\star, 0)$ is a M-matrix (the off-diagonal elements of A are non-negative) and Υ_2 is the region where the model makes biological sense. If the system (5.18) satisfies the conditions in (5.19) the the next theorem follows.

Theorem 5.3.2 *The fixed point $U_A = (X_A^\star, 0)$ is a globally asymptotically stable equilibrium of the system (5.18) provided that $R_H < 1$ and that the assumptions in (5.19) are satisfied.*

Proof Let

$$F_A(X_A, 0) = [\lambda^\alpha - \mu^\alpha S] \tag{5.20}$$

$$A_A = \begin{pmatrix} \beta_H^\alpha - (\sigma_H^\alpha + \mu^\alpha + \delta_3^\alpha) & \tau_2^\alpha \\ \sigma_H^\alpha & -(\tau_2^\alpha + \mu^\alpha + \delta_4^\alpha) \end{pmatrix} \tag{5.21}$$

and

$$\hat{G}_A(X_A, Z_A) = \begin{pmatrix} \hat{G_{11}}(X_A, Z_A) \\ \hat{G_{22}}(X_A, Z_A) \end{pmatrix} = \begin{pmatrix} \lambda_T N \left(1 - \frac{S}{N}\right) \\ 0 \end{pmatrix} \tag{5.22}$$

Thus $\hat{G_{11}}(X_A, Z_A) \geq 0$ and $\hat{G_{22}}(X_A, Z_A) = 0 \Rightarrow \hat{G}_A(X_A, Z_A) \geq 0$. Conditions in (5.19) are satisfied, thus the disease-free equilibrium of the submodel (5.8) is globally asymptotically stable for $R_H < 1$.

■

The procedure is now applied to find the global asymptotic stability of the disease-free equilibrium of the full model. Again, the model (5.1) is rewritten as:

$$\begin{aligned} \tfrac{d^\alpha X}{dt^\alpha} &= F(X, Z) \\ \tfrac{d^\alpha Z}{dt^\alpha} &= G(X, Z), \qquad G(X, 0) = 0 \end{aligned} \tag{5.23}$$

when $X = (S, R)$ and $Z = (E_T, I_T, T_R, I_H, A, E_T I_H, E_T A, I_{TH}, I_T A, R I_H, T_R I_H)$, with $X \in \mathbb{R}^2_+$ denoting the number of uninfected individuals and $Z \in \mathbb{R}^{11}_+$ denoting the number of infected individuals.

The disease-free equilibrium is denoted by $U_0 = (X^\star, 0)$, where $X^\star = \left(\frac{\lambda^\alpha}{\mu^\alpha}, 0\right)$.

The conditions H_1 and H_2 must be met to guarantee global asymptotic stability of the disease-free equilibrium of the model (5.1):

$$\begin{aligned} (H_1): &\ \text{For } \tfrac{d^\alpha X}{dt^\alpha} = F(X, 0), \ X^\star \qquad \text{is globally asymptotic stable} \\ (H_2): &\ G(X, Z) = AZ - \hat{G}(X, Z), \ \hat{G} \geq 0, \ \text{for } (X, Z) \in \Upsilon \end{aligned} \tag{5.24}$$

where $A = D_Z G(X^\star, 0)$ is a M-matrix (the off-diagonal elements of A are non-negative) and Υ is the region where the model makes biological sense. If the system (5.23) satisfies the conditions in (5.24), the following theorem is valid.

Theorem 5.3.3 *The fixed point $U_0 = (X^\star, 0)$ is a globally asymptotically stable equilibrium of the system (5.23) provided that $R_0 < 1$ and that the assumptions in (5.24) are satisfied.*

Proof Let

$$F(X,0) = \begin{pmatrix} \lambda^{\alpha} - \mu^{\alpha} S \\ -(\rho^{\alpha} + \mu^{\alpha}) R \end{pmatrix} \tag{5.25}$$

$$A = \begin{pmatrix}
-(\epsilon^{\alpha}+\mu^{\alpha}) & \beta_T^{\alpha} & 0 & 0 & 0 & 0 & 0 & \beta_T^{\alpha}\eta_{TH} & 0 & 0 & \beta_T^{\alpha}\eta_{TH} \\
\epsilon^{\alpha} & -(\gamma^{\alpha}+\sigma_T^{\alpha}+\mu^{\alpha}+\delta_1^{\alpha}) & 0 & 0 & 0 & 0 & 0 & 0 & 0 & 0 & 0 \\
0 & \sigma_T^{\alpha} & -(a^{\alpha}+\mu^{\alpha}+\delta_2^{\alpha}) & 0 & 0 & 0 & 0 & 0 & 0 & 0 & 0 \\
0 & 0 & 0 & \beta_H^{\alpha}-(\sigma_H^{\alpha}+\mu^{\alpha}+\delta_3^{\alpha}) & \tau_2^{\alpha} & \beta_H^{\alpha} & 0 & \beta_H^{\alpha}\eta_H & 0 & \beta_H^{\alpha}+\rho^{\alpha} & \beta_H^{\alpha}\eta_H \\
0 & 0 & 0 & \sigma_H^{\alpha} & -(\tau_2^{\alpha}+\mu^{\alpha}+\delta_4^{\alpha}) & 0 & 0 & 0 & 0 & 0 & 0 \\
0 & 0 & 0 & 0 & 0 & -(\eta_1\epsilon^{\alpha}+\theta_1\sigma_H^{\alpha}+\mu^{\alpha}+\delta_5^{\alpha}) & \tau_2^{\alpha} & 0 & 0 & 0 & 0 \\
0 & 0 & 0 & 0 & 0 & \theta_1\sigma_H^{\alpha} & -(\eta_2\epsilon^{\alpha}+\tau_2^{\alpha}+\mu^{\alpha}+\delta_6^{\alpha}) & 0 & 0 & 0 & 0 \\
0 & 0 & 0 & 0 & 0 & \eta_1\epsilon^{\alpha} & 0 & -(\gamma_1^{\alpha}+\sigma_{T1}^{\alpha}+\theta_2\sigma_H^{\alpha}+\mu^{\alpha}+\delta_7^{\alpha}) & \tau_3^{\alpha} & 0 & 0 \\
0 & 0 & 0 & 0 & 0 & 0 & \eta_2\epsilon^{\alpha} & \theta_2\sigma_H^{\alpha} & -(\tau_3^{\alpha}+\mu^{\alpha}+\delta_8^{\alpha}) & 0 & 0 \\
0 & 0 & 0 & 0 & 0 & 0 & 0 & \gamma_1^{\alpha} & 0 & -(\rho^{\alpha}+\mu^{\alpha}+\delta_3^{\alpha}) & a_1^{\alpha} \\
0 & 0 & 0 & 0 & 0 & 0 & 0 & \sigma_{T1}^{\alpha} & 0 & 0 & -(a_1^{\alpha}+\mu^{\alpha}+\delta_9^{\alpha})
\end{pmatrix} \tag{5.26}$$

and

$$\hat{G}(X,Z) = \begin{pmatrix} \hat{G_1}(X,Z) \\ \hat{G_2}(X,Z) \\ \hat{G_3}(X,Z) \\ \hat{G_4}(X,Z) \\ \hat{G_5}(X,Z) \\ \hat{G_6}(X,Z) \\ \hat{G_7}(X,Z) \\ \hat{G_8}(X,Z) \\ \hat{G_9}(X,Z) \\ \hat{G_{10}}(X,Z) \\ \hat{G_{11}}(X,Z) \end{pmatrix} = \begin{pmatrix} \lambda_T N\left(1-\frac{S}{N}\right) + \lambda_H E_T \\ \psi_3 \lambda_H I_T \\ 0 \\ \lambda_H N\left(1-\frac{S}{N}\right) + \psi_1 \lambda_T I_H \\ \psi_2 \lambda_T A \\ -\lambda_H E_T - \psi_1 \lambda_T I_H \\ -\psi_2 \lambda_T A \\ -\psi_3 \lambda_H I_T \\ 0 \\ 0 \\ 0 \end{pmatrix} \tag{5.27}$$

Condition H_2 in (5.24) is not satisfied since $\hat{G}_6 < 0$, $\hat{G}_7 < 0$ and $\hat{G}_8 < 0$. Consequently, U_0 may not globally asymptotically stable. Thus, in this case, a backward bifurcation seems to occur at $R_0 = 1$ and the double endemic equilibria exists for $R_0 < 1$. Note that the negative terms are associated with the coinfection.

■

5.4 Sensitivity analysis

In this section sensitivity analysis of the reproduction number, R_0, to relevant parameters of model (5.1) is performed. This analysis measures the relative change in a variable subjected to the variation of a given parameter. Following is the procedure developed in [27]. Since R_0 is the threshold for the existence of disease, it becomes imperative to compute the sensitivity indices for R_0.

The calculations are done for the parameter values given in Table 5.2. The signs of the sensitivity indices may be found in Table 5.1. A positive sign indicates an increase in the value of R_0 as the parameter is increased. Inversely a negative sign of the index means that R_0 decreases as the parameter is increased. For example, increasing the effective contact rates for HIV or TB, β_H^α and β_T^α, respectively, will increase the number of infectious individuals in the population, leading to a boost of the epidemics.

Parameter	Sensitivity index sign
β_T^α	+
η_T	+
σ_T^α	+
a^α	-
δ_2^α	-
μ^α	-
ϵ^α	+
γ^α	-
δ_1^α	-
β_H^α	+
τ_2^α	+
δ_4^α	-
δ_3^α	-
σ_H^α	-

Table 5.1: Sensitivity indexes for relevant parameters of model (5.1).

5.5 Numerical results

Simulations of the model (5.1) for different values of the order of the fractional derivative, $\alpha \in]0, 1]$, and for biologically relevant parameters are done. The predictor-corrector PECE method of Adams-Bashford-Moulton type [38] is applied. The parameters used in the simulations are given in Table 5.2 and the initial conditions are set to: $S(0) = 5 \times 10^5$, $E_T(0) = 4 \times 10^3$, $I_T(0) = R(0) = T_R(0) = I_H(0) = A(0) = E_T I_H(0) = E_T A(0) = I_{TH}(0) = I_T A(0) = R I_H(0) = T_R I_H(0) = 1000$.

Parameter	Value	Reference
Λ	50000	[125]
β_T	0.75	[4]
η_T	1.02	[15]
η_{TH}	1.02	[15]
β_H	0.45	[4]
η_H	1.05	[15]
ρ	0.05	[118]
μ	0.02	[125]
ψ_3	1.03	[15]
ϵ	0.25	[118]
γ	0.2	[15]
σ_T	0.003	[115]
δ_1	0.01	[125]
a	0.11	[118]
δ_2	0.02	[125]
τ_2	0.33	[131]
ψ_1	1.1	Estimated
ψ_2	1.2	[15]
σ_H	0.1	[4]
δ_3	0.01	[125]
δ_4	0.02	[125]
η_1	1.5	[15]
θ_1	1.02	[15]
δ_5	0.03	[125]
η_2	1.8	[15]
δ_6	0.03	[125]
γ_1	0.13	Estimated
σ_{T1}	0.003	Estimated
τ_3	0.33	Estimated
a_1	0.10	Estimated
θ_2	2.5	[15]
δ_7	0.03	[125]
δ_8	0.03	[125]
δ_9	0.03	[125]

Table 5.2: Parameters used in the numerical simulations of models (5.1), where appropriate the units are yr^{-1}.

In Figures 5.2-5.4, it is shown the dynamics of relevant variables of system (5.1) for different values of η_T, the increased infectiousness of the MRD-TB drug-resistant infected individuals, when compared to individuals infected with non-resistant TB strains, and for

three values of α. It is observed that an increase in η_T boosts the number of individuals infected with TB, suggesting that the increased infectiousness of the MRD-TB strains influences negatively the recovery of TB infection. Similar patterns are present for all values of the order of the fractional derivative, α. To avoid an excessive number of figures in the paper and some redundancy in terms of results, only the figures for three values of α are left here.

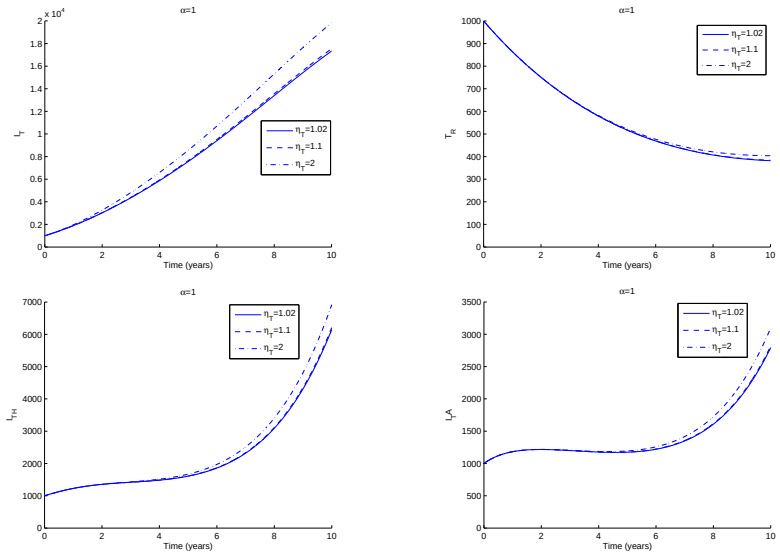

Figure 5.2: Dynamics of the relevant variables of system (5.1) for different values of η_T, the increased infectiousness of the MRD-TB infected individuals when compared to individuals infected with non-resistant TB strains, and $\alpha = 1$. Parameter values and initial conditions are in the text. ($\eta_T = 1.02$ - $R_T = 3.0412$, $R_H = 11.0265$, $R_0 = 11.0265$, $\eta_T = 1.1$ - $R_T = 3.0460$, $R_H = 11.0265$, $R_0 = 11.0265$ and $\eta_T = 2$ - $R_T = 3.0997$, $R_H = 11.0265$, $R_0 = 11.0265$)

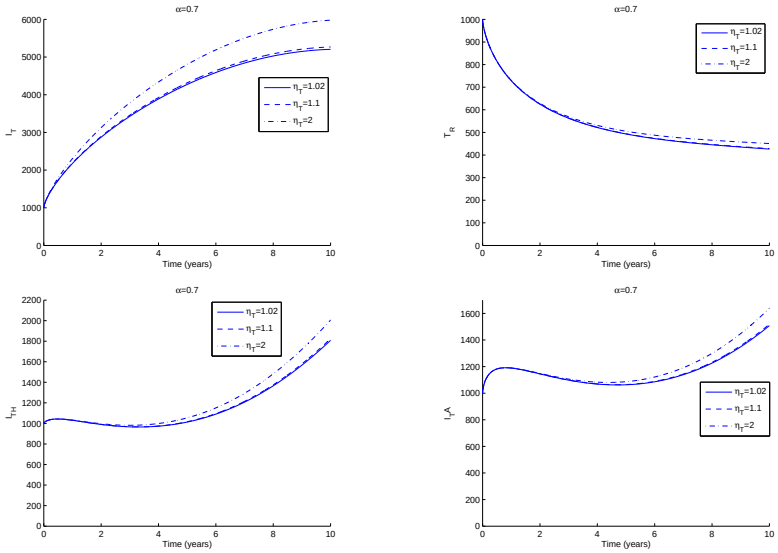

Figure 5.3: Dynamics of the relevant variables of system (5.1) for different values of η_T, the increased infectiousness of the MRD-TB infected individuals when compared to individuals infected with non-resistant TB strains, and $\alpha = 0.7$. Parameter values and initial conditions are in the text. ($\eta_T = 1.02$ - $R_T = 1.6467$, $R_H = 3.8568$, $R_0 = 3.8568$, $\eta_T = 1.1$ - $R_T = 1.6530$, $R_H = 3.8568$, $R_0 = 3.8568$ and $\eta_T = 2$ - $R_T = 1.7235$, $R_H = 3.8568$, $R_0 = 3.8568$)

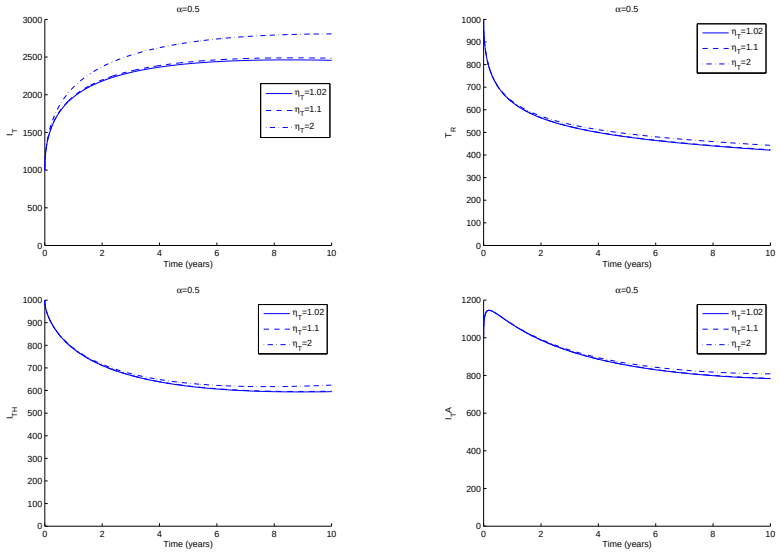

Figure 5.4: Dynamics of the relevant variables of system (5.1) for different values of η_T, the increased infectiousness of the MRD-TB infected individuals when compared to individuals infected with non-resistant TB strains, and $\alpha = 0.5$. Parameter values and initial conditions are in the text. ($\eta_T = 1.02$ - $R_T = 0.9907$, $R_H = 1.9402$, $R_0 = 1.9402$, $\eta_T = 1.1$ - $R_T = 0.9971$, $R_H = 1.9402$, $R_0 = 1.9402$ and $\eta_T = 2$ - $R_T = 1.07$, $R_H = 1.9402$, $R_0 = 1.9402$)

In Figures 5.5-5.7, are seen the dynamics of the variables of system (5.1) for different values of η_{TH}, the increased infectiousness of individuals coinfected with HIV and TB, when compared to individuals solely infected with TB, and for three values of α. The figures show that as η_{TH} increases, there is an overall increase in the numbers of individuals infected with TB and coinfected with HIV and TB, showing or not symptoms of AIDS. Thus, the coinfection adds severity to the epidemics. The behaviour is similar for all values of α.

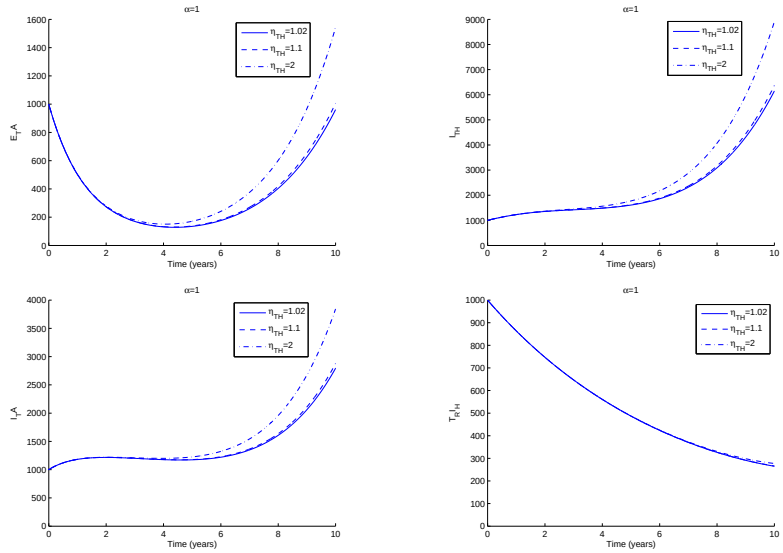

Figure 5.5: Dynamics of the relevant variables of system (5.1) for different values of η_{TH}, the increased infectiousness of individuals coinfected with HIV and TB, when compared to individuals solely infected with TB, and $\alpha = 1$. Parameter values and initial conditions are in the text. ($R_T = 3.0412$, $R_H = 11.0265$, $R_0 = 11.0265$)

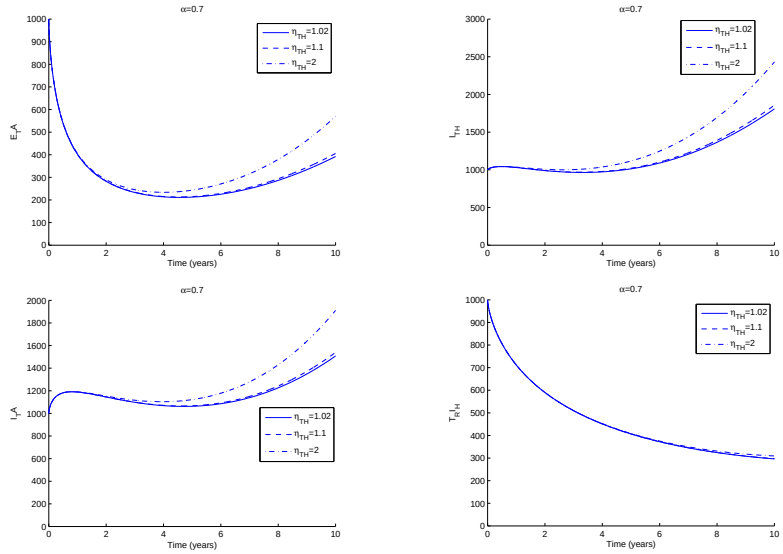

Figure 5.6: Dynamics of the relevant variables of system (5.1) for different values of η_{TH}, the increased infectiousness of individuals coinfected with HIV and TB, when compared to individuals solely infected with TB, and $\alpha = 0.7$. Parameter values and initial conditions are in the text. ($R_T = 1.6467$, $R_H = 3.8568$, $R_0 = 3.8568$)

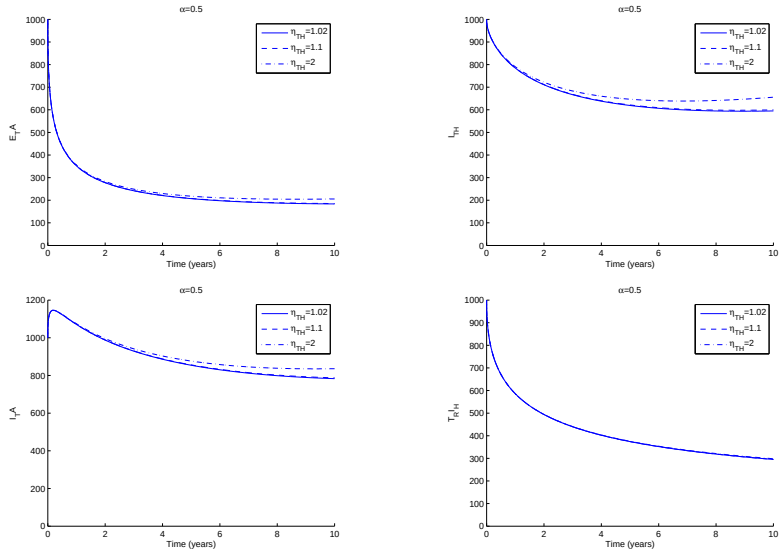

Figure 5.7: Dynamics of the relevant variables of system (5.1) for different values of η_{TH}, the increased infectiousness of individuals coinfected with HIV and TB, when compared to individuals solely infected with TB, and $\alpha = 0.5$. Parameter values and initial conditions are in the text. ($R_T = 0.9907$, $R_H = 1.9402$, $R_0 = 1.9402$)

Figures 5.8-5.10, depict the dynamics of the variables of system (5.1) for different values of η_H, the increased infectiousness of individuals coinfected with HIV and TB, when compared to individuals solely infected with HIV, and three values of α. Larger values of η_H promote higher numbers of individuals infected solely with HIV and of individuals coinfected with HIV and TB, showing or not symptoms of AIDS. Again, the coinfection seems to accelerate the epidemics. This occurs for all values of α.

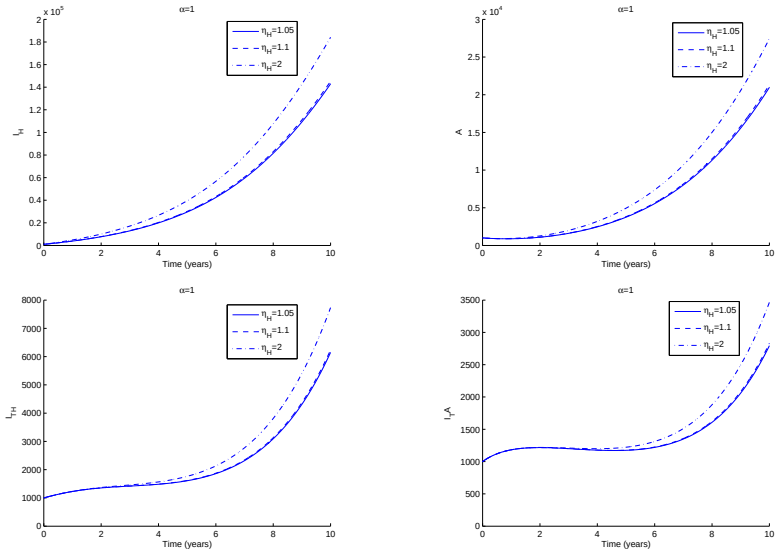

Figure 5.8: Dynamics of the relevant variables of system (5.1) for different values of η_H, the increased infectiousness of individuals coinfected with HIV and TB, when compared to individuals solely infected with HIV, and $\alpha = 1$. Parameter values and initial conditions are in the text. ($R_T = 3.0412$, $R_H = 11.0265$, $R_0 = 11.0265$)

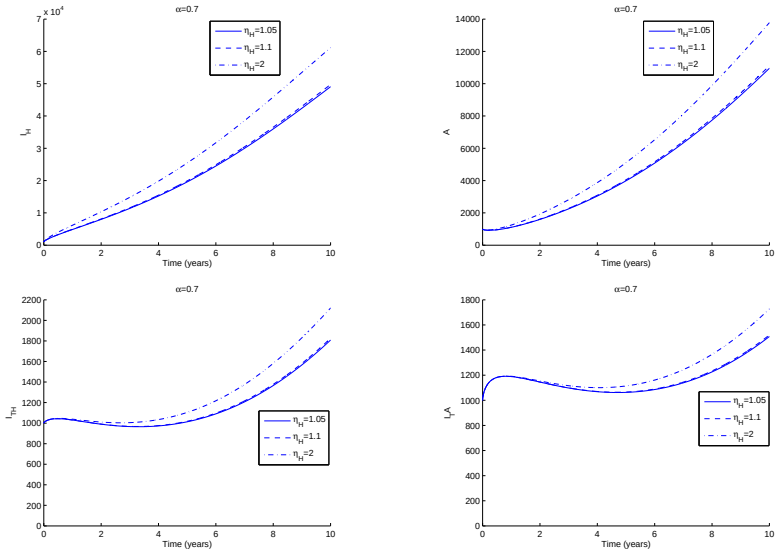

Figure 5.9: Dynamics of the relevant variables of system (5.1) for different values of η_H, the increased infectiousness of individuals coinfected with HIV and TB, when compared to individuals solely infected with HIV, and $\alpha = 0.7$. Parameter values and initial conditions are in the text. ($R_T = 1.6467$, $R_H = 3.8568$, $R_0 = 3.8568$)

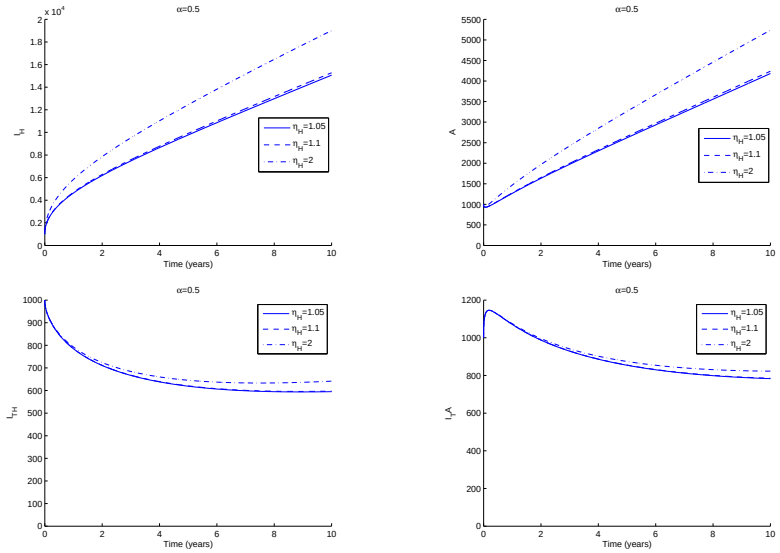

Figure 5.10: Dynamics of the relevant variables of system (5.1) for different values of η_H, the increased infectiousness of individuals coinfected with HIV and TB, when compared to individuals solely infected with HIV, and $\alpha = 0.5$. Parameter values and initial conditions are in the text. ($R_T = 0.9907$, $R_H = 1.9402$, $R_0 = 1.9402$)

Figures 5.11-5.13, show the dynamics of the variables of system (5.1) for different values of σ_T, the rate of TB infected individuals that become resistant to the first line of TB treatment, and three values of α. From the observation of the figures, one concludes that an increase in the resistance to treatment, due, for e.g., to lack of adherence, induces higher numbers of the MDR-TB infected individuals, and of TB exposed individuals. More exposed individuals, with drug-resistant strains, imply, on the long run, a TB transmission dominated by the MDR-TB strains, which could impair TB control and final elimination in the future. This behaviour is repeated for all values of α.

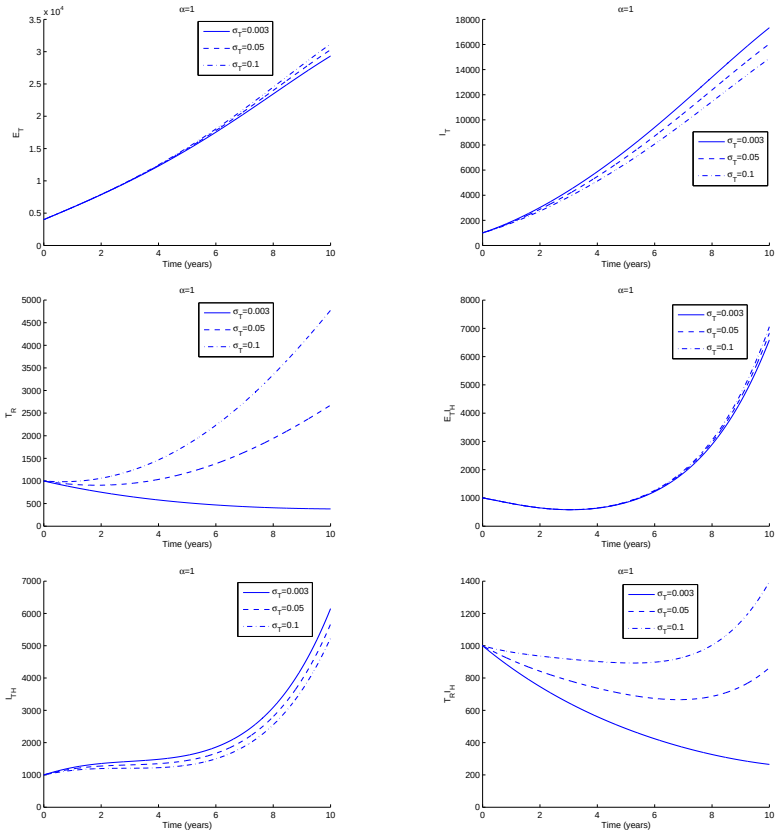

Figure 5.11: Dynamics of the relevant variables of system (5.1) for different values of σ_T, the rate of the TB infected individuals that become resistant to the first line of TB treatment, and $\alpha = 1.0$. Parameter values and initial conditions are in the text, except $\sigma_{T1} = \sigma_T$. ($\sigma_T = 0.005$ - $R_T = 3.0556$, $R_H = 11.0265$, $R_0 = 11.0265$, $\sigma_T = 0.05$ - $R_T = 3.3234$, $R_H = 11.0265$, $R_0 = 11.0265$ and $\sigma_T = 0.1$ - $R_T = 3.5354$, $R_H = 11.0265$, $R_0 = 11.0265$)

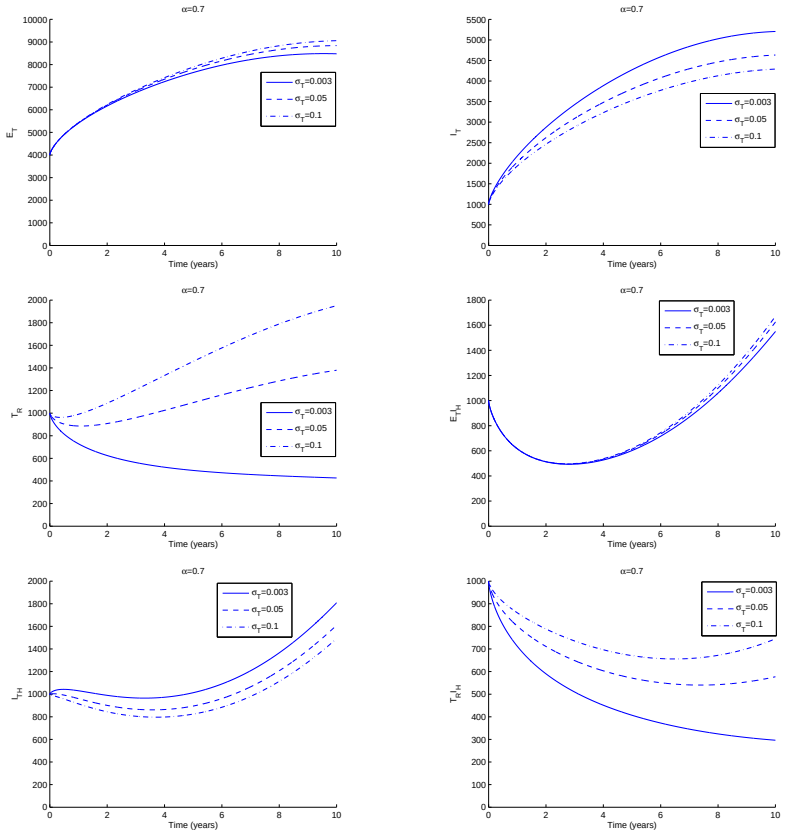

Figure 5.12: Dynamics of the relevant variables of system (5.1) for different values of σ_T, the rate of the TB infected individuals that become resistant to the first line of TB treatment, and $\alpha = 0.7$. Parameter values and initial conditions are in the text, except $\sigma_{T1} = \sigma_T$. ($\sigma_T = 0.005$ - $R_T = 1.6538$, $R_H = 3.8568$, $R_0 = 3.8568$, $\sigma_T = 0.05$ - $R_T = 1.7296$, $R_H = 3.8568$, $R_0 = 3.8568$ and $\sigma_T = 0.1$ - $R_T = 1.7723$, $R_H = 3.8568$, $R_0 = 3.8568$)

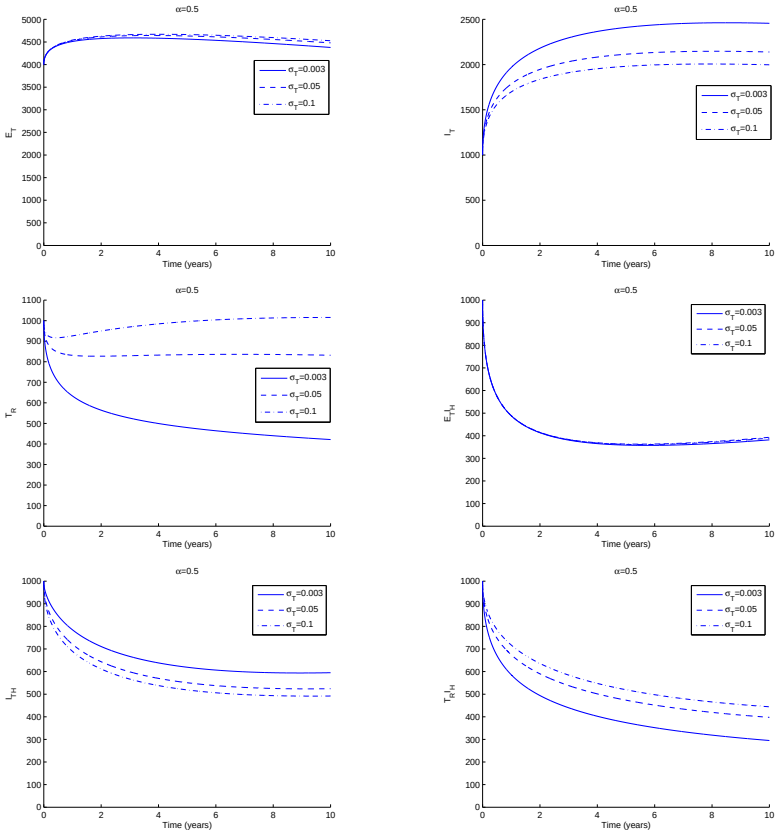

Figure 5.13: Dynamics of the relevant variables of system (5.1) for different values of σ_T, the rate of the TB infected individuals that become resistant to the first line of TB treatment, and $\alpha = 0.5$. Parameter values and initial conditions are in the text, except $\sigma_{T1} = \sigma_T$. ($\sigma_T = 0.005$ - $R_T = 0.9934$, $R_H = 1.9402$, $R_0 = 1.9402$, $\sigma_T = 0.05$ - $R_T = 1.0147$, $R_H = 1.9402$, $R_0 = 1.9402$ and $\sigma_T = 0.1$ - $R_T = 1.0245$, $R_H = 1.9402$, $R_0 = 1.9402$)

In Figures 5.14-5.16 show the dynamics of the variables of system (5.1) for different values of τ_2 the rate of individuals infected with AIDS are treated for HIV, respectively, and three values of α. It is observed that as τ_2 increases there is a decrease in the number of TB infected individuals and a decrease in the number of individuals showing symptoms of AIDS. ART enhances the immunity, which translates in an improvement of patients' health status. This is seen for all values of α.

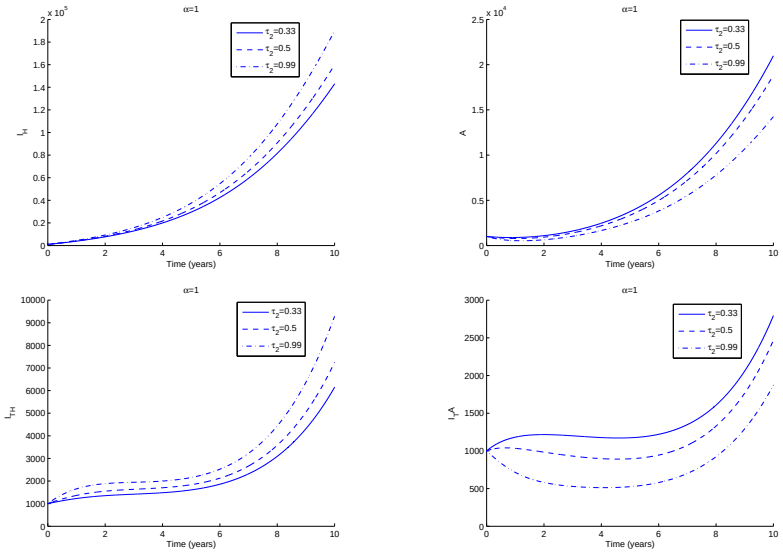

Figure 5.14: Dynamics of the relevant variables of system (5.1) for different values of τ_2, the rate of individuals infected with AIDS are treated for HIV, respectively, and $\alpha = 1.0$. Parameter values and initial conditions are in the text, except $\tau_3 = \tau_2$. ($\tau_2 = 0.33$ - $R_T = 3.0412$, $R_H = 11.0265$, $R_0 = 11.0265$, $\tau_2 = 0.5$ - $R_T = 3.0412$, $R_H = 12.0297$, $R_0 = 12.0297$ and $\tau_2 = 0.99$ - $R_T = 3.0412$, $R_H = 13.2808$, $R_0 = 13.2808$)

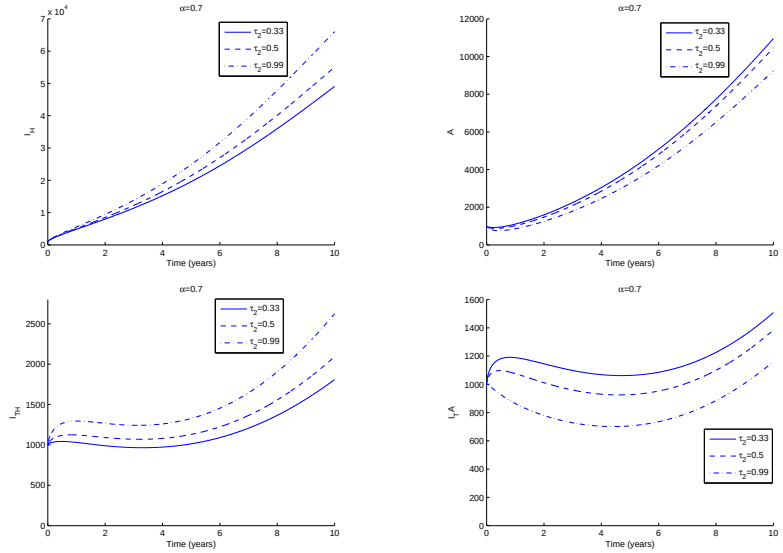

Figure 5.15: Dynamics of the relevant variables of system (5.1) for different values of τ_2, the rate of individuals infected with AIDS are treated for HIV, respectively, and $\alpha = 0.7$. Parameter values and initial conditions are in the text, except $\tau_3 = \tau_2$. ($\tau_2 = 0.33$ - $R_T = 1.6467$, $R_H = 3.8568$, $R_0 = 3.8568$, $\tau_2 = 0.5$ - $R_T = 1.6467$, $R_H = 4.1099$, $R_0 = 4.1099$ and $\tau_2 = 0.99$ - $R_T = 1.6467$, $R_H = 4.4855$, $R_0 = 4.4855$)

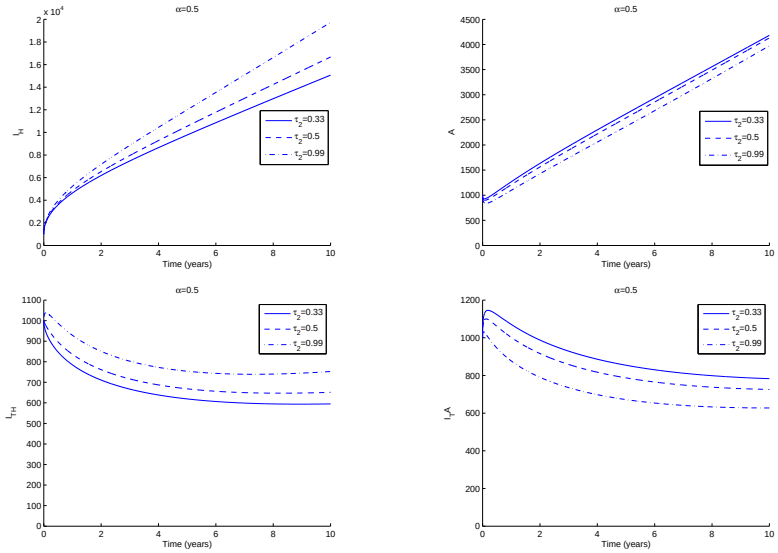

Figure 5.16: Dynamics of the relevant variables of system (5.1) for different values of τ_2, the rate of individuals infected with AIDS are treated for HIV, respectively, and $\alpha = 0.5$. Parameter values and initial conditions are in the text, except $\tau_3 = \tau_2$. ($\tau_2 = 0.33$ - $R_T = 0.9907$, $R_H = 1.9402$, $R_0 = 1.9402$, $\tau_2 = 0.5$ - $R_T = 0.9907$, $R_H = 2.0219$, $R_0 = 2.0219$ and $\tau_2 = 0.99$ - $R_T = 0.9907$, $R_H = 2.1541$, $R_0 = 2.1541$)

The results of the simulations of our model support evidence that HIV and TB coinfection poses a significant threat to the public health care system. Coinfection is responsible for more infectious individuals, who are more prone to spread the epidemics. Moreover, the MDR-TB strains transmission in the population, together with HIV infection, constitutes a major challenge with respect to treatment, which requires anti-tuberculosis and ART to be administered unitedly. The later raises important issues, namely pill burden, patient compliance, drug interactions and toxic effects, as well as immune reconstitution inflammatory syndrome. All together, the coinfection burden increases concerns of an extreme difficulty in TB control and elimination worldwide, as well as jeopardizes the ending of AIDS epidemic. Note that the 90-90-90 ambitious treatment target to help end the AIDS epidemics relies on three premisses by 2020: 90% of all people living with HIV will know their HIV status; 90% of all people with diagnosed HIV infection will receive sustained ART; and 90% of all people receiving ART will have viral suppression [92].

The fractional order derivative brings additional information on the epidemics, which may be associated with individuals' specificities of the immune system (for e.g., on HIV progression one can distinguish the rapid progressors, the long-term non progressors and the elite controllers), existence of other comorbidities, access to medical care, and the issues related to treatment (adherence, toxicity, etc).

5.6 Conclusions

A FO model is proposed for the coinfection of HIV and TB, in the presence of MDR-TB strains and treatment for both diseases. The model's behaviour is analyzed for distinct values of the order of the fractional derivative, α, and for biologically relevant parameters, namely the ones related with the coinfection and treatment. It is observed that the coinfection burden increases the severity of the disease and poses a significant threat to the public health care system. Coinfection is responsible for more infectious individuals, who are more prone to spread the epidemics. Moreover, the MDR-TB strains transmission in the population, together with HIV infection, constitutes a major challenge with respect to treatment, which requires anti-tuberculosis and ART to be administered unitedly. All together, the coinfection burden increases concerns of an extreme difficulty in TB control and elimination worldwide, as well as jeopardizes the ending of AIDS epidemic. The order of the fractional derivative, α, may be associated with differences in individuals' immune system, age, treatment compliance, treatment toxicities, other comorbidities, amongst others.

Chapter 6

Conclusions

For those who work in compartmental models, mathematical models are the equivalent of a laboratory. Models are mathematical representations of biological processes that allow transparency and precision in relation to the epidemiological assumptions. They allow to test the understanding of the epidemiology of the disease, comparing the results of the model and the observed patterns. These methods provide the tools to bridge the micro and macro gap in the study of HIV population dynamics. As models become more sophisticated and more capable of capturing the heterogeneities observed in the data, one begins to think of the changes induced by the model in spread of the disease. Mathematical models and computational simulations are thus useful experimental tools for constructing and testing theories, evaluating quantitative conjectures, answering specific questions, determining sensitivities to changes in parameter values and the key to estimating model parameters. Model analysis and predictions provide crucial data that can be used in treatment strategies and prevention. Moreover, they are the tools needed to demonstrate the impact of a social or behavioral intervention in a population. On the other hand, an important role of modeling is that it can alert us to deficiencies in our current understanding of the epidemiology of various infectious diseases and suggest crucial questions for research and data that need to be collected.

In this work, mathematical models for HIV/AIDS virus transmission and relevant coinfections are studied. The major limitation of studies of this type is the lack of real data that would allow one to compare the results of the theoretical models with the real data. For this reason, most of the parameter values used in the simulations of the proposed models are based on the HIV/AIDS literature. Future work will focus on studying models of HIV/AIDS and fitting the simulations of the models to real data. Permissions to ethical commissions of Portuguese hospitals have already been asked

with some positive replies. The data from real HIV infected Portuguese patients is being collected to be further analyzed.

6.1 Thesis results

The present thesis originated results presentation to the scientific community in the form of articles. The following are the results:

- C.M.A. Pinto and A.R.M. Carvalho, *New findings on the dynamics of HIV and TB coinfection models*, Applied Mathematics and Computation 242, 36–46, 2014.

  Abstract: In this paper we study a model for HIV and TB coinfection. We consider the integer order and the fractional order versions of the model. Let $\alpha \in [0.78; 1.0]$ be the order of the fractional derivative, then the integer order model is obtained for $\alpha = 1.0$. The model includes vertical transmission for HIV and treatment for both diseases. We compute the reproduction number of the integer order model and HIV and TB submodels, and the stability of the disease free equilibrium. We sketch the bifurcation diagrams of the integer order model, for variation of the average number of sexual partners per person and per unit time, and the tuberculosis transmission rate. We analyze numerical results of the fractional order model for different values of α, including $\alpha = 1$. The results show distinct types of transients, for variation of α. Moreover, we speculate, from observation of the numerical results, that the order of the fractional derivative may behave as a bifurcation parameter for the model. We conclude that the dynamics of the integer and the fractional order versions of the model are very rich and that together these versions may provide a better understanding of the dynamics of HIV and TB coinfection.

- A.R.M. Carvalho and C.M.A. Pinto, *A coinfection model for HIV and HCV*, BioSystems 124, 46–60, 2014.

  Abstract: We study a mathematical model for the human immunodeficiency virus (HIV) and hepatites C virus (HCV) coinfection. The model predicts four distinct equilibria: the disease free, the HIV endemic, the HCV endemic, and the full endemic equilibria. The local and global stability of the disease free equilibrium was calculated for the full model and the HIV and HCV submodels. We present numerical simulations of the full model where the distinct equilibria can be observed. We show simulations of the qualitative changes of the dynamical behavior of the full model for variation of relevant parameters. From the results of the model, we infer possible measures that could be implemented in order to reduce the number of infected individuals.

- C.M.A. Pinto and A.R.M. Carvalho, *Effects of treatment, awareness and condom use in a coinfection model for HIV and HCV in MSM*, Journal of Biological Systems 23(2), 165–193, 2015.

  Abstract: We develop a new a coinfection model for hepatitis C virus (HCV) and the human immunodeficiency virus (HIV). We consider treatment for both diseases, screening, unawareness and awareness of HIV infection, and the use of

condoms. We study the local stability of the disease-free equilibria for the full model and for the two submodels (HCV only and HIV only submodels). We sketch bifurcation diagrams for different parameters, such as the probabilities that a contact will result in a HIV or an HCV infection. We present numerical simulations of the full model where the HIV, HCV and double endemic equilibria can be observed. We also show numerically the qualitative changes of the dynamical behavior of the full model for variation of relevant parameters. We extrapolate the results from the model for actual measures that could be implemented in order to reduce the number of infected individuals.

- C.M.A. Pinto and A.R.M. Carvalho, *Fractional Modeling of Typical Stages in HIV Epidemics with Drug-Resistance*, Progress in Fractional Differentiation and Applications 1(2), 111–122, 2015.

  Abstract: In this paper it is studied a fractional order model for the three stages of HIV epidemics with drug-resistance. The model includes CD4^+ T cells, CTLs, macrophages, and the virus populations. We simulate the model for different values of the fractional derivative $\alpha \in [0.5, 1.0]$. The fractional order system untangles generous dynamical characteristics, such as faster transients and slower evolutions as time increases. These traits are not seen in integer-order models, since they are customary of memory-preserving systems.

- A.R.M. Carvalho and C.M.A. Pinto, *Emergence of drug-resistance in HIV dynamics under distinct HAART regimes*, Communications in Nonlinear Science and Numerical Simulation 30, 207–226, 2016.

  Abstract: In this paper we propose a model for the dynamics of HIV epidemics under distinct HAART regimes, and study the emergence of drug-resistance. The model predicts HIV dynamics of untreated HIV patients for all stages of the infection. We compute the local and the global stability of the disease-free equilibrium of the model. We simulate the model for two distinct HIV patients, the rapid progressors and the long-term non-progressors. We study the effects of equal RTI and PI efficacies, as well as distinct drug efficacies, namely RTI-based and PI-based therapeutics. Treatment is initiated when the CD4^+ T cells count is less than 350 cells mm^{-3}. The PI-based drugs seem to produce better outcomes, with respect to disease progression, than RTI-based regimes.

- C.M.A. Pinto and A.R.M. Carvalho, *Fractional complex-order model for HIV infection with drug resistance during therapy*, Journal of Vibration and Control 22(9), 2222–2239, 2016.

  Abstract: We propose a fractional complex-order model for drug-resistance in HIV infection. We consider three distinct growth rates for the CD4^+ T helper cells. We simulate the model for different values of the fractional derivative of complex order $D^{\alpha \pm j\beta}$, where $\alpha, \beta \in \mathbf{R}^+$, and for the distinct growth rates. The fractional derivative of complex order is a generalization of the integer order derivative where $\alpha = 1$ and $\beta = 0$. The fractional complex-order system reveals rich dynamics and variation of the value of the complex-order derivative sheds new light on the modeling of the intracellular delay. Additionally, fractional patterns are characterized by time responses with faster transients and slower evolutions towards the steady-state.

- C.M.A. Pinto and A.R.M. Carvalho, *A latency fractional order model for HIV dynamics*, Journal of Computational and Applied Mathematics 31, 240–256, 2017.

  Abstract: We study a fractional order model for HIV infection where latent T helper cells are included. We compute the reproduction number of the model and study the stability of the disease free equilibrium. We observe that the reproduction number varies with the order of the fractional derivative α. In terms of epidemics, this suggests that varying α induces a change in the patients' epidemic status. Moreover, we simulate the variation of relevant parameters, such as the fraction of uninfected CD4^+ T cells that become latently infected, and the CTLs proliferation rate due to infected CD4^+ T cells. The model produces biologically reasonable results.

- A.R.M. Carvalho and C.M.A. Pinto, *Within-host and synaptic transmissions: contributions to the spread of HIV infection*, Mathematical Methods in the Applied Sciences 40(4), 1231–1264, 2017.

  Abstract: We study the contributions of within-host (virus-to-cell) and synaptic (cell-to-cell) transmissions in a mathematical model for human immunodeficiency virus epidemics. The model also includes drug resistance. We prove the local and global stability of the disease-free equilibrium and the local stability of the endemic equilibrium. We analyse the effect of the cell-to-cell transmission rate on the value of the reproduction number, R_0. Moreover, we show evidence of a qualitative change in the models' dynamics, subjected to the value of the drug efficacy. In the end, important inferences are drawn.

- C.M.A. Pinto and A.R.M. Carvalho, *The role of synaptic transmission in a HIV model with memory*, Applied Mathematics and Computation 292, 76–95, 2017.

  Abstract: We propose a mathematical model with memory for the dynamics of HIV epidemics, where two transmission modes, cell-to-cell and virus-to-cell, and drug resistance are considered. Systems with memory, or fractional order systems, have largely been applied to the modeling of several real life phenomena. Here, we consider a fractional model where the order of the non-integer derivative takes values in the interval $[0.5, 1.0]$. We prove the local and global stability of the disease-free equilibrium. We study the role of the cell-to-cell transmission probability on the dynamics of the model, and on the value of the reproduction number, R_0, for distinct values of the fractional order derivative, α. Moreover, we show evidence of an improvement of HIV infected patients quality of life, due to the increase of the drug efficacy. In the end, important inferences are drawn.

- C.M.A. Pinto and A.R.M. Carvalho, *The HIV/TB coinfection severity in the presence of TB multi-drug resistant strains*, Ecological Complexity 32, 1–20, 2017.

  Abstract: We introduce a novel fractional-order model for the coinfection of HIV and tuberculosis (TB), in the presence of multi-drug resistant TB strains (MDR-TB) and treatment for both diseases. We compute the reproduction number of the HIV and TB submodels and of the full model and the local and global stabilities of the disease-free equilibria. Numerical simulations show the different dynamics of the model for variation of biologically relevant parameters, and for the order of the fractional derivative $\alpha \in]0, 1]$. The results obtained highlight the importance of treatment for HIV and TB and the role of the MDR-TB strains in the severity of the coinfection. Moreover, the order of the fractional derivative is a significant player in the epidemics theatre.

- Ana R.M. Carvalho and Carla M.A. Pinto, *New developments on AIDS-related cancers: the role of the delay and treatment options*, Mathematical Methods in the Applied Sciences, 1–14, DOI: 10.1002/mma.4657, 2017.

  Abstract: We propose a simple delay mathematical model for the dynamics of AIDS-related cancers with treatment for HIV and chemotherapy. The main goals are to study the effects of the delay and of treatment (HAART and chemotherapy) in cancer cells growth. The model was simulated for several biologically reasonable values of the delay, of HAART efficacies and of chemotherapeutic drugs decay rates. The results of the simulations reveal an epidemiologically well-defined model. Important inferences are drawn for designing future treatment protocols.

- C.M.A. Pinto and A.R.M. Carvalho, *Fractional dynamics of a HIV infection model with time-varying drug exposure*, Journal of Computational and Nonlinear Dynamics, 2017, DOI: 10.1115/1.4038643.

  Abstract: We introduce a fractional order model for the human immunodeficiency virus dynamics, where time-varying drug-exposure and drug-resistance are assumed. We derive conditions for the local and global asymptotic stability of the disease-free equilibrium. We find periodic stable endemic states for certain parameter values, for sinusoidal drug efficacies and when considering a density dependent decay rate for the T cells. Other classes of periodic drug-efficacies are considered and the effect of the phases of these functions on the dynamics of the model are also studied. The order of the fractional derivative plays an important role in the severity of the epidemics.

- C.M.A. Pinto and A.R.M. Carvalho, *The impact of pre-exposure prophylaxis (PrEP) and screening on the dynamics of HIV*, Journal of Computational and Applied Mathematics, 2017, https://doi.org/10.1016/j.cam.2017.10.019.

  Abstract: We analyse the impact of pre-exposure prophylaxis (PrEP) and screening effects on HIV dynamics in infected patients. Our model incorporates condom use, the number of sexual partners, and treatment for HIV. Numerical simulations are performed and the model is fitted to data on the cumulative HIV and AIDS cases in Portugal. Moreover, critical epidemiological parameters are also varied. Inferences are made concerning the epidemiological consequences of the model's predictions on public HIV/AIDS planning. The order of the fractional derivative is suggested to have a powerful role in the drama of HIV epidemics.

- A.R.M. Carvalho, C.M.A. Pinto and D. Baleanu, *HIV/HCV coinfection model: a fractional order perspective for the effect of the HIV viral load*, Advances in Difference Equations 2018(2): 1–22, 2018.

  Abstract: We study the burden of the HIV viremia and of treatment efficacy in the severity of the patterns of the HIV/HCV coinfection. For this, we derive a simple non-integer order (fractional order) model for the coinfection patterns. The basic reproduction number and the stability of the disease-free equilibrium are computed. The numerical results suggest that the HIV viral load impacts impressively the severity of the HCV infection. The treatment efficacy is also found to influence the natural progression of HCV on the HIV/HCV coinfection. The later repeats for all values of the order of the fractional derivative.

- Ana R.M. Carvalho and Carla M.A. Pinto, *Non-integer order analysis of the impact of diabetes and resistant strains in a model for TB infection*, Communications in Nonlinear Science and Numerical Simulation, Accept, January 2018.

Abstract: We study the impact of diabetes and multi-drug resistant strains in a model for tuberculosis (TB) infection in a community. We compute the reproduction number, R_0, of the model and analyse its behaviour numerically for variation of epidemiologically relevant parameters. Namely, the increased susceptibility to TB due to diabetes, the diabetes recruitment rate, and the increased progression of non-diabetics TB infectious to diabetic TB infectious individuals, due to their active TB status. Moreover, we have also performed numerical simulations of the model for the mentioned parameters and the results confirm the dynamics predicted by the value of R_0. The sensitivity indices of R_0 were also determined. The order of the fractional derivative adds more information on the dynamics of the model and may help distinguishing dynamical traits in distinct patients.

References

[1] UL Abbas, R Glaubius, A Mubayi, G Hood, and JW Mellors. Antiretroviral therapy and pre-exposure prophylaxis: Combined impact on HIV transmission and drug resistance in South Africa. *The Journal of Infectious Diseases*, 208(2):224–234, 2013.

[2] LJ Abu-Raddad, JT Schiffe, R Ashley, G Mumtaz, RA Alsallaq, FA Akala, I Semini, G Riedner, and D Wilson. HSV-2 serology can be predictive of HIV epidemic potential and hidden sexual risk behavior in the Middle East and North Africa. *Epidemics*, 2(4):173–182, 2010.

[3] LM Agosto, PD Uchi, and W Mothes. HIV cell-to-cell transmission: effects on pathogenesis and antiretroviral therapy. *Trends in Microbiology*, 23(5):289–295, 2015.

[4] FB Agusto and AI Adekunle. Optimal control of a two-strain tuberculosis - HIV/AIDS co-infection model. *BioSystems*, 119:20–44, 2014.

[5] HK Alexander and S Bonhoeffer. Pre-existence and emergence of drug resistance in a generalized model of intra-host viral dynamics. *Epidemics*, 4(4):187–202, 2012.

[6] MJ Alter. Epidemiology of viral hepatitis and HIV co-infection. *Journal of Hepatology*, 44(1 Suppl):S6–9, 2006.

[7] P An and CA Winkler. Host genes associated with HIV/AIDS: advances in gene discovery. *Trends in Genetics*, 26(3):119–131, 2010.

[8] R Arnaout, M Nowak, and D Wodarz. HIV-1 dynamics revisited: Biphasic decay by cytotoxic lymphocyte killing? *Proceedings of the Royal Society London B*, 267(1450):1347–1354, 2000.

[9] LO Arthur, JW Bess, RC Sowder, RE Benveniste, DL Mann, JC Chermann, and LE Henderson. Cellular proteins bound to immunodeficiency virus: implications for pathogenesis and vaccines. *Science*, 258:1935–1938, 1992.

[10] B Asquith, C Edwards, M Lipsitch, and A McLean. Inefficient cytotoxic T lymphocyte-mediated killing of HIV-1-infected cells in vivo. *PLoS Biology*, 4(4):583–592, 2006.

[11] SH Bajaria, G Webb, M Cloyd, and D Kirschner. Dynamics of naive and memory $CD4^+$ T lymphocytes in HIV-1 disease progression. *Journal of Acquired Immune Deficiency Syndromes*, 30(1):41–58, 2002.

[12] P Barreiro, C de Mendoza, J Gonzalez-Lahoz, and V Soriano. Superiority of protease inhibitors over non-nucleoside reverse-transcriptase inhibitors when highly active antiretroviral therapy resumed after treatment interruption. *Clinical Infectious Diseases*, 41(6):897–900, 2005.

[13] JM Benito, M López, and V Soriano. The role of $CD8^+$ T-cell response in HIV infection. *AIDS Reviews*, 6(2):79–88, 2004.

[14] CP Bhunu. Mathematical analysis of a three-strain tuberculosis transmission model. *Applied Mathematical Modelling*, 35(9):4647–4660, 2011.

[15] CP Bhunu, W Garira, and Z Mukandavire. Modeling HIV/AIDS and tuberculosis coinfection. *Bulletin of Mathematical Biology*, 71(7):1745–1780, 2009.

[16] CP Bhunu and S Mushayabasa. Modelling the transmission dynamics of HIV/AIDS and hepatitis C virus co-infection. *HIV & AIDS Review*, 12(2):37–42, 2013.

[17] R Birger, R Kouyos, J Dushoff, and B Grenfell. Modeling the effect of HIV coinfection on clearance and sustained virologic response during treatment for hepatitis C virus. *Epidemics*, 12:1–10, 2015.

[18] CJ Browne and SS Pilyugin. Periodic multidrug therapy in a within-host virus model. *Bulletin of Mathematical Biology*, 74(3):562–589, 2012.

[19] L Capa, V Soriano, J Garcia-Samaniego, M Nunez, M Romero, A Cascarejo, F Muñoz, J González-Lahoz, and JM Benito. Influence of HCV genotype and co-infection with human immunodeficiency virus on $CD4^+$ and $CD8^+$ T-cell responses to hepatitis C virus. *Journal of Medical Virology*, 49(5):503–510, 2007.

[20] M Caputo. Linear model of dissipation whose Q is almost frequency independent - II. *Geophysical Journal of the Royal Astronomical Society*, 13:529–539, 1967.

[21] ARM Carvalho and CMA Pinto. A coinfection model for HIV and HCV. *BioSystems*, 124:46–60, 2014.

[22] ARM Carvalho and CMA Pinto. Emergence of drug-resistance in HIV dynamics under distinct HAART regimes. *Communications in Nonlinear Science and Numerical Simulation*, 30(1–3):207–226, 2016.

[23] ARM Carvalho and CMA Pinto. Within-host and synaptic transmissions: contributions to the spread of HIV infection. *Mathematical Methods in the Applied Sciences*, 40(4):1231–1264, 2017.

[24] C Castillo-Chavez and Z Feng. To treat or not to treat: the case of tuberculosis. *Journal Mathematical Biology*, 35(6):629–656, 1997.

[25] BS Chan and P Yu. Bifurcation analysis in a model of cytotoxic T-lymphocyte response to viral infections. *Nonlinear Analysis: Real World Applications*, 13(1):64–77, 2012.

[26] CY Chiang and LW Riley. Exogenous reinfection in tuberculosis. *The Lancet Infectious Diseases*, 5(10):629–636, 2005.

[27] N Chitnis, JM Hyman, and JM Cushing. Determining important parameters in the spread of malaria through the sensitivity analysis of a mathematical model. *Bulletin of Mathematical Biology*, 70(5):1272–1296, 2008.

[28] MS Ciupe, BL Bivort, DM Bortz, and PW Nelson. Estimating kinetic parameters from HIV primary infection data through the eyes of three different mathematical models. *Mathematical Biosciences*, 200(1):1–27, 2006.

[29] T Cohen, M Lipsitch, RP Walensky, and M Murray. Beneficial and perverse effects of isoniazid preventive therapy for latent tuberculosis infection in HIV-tuberculosis coinfected populations. *Proceedings of the National Academy of Sciences of the United States of America*, 103(18):7042–7047, 2006.

[30] JM Conway and AS Perelson. Post-treatment control of HIV infection. *Proceedings of the National Academy of Sciences of the United States of America*, 112(17):5467–5472, 2015.

[31] JM Conway and AS Perelson. Residual viremia in treated HIV^+ individuals. *PLOS Computational Biology*, 12(1):1–19, 2016.

[32] S Corson, D Greenhalgh, A Taylor, N Palmateer, D Goldberg, and S Hutchinson. Modelling the prevalence of HCV amongst people who inject drugs: An investigation into the risks associated with injecting paraphernalia sharing. *Drug and Alcohol Dependence*, 133(1):172–179, 2013.

[33] RV Culshaw and S Ruan. A delay-differential equation model of HIV infection of $CD4^+$ T-cells. *Mathematical Biosciences*, 165(1):27–39, 2000.

[34] M Danta, N Semmo, P Fabris, D Brown, OG Pybus, CA Sabin, S Bhagani, VC Emery, GM Dusheiko, and P Klenerman. Impact of HIV on host-virus interactions during early hepatitis C virus infection. *The Journal of Infectious Diseases*, 197(11):1558–1566, 2008.

[35] LG de Pillis, W Gu, and AE Radunskaya. Mixed immunotherapy and chemotherapy of tumors: modeling, applications and biological interpretations. *Journal of Theoretical Biology*, 238(4):841–862, 2006.

[36] A de Vos, JJ van der Helm, M Prins, and M Kretzschmar. Determinants of persistent spread of HIV in HCV-infected populations of injecting drug users. *Epidemics*, 4(2):57–67, 2012.

[37] K Diethelm. A fractional calculus based model for the simulation of an outbreak of dengue fever. *Nonlinear Dynamics*, 71(4):613–619, 2013.

[38] K Diethelm and AD Freed. The Frac PECE subroutine for the numerical solution of differential equations of fractional order. *In: Heinzel, S., Plesser, T. (Eds.), Forschung und Wissenschaftliches Rechnen 1998. Gessellschaft fur Wissenschaftliche Datenverarbeitung, Gottingen*, pages 57–71, 1999.

[39] A Engelman and P Cherepanov. The structural biology of HIV-1: Mechanistic and therapeutic insights. *Nature reviews. Microbiology*, 10:279–290, 2012.

[40] B Ermentrout. XPPAUT®– the differential equations tool, version 5.98, 2006. `http://www.math.pitt.edu/~bard/xpp/xpp.html7`.

[41] Z Feng, C Castillo-Chavez, and AF Capurro. A model for tuberculosis with exogenous renfection. *Theoretical Population Biology*, 57(3):235–247, 2000.

[42] European Centre for Disease Prevention and Control. Annual epidemiological report reporting on 2011 surveillance data and 2012 epidemic intelligence data. Technical report, 2013.

[43] A Franciscus. A guide to: HIV/HCV coinfection. Technical report, Hepatitis C Support Project, 2012.

[44] EO Freed. HIV-1 replication. *Somatic Cell and Molecular Genetics*, 26:13–33, 2002.

[45] S Gakkhar and N Chavda. A dynamical model for HIV-TB co-infection. *Applied Mathematics and Computation*, 280(18):9261–9270, 2012.

[46] NR Gandhi, P Nunn, K Dheda, HS Schaaf, M Zignol, D van Soolingen, P Jensen, and J Bayona. Multidrug-resistant and extensively drug-resistant tuberculosis: a threat to global control of tuberculosis. *Lancet*, 375(9728):1830–1843, 2010.

[47] GAT. Guia sobre hepatite C para as pessoas que vivem com o VIH: Testes, co-infeção e tratamento. Technical report, 2009.

[48] MM Hadjiandreou, R Conejeros, and DI Wilson. Long-term HIV dynamics subject to continuous therapy and structured treatment interruptions. *Chemical Engineering Science*, 64(7):1600–1617, 2009.

[49] AD Harries, SD Lawn, H Getahun, R Zachariah, and DV Havlir. HIV and tuberculosis - science and implementation to turn the tide and reduce deaths. *Journal of the International AIDS Society*, 15(17396):1–11, 2012.

[50] PR Harrigan, M Whaley, and JS Montaner. Rate of HIV-1 RNA rebound upon stopping antiretroviral therapy. *AIDS*, 13(9):59–62, 1999.

[51] MD Hernandez and KE Sherman. HIV/HCV coinfection natural history and disease progression, a review of the most recent literature. *Current Opinion in HIV and AIDS*, 6(6):478–482, 2011.

[52] EA Hernandez-Vargas and RH Middleton. Modeling the three stages of HIV infection. *Journal of Theoretical Biology*, 320:33–40, 2013.

[53] M Heusinkveld and SH van der Burg. Identification and manipulation of tumor associated macrophages in human cancers. *Journal of Translational Medicine*, 9(216):1–13, 2011.

[54] TD Hollingsworth, RM Anderson, and C Fraser. HIV-1 transmission, by stage of infection. *Journal of Infectious Diseases*, 198(5):687–693, 2008.

[55] D Huang, X Zhang, Y Guo, and H Wang. Analysis of an HIV infection model with treatments and delayed immune response. *Applied Mathematical Modelling*, 40(4):3081–3089, 2016.

[56] LE Jones and AS Perelson. Opportunistic infection as a cause of transient viremia in chronically infected HIV patients under treatment with HAART. *Bulletin of Mathematical Biology*, 67(2):1227–1252, 2005.

[57] Y Kakizoe, S Nakaoka, CAA Beauchemin, S Morita, H Mori, T Igarashi, K Aihara, T Miura, and S Iwami. A method to determine the duration of the eclipse phase for in vitro infection with a highly pathogenic SHIV strain. *Scientific Reports*, 5(10371):1–14, 2015.

[58] WO Kermack and AG McKendrick. Contribution to the mathematical theory of epidemics. *Proceedings of the Royal Society of London A: Mathematical, Physical and Engineering Sciences*, 115(772):700–721, 1927.

[59] H Kim and AS Perelson. Viral and latent reservoir persistence in HIV-1–infected patients on therapy. *PLoS Computational Biology*, 2(10):1232–1247, 2006.

[60] SE Kline, LL Hedemark, and SF Davies. Outbreak of tuberculosis among regular patrons of a neighborhood bar. *New England Journal of Medicine*, 333(4):222–227, 1995.

[61] NL Komarova, D Anghelina, I Voznesensky, B Trinité, DN Levy, and D Wodarz. Relative contribution of free-virus and synaptic transmission to the spread of HIV-1 through target cell populations. *Biology Letters*, 9(1):1–6, 2013.

[62] H Koppensteiner, R Brack-Werner, and M Schindler. Macrophages and their relevance in human immunodeficiency virus type I infection. *Retrovirology*, 9(82):1–11, 2012.

[63] V Lakshmikantham, S Leela, and A Martynyuk. *Stability Analysis of Nonlinear Systems*. Marcel Dekker Inc., New York and Basel, 1989.

[64] S LeBlanc. *The Long and the Short of AIDS Progression*. The Bay Area Report, 1996.

[65] JA Levy. The importance of the innate immune system in controlling HIV infection and disease. *Trends in Immunology*, 22(6):312–316, 2001.

[66] MY Li and L Wang. Backward bifurcation in a mathematical model for HIV infection in vivo with anti-retroviral treatment. *Nonlinear Analysis: Real World Applications*, 17:147–160, 2014.

[67] W Lin. Global existence theory and chaos control of fractional differential equations. *Journal of Mathematical Analysis and Applications*, 332(1):709–726, 2007.

[68] R Lorenzo-Redondo, HR Fryer, T Bedford, EY Kim, J Archer, SL Kosakovsky Pond, YS Chung, S Penugonda, JG Chipman, CV Fletcher, TW Schacker, MH Malim, A Rambaut, AT Haase, AR McLean, and SM Wolinsky. Persistent HIV-1 replication maintains the tissue reservoir during therapy. *Nature*, 530(7588):51–56, 2016.

[69] J Lou and T Ruggeri. A time delay model about AIDS-related cancer: equilibria, cycles and chaotic behavior. *Ricerche di Matematica*, 56(2):195–208, 2007.

[70] J Lou, T Ruggeri, and Z Ma. Cycles and chaotic behavior in an AIDS-related cancer dynamic model in vivo. *Journal of Biological Systems*, 15(2):149–168, 2007.

[71] J Lou, T Ruggeri, and C Tebaldi. Modeling cancer in HIV-1 infected individuals: equilibria, cycles and chaotic behavior. *Mathematical Biosciences and Engineering*, 3(2):313–324, 2006.

[72] Y Louzoun, C Xue, GB Lesinski, and A Friedman. A mathematical model for pancreatic cancer growth and treatments. *Journal of Theoretical Biology*, 351:74–82, 2014.

[73] O Lund, E Mosekilde, and J Hansen. Period doubling route to chaos in a model of HIV infection of the immune system: A comment on the Anderson-May model. *Simulation Practice and Theory*, 1(2):49–55, 1993.

[74] R Luo, MJ Piovoso, J Martinez-Picado, and R Zurakowski. HIV model parameter estimates from interruption trial data including drug efficacy and reservoir dynamics. *PLoS ONE*, 7(7):1–12, 2012.

[75] MG Madariaga, UG Lalloo, and S Swindells. Extensively drug-resistant tuberculosis. *The American journal of medicine*, 121(10):835–844, 2008.

[76] A Mallela, S Lenhart, and NK Vaidya. HIV-TB co-infection treatment: Modeling and optimal control theory perspectives. *Journal of Computational and Applied Mathematics*, 307:143–161, 2016.

[77] ES McBryde, MT Meehan, TN Doan, R Ragonnet, BJ Marais, V Guernier, and JM Trauer. The risk of global epidemic replacement with drug-resistant mycobacterium tuberculosis strains. *International Journal of Infectious Diseases*, 56:14–20, 2017.

[78] AJ McMichael, P Borrow, GD Tomaras, N Goonetilleke, and BF Haynes. The immune response during acute HIV-1 infection: clues for vaccine development. *Nature Reviews Immunology*, 10(1):11–23, 2010.

[79] JS Montaner, M Harris, T Mo, and PR Harrigan. Rebound of plasma viral load following prolonged supression with combination therapy. *AIDS*, 12(11):1398–1399, 1998.

[80] Y Nakamura, Y Obase, N Suyama, Y Miyazaki, H Ohno, M Oka, M Takahashi, and S Kohno. A small outbreak of pulmonary tuberculosis in non-close contact patrons of a bar. *Internal Medicine Journal*, 43(3):263–267, 2004.

[81] R Naresh and A Tripath. Modelling and analysis of HIV-TB co-infection in a variable size population. *Mathematical Modelling and Analysis*, 10(3):275–286, 2005.

[82] R Nazari and S Joshi. CCR5 as target for HIV-1 gene therapy. *Current Gene Therapy*, 8(4):264–272, 2008.

[83] J Newcomb-Fernandez. Cancer in the HIV-infected population. the body - the complete HIV/AIDS resource. `http://www.thebody.com/content/art16834.html`.

[84] F Nyabadza. A mathematical model for combating HIV/AIDS in Southern Africa: will multiple strategies work? *Journal of Biological Systems*, 14(3):357–372, 2006.

[85] F Nyabadza and Z Mukandavire. Modeling HIV/AIDS in the presence of an HIV testing and screening campaign. *Journal of Theoretical Biology*, 280(1):167–179, 2011.

[86] ZM Odibat and NT Shawagfeh. Generalized Taylor's formula. *Applied Mathematics and Computation*, 186(1):286–293, 2007.

[87] Center of Disease Control and Prevention. HIV/AIDS and HCV. `http://www.cdc.gov/hepatitis/hcv/pdfs/hepcgeneralfactsheet.pdf` and `http://www.cdc.gov/HIV`.

[88] U.S. Department of Health & Human Services. HIV/AIDS glossary. https://aidsinfo.nih.gov/understanding-hiv-aids/glossary/325/human-immunodeficiency-virus.

[89] School of Medicine & Health Sciences. HIV and the AIDS pandemic. https://smhs.gwu.edu/nixon-lab/research.

[90] AA Okoye and LJ Picker. $CD4^+$ T cell depletion in HIV infection: mechanisms of immunological failure. *Immunological Reviews*, 254(1):54–64, 2013.

[91] KB Oldham and J Spanier. *The fractional calculus: theory and application of differentiation and integration to arbitrary order*. Academic Press, 1974.

[92] Joint United Nations Programme on HIV/AIDS (UNAIDS). Report on the global AIDS epidemic. http://data.unaids.org/pub/GlobalReport/2008/JC1511_GR08_ExecutiveSummary_en.pdf.

[93] World Health Organization. HIV/AIDS. http://www.who.int/hiv/en/.

[94] World Health Organization. Tuberculosis and HIV. http://www.who.int/hiv/topics/tb/about_tb/en/.

[95] R Ouifki and G Witten. Stability analysis of a model for HIV infection with RTI and three intracellular delays. *BioSystems*, 95(1):1–6, 2009.

[96] AS Perelson, DE Kirschner, and R De Boer. Dynamic of HIV infection of $CD4^+$ T cells. *Mathematical Biosciences*, 114(1):81–125, 1993.

[97] AS Perelson, AU Neumann, M Markowitz, JM Leonard, and DD Ho. HIV-1 dynamics in vivo: virion clearance rate, infected cell life-span, and viral generation time. *Science*, 271(5255):1582–1586, 1996.

[98] AS Perelson and RM Ribeiro. Modeling the within-host dynamics of HIV infection. *BMC Biology*, 11(96):1–10, 2013.

[99] CMA Pinto and ARM Carvalho. Mathematical model for HIV dynamics in HIV-specific helper cells. *Communications in Nonlinear Science and Numerical Simulation*, 19(3):693–701, 2014.

[100] CMA Pinto and ARM Carvalho. New findings on the dynamics of HIV and TB coinfection models. *Applied Mathematics and Computation*, 242:36–46, 2014.

[101] CMA Pinto and ARM Carvalho. Effects of treatment, awareness and condom use in a coinfection model for HIV and HCV in MSM. *Journal of Biological Systems*, 23(2):165–193, 2015.

[102] CMA Pinto and ARM Carvalho. Fractional modeling of typical stages in HIV epidemics with drug-resistance. *Progress in Fractional Differentiation and Applications*, 1(2):111–122, 2015.

[103] CMA Pinto and ARM Carvalho. Fractional complex-order model for HIV infection with drug-resistance during therapy. *Journal of Vibration and Control*, 22(9):2222–2239, 2016.

[104] CMA Pinto and ARM Carvalho. The impact of pre-exposure prophylaxis (PrEP) and screening on the dynamics of HIV. *Journal of Computational and Applied Mathematics*, 2017.

[105] CMA Pinto and ARM Carvalho. A latency fractional order model for HIV dynamics. *Journal of Computational and Applied Mathematics*, 312:240–256, 2017.

[106] CMA Pinto and ARM Carvalho. The role of synaptic transmission in a HIV model with memory. *Applied Mathematics and Computation*, 292:76–95, 2017.

[107] M Pitchaimani, C Monica, and M Divya. Stability analysis for HIV infection delay model with protease inhibitor. *BioSystems*, 114(2):118–124, 2013.

[108] L Platt, P Easterbrook, E Gower, B McDonald, K Sabin, C McGowan, I Yanny, H Razavi, and P Vickerman. Prevalence and burden of HCV co-infection in people living with HIV: a global systematic review and meta-analysis. *The Lancet Infectious Diseases*, 16(7):797–808, 2016.

[109] M Prakash and P Balasubramaniam. Bifurcation analysis of macrophages infection model with delayed immune response. *Communications in Nonlinear Science Numerical Simulation*, 35:1–16, 2016.

[110] B Ramratnam, JE Mittler, L Zhang, D Boden, A Hurley, F Fang, CA Macken, AS Perelson, M Markowitz, and DD Ho. The decay of the latent reservoir of replication-competent HIV-1 is inversely correlated with the extent of residual viral replication during prolonged anti-retroviral therapy. *Nature Medicine*, 6(1):82–85, 2000.

[111] R Reinke, NR Steffen, and ER Jr. Natural selection results in conservation of HIV-1 integrase activity despite sequence variability. *AIDS*, 15:823–830, 2001.

[112] R Reynoso, M Wieser, D Ojeda, M Bonisch, H Kuhnel, F Bolcic, H Quendler, J Grillari, R Grillari-Voglauer, and J Quarleri. HIV-1 induces telomerase activity in monocyte-derived macrophages, possibly safeguarding one of its reservoirs. *Journal of Virology*, 86(19):10327–10337, 2012.

[113] FA Rihan and DHA Rahman. Delay differential model for tumour–immune dynamics with HIV infection of CD4^+ T-cells. *International Journal of Computer Mathematics*, 90(3):594–614, 2013.

[114] JK Rockstroh. Influence of viral hepatitis on HIV infection. *Journal of Hepatology*, 44(Suppl 1):S25–S27, 2006.

[115] P Rodrigues, MGM Gomes, and C Rebelo. Drug resistance in tuberculosis - a reinfection model. *Theoretical Population Biology*, 71(2):196–212, 2007.

[116] LI Roeger, Z Feng, and C Castillo-Chavez. Modeling TB and HIV co-infections. *Mathematical Biosciences and engineering*, 6(4):815–837, 2009.

[117] L Rong, RM Ribeiro, and AS Perelson. Modeling quasispecies and drug resistance in hepatitis C patients treated with a protease inhibitor. *Bulletin of Mathematical Biology*, 74(8):1789–1817, 2012.

[118] M Ronoh, R Jaroudi, P Fotso, V Kamdoum, N Matendechere, J Wairimu, R Auma, and J Lugoye. A mathematical model of tuberculosis with drug resistance effects. *Applied Mathematics*, 7:1303–1316, 2016.

[119] R Ross. *The prevention of malaria*. New York, E.P. Dutton & company, 1911.

[120] SM Roy and D Wodarz. Infection of HIV-specific CD4$^+$ T helper cells and the clonal composition of the response. *Journal of Theoretical Biology*, 304:143–151, 2012.

[121] A Rubbert, G Behrens, and M Ostrowski. Pathogenesis of HIV-1 infection. `https://hivbook.com/tag/structure-of-hiv-1/`.

[122] SG Samko, AA Kilbas, and OI Marichev. *Fractional integrals and derivatives: theory and applications*. Gordon and Breach Science Publishers, 1993.

[123] AYC Sanchez, M Aerts, Z Shkedy, P Vickerman, F Faggiano, G Salamina, and N Hens. A mathematical model for HIV and hepatitis C co-infection and its assessment from a statistical perspective. *Epidemics*, 5(1):56–66, 2013.

[124] R Sergeev, C Colijn, M Murray, and T Cohen. Modeling the dynamic relationship between HIV and the risk of drug-resistant tuberculosis. *Science Translational Medicine*, 4(135):135–167, 2012.

[125] O Sharomi, CN Podder, AB Gumel, and B Song. Mathematical analysis of the transmission dynamics of HIV/TB co-infection in the presence of treatment. *Mathematical Biosciences and Engineering*, 5(1):145–174, 2008.

[126] MP Sherman and WC Greene. Slipping through the door: HIV entry into the nucleus. *Microbes and Infection*, 4:67–73, 2002.

[127] CI Siettos and L Russo. Mathematical modeling of infectious disease dynamics. *Virulence*, 4(4):295–306, 2013.

[128] A Sigal, JT Kim, AB Balazs, E Dekel, A Mayo, R Milo, and D Baltimore. Cell-to-cell spread of HIV permits ongoing replication despite antiretroviral therapy. *Nature*, 477(7362):95–98, 2011.

[129] JD Siliciano, J Kajdas, D Finzi, TC Quinn, K Chadwick, JB Margolick, C Kovacs, SJ Gange, and RF Siliciano. Long-term follow-up studies confirm the stability of the latent reservoir for HIV-1 in resting $CD4^+$ T cells. *Nature Medicine*, 9:727–728, 2003.

[130] C Silva, H Maurer, and DFM Torres. Optimal control of a tuberculosis model with state and control delays. *Mathematical Biosciences and Engineering*, 14(1):321–337, 2017.

[131] CJ Silva and DFM Torres. A SICA compartmental model in epidemiology with application to HIV/AIDS in Cape Verde. *Ecological Complexity*, 30:70–75, 2017.

[132] L Simpson and AB Gumel. Mathematical assessment of the role of pre-exposure prophylaxis on HIV transmission dynamics. *Applied Mathematics and Computation*, 293:168–193, 2017.

[133] HL Smith and P Waltman. *The Theory of the Chemostat*. Cambridge University Press, 1995.

[134] JI Spouge, RI Shrager, and DS Dimitrov. HIV-1 infection kinetics in tissue cultures. *Mathematical Biosciences*, 138(1):1–22, 1996.

[135] SI Staprans, AP Barry, G Silvestri, JT Safrit, N Kozyr, B Sumpter, H Nguyen, H McClure, D Montefiori, JI Cohen, and MB Feinberg. Enhanced SIV replication

and accelerated progression to AIDS in macaques primed to mount a $CD4^+$ T cell response to the SIV envelope protein. *Proceedings of the National Academy of Sciences USA*, 101(35):13026–13031, 2004.

[136] KE Starkov and C Plata-Ante. On the global dynamics of the cancer AIDS-related mathematical model. *Kybernetika*, 50(4):563–579, 2014.

[137] Consensus statement. EASL international consensus conference on hepatitis C. Paris, 26-28 february 1999. *Journal of Hepatology*, 30(5):956–961, 1999.

[138] MS Sulkowski. Viral hepatitis and HIV coinfection. *Journal of Hepatology*, 48(2):353–367, 2008.

[139] NH Sweilam and SM AL-Mekhlafi. Numerical study for multi-strain tuberculosis (TB) model of variable-order fractional derivatives. *Journal of Advanced Research*, 7(2):271–283, 2016.

[140] NH Sweilam and SM AL-Mekhlafi. On the optimal control for fractional multi-strain TB model. *Optimal Control Applications and Methods*, 37(6):1355–1374, 2016.

[141] MS Tavazoei and M Haeri. Chaotic attractors in incommensurate fractional order systems. *Physica D: Nonlinear Phenomena*, 237(20):2628–2637, 2008.

[142] LE Taylor, T Swan, and KH Mayer. HIV coinfection with hepatitis C virus: evolving epidemiology and treatment paradigms. *Clinical Infectious Diseases*, 55(Suppl 1):S33–S42, 2012.

[143] A Telesnitsky and SP Goff. *Reverse Transcriptase and the Generation of Retroviral DNA*. Cold Spring Harbor Laboratory Press, Cold Spring Harbor (NY), 1997.

[144] HH Thein, Q Yi, GJ Dore, and MD Krahn. Natural history of hepatitis C virus infection in HIV-infected individuals and the impact of HIV in the era of highly active antiretroviral therapy: a meta-analysis. *AIDS*, 22(15):1979–1991, 2008.

[145] BK Titanji, MA Chapman, D Pillay, and C Jolly. Protease inhibitors effectively block cell-to-cell spread of HIV-1 between T cells. *Retrovirology*, 10:161–171, 2013.

[146] JM Trauer, JT Denholm, and ES McBryde. Construction of a mathematical model for tuberculosis transmission in highly endemic regions of the Asia-Pacific. *Journal of Theoretical Biology*, 358:74–84, 2014.

[147] BG Turner and MF Summers. Structural biology of HIV. *Journal of Molecular Biology*, 285:1–32, 1999.

[148] PW Uys, PD van Helden, and JW Hargrove. Tuberculosis reinfection rate as a proportion of total infection rate correlates with the logarithm of the incidence rate: a mathematical model. *Journal of The Royal Society Interface*, 6(6):11–15, 2009.

[149] TJ van de Laar, GV Matthews, M Prins, and M Danta. Acute hepatitis C in HIV-infected men who have sex with men: an emerging sexually transmitted infection. *AIDS*, 24(12):1799–1812, 2010.

[150] P van den Driessche and P Watmough. Reproduction numbers and sub-threshold endemic equilibria for compartmental models of disease transmission. *Mathematical Biosciences*, 180(1–2):29–48, 2002.

[151] S Verver, RM Warren, N Beyers, M Richardson, GD van der Spuy, MW Borgdorff, DA Enarson, MA Behr, and PD van Helden. Rate of reinfection tuberculosis after successful treatment is higher than rate of new tuberculosis. *American Journal of Respiratory and Critical Care Medicine*, 171(12):1430–1435, 2005.

[152] P Vickerman, NK Martin, and M Hickman. Understanding the trends in HIV and hepatitis C prevalence amongst injecting drug users in different settings: implications for intervention impact. *Drug and Alcohol Dependence*, 123(1–3):122–131, 2012.

[153] P Vickerman, A Miners, and J Williams. Assessing the cost-effectiveness of interventions linked to needle and syringe programmes for injecting drug users: an economic modelling report. Technical report, Department of Public Health and Policy, London School of Hygiene and Tropical Medicine, Keppel Street, London, UK, 2008.

[154] LM Wahl and MA Nowak. Adherence and drug resistance: predictions for therapy outcome. *Proceedings of Biological Sciences*, 267(1445):835–843, 2000.

[155] X Wang, X Song, S Tang, and L Rong. Dynamics of an HIV model with multiple infection stages and treatment with different drug classes. *Bulletin of Mathematical Biology*, 78(2):322–349, 2016.

[156] Y Wang, F Brauer, J Wu, and JM Heffernan. A delay-dependent model with HIV drug resistance during therapy. *Journal of Mathematical Analysis and Applications*, 414(2):514–531, 2014.

[157] AS Waziri, ES Massawe, and OD Makinde. Mathematical modelling of HIV/AIDS dynamics with treatment and vertical transmission. *Applied Mathematics*, 2(3):77–89, 2012.

[158] X Wei, SK Ghosh, ME Taylor, VA Johnson, EA Emini, P Deutsch, JD Lifson, S Bonhoeffer, MA Nowak, BH Hahn, MS Saag, and GM Shaw. Viral dynamics in human immunodeficiency virus type 1 infection. *Nature*, 373(6510):117–122, 1995.

[159] LM Wein, RM D'Amato, and AS Perelson. Mathematical analysis of antiretroviral therapy aimed at HIV-1 eradication or maintenance of low viral loads. *Journal of Theoretical Biology*, 192(1):81–98, 1998.

[160] LS Weinhardt, MP Carey, BT Johnson, and NL Bickham. Effects of HIV counseling and testing on sexual risk behavior: a meta-analytic review of published research, 1985–1997. *American Journal of Public Health*, 89(9):1397–1405, 1999.

[161] Q Wen and J Lou. The global dynamics of a model about HIV-1 infection in vivo. *Ricerche di Matematica*, 58(1):77–90, 2009.

[162] D Wodarz and DH Hamer. Infection dynamics in HIV-specific $CD4^+$ T cells: does a $CD4^+$ T cell boost benefit the host or the virus? *Mathematical Biosciences*, 209(1):14–29, 2007.

[163] Y Yang and Y Xiao. Threshold dynamics for an HIV model in periodic environments. *Journal of Mathematical Analysis and Applications*, 361(1):59–68, 2010.